

1999

ANTIMONY SPECIATION BY CHROMATOGRAPHIC SAMPLE INTRODUCTION TO PLASMA SPECTROSCOPY

GUY, ALAN BRUCE

<http://hdl.handle.net/10026.1/1675>

<http://dx.doi.org/10.24382/3456>

University of Plymouth

All content in PEARL is protected by copyright law. Author manuscripts are made available in accordance with publisher policies. Please cite only the published version using the details provided on the item record or document. In the absence of an open licence (e.g. Creative Commons), permissions for further reuse of content should be sought from the publisher or author.

ANTIMONY SPECIATION BY CHROMATOGRAPHIC SAMPLE INTRODUCTION TO PLASMA SPECTROSCOPY

by

ALEN BRUCE GUY
BSc (Hons), GRSC

A thesis submitted to the University of Plymouth
in partial fulfilment for the degree of

DOCTOR OF PHILOSOPHY

Department of Environmental Sciences
University of Plymouth
Drake Circus
Plymouth
PL4 8AA

In collaboration with:

Engineering & Physical Sciences Research Council; and

ICI Technology
Wilton
Middlesborough
Teesside

February 1999

LIBRARY STORE

90 0392055 1



UNIVERSITY OF PLYMOUTH	
Item No.	9003920551
Date	- 8 JUL 1999 S
Class No.	T 543.0858
Contl. No.	X703901647
LIBRARY SERVICES	

GUY

REFERENCE ONLY

Abstract

“Antimony Speciation by Chromatographic Sample Introduction to Plasma Spectroscopy”

Alen Guy

Antimony (Sb), an element in Group V of the Periodic Table, has an ancient and varied chemistry with many applications in industry and medicine. However, although sensitive analytical methods exist for the determination of Sb very little is known about the speciation of the element. It is widely known that the toxicity of Sb is not only dependent upon its oxidation state but also its molecular form. Thus this study has utilised chromatographic sample introduction directly coupled to plasma spectroscopic instruments to facilitate separations of Sb based upon molecular form coupled with sensitive detection methods.

Fundamental studies, using NMR to investigate physical changes in ligands and ESI-MS to investigate molecular ions, have shown that complexes of Sb(V) can form with compounds that might exist in biological/environmental systems, such as α -hydroxyacids. These complexes have been separated using ion-exchange and reversed-phase chromatography for the first time. A fundamental investigation of the nebuliser/spray chamber assembly was carried out in terms of the effect on the quality of the chromatographic separations. It was found that the resolution was strongly dependent upon choice of nebuliser and spray-chamber. Five nebulisers and two spray-chambers were studied with the Burgener nebuliser/cyclonic spray-chamber pairing being the most useful analytically. The methods developed from these fundamental studies were applied to environmental water, plant and sediment sample extracts as well as industrial polymer leachates.

These studies have shown that Sb(V) was the favoured form in terrestrial water samples, agreeing with thermodynamic assumptions. However, more unidentified Sb species were detected in sediment and plant (liverwort, moss) extracts. Hydride generation (HG) apparatus placed in-line between the HPLC and the plasma instrument facilitated analysis of reducible species and it was found that for many samples not all the Sb was in a reducible form. This was confirmed by comparison with chromatograms for analysis without HG. Sample spiking experiments showed that dissolved complexing agents from the samples would produce striking differences in chromatograms, i.e. in one case all peaks would respond to the spike whereas in another sample only one peak would respond. This was a novel discovery in this field of speciation and has highlighted possible new chemistries for trace levels of environmental Sb. This indicated the need for further studies of the complex nature of Sb in trace and ultra-trace levels in the environment leading to the production of specific reference materials. Investigation of industrial samples showed that significant work is still required especially in the area of the chromatographic elution of Sb(III) species from columns packed with a high percentage of aromatic organic material.

CONTENTS

SECTION	PAGE
Copyright Statement	I
Title Page	II
Abstract	III
List of Contents	IV
List of Tables	XI
List of Figures	XIV
Acknowledgements	XXIII
Authors Declaration	XXV
Chapter 1. Chemistry of Antimony, Literature Review and Aims and Objectives of the Study	1
1.1 Introduction	1
1.2 The Chemistry and Uses of Antimony	1
1.2.1 Elemental Antimony	1
1.2.2 The Hydride, Stibine, SbH_3	2
1.2.3 Trivalent Antimony	3
1.2.3.1 Trihalides, SbX_3	3
1.2.3.2 Antimony Oxides	4
1.2.3.3 Antimony Sulphides	4
1.2.4 Pentavalent Antimony	5
1.2.4.1 Halides, SbX_5 and $[\text{SbX}_6]^-$	5
1.2.4.2 Antimony Oxides	5
1.2.5 The Coordination Chemistry of Antimony	5
1.2.6 Applications of Antimony	15

1.2.6.1 Historical Uses and Background	15
1.2.6.2 Industrial Applications of Antimony	15
1.2.6.3 Medical Applications for Antimony	17
1.2.6.4 Abstraction of Antimony	17
1.2.7 Toxicology of Antimony	19
1.2.7.1 Intoxication	21
1.2.7.2 Environmental Antimony	21
1.2.8 Summary	23
1.3 Review of Methods of Determination	24
1.3.1 UV/Vis Spectrophotometry	24
1.3.2 Flame and Electrothermal Atomisation-Atomic Absorption Spectroscopy	28
1.3.3 Inductively Coupled Plasma-Atomic Emission Spectroscopy	32
1.3.4 Inductively Coupled Plasma-Mass Spectrometry	35
1.3.5 Other Methods	38
1.3.6 Discussion	41
1.4 Review of Speciation of Antimony	41
1.4.1 Voltammetric and Instrumental Neutron Activation Analysis Methods	41
1.4.2 UV/Vis Spectrophotometric Methods	43
1.4.3 Hydride Generation-Atomic Absorption/Fluorescence Spectroscopy	44
1.4.4 Electrothermal Atomisation-Atomic Absorption Spectroscopy	46
1.4.5 Gas Chromatography	48
1.4.6 Liquid Chromatography (LC) Methods	50
1.4.7 Discussion	53

1.5 Aims and Objectives of Study	55
1.5.1 Antimony Speciation	55
1.5.1.1 Environmental Samples	56
1.5.1.2 Industrial Samples	57
1.5.2 Fundamental Studies	57
 Chapter 2. Instrumentation	 59
2.1 Principles of Chromatography	59
2.1.1 Introduction	59
2.1.2 Categories of Chromatography	60
2.2 Atomic Spectroscopy	72
2.2.1 Introduction	72
2.2.2 Inductively Coupled Plasma-Optical Emission Spectroscopy	72
2.2.2.1 The Inductively Coupled Plasma (ICP)	72
2.2.2.2 Sample Introduction	75
2.2.2.3 Optical Spectrometer	82
2.2.2.4 Detection and Data Manipulation	85
2.2.3 Inductively Coupled Plasma-Mass Spectrometry (ICP-MS)	87
2.2.3.1 Ion Formation in the Plasma	87
2.2.3.2 ICP-Mass Analyser Interface	89
2.2.3.3 Detection and Data Manipulation	93
2.2.4 ICP-AES/MS Analytical Merits and Applications	94
2.2.5 Hydride Generation (HG)	95
2.2.5.1 Introduction	95
2.2.5.2 Principles	97

2.3 Nuclear Magnetic Resonance	99
2.3.1 Principles of Nuclear Magnetic Resonance (N.M.R.)	99
2.3.2 Sampling	104
2.3.3 Applications	104
2.4 Electrospray Ionisation-Mass Spectrometry	105
2.4.1 Principles	105
2.4.2 Sampling	106
2.4.3 Spectra and Applications	107
 Chapter 3. The Determination of Sb:α-hydroxyacid Complexes	 108
3.1 Introduction	108
3.2 Experimental	113
3.2.1 Instrumentation	113
3.2.2 Reagents	114
3.3 Method Development	114
3.4 Results	119
3.4.1 NMR Interpretation	119
3.4.1.1 Sb:Citric Acid	119
3.4.1.2 Sb:Malic Acid	124
3.4.1.3 Sb:Mandelic Acid	124
3.4.2 Determination of Complexes by IC-ICP-AES	129
3.4.2.1 Preliminary Results	129
3.4.2.2 Detailed Investigation and Application of Stoichiometric Model	133
3.4.2.2.1 [Sb(OH) _x (citrate) _n]	133
3.4.2.2.2 [Sb(OH) _x (malate) _n]	138

3.4.2.2.3 [Sb(OH) _x (mandelate) _n]	141
3.4.3 Electrospray Ionisation-Mass Spectrometry (ESI-MS)	145
3.4.3.1 Spectra Interpretation	145
3.4.4 Further Complex Determinations by HPLC	148
3.5 Discussion	156
3.5.1 Structural Evaluation of Sb,α-hydroxyacid Compounds	156
3.5.2 Application of Sb,α-hydroxyacid Complexation to Separation	157
Methodology and Determination of Sb Compounds in Real	
Samples	
3.6 Conclusions	158
 Chapter 4. Speciation of Antimony in Environmental Samples	 159
4.1 Introduction	159
4.1.1 Antimony in the Environment	159
4.2 Experimental	165
4.2.1 Instrumentation	165
4.2.2 Reagents	165
4.2.3 Method Development	166
4.3 Results	173
4.3.1 Ion-exchange Chromatography and Conductivity	173
Detection (CD)	
4.3.2 ICP-AES	173
4.3.2.1 Initial Coupling of HPLC with ICP-AES	173
4.3.2.2 Determination of Antimony by HG-ICP-AES	183
4.3.3 Determination of Antimony by ICP-MS and HPLC-ICP-MS	188

4.3.3.1 Continued Method Development using Ion Exchange Chromatography	188
4.3.3.2 Determination of Antimony in H ₂ O and 0.2 M Acetic Acid Extracts of Plant and Sediment Samples by HPLC-ICP-MS	201
4.3.3.3 Analysis of Mine Site Samples by HPLC-HG-ICP-MS	208
4.4 Conclusions	213
Chapter 5.	215
5.1 Nebuliser and Spray-Chamber Effects on Post-Column Dispersion and Resolution in High Performance Liquid Chromatography-Inductively Coupled Plasma-Mass Spectrometry	215
5.1.1 Introduction	215
5.1.2 HPLC-ICP-MS and Post-Column Dispersion	216
5.1.2.1 The Nebuliser and Spray Chamber Assembly	218
5.1.3 Instrumentation	221
5.1.4 Reagents	221
5.1.5 Experimental	223
5.1.5.1 Nebuliser Comparison with Double-Pass Spray-Chamber	223
5.1.5.2 Comparison of Cyclonic and Double-Pass Spray-Chamber, and the Concentric and Burgener Nebuliser with the Cyclonic Spray-Chamber	224
5.1.6 Results	224
5.1.6.1 Comparison of Nebulisers when used with Double-Pass Spray-Chamber	224
5.1.6.2 Comparison of Spray-Chambers	228

5.1.6.3 Comparison of Nebulisers with the Cyclonic Spray-Chamber	228
5.1.7 Discussion	231
5.1.7.1 Nebuliser Comparison with Double-Pass Spray-Chamber	231
5.1.7.2 Comparison of Spray-Chambers	232
5.1.7.3 Comparison of Burgener and Concentric Nebulisers with Cyclonic Spray-Chamber	233
5.1.8 Conclusions	234
5.2 Investigation of Antimony in Organic Matrices	235
5.2.1 Introduction	235
5.2.2 Experimental	237
5.2.2.1 Instrumentation	237
5.2.2.2 Reagents	237
5.2.2.3 Sample Preparation (University of Plymouth)	237
5.2.3 Results	237
5.2.4 Discussion	247
5.2.5 Conclusion	249
Chapter 6. Conclusions and Future Work	250
6.1 Conclusions	250
6.2 Future Work	254
6.2.1 HPLC Separations of Antimony Species	254
6.2.2 HPLC Coupled to ICP-MS	255
6.2.3 Sb, α -hydroxyacid Complexes	256
References	257
Published Work	269
Conference Presentations	269

LIST OF TABLES

CHAPTER ONE	PAGE
1.1 Properties of stibine and arsine	2
1.2 Properties of Sb trihalides	3
1.3 Examples of applications for antimony trihalides	4
1.4 Summary of coordination chemistry literature for Sb complexes of Sb(V) and Sb(III)	8
1.5 Examples of total Sb analysis by UV/Vis spectrophotometry	26
1.6 Examples of total Sb analysis by flame and electrothermal atomisation-atomic absorption spectrometry	29
1.7 Examples of total Sb analysis by ICP-AES	33
1.8 Examples of total Sb analysis by ICP-MS	36
1.9 Examples of less common detection methods for the determination of total Sb	39
1.10 Limits of detection for methods utilised by Smichowski <i>et al</i> ⁽¹⁵⁹⁾	51
 CHAPTER TWO	
2.1 Classification of column chromatographic methods with some examples of applications	61
2.2 Modes of LC separation and the general mechanism	67
2.3 Functional groups used in ion-exchange chromatography (IEC) and their ion exchange strength	68
2.4 Examples of interfering molecular ions for some elements in ICP-MS analysis	92

2.5	Limits of detection for selected elements by a range of atomic spectroscopy instruments	94
2.6	Examples of the application base for plasma instruments. CN - Continuous Nebulisation, FI - Flow Injection, HPLC - High Performance Liquid Chromatography	95
2.7	Relationship between mass/atomic numbers and spin quantum number	100

CHAPTER THREE

3.1	Molar ratios of Sb:α-hydroxyacid used in HPLC-ICP-AES investigation	116
3.2	Figures of significance for preliminary separations of Sb,α-hydroxyacids	133
3.3	Summary of results for Sb: citric acid system including the calculated levels of association	137
3.4	Summary of results for Sb:DL-malic acid system including the calculated levels of association	140
3.5	Summary of results for Sb:(±) mandelic acid system including the calculated levels of association	142
3.6	Hypothesised m/z values and formulae for the complexes	141

CHAPTER FOUR

4.1	Summary of sample types, detection method, typical concentration range and limits of detection for Sb reported in the literature over the last 20 years	160
4.2	Comparison of sample analyses by HG-ICP-AES with ICP-MS	188
4.3	Summary of total Sb analyses for water samples and water soluble extracts of sediment samples	193

4.4	Summary of HPLC-ICP-MS results for Sb(V) using 5 mM Cl ⁻ eluent at 0.35 ml min ⁻¹ , AS-11 anion exchange column	199
4.5	pH ranges for 0.2 M acetic acid extracts	202
4.6	Summary of peak data for sample extracts, all 0.2 M acetic acid except where indicated	202

CHAPTER FIVE

5.1	Summary of tuning process for the nebulisers with a double-pass spray-chamber using a continuously nebulised solution of ¹¹⁵ In (100 µg l ⁻¹)	224
5.2	Summary of chromatographic parameters for comparison of nebulisers with double-pass spray-chambers	225
5.3	Summary of SBR's for the nebuliser study with a double-pass spray-chamber	227
5.4	Extra-column volumes and changes in i.d. in the interface associated with each nebuliser	227
5.5	Key results from the spray-chamber comparison using a Burgener nebuliser	228
5.6	Summary of analysis of coke samples from both a can and a PET bottle	244

LIST OF FIGURES

CHAPTER ONE	PAGE
1.1 Structure of SbF_6 bridged octahedra polymeric chain	6
1.2 Structural representations of $[\text{SbCl}_5(\text{OPCl}_3)]$ and $[\text{SbF}_5(\text{OSO})]$	6
1.3 Structural representations of tartar emetic, stibophen and astiban	18
 CHAPTER TWO	
2.1 Representation of a Chromatographic Separation of Two Species	63
2.2 The van Deemter Plot	66
2.3 Diagram showing the make-up of Ionpac packing material and the functionalisation utilised by Dionex	69
2.4 Structural representation of cross-linked polystyrene divinylbenzene copolymer with sulfonate groups	70
2.5 Processes of absorption/emission of energy in AES, AAS and AFS	73
2.6 Schematic diagram of a torch and inductively coupled plasma	74
2.7 The components of a typical sample introduction arrangement for ICP	76
2.8 Nebulisers utilised for sample introduction to ICP-AES	78
2.9 The Venturi effect	79
2.10 Spray chambers for ICP. a) The double pass; b) single pass with impact bead; c) cyclonic spray chamber; and d) dimple modified cyclonic spray chamber	81
2.11 Schematic diagrams for monochromator types used in ICP-AES	83
2.12 Schematic diagrams of typical arrangements for a) ICP-AES and b) ICP-MS	88
2.13 Schematic diagram of a typical ICP-MS interface	90

2.14	Schematic diagrams for a quadrupole mass analyser and potential arrangement	91
2.15	Typical hydride generation arrangement	98
2.16	Representation of precessing nuclei under the influence of an external magnetic field B_0	101
2.17	^1H N.M.R. of ethanol, $\text{CH}_3\text{CH}_2\text{OH}$	103

CHAPTER THREE

3.1	Structures of selected α -hydroxyacids. a) Mandelic acid; b) Citric acid; c) Malic acid; and d) Lactic acid	109
3.2	Molecular configuration for the complex $[\text{SbNa}(\text{C}_6\text{H}_6\text{O}_7)_2(\text{H}_2\text{O})] \cdot \text{H}_2\text{O}$	112
3.3	Model developed to determine metal:ligand ratios for Sb: α -hydroxyacid complexes	117
3.4	^1H NMR for 2% (w/v) citric acid in MilliQ. Inset is structure and annotation	120
3.5	^1H NMR for an equimolar solution of Sb(V) and citric acid in MilliQ	121
3.6	^{13}C NMR for 2% (w/v) citric acid in MilliQ	122
3.7	^{13}C NMR for an equimolar solution of Sb(V) and citric acid in MilliQ	123
3.8	^1H NMR for a) 2% (w/v) DL-malic acid and b) equimolar solution of Sb(V) and DL-malic acid in MilliQ. Inset is structure.	125
3.9	^{13}C NMR for an equimolar solution of Sb(V) and DL-malic acid in MilliQ	126
3.10	^1H NMR for a) 2% (w/v) mandelic acid and b) equimolar solution of Sb(V) and mandelic acid in MilliQ. Inset is structure	127

3.11	^{13}C NMR for a) 2% (w/v) mandelic acid and b) as a) ^{13}C DEPT experiment, and c) an equimolar solution of Sb(V) and mandelic acid in MilliQ	128
3.12	Separation of 5 mg l^{-1} Sb(V) and Sb(V)citrate. 10 mM KNO_3 eluent at pH3. Flow rate 1 ml min^{-1} . AS4A column. ICP-AES detection @217.581 nm	130
3.13	Injections of 5 mg l^{-1} Sb(V) in excesss DL-malic acid followed by an aliquot of Sb(V). 10 mM KNO_3 eluent at pH3. Flow rate 1 ml min^{-1} . AS4A column ICP-AES detection @217.581 nm	130
3.14	Chromatogram for three repeat injections of a 10 mg l^{-1} as Sb mixture of $[\text{Sb}(\text{OH})_6]$, $\text{Sb}(\text{OH})_x(\text{malate})_n$ and $\text{Sb}(\text{OH})_x(\text{citrate})_n$. 10 mM KNO_3 eluent at pH3. Flow rate 1 ml min^{-1} . AS4A column. ICP-AES detection @217.581 nm	132
3.15	Injection of 1:1 solution of Sb(V):citric acid. 20 mM NH_4Cl eluent at <pH 3. Flow rate 1 ml min^{-1} . AS4A column. ICP-AES detection @187.115 nm	134
3.16	Injection of 1:1 solution of Sb(V):citric acid. 20 mM NH_4Cl eluent at <pH3. Flow rate 1 ml min^{-1} . AS4A column. ICP-AES detection @193.026 nm	134
3.17	Chromatograms for Sb-citric acid system. a) Individual components; b) 1:1 ratio; c) 2:1 ratio; d) 3:1 ratio; and e) 1:2 ratio. Solid lines, Sb 204.957 nm; dashed lines, C 193.018nm	136
3.18	Injection of 1:1 solution of Sb(V):DL-malic acid. 20 mM NH_4Cl eluent at <pH3. Flow rate 1 ml min^{-1} . AS4A column. ICP-AES detection @187.115 nm	139

3.19	Injection of 1:1 solution of Sb(V):DL-malic acid. 20 mM NH ₄ Cl eluent at <pH3. Flow rate 1 ml min ⁻¹ . AS4A column. ICP-AES detection @193.026 nm	139
3.20	Chromatograms for C analysis @ 193.026 nm. a) 1:1 mandelic acid; b) 1:2 Sb:mandelic acid; c) 1:3 Sb:mandelic acid; and d) Sb:mandelic acid. 20 mM NH ₄ Cl eluent at <pH3. Flow rate 1 ml min ⁻¹ . AS4A column	143
3.21	Chromatograms for Sb analysis @ 187.115 nm. a) 2:1 Sb:mandelic acid; and b) 3:1 Sb:mandelic acid. 20 mM NH ₄ Cl eluent at <pH3. Flow rate 1 ml min ⁻¹ . AS4A column	144
3.22	Electrospray ionisation-mass spectra for solution of KSb(OH) ₆	146
3.23	Electrospray ionisation-mass spectra for solution of Sb with citric acid	147
3.24	Electrospray ionisation-mass spectra for solution of Sb with malic acid	149
3.25	Electrospray ionisation-mass spectra for solution of Sb with mandelic acid	150
3.26	Chromatograms obtained for injections of 250 µg l ⁻¹ Sb(V) with citric acid. 1) 5 mM H ₂ SO ₄ eluent; 2) 1 mM; and 3) 0.2 mM. Flow rate 0.35 ml min ⁻¹ . AS11-SC column	151
3.27	Chromatograms obtained for injections of 250 µg l ⁻¹ Sb(V) with 1)DL-malic acid; and 2) mandelic acid. 1 mM H ₂ SO ₄ eluent. Flow rate 0.35 ml min ⁻¹ . AS11-SC column	152
3.28	Chromatogram for injection of 250 µg l ⁻¹ Sb(V):α-hydroxyacid mixture. 1)DL-malic; 2)DL-malic; 3) mandelic; and 4) citric acid. 0.2 mM H ₂ SO ₄ eluent at 0.35 ml min ⁻¹ . AS11-SC column	154

3.29	Chromatograms for injection of 4×10^{-6} M Sb(V) added to 1.33×10^{-4} M mixture of α -hydroxyacids; and separate standards of $63 \mu\text{g l}^{-1}$ Sb(V) in each acid. 1) Uncomplexed Sb(V); 2) mandelic; 3) DL-malic; 4) DL-malic; 5) mandelic; and 6) citric acid. 0.2 mM H_2SO_4 eluent @ 0.35 ml min^{-1} . AS11-SC column.	155
------	--	-----

CHAPTER FOUR

4.1	Schematic diagram of the HPLC-ICP-AES system	168
4.2	Schematic diagram showing the coupling of hydride generation system to the ICP-AES	169
4.3	A map of the Wheal Emily antimony mine site showing the positions of the sampling points. A scale map is available, Ordnance Survey 1866 Edition, Devonshire Sheet 130.0	171
4.4	Chromatograms for the separation of Sb(V) from Sb(III) by HPLC-CD. a) 50 mg l^{-1} Sb(V); b) 50 mg l^{-1} Sb(III); and c) 25 mg l^{-1} mixed standard. Omnipac Pax-500 anion exchange column. 40 mM NaOH/5% MeOH mobile phase at 0.9 ml min^{-1} . 20 mN H_2SO_4 regenerant in anion micromembrane conductivity suppressor	174
4.5	Calibration data for Sb(V) and Sb(III) by HPLC-CD	175
4.6	a) Chromatogram for 10 mg l^{-1} Sb(V); & b) chromatogram for 10 mg l^{-1} Sb(III). Elution protocol as for conductivity detection. Omnipac PAX-500 column	176
4.7	Chromatogram showing the separation of Sb(V) and SbCl_3 . 5 mM phthalic acid/1% MeCN mobile phase at 1.0 ml min^{-1} ; pH 4.45. Omnipac PAX-500 column.	178

4.8	Chromatogram of Sb species at 10 mg l ⁻¹ . a) Sb(V); b) SbF ₃ and SbCl ₃ ; and c) potassium antimonyl tartrate. 10 mM phthalic acid mobile phase at 1.0 ml min ⁻¹ , pH 4.7. Ionpac AS4A column.	179
4.9	a) Effect of NO ₃ ⁻ concentration on retention time of Sb species. b) Effect of Cl ⁻ concentration on retention time of Sb(V).	181
4.10	Chromatogram showing two consecutive injections of 10 mg l ⁻¹ mixed species. a) Sb(V), antimonyl(III) tartrate and SbCl ₃ and Sb(V)citrate; and b) as a) but including Sb(III) with citric acid.	182
4.11	Separation of Sb(V);α-hydroxyacid complexes. 20 mM Cl ⁻ mobile phase at 1.0 ml min ⁻¹ , pH 3.	184
4.12	Wavelength scans for a) 10 mg l ⁻¹ SbCl ₃ solution; b) 0.5 mg l ⁻¹ SbCl ₃ with HG; and c) blank solution with HG	186
4.13	Calibration graphs for a) SbCl ₃ ; b) antimonyl tartrate; c) KSb(OH) ₆ without KI; & d) as c) with KI	187
4.14	Calibration graphs for a) TMSbBr ₂ without KI; and b) TMSbBr ₂ with KI	189
4.15	Wavelength scan for 1 mg l ⁻¹ TMSb by HG in the presence of citric acid	190
4.16	Chromatograms obtained for repeat injections of 20 µg l ⁻¹ Sb(V) and Sb(V)citrate mix with a) 20 mM NH ₄ NO ₃ mobile phase; and b) 20 mM KNO ₃ mobile phase at 1.0 ml min ⁻¹ , pH 3, AS4A anion exchange column	192
4.17	Chromatogram for 100 µg l ⁻¹ [Sb(OH) ₆] ⁻ and antimonyl(III) tartrate solution, 5 mM SO ₄ ²⁻ mobile phase at 0.35 ml min ⁻¹ , AS11 anion exchange column	195
4.18	Chromatograms for injections of standards and samples with and without citric acid	197
4.19	Chromatograms obtained from spoil heap runoff as the Sb formed the complex with the citric acid	198

4.20	Calibration set for separation of TMSb and Sb(V). 1 mM OH ⁻ mobile phase at 0.35 ml min ⁻¹ , AS11 column. Concentration set: 1, 5, 10, 20 and 40 µg l ⁻¹	200
4.21	Chromatograms illustrating the effect of H ₂ SO ₄ concentration on the elution profile of a 0.2 M acetic acid extract of a moss sample taken from the mine adit mouth	203
4.22	Chromatogram obtained from a sample of liverwort taken from the mine site. 0.5 mM H ₂ SO ₄ mobile phase at 0.35 ml min ⁻¹ . AS11 column	204
4.23	Chromatogram obtained from a sample of moss taken from the spoil heap. 0.5 mM H ₂ SO ₄ mobile phase at 0.35 ml min ⁻¹ . AS11 column	204
4.24	Chromatogram from the BCR reference material No. 61. <i>Platyhypnidium riparoides</i> (aquatic moss). 0.5 mM H ₂ SO ₄ mobile phase at 0.35 ml min ⁻¹ . AS11 column	205
4.25	Chromatogram obtained from the spoil heap sediment. 0.5 mM H ₂ SO ₄ mobile phase at 0.35 ml min ⁻¹ . AS11 column	205
4.26	Chromatogram obtained from the adit mouth sediment. 0.5 mM H ₂ SO ₄ mobile phase at 0.35 ml min ⁻¹ . AS11 column	206
4.27	Chromatogram obtained from the adit trail sediment in H ₂ O. 0.4 mM H ₂ SO ₄ mobile phase at 0.35 ml min ⁻¹ . AS11 column	206
4.28	Chromatogram obtained from the spoil heap sediment in H ₂ O. 0.4 mM H ₂ SO ₄ mobile phase at 0.35 ml min ⁻¹ . AS11 column	207
4.29	Chromatograms obtained from the adit mouth moss extracts with and without a Sb(V) spike. 0.4 mM H ₂ SO ₄ mobile phase at 0.35 ml min ⁻¹ . AS11 column	207

4.30	Chromatogram obtained from the spoil heap moss extracts with and without a Sb(V) spike. 0.4 mM H ₂ SO ₄ mobile phase at 0.35 ml min ⁻¹ . AS11 column	209
4.31	Chromatogram obtained for 10 µg l ⁻¹ Sb(V) in 0.2 M acetic acid. 0.4 mM H ₂ SO ₄ mobile phase at 0.35 ml min ⁻¹ . AS11 column	209
4.32	Chromatograms obtained from spoil heap sediment in 0.2 M acetic acid by HPLC-HG-ICP-MS with and without a pre-reductant. 0.4 mM H ₂ SO ₄ mobile phase at 0.35 ml min ⁻¹ . AS11 column	210
4.33	Chromatograms obtained from spoil heap moss in 0.2 M acetic acid by HPLC-HG-ICP-MS with and without a pre-reductant. 0.4 mM H ₂ SO ₄ mobile phase at 0.35 ml min ⁻¹ . AS11 column	211

CHAPTER FIVE

5.1	Parabolic flow of mobile phase through a tube	217
5.2	Schematic diagrams of nebulisers utilised in this study. a) concentric glass (MN); b) Burgener (BGN); c) de Galan (DGN); d) Ebdon type V-Groove (EUM); and e) modified V-groove (MOD)	219
5.3	Schematic diagrams of spray-chambers used in this study	222
5.4	Chromatograms obtained for the separation of Sb species using the nebulisers shown in Figure 5.2	226
5.5	Chromatograms obtained for the separation of the Sb species using the cyclonic and double pass spray-chambers	229
5.6	Chromatograms obtained for the separation of the Sb species using the cyclonic spray-chamber with the concentric glass and Burgener nebulisers	230

5.7	a) Chromatogram for 15% ethanol from ICI; & b) Chromatogram for repeat injections of 15% ethanol sample. 0.1 mM OH ⁻ mobile phase at 0.35 ml min ⁻¹	239
5.8	a) Chromatogram obtained for repeat injections of 3% acetic acid blank; & b) chromatogram for repeat injections of approx. 40 µg l ⁻¹ Sb in 3% acetic acid sample. (both samples obtained from ICI, Wilton)	240
5.9	a) Chromatogram obtained from 3% acetic acid blank (blue line) and 3% acetic acid sample (purple line); & b) Chromatograms for 15% ethanol blank (red line), and 15% ethanol sample (blue line). 5 mM SO ₄ ²⁻ mobile phase at 0.35 ml min ⁻¹	241
5.10	Chromatograms obtained for solutions of 3% acetic acid. 0.2 mM H ₂ SO ₄ mobile phase at 0.35 ml min ⁻¹	242
5.11	Chromatograms obtained for 15% ethanol and 95% ethanol samples from ICI. The 15% ethanol sample contains approximately 20 µg l ⁻¹ Sb. 0.4 mM H ₂ SO ₄ mobile phase at 0.35 ml min ⁻¹	243
5.12	Chromatograms obtained for a) 3% acetic acid extract of poly(ethylene terephthalate), PET, from a coke bottle; and b) 3% acetic acid extract of PET from a sprite bottle. 0.4 mM H ₂ SO ₄ mobile phase at 0.35 ml min ⁻¹ .	245
5.13	Aliquots of continuously nebulised solutions of 3% acetic acid, Sprite bottle and coke bottle extract	246
5.14	Wavelength scans 217.550 to 217.613 nm for a) 15% ethanol; b) approx. 20 µg l ⁻¹ Sb in 15% ethanol sample; c) as b) but with citric acid; d) approx. 40 µg l ⁻¹ Sb in 3% acetic acid sample; & e) as d) with citric acid. Analysis by HG-ICP-AES. 2 M acetic acid carrier, 1% NaBH ₄ reductant	248

ACKNOWLEDGEMENTS

I would first of all like to thank my Director of Study Professor Steve Hill for guiding me through the last three years and forgiving my occasional leaps of faith. I thank Professor Hill for giving me the perfect excuse to go to the Departmental Office.

I am very grateful to Dr Phil Jones for his support and help with much of the separation science.

I would particularly like to thank the Engineering and Physical Sciences Research Council for financial support throughout this project and ICI Technology for the provision of a CASE award. Special thanks go to Prof. John Marshall and Dr. Jeff Franks at ICI in Wilton for their guidance, ideas and time when I worked at their laboratory.

The technical support I have received at the University of Plymouth has been second to none, so I must mention Ian even if we did get crossed wires early on, Dr. Roger Evens for his NMR expertise, Andy and Andrew, Roger Bowers for some great glasswork and last but not least Rob Harvey, without whom many a great ICP project would be lost.

Dr. Andy Fisher, Dr. Cristina Rivas and Dr. Kathryn Lamble got me started on the ICP's and deserve thanks, and Andy kept me going on ICP's even in a few of the darker moments. Others who have helped me out with individual moments have been Dr. Gavin O'Connor and Dr. Simon Belt, for there invaluable work with organic analysis.

Anyone I have left out from Davy I'm sorry but the thesis is long enough. However, I will thank Simon Neville and Simon Coles for always being willing to have a chat and a drink!! whatever the stress levels and.

My Mother and Pat deserve enormous thanks, I will be forever grateful for your support through my time at University. You have always been there when I most needed you and I couldn't have done any of this without you.

Finally I wish to thank Kathryn, my Wife. I have been enormously lucky to have had you during this time. You have been a tower of strength just by allowing me the space to get on with it, and you have pushed me when I needed it. Mind you, you know I'll most likely repay your effort thrice over. I hope your investment in me has paid off.

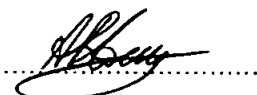
Authors Declaration

At no time during the registration of the degree of Doctor of Philosophy has the author been registered for any other university award.

This study was financed by a CASE studentship from the Engineering and Physical Sciences Research Council in collaboration with ICI Technology, Wilton, Middlesborough, Teeside.

Relevant Scientific seminars and conferences were regularly attended at which work was often presented; external institutions were visited for consultation purposes and several papers prepared for publication.

Signed



Date

17th May 1999

Chapter One. Chemistry of Antimony, Literature Review and Aims and Objectives of the Study

1.1 Introduction

The following sections serve as an introduction to this thesis by providing a short treatise of antimony (Sb) chemistry as given in established and recent research literature.

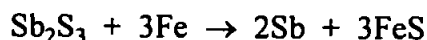
This will be followed by a literature review covering total Sb analysis and Sb speciation. Finally, the aims and objectives of the study will be described.

1.2 The Chemistry and Uses of Antimony

Antimony, Sb, is in Group V of the Periodic Table with the electronic structure $[\text{Kr}]4d^{10}5s^25p^3$. Sb is the 64th most abundant element in the Earth's crust, by weight, at 0.20 ppm. The most important oxidation states of Sb are (V) and (III). Although there are many isotopes of Sb the most abundant natural isotopes of Sb are ^{121}Sb (57.25%) and ^{123}Sb (42.75%). The atomic mass of Sb is 121.75 amu.

1.2.1 Elemental Antimony

Antimony sulphide, Sb_2S_3 , otherwise known as stibnite is the most important ore of Sb and metallic Sb can be obtained from fusing with iron:



Antimony is a blue-white lustrous metal with a melting point of 630°C and a boiling point of 1640°C.

The applications for elemental Sb are mainly in alloys such as with lead for storage batteries, bearings, ammunition, solder, type metal and sheet pipe. Alloys of Sb with Al, Ga and In have also been used in infra-red devices and diodes⁽¹⁾.

Antimony is stable to air and moisture at room temperature and oxidises on being heated to give Sb_2O_3 , Sb_2O_4 or Sb_2O_5 . It reacts vigorously with Cl_2 but less so with Br_2 and I_2 to give SbX_3 , the trihalides. It will also combine with sulphur on heating. It will not react directly with H_2 but will form a hydride (reaction discussed later) that is both very poisonous and very unstable thermally. Sb is unaffected by dilute acid but reacts readily with oxidising acids; HNO_3 gives hydrated Sb_2O_5 , aqua regia gives a solution of SbCl_5 , and hot H_2SO_4 will give a $\text{Sb}_2(\text{SO}_4)_3$ salt.

Sb will form many intermetallic compounds but with the large range of stoichiometries and the complexity of the structures classification is difficult and such compounds bear no relation to this study.

1.2.2 The Hydride, Stibine, SbH_3 .

Antimony hydride, SbH_3 , or stibine is a very poisonous, thermally unstable colourless gas. The properties of stibine are given in Table 1.1 and are compared with those of arsine, AsH_3 .

Table 1.1 Properties of stibine and arsine.

Property	SbH_3	AsH_3
Melting point / °C	-88	-116.3
Boiling point / °C	-18.4	-62.4
Density / g cm ⁻³ (T °C)	2.204(-18)	1.640(-64)
ΔH_f° / kJ mol ⁻¹	145.1	66.4
M-H distance / pm	170.7	151.9
H-M-H angle	91.3°	91.8°

SbH₃ will steadily decompose at room temperature. The reaction to produce stibine will be directly discussed in Chapter 2.

1.2.3 Trivalent Antimony

The general chemistry of Sb(III) is extensive and varied and can be found in many general chemistry texts⁽¹⁻⁵⁾. Exhaustive detail is not required for this study but short examples of typical reactions will be given.

1.2.3.1 Trihalides, SbX₃

Antimony will form trihalides with F, Cl, Br and I. The physical properties of the trihalides are given in Table 1.2

Table 1.2 Properties of Sb trihalides

Compound	Appearance	Melting point / °C	Boiling point / °C	ΔH_f° / kJ mol ⁻¹
SbF ₃	Colourless crystal	290	~345	-915.3
SbCl ₃	White	73.4	223	-382.2
SbBr ₃	White	96	288	-259.4
SbI ₃	Red crystal	170.5	401	-100.4

The trifluoride can be prepared by the action of HF on Sb₂O₃, whereas the trichloride, tribromide and triiodide can be prepared by direct reaction of the respective halide with Sb or Sb₂O₃. SbF₃ is relatively soluble in water but SbCl₃ will hydrolyse to the insoluble oxychloride, SbOCl. Table 1.3 gives examples of uses for some of the trihalides.

Table 1.3 Examples of applications for antimony trihalides

Trihalide	Application
SbF ₃	Prep ⁿ of organofluorines (Swarts Reaction) ; $R_3PS + SbF_3 \rightarrow R_3PF_2$
SbCl ₃	Non-aqueous solvent, $\eta = 2.58$ at 75 °C and $\epsilon = 33.2$. For Cl ⁻ transfer.
SbCl ₃	Prep ⁿ of antimonate esters ; $SbCl_3 + 3Bu^iOH + 3NH_3 \rightarrow Sb(OBu^i)_3 + 3NH_4Cl$

η is viscosity
 ϵ is dielectric constant
BuⁱOH is butanol
Prepⁿ is preparation

1.2.3.2 Antimony Oxides

Antimony trioxide, Sb₂O₃, can be obtained by the roasting of sulphide ores such as ZnS or Sb₂S₃ in air. The zinc ore like many metal ores will have some level of antimony associated with it. Hence the early derivation of antimony from *antimonos*, Greek meaning anti-loneliness, i.e. this metal was frequently found in the ores of other metals. Sb₂O₃ is the most important compound of Sb with applications mainly in polymer production either as a fire retardent or as a catalyst. This compound has also seen use as a fire retardent in fabrics, paper, paint, epoxy resins and adhesives.

Sb₂O₃ has a very limited solubility in pure water and the main species in solution will probably be the poorly characterised antimonious acid, H₃SbO₃. Though, it has been surmised that depending upon the pH of the solution it could also exist as SbO₂⁻ or Sb(OH)₃.

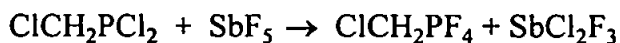
1.2.3.3 Antimony Sulphides

The sulphide, Sb₂S₃, occurs as the mineral ore stibnite and has been applied to the manufacture of safety matches, ammunition and explosives. The sulphides have flame retardent properties and have been used in plastics for a dual role of pigment and flame-retardent.

1.2.4 Pentavalent Antimony

1.2.4.1 Halides, SbX_5 and $[\text{SbX}_6]^-$

The pentafluoride can be prepared by direct reaction of F_2 with the oxide, Sb_2O_3 . The pentachloride, SbCl_5 , is made by the reaction of Cl_2 with SbCl_3 , and is a trigonal bipyramid molecule. SbF_5 is a very viscous liquid with polymeric chains of bridged (SbF_6) octahedra, Figure 1.1. SbF_5 is a powerful fluorinating agent.



If SbCl_5 is added to SbF_5 the viscosity of the pentafluoride decreases because the Sb-F-Sb linkage is broken. The electrical conductivity increases and the mixed halide becomes an even more powerful fluorinating agent than SbF_3 .

Halide complexes of Sb(V) are well known and are made by the direct reaction of the pentahalide with the appropriate ligand. Salts of $[\text{SbF}_6]^-$, $[\text{SbCl}_6]^-$ and $[\text{Sb}(\text{OH})_6]^-$ have octahedral geometry. Complexes are also formed by a variety of oxygen donors, e.g. $[\text{SbCl}_5(\text{OPCl}_3)]$ and $[\text{SbF}_5(\text{OSO})]$, Figure 1.2.

1.2.4.2 Antimony Oxides

Antimony(V) oxide has been formed by the hydrolysis of SbCl_5 with aqueous ammonia followed by dehydration at 275 °C.

1.2.5 The Coordination Chemistry of Antimony

The coordination chemistry of Sb is too extensive to overview in a brief review, however Table 1.4 gives a general summary of the classes of organometallic coordination

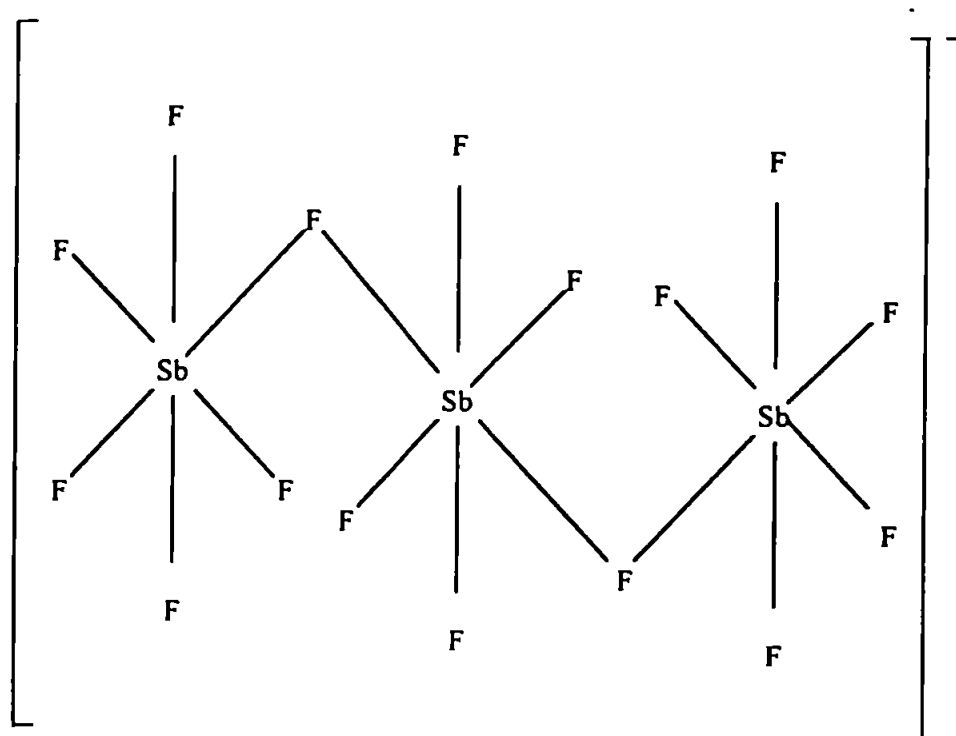


Figure 1.1 Structure of SbF_6 bridged octahedra polymeric chain

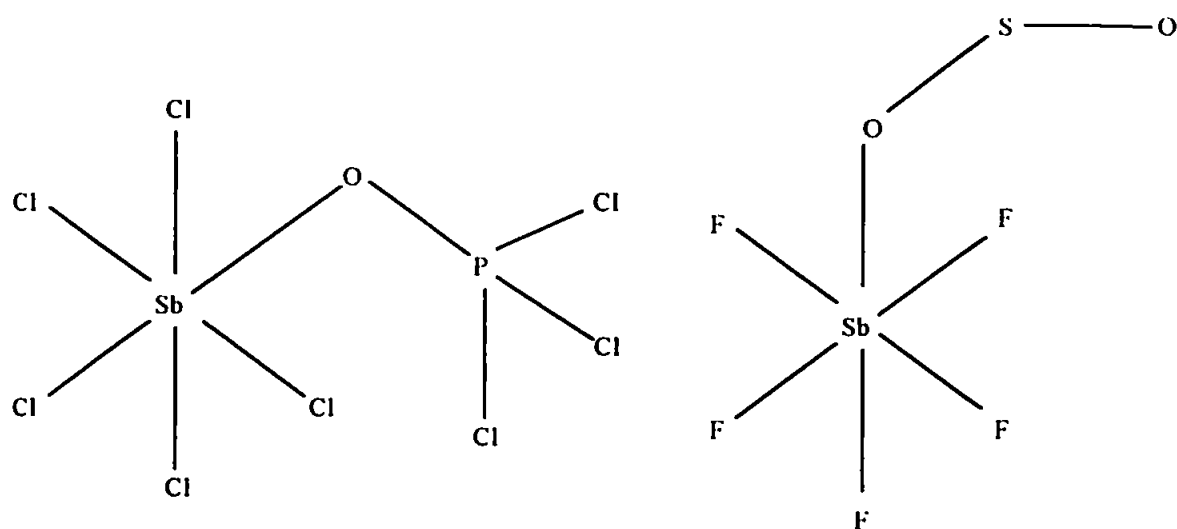


Figure 1.2 Structural representation of $[\text{SbCl}_5(\text{OPCl}_3)]$ and $[\text{SbF}_5(\text{OSO})]$

compounds of Sb and their applications. The bond types given in this table are Sb-C, Sb-O, Sb-S and Sb-N.

In the opinion of the author the most interesting reactions involve the Schiff's base complexes of urea and thiourea⁽¹⁴⁾, and the citrate complexes^(24,25). Both of these are with Sb(III) species although complexes of Sb(V) have been described with dicarboxylic acids⁽²³⁾. The Schiff's base complexes are interesting because of the biological implications of Sb complexation in such matrices, although they will not be discussed here. Two important papers in relation to this study have been published by Smith *et al.*^(26,27). In the first the authors refer to earlier work^(24,25) and state that α -hydroxy oxygens bond with Sb, 'the observation is that deprotonation of the α -hydroxy group occurs at quite low pH (ca 1.5) due to lowering of its effective pKa after initial coordination of the adjacent carboxyl group'. Thus an intermediate where only the carboxylate oxygen is coordinated must exist. Smith and Kennard⁽²⁷⁾ also prepared and Sb(III) complex with hydroxyacetic acid $(\text{NH}_4)[\text{Sb}(\text{C}_2\text{H}_2\text{O}_3)_2]$. This was an anionic monomer species, the first of its type.

The use of Sb(III) is most often referenced with limited reference to Sb(V) compounds and in particular there is limited information available for Sb(V) oxoanion complexes.

What these two references and those in Table 1.4 show is that given the right circumstances i.e. anaerobic, reducing conditions and the environmental functionalities in, for example, humic substances that may complex with Sb, it is conceivable that in trace concentrations such complexes, as have been described here, may form.

Table 1.4 Summary of organometallic chemistry literature for Sb complexes of Sb(V) and Sb(III)

Sb(V)/(III)	Complex Formulae/Structure	Reaction	Application	Reference
(III)	$\text{SbCl}_3(\text{MeNHCOCOONHMe})$ Bond : Sb-O	Direct addition of SbCl_3 and $\text{N,N}'$ -dimethyloxamide. Benzene solutions, N_2 atmosphere	Formation of 6 coordinate Sb(III) complex. O,O bonding leading to four membered $\text{Sb}(\mu\text{-O})_2$ ring.	6
(III)	$[\text{H}_2\text{L}]^{2+}[\text{Sb}_2\text{OCl}_6]^{2-}$ L=1,4,8,11-tetramethyl-1,4,8,11-tetraazacyclotetradecane Bond : Sb-O	Under N_2 , SbCl_3 added to solution of L and water.		7
(V)/(III)	Ph_3SbI_2 and $[\text{Ph}_4\text{Sb}]\text{I}_3$ Bond : Sb-C	Anaerobic reaction of tertiary stibine with dihalogen in diethyl ether. Ionisation, dissolution in acetonitrile for 3 d.	Investigation of Ph_3SbX_2 structure and ionisation products. Ph_3SbI_2 has a distorted trigonal-bipyramid structure.	8
(V)/(III)	$\text{MeC}_6\text{H}_4\text{SbX}_2$ (X = Cl, Br) Ph_2SbBr (biphenyl-2,2'-diyl) SbCl . Bis(2-chlorobiphenyl-2-yl) SbCl_3 Bond :Sb-C	Too complex for this discussion.	Sb(V) unusual in that it is monomeric and Cl is in both axial and equatorial sites.	9

Table 1.4 Continued

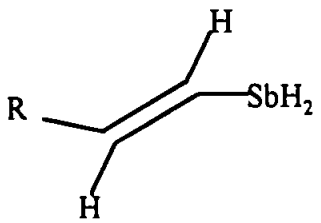
Sb(V)/(III)	Complex Formulae/Structure	Reaction	Application	Reference
(III)	 <p>Where R = H, Me</p>	SbCl ₃ + vinyltributylstannane in N ₂ atmosphere. Chlorostibine reduced to vinylstibine with tributylstannane.	Considering synthesis of potential precursors for stibalkenes or -alkynes.	10
(V)/(III)	Sb(III) phthalocyanine and [Phthalocyanine)Sb(OH) ₂] ⁺	Free base phthalocyanine & SbF ₃ cautiously heated. Extracted with methanol. Sb(V) derivative obtained by treatment of reaction mixture with H ₂ O and acetone extraction.	Investigation of spectral properties. Sb(V) derivative exhibited luminescence at 420 nm upon UV excitation. No observed emission for Sb(III) derivative.	11
(V)/(III)	SbCl ₃ .2R'COCHC(NHR)Me & SbCl ₃ .MECOCHC(NHR)Me (R' = Me, Ph; R = Me, Et, i-Pr)	<p>β-ketoamine in benzene added to solution of SbCl₃ dropwise at ~ 15° C. Stirred for 4 h and filtered.</p> <p>β-ketoamine in chloroform added dropwise to SbCl₃ and stirred for 8 h. Oily product separated by decantation.</p>	<p>IR spectra of Sb adducts with β-ketoamines suggested coordination through N atom. Adducts insoluble in polar solvents.</p> <p>Sb(III) adduct - square pyramidal Sb(V) adduct - octahedral</p>	12

Table 1.4 Continued

Sb(V)/(III)	Complex Formulae/Structure	Reaction	Application	Reference
(III)	$\text{SbCl}_{3-n}(\text{L})_n$ L = $\text{RC}(\text{O})\text{CH}_2\text{C}(\text{CH}_3):\text{NCH}_2\text{C}(\text{O})\text{O}$; (R = Ph, Me; n = 1,2,3) Bond : Sb-O	$\text{SbCl}_3 + n\text{LK} \rightarrow \text{SbCl}_{3-n}(\text{L})_n + n\text{KCL}_{(s)}$ (In dry methanol)	IR spectra suggests unidentate behaviour of COO^- group. Insolubility suggests polymeric species.	13
(III)	Schiff's base complexes with Sb(III)	Amine, amide, urea or thiourea with salicylaldehyde in chloroform. Warm chloroform solution of SbCl_3 added slowly with shaking. 45°C for 2-3 h. Solids filtered & recrystallised from hot THF.	IR spectra evidence for Sb-O and Sb-N coordination.	14
(III)	$\text{SbPh}_2(\text{S}_2\text{PR}_2)$ R = Me, Et & Ph. Bond : Sb-S	Example. $(\text{SbPh}_2\text{OBr})_2 + 2\text{Na}(\text{S}_2\text{PMe}_2) \cdot 2\text{H}_2\text{O} \rightarrow$ $\text{SbPh}_2(\text{S}_2\text{PMe}_2) + \text{SbPh}_2(\text{O}_2\text{PMe}_2) +$ $2\text{NaBr} + 2\text{S} + 4\text{H}_2\text{O}$ Benzene solvent refluxed for 2 h.	Diphenylantimony(V) reduced by dithiophosphinate. The Sb(III) dithiophosphinates are weakly associated dimers where R = Me and intermediate for R = Ph and Et.	15

Table 1.4 Continued

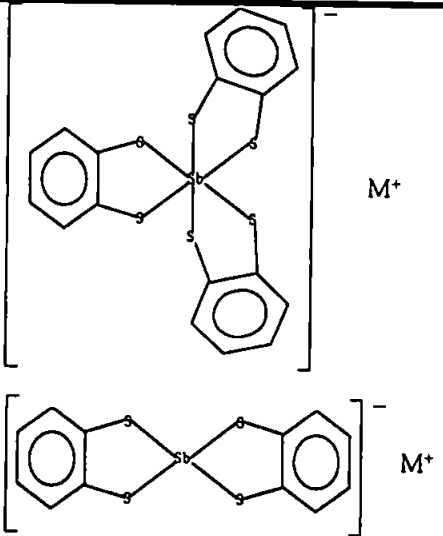
Sb(V)/(III)	Complex Formulae/Structure	Reaction	Application	Reference
(V)/(III)	 <p>The first structure shows a central antimony atom (Sb) coordinated to two phenyl rings and two sulfur atoms, which are part of a 1,2-dithiolene group. The second structure shows a central antimony atom (Sb) coordinated to two phenyl rings and two sulfur atoms, which are part of a 1,2-dithiolene group.</p>	<p>Anaerobic treatment of SbCl_3 with 1,2-$(\text{LiS})_2\text{C}_6\text{H}_4$ for $[\text{Sb}(1,2\text{-S}_2\text{C}_6\text{H}_4\text{O}_2)]^-$ & on reaction with 1,2-$(\text{HS})_2\text{C}_6\text{H}_4 + \text{O}_2$ yields $[\text{Sb}(1,2\text{-S}_2\text{C}_6\text{H}_4)_3]^-$.</p>	<p>Sb(III) ψ-trigonal-bipyramidal distorted by lone electron pair. Sb(V) is slightly distorted octahedral</p>	16
(V)	<p>$\{\text{SbPh}_2\text{Cl}[\text{O}_2\text{P}(\text{C}_6\text{H}_{11})_2]\}\text{O}$ & $[\text{SbPh}_2(\text{O}_2\text{CPh})_2]_2\text{O}$. Bond : Sb-O</p>	<p>$2\text{SbPh}_2\text{Cl}_3 + 2\text{AgO}_2\text{P}(\text{C}_6\text{H}_{11})_2 \rightarrow$ $\{\text{SbPh}_2\text{Cl}[\text{O}_2\text{P}(\text{C}_6\text{H}_{11})_2]\}\text{O} + 2\text{AgCl}$ $2\text{SbPh}_2\text{Cl}_3 + 6\text{AgO}_2\text{CR} \rightarrow$ $[\text{SbPh}_2(\text{O}_2\text{CR})_2\text{O}] + 2\text{RCO}_2\text{H} + 6\text{AgCl}$. $\text{R} = \text{Ph}, \text{CHPh}_2, 2,4,6\text{-Me}_3\text{C}_6\text{H}_2, 2\text{-MeC}_6\text{H}_4, 4\text{-MeC}_6\text{H}_4$.</p>	<p>Oxo-bridged dimers (Nearly linear Sb-O-Sb at 173.9°). Phosphinates are octahedral Carboxylates are pentagonal bipyramidal.</p>	17

Table 1.4 Continued

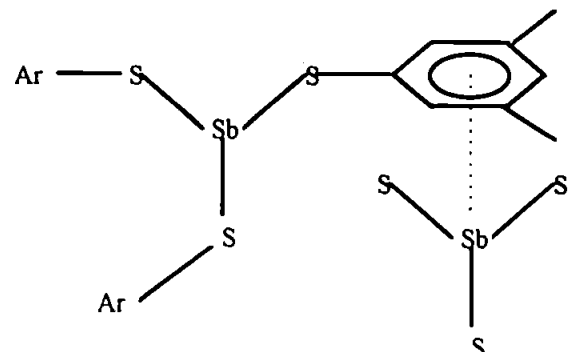
Sb(V)/(III)	Complex Formulae/Structure	Reaction	Application	Reference
(III)	$\text{Sb}(\text{SR})_3$ $\text{R} = 4\text{-MeC}_6\text{H}_4, 3,5\text{-Me}_2\text{C}_6\text{H}_3$	Under dry N_2 conditions $\text{Na}[\text{SC}_6\text{H}_3\text{Me}_2-3,5]$ or $(\text{HSC}_6\text{H}_4\text{Me}-4)$ in THF added to SbCl_3 . Stirred for 1 h. Crude product dissolved in Et_2O & filtered. Solvent diffused with hexane	<p>These thiolates showed trigonal bipyramid Sb centre for both complexes. Additional $\text{Sb}^{\cdots}\text{S}$ interactions and $\text{Sb}^{\cdots}\text{arene}$ ring interactions for 3,5-$\text{Me}_2\text{C}_6\text{H}_3$ complex.</p> 	18
(V)	$\text{R}_3\text{Sb}(\text{O}_2\text{PR}')_2$ & $\text{R}_3\text{Sb}(\text{OH})(\text{O}_2\text{PR}'_2)$ R and $\text{R}' = \text{Me}, \text{Ph}$ Bond : Sb-O	$\text{R} \ \& \ \text{R}' = \text{Me} : \text{R}_3\text{SbCl}_2 + \text{R}'_2\text{PO}_2\text{Na}$ in CH_3CN stirred for 2h under reflux. $\text{R}, \text{Me} \ \& \ \text{R}', \text{Ph} : 2\text{h}$ reflux in MeOH $\text{R}, \text{Ph} \ \& \ \text{R}', \text{Me} : 4\text{h}$ reflux in CH_3CN $\text{R} \ \& \ \text{R}' = \text{Ph} : 2\text{h}$ reflux in MeOH	<p>Trimethylderivatives soluble in H_2O. When $\text{R}' = \text{Ph}$, if moisture is not excluded one phosphinato hydrolytically transforms to an OH forming $\text{Me}_3\text{Sb}(\text{OH})[\text{O}_2\text{PPh}_2]$.</p> <p>Trigonal bipyramidal structure. There is chain polymerisation through H-bonding.</p>	19

Table 1.4 Continued

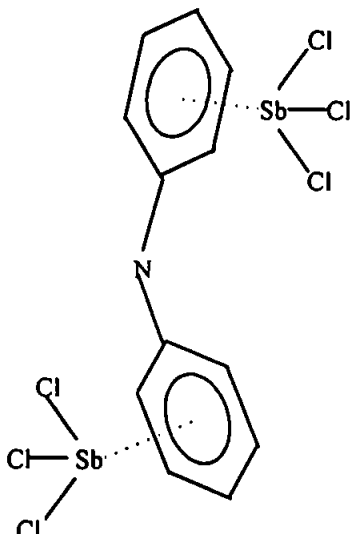
Sb(V)/(III)	Complex Formulae/Structure	Reaction	Application	Reference
(III)	$\text{Ph}_2\text{SbS}_2\text{PPh}_2$ & $\text{Ph}_2\text{SbS}_2\text{P}(\text{OPr}^1)_2$ Bond : Sb-S and Sb-C	DiphenylSb(III) acetate & diphenyldithiophosphinic acid in acetone. Direct reaction. DiphenylSb(III) acetate & ammonium diisopropyldithiophosphate. Direct reaction.	Solid state structure not determined. These compounds have exhibited antineoplastic properties against Ehrlich ascite tumor cells when injected intraperitoneal (i.p.) 1st organoSb(III) compound with antitumour properties.	20
(III)	$(\text{C}_6\text{H}_5)_2\text{NH} \cdot 2\text{SbCl}_3$ 	Components sealed in ampoules under vacuum, heated to melting in oil bath and violently stirred.	There are Sb interactions with π electrons of aromatic rings, but, coordination and dipole-dipole interactions are more important than Sb-hydrocarbon interaction in the structure formation of lattice cell.	21

Table 1.4 Continued

Sb(V)/(III)	Complex Formulae/Structure	Reaction	Application	Reference
(III)	2SbCl ₃ .C ₆ H ₆ , 2SbCl ₃ .1,1'-(C ₆ H ₅) ₂ and 2SbCl ₃ .phenanthrene	As Ref. 21	Study of molecular dynamics	22
(V)	Ph ₄ SbOC(O)-R-OC(O)SbPh ₄ R = maleic, tartaric & adipic acids Bond : Sb-O	1:1 or 2:1 mole ratios of Ph ₅ Sb & dicarboxylic acid in toluene or dioxane. Either left at room temperature for 24 h. or heated at 60° for between 15 min. and 1 h. then left to stand for 12 h. at room temperature. Recrystallised from benzene-isopropyl alcohol (4:1)	Trigonal bipyramidal geometry about Sb centre. Sb-O bond not considered ionic as coordination polyhedron of Sb corresponded to d ² sp ² hybridisation.	23
(III)	[Sb ₂ Ag ₂ (C ₆ H ₆ O ₇) ₄] & [SbNa(C ₆ H ₆ O ₇) ₂].H ₂ O	Digestion of Sb ₂ O ₃ with aqueous citric acid at 90° C. Aqueous silver or sodium nitrate added to filtrate. Colourless crystals formed in several days.	The citrate ligand is dianionic. SbAg complex is a discrete dimeric unit. SbNa complex is a monomeric compound. O-Sb-O bonding via carboxylate and α-hydroxyl oxygens	24
(III)	CuSb(C ₆ H ₆ O ₇ ²⁻)(C ₆ H ₅ O ₇ ³⁻)(H ₂ O) ₂ .2½H ₂ O	As Ref. 24 but with addition of copper nitrate.	Pseudo trigonal bipyramidal stereochemistry. Terminal carboxylate in citrato(3-) ligand bonds with Cu and provides cross link to the polymer chain.	25

1.2.6 Applications of Antimony

1.2.6.1 Historical Uses and Background

Antimony, like arsenic, was known to the ancients with examples of Sb laden pottery dating from 4000 BC and antimony coated copper items used in Egypt ca. 2500 BC. The name stibium was given by Pliny, AD 50, and the name antimonium appeared in AD 80. The ancient Egyptians also made extensive use of antimony pigments for make-up such as the red antimony compound *kermesite* for lip-reddening and *buornonite*, a black antimony pigment, for eye make-up. Pliny prescribed stibium as a pharmaceutical agent, as well as describing its cosmetic uses, for the treatment of eye disease⁽²⁸⁾.

However, Sb compounds are still used in the Middle and Far Eastern countries as kohl, a therapeutic concoction used as eye make-up. Pure kohl contains antimony sulphide and trisulphide as its main constituents⁽²⁹⁾. It has folk remedy status in these countries owing to a 'strong traditional belief that kohl has a curative effect on the treatment of eye diseases'⁽³⁰⁾. However, the literature^(29,30) reports that although Sb is the traditional constituent, lead based kohl formulations are more likely to be found nowadays.

1.2.6.2 Industrial Applications of Antimony

The use of Sb metal in the formulation of alloys has already been mentioned. Antimony has the property of imparting hardness and mechanical strength on metal products, indeed the use of Sb for plates in lead/acid batteries, cable sheathing, anti-friction bearings and type metal accounted for nearly half of all Sb metal produced in the 1980's⁽³¹⁾.

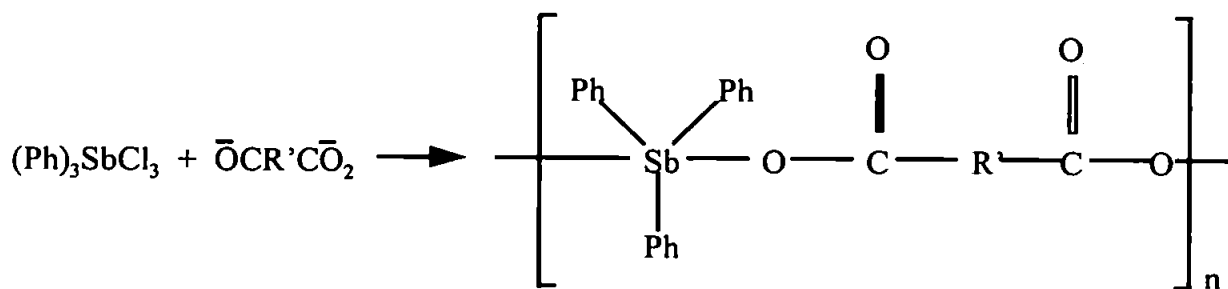
Antimony is also used in ceramics and primers, fireworks, pigments, ammunition and ammunition primers. In a study of firearms instructors in the Chicago Police dept., blood Sb levels were found to be as high as $130 \mu\text{g l}^{-1}$. From the data presented the average level was $33.75 \mu\text{g l}^{-1}$. Levels of blood Sb in unexposed populations were found to be $10 \mu\text{g}$

1⁻¹ or less⁽³²⁾. Analysis of Sb as well as other metals, Pb, Ba, Cu, Zn and Fe, in human tissue and clothing, has helped in the interpretation of events surrounding gunshot incidents⁽³³⁾.

Sb is used in plastics and rubber products as either a catalyst or as a flame retardent in adhesives, paper, pigments, textiles, plastics and rubber.

Antimony trioxide, Sb₂O₃, has been used as a catalyst in polymer production since at least 1946 when Whinfield and Dickson patented the polymer, poly(ethylene terephthalate), PET⁽³⁴⁾. Examples of Sb(V) catalysis are available especially the use of pentavalent organoantimony as a catalyst for the production of oxiranes such as ethylene oxide⁽³⁵⁾. As an additive for flame retardent application Sb₂O₃ is the most popular compound⁽³⁶⁾ and is typically used in flexible PVC⁽³⁷⁾ and epoxides⁽³⁶⁾. Organoantimony compounds such as (Ph)₃SbBr₂ and derivatives of triphenylantimony(V) with tribromo-, trichloro- and pentachlorophenols as well as antimony trichloride have also been utilised for flame retardent functions^(36, 38-40). They may also be used as polymeric flame retardents. They would differ from Sb₂O₃ flame retardents as the Sb would be locked in the polymer backbone chain or in the groups connected to the polymer. This would be achieved by σ or π bonds to carbon, coordination bonds to elements containing free electron pairs or, less commonly, by σ or π bonds to other elements⁽⁴²⁾.

The synthesis of an Sb polyester could be shown as :



where R'(CO₂H)₂ = terephthalic acid, oxalic acid, fumaric, dimethyl and 1,1'-ferrocenedicarboxylic acid⁽⁴⁸⁾.

1.2.6.3. Medical Applications for Sb

The medicinal use of kohl has already been mentioned, but antimonial compounds generally have been used throughout history in physiological or medicinal applications.

Probably the most well known Sb prescription is the 'tartar emetic', potassium antimonyl(III) tartrate. Figure 1.3 gives a representation of this compound. The action of Sb as an emetic was known to the Romans who would drink wine from a goblet rich in Sb. These *calices vomitorium* provoked vomiting following a feast. The emetic action is caused by the irritant action on the gastric mucosa. Paracelsus prescribed Sb preparations in the 16th century and one of his disciples was probably the first to synthesise tartar emetic⁽⁴³⁾. Potassium antimonyl(III) tartrate has also been used in the treatment of tropical parasitic diseases such as schistosomiasis, bilharzia, leishmaniasis and trypanosomiasis⁽⁴⁴⁻⁴⁷⁾. Also, Sb containing polymers have been described for use as biomaterials in therapeutic agents against tropical parasitic diseases as well as antibacterial additives and fungicides⁽⁴⁸⁾. Other compounds of Sb used in the treatment of these diseases include stibophen and astiban, both of which are shown in Figure 1.3.

The therapeutic action of these compounds can also be responsible for toxic effects, namely the combining with sulphydryl groups of cellular constituents and enzymes, thus blocking their activity. The toxic implications of Sb are discussed later in section 1.2.7.

Other areas of medical application have been in the treatment of AIDS where the compound ammonium-5-tungsto-2-antimoniate has been demonstrated to inhibit reverse transcriptase⁽⁴⁹⁾ and in antitumour compounds⁽⁴³⁾.

1.2.6.4 Abstraction of Antimony

The most important ore of Sb is stibnite, Sb_2S_3 . Worldwide production of Sb in 1989 was approximately 68,000 metric tons, not including that produced in the U.S.⁽³¹⁾. However, as much as 50% of this figure is released to the environment as a result of human activity

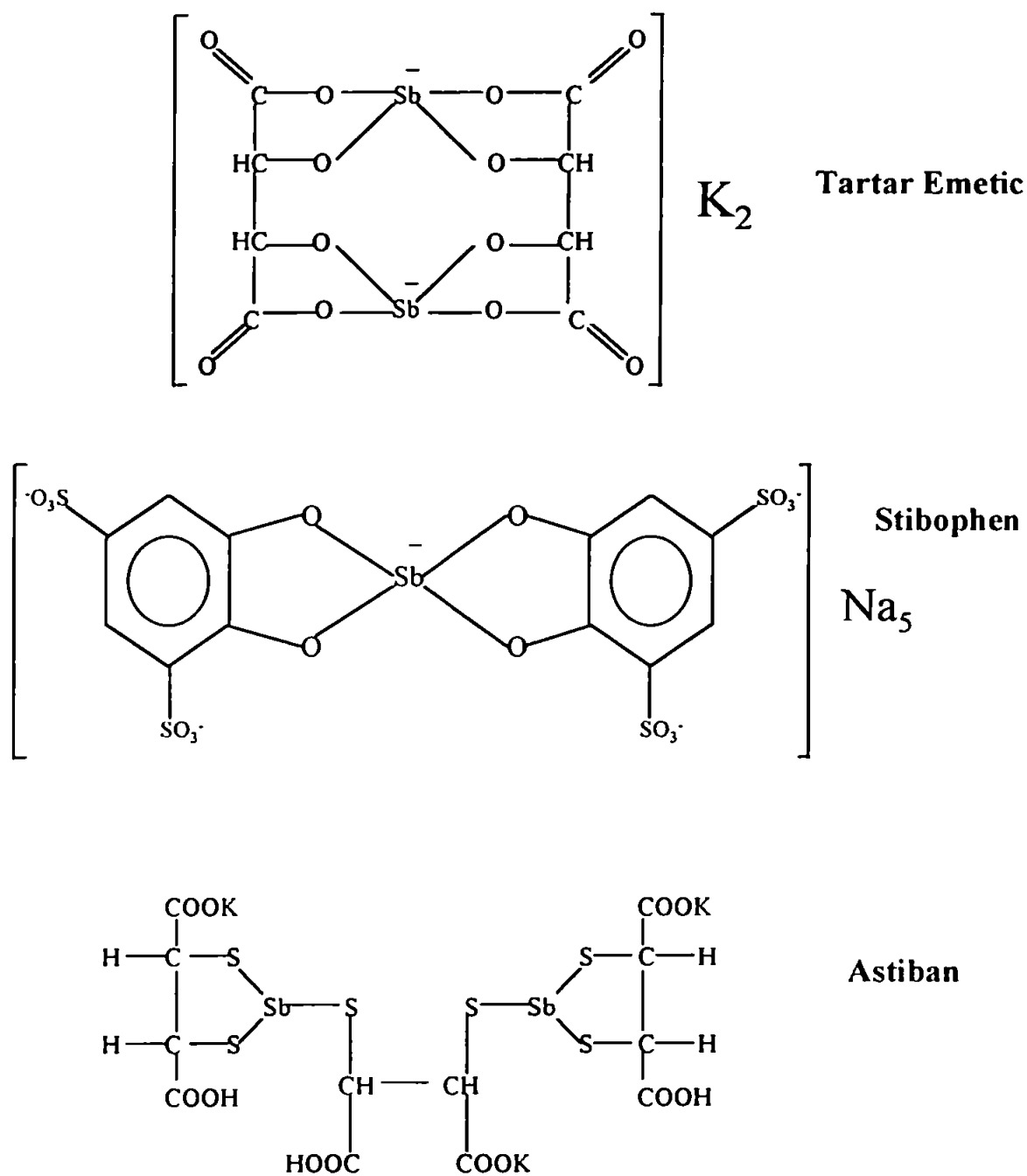


Figure 1.3 Structural representations of tartar emetic, Stibophen and Astiban

such as energy production, mining (waste), smelting and refining, and waste incineration.

The combustion of coal alone releases 10000 tonnes Sb y^{-1} to the atmosphere.

There has been a history of Sb production in South West England. In fact >300 tonnes of Sb ores were produced but mostly ca. 18th C or earlier⁽⁵⁰⁾. The ores in S.W. England mostly comprised of Sb₂S₃ or were associated with Pb (jamesonite), Cu (buromonite) or Ag⁽⁵¹⁾. The main commercial production was on the North Coast of Cornwall around Wadebridge, and in an area S.E. of Callington and Tavistock district^(51,52). Dines⁽⁵²⁾ and a report from 1922 by Toll and Barclay⁽⁵³⁾ name a small mine called Wheal Emily, 4 miles S by E of Plympton, South Devon as a source of Sb ore with one shaft and two adits. While the British Geological Survey have reported the South Hams district as being anomalously rich in Sb⁽⁵⁴⁾.

As such, like arsenic, there is an antimony mining legacy in Devon and Cornwall but unlike As, it has remained relatively uninvestigated.

1.2.7 Toxicology of Sb

Antimony is considered a non-essential element⁽⁵⁵⁾. However, as the feasting Romans have shown, the toxic effects of Sb have been well known for centuries. The Faculty of Physicians at the University of Paris even prohibited the medicinal use of Sb until a hundred years after this decision, in 1657, Louis XIV of France appeared to be cured of typhoid with a prescription of Sb.

In 1997 Gebel⁽⁵⁶⁾ stated that although Sb is an environmental contaminant, because it is not widely distributed in the environment, too little is known about Sb to evaluate its toxicology and determine its impact on the environment and human health. Although there is evidence of lung carcinogenicity caused by Sb in rats^(57,58), it is not yet clear whether Sb is a human carcinogen.

What is clear is that Sb(III) compounds are generally more toxic than Sb(V) compounds. An excellent review of the toxicological effects of Sb compounds has been prepared by Leonard and Gerber⁽⁵⁹⁾. This review succinctly covers many of the known, or little known, aspects of Sb toxicity.

A study in 1995 did find that lung cancer was in excess among U.S. Sb smelter workers⁽⁶⁰⁾. However, there is a difficulty with correlating Sb exposure with cancer in such facilities as Sb is almost always associated with metals and metalloids like As that might also be carcinogenic.

Other studies have shown that either by oral or intravenous administration antimony concentrates most in the liver followed by spleen, thyroid, kidneys, heart and lungs. The use of radioactive ¹²⁴Sb has shown that antimony(III) migrates to erythrocytes. In biological media Sb(V) predominates in the form $[\text{Sb}(\text{OH})_6]^-$ and Sb(III) will be in the uncharged $\text{Sb}(\text{OH})_3$ form⁽⁶¹⁾. In experiments with hamsters the uncharged Sb(III) showed a greater affinity for erythrocytes than for charged Sb(V). Thus, Sb(III) in this state will freely permeate cell membranes by diffusion, charged Sb(V) would not be able to do this. There is approximately 5-10% change in valency of Sb after administration with little evidence of methylation. Thus, any intake of Sb(III) is not likely to be detoxified to any great extent. Antimony-glutathione complexes have a limited stability and excretion in human bile does not seem high although studies are ongoing⁽⁶²⁾. Charged Sb(V) is excreted more quickly than Sb(III).

Stibine, SbH_3 , has the highest toxicity of any Sb compound and as a consequence is the most strictly controlled of the Sb species. Most studies have centred around exposure to SbH_3 by workers in lead battery production. As has already been described Sb is used in the production of these batteries and volatile SbH_3 can be generated while charging the battery plates⁽⁶³⁾. Currently the occupational exposure limit (OEL) for stibine is 0.1 mg dm^{-3} (8 hour time-weighted average)⁽⁶⁴⁾.

1.2.7.1 Intoxication

Symptoms of acute intoxication are metallic taste, headache, dizziness, nausea and salivation followed by vomiting, gastric and intestinal spasms and diarrhoea. Oral administration of tartar emetic will cause vomiting within approximately 15 minutes while the same dose by intravenous administration will take 60 - 90 minutes to have the same effect⁽²⁸⁾. 'Antimony spots' may occur⁽⁶⁴⁾ on the skin and pneumoconiosis.

Chronic exposure may cause cachexia, reduced libido, oppression, dyspnea with coughing and chest pains. Breiger *et al.*⁽⁶⁵⁾ also observed an apparent increase in heart abnormalities in workers exposed to antimony trisulphide. If the liver and spleen are damaged this can be indicated by lymphocytosis, a reduction in white blood cell and platelet counts, and an increase in red blood cells with basophilic speckling.

Further medical affects can be found in the literature relating to the cardiovascular and respiratory systems and their failure upon administration of lethal doses⁽⁶⁶⁻⁶⁸⁾.

Current permissible limits are as follows; 10 $\mu\text{g l}^{-1}$ Sb in surface and potable waters⁽⁶⁹⁾, 0.5 mg dm^{-3} as an 8 hour time-weighted average (maximum exposure limit) for Sb and its compounds (except SbH_3)⁽⁶⁴⁾, 0.1 mg dm^{-3} OEL for SbH_3 (8 hour time-weighted average). As of 1989-1990 the U.S. standards for the place of work was 0.05 mg dm^{-3} for Sb, (TLV, threshold limit value)⁽⁷⁰⁾.

1.2.7.2 Environmental Antimony

Most of the preceding review has covered the uses of antimony and its effect on humans, both toxic and questionably beneficial. However although the source of antimony, the ores, have already been mentioned the areas of environmental metabolism or biogeochemical pathways have not and will now be discussed in this section.

Section 1.2 gives abundance data for Sb in the Earth's crust at an average of 0.2 mg kg^{-1} . This translates to areas that have high concentrations and a lot more that have a generally low concentration. The determinations of Sb and Sb species are discussed in the next two sections although the number of species determined to date however has been limited. Currently the level of understanding of the biogeochemistry of Sb is poor when compared to As, the metalloid to which Sb is most compared. Only Sb(III), Sb(V), methylstibinic acid $[\text{MeSbO}(\text{OH})_2]$ and dimethylstibonic acid $[\text{Me}_2\text{SbO}(\text{OH})]$ have been reported as being determined in fresh, estuarine and marine waters, without appropriate mass spectrometric supporting evidence. Although thermodynamic evidence suggests that Sb(V) should exist as $[\text{Sb}(\text{OH})_6]^-$ in these waters and that Sb(III) will exist as either SbO_2^- or $\text{Sb}(\text{OH})_3$, no definitive identification has been achieved.

The mechanisms of biomethylation of Sb are only now beginning to be elucidated, although research activity in this area has existed for some time especially since Richardson suggested the microbial generation of volatile Sb species from mattress covers treated with Sb_2O_3 as a flame retardent⁽⁷¹⁾.

The determination of methylated species in marine organisms and plants does suggest that biomethylation of Sb is possible. Indeed in 1976 Parris and Brinckman stated that there was no obvious thermodynamic or kinetic barrier to biomethylation and that the chemical similarities between Sb and Sn, Pb, As, Se and Te would suggest biomethylation pathways for Sb could exist⁽⁷²⁾. They also warned of the potential for discarded consumer items as a source for biodegradation and the subsequent risk of leaching Sb that may be metabolised or solubilised, thus contributing to pollution of waterways.

Twenty years later two papers discussed Sb leachate from fly-ash after incineration of municipal waste or fossil fuels. Both papers highlighted very significant levels of Sb were being leached but that speciation results were unreliable^(73,74). Maeda *et al.*⁽⁷⁵⁾ investigated the bioaccumulation of Sb by freshwater alga in an arsenic polluted environment. When the

alga was cultured in an Sb(III) rich medium the excreted Sb was in both oxidation states, (V) and (III), 40% and 60% respectively. Therefore, the algal cells were effectively detoxifying much of the Sb, although no evidence was provided as to the molecular form of the Sb(V). So, even though a biotransformation of Sb was shown, clearly more work was required to establish the pathway and the forms of Sb produced. At the same time Gürleyuk *et al.*⁽⁷⁶⁾ reported the production of $(\text{CH}_3)_3\text{Sb}$ and its determination in the headspace from soil samples amended with Sb(III) and (V) species although the microorganisms believed to be responsible were not isolated. In 1998 however Jenkins *et al.*⁽⁷⁷⁾ reported the formation of $(\text{CH}_3)_3\text{Sb}$ by a characterised microorganism *Scopulariopsis brevicaulis*. Dodd *et al.*⁽⁷⁸⁾ also found evidence of methylated Sb species in plant extracts. The plants were from a lake influenced by gold-mine effluent. This mine effluent also contained As, Cu, Pb, Fe and Zn, metals with which Sb is known to associate in mineral ores. This study is reviewed in greater detail in section 1.4.5.

So, although authors are now beginning to surmise that Sb may have as rich an environmental chemistry as arsenic, very little information is known on the metabolic pathways or biogeochemistry of Sb. As a result the environmental toxicity of this element is not known. Antimony is so often associated with other metals and metalloids in the environment that the impact of Sb on the environment is also difficult to characterise. This is because many of the metals with which Sb is associated have been extensively researched, i.e. As, Pb and Zn and if Sb has a similar toxic effect it could well be masked by these other metals.

1.2.8. Summary

As can be seen the chemistry of Sb is extensive and the applications are varied. Some information is available on the element's detrimental effects and how these are governed

by its molecular form and oxidation state, i.e., Sb(III) more toxic than Sb(V) and inorganic Sb generally being more toxic than organic Sb.

Very little is understood about the chemistry of Sb in the environment and as such less is known about the toxic impact of Sb on the environment compared to many other metals. Much of the research to date has been produced at concentrated or pure Sb levels, and as such is not very applicable to environmental considerations where analysis of Sb is often restricted to trace or ultra-trace levels (discussed further in the Section 1.3). The rich variations in Sb chemistry, especially in the area of organometallic compounds, indicates that with advances in instrumental methods of determination analysts can progress from merely determining simple Sb(III) and (V) species and concentrate on the molecular forms of Sb compounds. The progressive development of instrumental methods and the findings of the analysts involved with Sb will now be discussed.

1.3 Review of Methods of Determination

Because of the long history of using Sb it would be unrealistic to establish a truly definitive point at which Sb was first identified, and the analytical techniques employed have been many and varied. This review summarises many of the methods utilised using tables to group together applications utilising the same or similar methodology.

1.3.1 UV/Vis spectrophotometry

Table 1.5 gives examples of the determination of total Sb by UV/Vis spectrophotometric methods. All of these techniques rely upon a selective complexation process. In many cases either Sb(V) is reduced or Sb(III) is oxidised to obtain a complex and therefore facilitate total Sb present in the sample. Although such methodology can be modified to allow speciation studies the authors did not highlight this.

What Table 1.5 shows is that such techniques can be utilised for total Sb concentrations in a wide concentration range (a few ppb⁽⁸⁶⁾ to a few percent⁽⁸¹⁾) for a variety of matrices. Complex reactions that are highly selective can be used in order to remove analytically difficult matrices. However, UV/Vis spectrophotometry is not sufficiently sensitive to be used for analysis of very low concentrations of Sb without preconcentration. Such sample pre-treatment is not always possible if the sample volume is limited.

Table 1.5 Examples of total Sb analysis by UV/Vis spectrophotometry.

Matrix	λ , nm	Complex	Sample Preparation	Concentration Range	Limit of Detection	Reference
Synthetic alloy solutions	560	1:1 complex of Sb(III) with 2,4,6-tris(1-hydroxy-4-sulphonaphthyl-2-azo) pyrimidine. Violet coloured	1 ml acetate buffer (pH 5.5), 0.5 ml 1×10^{-3} M THPm-4S + aliquot 5 - 30 μg Sb(III) diluted to 10 ml. Warmed at 60° C then cooled and analysed	10 - 46 $\mu\text{g ml}^{-1}$	N.R.	79
Aqueous	660	Phosphate-heptamolybdate/Sb (poorly characterised)	FIA method wherein the complex enhancement of molybdenum blue reaction is measured	0 - 100 mg l^{-1}	0.5 mg l^{-1}	80
Sb in glass	507.2	Pink-red Sb(III) complex with iodide and dithizone	Sb(III)-I-dithizone complex sorped on polyurethane foam in H_2SO_4 medium. Eluted with H_2SO_4 acidified acetone	0.01 - 1.07 %	N.R.	81
Sb(III) in alloys & pharmaceuticals	Not given	Sb-Iodide. {bis(2,4,4-trimethylpentyl)monothiophosphinic acid}	Sb is extracted into cyanex 302 solution at pH 0.5 - 1.5. Sb is then stripped with water and the Sb-I complex is determined	Upto 0.5 % w/v	N.R.	82
Waste water	400,520	Sb-chromazurol-S	β -correction spectrophotometry	0.064 - 2.33 mg l^{-1}	9 $\mu\text{g l}^{-1}$	83
Aqueous	280	Sb(III)-tris(diethyldithiophosphate)	Sb(III) complex separated from As(III) & Bi(III) complexes by RP-HPLC	N.R.	2 ng in 1 ml	84

Table 1.5 Continued

Matrix	λ , nm	Complex	Sample Preparation	Concentration Range	Limit of Detection	Reference
Multi-metal solution	555	Sb-phenylfluorene	Sb extracted from HCl by silica gel coated with bis(2-ethylhexyl)phosphinic acid. Then stripped by strong acid	N.R.	N.R.	85
Rain water	620	Sb-cetylpyridinium chloride-triton X-100-brilliant green	Sb(III) oxidised to (V) by $\text{Ce}(\text{SO}_4)_2 \cdot (\text{NH}_4)_2\text{SO}_4$. Aliquot of sample added to 7 ml conc. HCl and oxidising agent. CPC & TX-100 added with toluene extraction solvent	10.3 - 24.6 ng ml ⁻¹	3 ng ml ⁻¹	86
Metal & water samples	535	ICl_2^- -Rhodamine 6G	Sb determination based upon enhancement of complex reaction	278 ng l ⁻¹ to 0.03 %	N.R.	87
Waste waters	590	Cr(VI)-I- reaction with I_3^- -starch complex indicator	Sb(III) induced Cr(VI)-I reaction. FLA method	0.33 - 1.65 $\mu\text{g ml}^{-1}$	0.014 $\mu\text{g ml}^{-1}$	88

1.3.2 Flame and Electrothermal Atomisation-Atomic Absorption Spectroscopy

Table 1.6 gives details on examples of total determinations of Sb by flame and electrothermal atomisation-AAS.

Although direct flame AAS is not generally utilised for Sb analysis, the use of hydride generation offers improved limits of detection ($\leq 1 \mu\text{g l}^{-1}$) and facilitates AAS analysis. The mechanism of hydride generation for analytical purposes is discussed in Chapter Two.

Electrothermal atomisation-AAS is a more sensitive technique but may require further sample preparation and modification prior to analysis. This technique has, with some labour, been applied to solid and slurry samples^(93,99), thus displaying a certain flexibility for different environmental matrices. However, this instrument is fundamentally a batch rather than continuous analysis tool, and the adaption of this instrument to speciation has been limited. It is worth noting that many authors using this approach do not quote analytical detection limits^(29,92,96,99,101).

Table 1.6 Examples of total Sb analysis by flame and electrothermal atomisation-atomic absorption spectrometry.

Flame/ETAAS	Matrix	Sample Preparation	Concentration Range	Limit of Detection	Reference
Flame	Fly-ash & municipal waste leachate. Fly-ash digests	SbH ₃ was produced by HG device, Sample acidified with HCl and reductant was NaBH ₄ .	Upto 1,100 mg kg ⁻¹	0.2 µg l ⁻¹	73
ETAAS	Ref. materials and whole blood	Acid digestion (microwave assisted) for solids. Sb determined by laser-induced fluorescence and an ICCD	0.01 - 15 ng ml ⁻¹	10 pg ml ⁻¹	89
ETAAS	Water, blood, serum.	-	0.2 - 10.2 mg kg ⁻¹ (blood) 10 - 237 µg l ⁻¹ (water, serum)	2.6 µg l ⁻¹	90
ETAAS	Biological material	Also analysed by HGAAS and γ-emission of radioactive samples	Upto 2.79 mmol l ⁻¹	0.001 mmol l ⁻¹	91
ETAAS	Pine needle ref NIST 1575 & Pondweed	Ref. material acid digested and pondweed extracted with either acetic acid or methanol/water solution	0.208 - 40 mg kg ⁻¹	N.R.	92
ETAAS	Soil & sediment	Samples were ground and slurried	0.61 - 177 µg g ⁻¹	0.03 µg g ⁻¹ (100 mg ml ⁻¹ suspension)	93

Table 1.6 Continued

Flame/ETAAS	Matrix	Sample Preparation	Concentration Range	Limit of Detection	Reference
ETAAS	Geological samples	Samples were acid digested then extracted with a toluene solution of hexene-1	8 - 45 $\mu\text{g g}^{-1}$	0.004 $\mu\text{g g}^{-1}$	94
Flame	Geological, steel and alloys	Digested samples extracted with MIBK	3 - 305 mg kg^{-1}	2 mg kg^{-1}	95
Flame	Organoantimony	Samples prepared in a range of solvents	N.R.	N.R.	96
ETAAS	Urine	Sample was digested with HNO_3 - HClO_4 - H_2SO_4 . Salt and interferences removed by cation exchange and Sb extracted in APDC-2-methyl-4-pentanone. Sb(V) reduced with KI	0.3 - 1.3 $\mu\text{g l}^{-1}$	0.01 μg	97
ETAAS	Biological fluids	-	-	-	98
ETAAS	PVC	A solid sampling procedure	2.04 - 3.34 (g per 100g)	N.R.	99
ETAAS	Kohl eyeliner	-	0 - 9.97%	N.R.	29
Flame	Vegetation and soils	Oven-dried and HNO_3 digested. Analysed by HG-FAAS. Sb(V) pre-reduced to Sb(III) with 25% KI (w/v)	Upto 1,489 mg kg^{-1} (Dry weight)	1.6 x 10 ⁻⁴ mg l^{-1}	100

Table 1.6 Continued

Flame/ETAAS	Matrix	Sample Preparation	Concentration Range	Limit of Detection	Reference
ETAAS	Sediments	Leach experiments with water, ammonium sulphate(exchangeable), hydroxylamine hydrochloride-HNO ₃ (easily reducible), oxalic acid-ammonium oxalate(moderately reducible)	0.5 - 8.3 µg g ⁻¹	N.R.	101
Flame	Blood, urine & air	Analysis of exposed workers. Urine samples unprepared. Air & blood, wet oxidative digestion	Air 0.6 - 41.5 µg m ⁻³ Blood 0.5 - 17.9 µg l ⁻¹ Urine 2.8 23.4 µg g ⁻¹	N.R.	63
Flame	Smelter products	Samples extracted with di-isopropyl ether and reductively stripped into aqueous phase. Sb(III) oxidised to (V) with sodium nitrite	0.0058 - 0.1150 %	N.R.	102
ETAAS	Blood, urine & mosquito larvae	-	10 - 500 µg l ⁻¹ (Blood & urine)	25 µg l ⁻¹ (blood/urine) 6 mg kg ⁻¹ (mosquito larvae)	103

ICCD - Intensified charge coupled device; MIBK - Methyl Isobutyl Ketone; PVC - Polyvinyl Chloride

1.3.3 Inductively Coupled Plasma - Atomic Emission Spectroscopy

This section concentrates on ICP-AES determinations of Sb whether by continuous nebulisation of samples or following sample pre-treatment using methods such as hydride generation. As with the other methods described in this chapter, Table 1.7 presents examples of the determination of total Sb by ICP-AES.

The seven papers in Table 1.7 demonstrate the good sensitivity of ICP-AES techniques, although very few workers make use of continuous nebulisation for Sb analysis. Instead the use of HG is very much the norm when using this type of instrument for the determination of Sb, facilitating an improvement of the detection limits typically by at least a factor of 20. However, the use of HG also allows speciation studies and this will be discussed more fully in Section 1.4

The previous section on UV/Vis techniques stated that complex formation/chelation of Sb can be highly selective and provide an excellent means for preconcentration and matrix removal. Two groups of workers^(108,110) attempted to utilise this with two similar chelates, APDC and dithiocarbamate, but unlike the study with UV/Vis spectrophotometry, the ICP-AES determinations were applied to samples where the Sb concentration was much lower than for the examples given in Table 1.5.

The final and most significant improvement, in analytical terms, when using ICP spectroscopy is the ability to analyse more than one element simultaneously. This attribute is discussed in greater detail in Chapter Two.

Table 1.7 Examples of total Sb analysis by ICP-AES.

Matrix	Application	Sample Preparation	Concentration Range	Limit of Detection	Reference
Housedust	Investigation of correlation between Sb in the domestic environment and Sudden Infant Death Syndrome (SIDS)	Samples will have been acid digested followed by analysis by HG-ICP-AES	Upto 1870 ppm	N.R.	104
Fertilisers	Soil pollution by heavy metals	HNO ₃ & HF digests of fertiliser and soil amendments	0.3 - 10.2 µg g ⁻¹	0.3 µg g ⁻¹	105
Soil, water & biological tissue	Analysis of reference materials and assessment of sample preparation procedures	Solid samples were appropriately digested. Samples analysed for total Sb by HG-ICP-AES. Sb(V) reduced with KI	0.1 - 75.3 µg g ⁻¹	0.41 µg l ⁻¹	106
Marine & estuarine refs.	Application of simultaneous determination of Sb, As, Bi, Ge, Se and Te in environmental samples	Samples were microwave digested with a solution of HNO ₃ :HCl (70:37). Determination by HG-ICP-AES	0.59 - 211 mg kg ⁻¹	0.3 µg l ⁻¹	107
Drainage waters	Preconcentration and determination of 22 trace elements in drainage and pond waters	Metals were chelated with ammonium pyrrolidinedithiocarbamate (APDC) and extracted into chloroform. Extract residue taken up by dilute HNO ₃ and analysed by simultaneous ICP-OES	N.R.	1 µg l ⁻¹	108

Table 1.7 Continued

Matrix	Application	Sample Preparation	Concentration Range	Limit of Detection	Reference
Sea waters	Application of HG-MIP-AES to determination of As, Sb and Se.	-	N.R.	0.9 µg l ⁻¹	109
Waters	Multi-element determination of As, Bi, Hg, Sb, Se and Sn in water samples	Sb sorbed onto dithiocarbamate loaded polyurethane foam. Preconcentration method. Eluted with methanol	Around 8 µg l ⁻¹	2 µg l ⁻¹	110

1.3.4. Inductively Coupled Plasma-Mass Spectrometry

Table 1.8. gives examples of the determination of total Sb utilising ICP-MS. This summary shows the following key features: 1) excellent sensitivity with L.O.D.s in the ppt range; 2) as many examples of analysis by continuously nebulised samples as there are by hydride generation sample introduction; 3) the samples are predominantly aqueous (organic media are generally avoided but this is briefly discussed in Chapter Two); and 4) extensive use of multi-element determinations for Sb and other toxic elements in the same sample.

The ever increasing availability of ICP-MS to metals analysts makes this type of instrument the one of choice for analysis of Sb as it has the required sensitivity for analysing Sb in natural waters and other environmentally important matrices. However, as with all the techniques given in this chapter so far, most studies are only obtaining part of the required information, i.e. total Sb and not the different species of Sb in the samples.

Table 1.8 Examples of total Sb analysis by ICP-MS.

Matrix	Application	Sample Preparation	Concentration Range	Limit of Detection	Reference
Mattress covers (PVC)	Investigation of toxic gas generation from plastic mattresses and implications for SIDS	Chemical analysis $\text{H}_2\text{SO}_4\text{:HNO}_3$ digest of covers. Mercuric chloride & silver nitrate test paper strips that were exposed during mycological experiments were digested in hot conc. HNO_3 , diluted with H_2O and analysed	Chemical content <50 - 31,050 ppm Test paper, <0.1 - 0.6 ng	N.R. 0.1 ng per strip	111
Seawater	Measurement of isotope ratio	Utilisation of flow injection-hydride generation. No other sample pre-treatment	N.R.	6 ng l ⁻¹	112
Reference waters	Determination of As, Sb and Se by ETV-ICP-MS to eliminate polyatomic interferences	A range of chemical modifiers were utilised	Linear 0 - 100 ng g ⁻¹	0.01 ng g ⁻¹	113
Water	Multi-element hydride generation method for As, Sb and Se	Pre-reduction of Sb(V) to Sb(III) with thiourea	2.78 - 8.5 µg g ⁻¹	0.06 ng g ⁻¹	114
Reference waters	Determination of As, Sb, Bi and Hg in waters by FI-HG-ICP-MS	Pre-reduction with L-cysteine	0.26 - 1.0 ng ml ⁻¹	0.017 ng ml ⁻¹	115
Sea water	Automated HG-ICP-MS determination of Se(IV), Sb, As and Ge	Methanol utilised to enhance sensitivity. L-cysteine used as pre-reductant	Around 277 ng l ⁻¹	2.2 ng l ⁻¹	116

Table 1.8 Continued

Matrix	Application	Sample Preparation	Concentration Range	Limit of Detection	Reference
Geological	Determination of Bi, Sb, Se and Te by HG-ICP-MS	Samples digested in Aqua regia or HF-HClO ₄ -HNO ₃ -HCl. Potential interferences removed by co-precipitation with La(OH) ₃ . KI pre-reductant	0.07 - 22.0 mg kg ⁻¹	6 µg kg ⁻¹	117
Dust, deposition & grasses	Association of Sb with traffic	Dust/deposition open digested in HNO ₃ :H ₂ O ₂ :HF Grass analysed for nitric acid soluble and HF digestible Sb	Ref materials 5.8 - 44 µg g ⁻¹ Airborne particles 1.26 - 16.7 ng m ⁻³ Grasses 0.015 - 1.88 mg kg ⁻¹ Depositions 0.6 - 16 µg m ⁻² d ⁻¹	0.3 mg kg ⁻¹	118
Human biological fluids or tissue	Determination of Sb in infant tissue. Investigation of sampling protocols		Urine 0.01 - 4.9 µg l ⁻¹ Blood/serum 0.17 - 0.78 µg l ⁻¹ Liver/lung 0.7 - 37 µg kg ⁻¹	0.004 µg l ⁻¹ 0.02 µg l ⁻¹ 0.5 - 1.0 ng g ⁻¹	119

1.3.5 Other Methods

This section covers those methods that have not been utilised to the extent that above spectroscopic methods have. Table 1.9 gives the method of detection and sample preparation details with references. This table also gives sample matrix and the concentration range for the Sb determined. It can be seen that the analysis of Sb is not totally dominated by AAS or ICP methodology, and in recent years studies using other approaches have been published^(33, 62, 123, 124, 126, 128 & 131).

Some of the electrochemical methods and neutron activation analysis methods have been applied to speciation studies and as such any discussion of these techniques will be dealt with in Section 1.4. The X-ray techniques generally lack sensitivity for analysis of many real environmental samples where levels of Sb would be below the limits of detection of these methods. As such they will not be discussed in this thesis.

Table 1.9 Examples of less common detection methods for the determination of total Sb.

Method of Determ ^a	Matrix	Sample Preparation	Sb Concentration Range	Limit of Detection	Reference
Gamma Spectrometry	Human Milk	Irradiation, 10-14 h.	$\leq 0.05 - 12.9 \text{ ng g}^{-1}$	0.05 ng g^{-1}	120
INAA/ γ spectrometry	Natural waters	Preconcentration on thionalide loaded acrylic polymer. Sb(V) pre-reduced to Sb(III)	$0.057 - 0.210 \text{ } \mu\text{g l}^{-1}$	$0.023 \text{ } \mu\text{g l}^{-1}$ (100 ml sample)	121
INAA	Car & Truck tyres	Some samples were ashed	$0.06 - 46 \text{ } \mu\text{g g}^{-1}$	N.R.	122
INAA	Snake Venom	Dried at room temperature under vacuum	$1.67 - 56.3 \text{ ng g}^{-1}$	N.R.	123
INAA	Brackish-water Coals	-	$0.07 - 1.49 \text{ mg kg}^{-1}$	N.R.	124
INAA	House & street dust	-	$1.83 - 30.6 \text{ } \mu\text{g g}^{-1}$	N.R.	125
X-ray fluorescence	Seawater	HG, preconcentration in solvent	Not applied to real samples	-	126
X-ray microfluorescence	Gunshot residue on human tissue and clothing	-	N.R.	N.R.	33
EDAX	Kohl eyeliner pencils	-	Approx. 10%	N.R.	30
EDAX	Biliary excretion	-	Effect of Sb on Se excretion analysed	N.R.	62

Table 1.9 Continued

Method of Determ ^a	Matrix	Sample Preparation	Sb Concentration Range	Limit of Detection	Reference
ASV	Humic acid	Solution of Sb added to humic acid. Supernatant analysed to measure sorption of Sb	N.R.	N.R.	127
DPP	Industrial waste water	1 litre evaporated to 250 ml, digested with 2 ml of HNO ₃ :H ₂ SO ₄ (10:1)	0.052 - 0.085 mg l ⁻¹	0.020 mg l ⁻¹	128
ASV	Hair & soil	Sample digestion	14.24 - 39.8 µg l ⁻¹ and 3.98 - 7.2 µg g ⁻¹	8.9 x 10 ⁻⁹ mol l ⁻¹	129
CSV	Estuarine water	-	Upto ≈ 2 nM	N.R.	130
CSV	Steel & brass	Sb(III) complexed with 2',3,4',5,7- pentahydroxyflavone (morin)	Around 30 µg g ⁻¹	7 x 10 ⁻¹⁰ mol l ⁻¹	131
ASV	Whole blood, urine, mosquito larvae	Spiked samples	10 - 500 µg l ⁻¹	2 µg l ⁻¹ (urine)	103
Polarography	Non-ferrous metal alloys	Digestion & complex with pyrocatechol violet, pharmacopoeia pyramidone	0.005 - 0.03%	Limit of determination 2.5 x 10 ⁻⁴ %	132
Oscillopolarography	Metallurgical leaching slimes	Sample acid digested	N.R.	N.R.	133

γ - Gamma; INAA - Instrumental Neutron Activation Analysis; EDAX - Energy Dispersive X-Ray Analysis; ASV - Anodic Stripping Voltammetry; DPP - Differential Pulse Polarography; CSV - Cathodic Stripping Voltammetry.

1.3.6 Discussion

At best all of the methods described in this section could be used for speciation of Sb as Sb(III) or (V). To give the best possible chance of observing Sb species on a molecular level separation methods need to be introduced that minimise chemical selectivity and maximise species discrimination, based upon the physical characteristics of the Sb molecules.

If the real picture is to be seen with Sb speciation and its toxic impact is to be assessed then the sample preparation has to maintain the integrity of the Sb species.

The attempts, to date, to achieve speciation of Sb by oxidation state or on a molecular level are reviewed in the next section.

1.4 Review of Speciation of Sb

1.4.1 Voltammetric and Instrumental Neutron Activation Analysis Methods

In 1997 Bond *et al.*⁽¹³⁴⁾ reported on the determination of Sb(III) and Sb(V) in zinc plant electrolyte using anodic stripping voltammetry. The application was straightforward, since Sb interferes with the electrochemical deposition of zinc. This study described how at high acid concentration (>4M HCl) both Sb(III) and Sb(V) could be reduced at a hanging mercury drop electrode to form Sb(Hg), antimony amalgam. At low concentrations of HCl (0.1M) only Sb(III) was reduced. Therefore the concentration of Sb(V) was determined by difference between total Sb and Sb(III). Sb(III) was determined down to $12 \mu\text{g l}^{-1}$ though the limit of detection was not reported.

Rúriková and Pocuchová⁽¹³⁵⁾ determined Sb in natural waters by differential pulse voltammetry. The Sb(III) was first complexed with catechol, then, after a rapid potential change to -0.1V a cathodic scan is carried out from -0.1V to -1.0V. As with the previous method this approach was selective for Sb(III). Sb(V) is pre-reduced with ascorbic acid.

The limit of detection was given as $0.1 \mu\text{g l}^{-1}$. However, only total Sb was reported for the samples at concentrations between 0.1 and $0.9 \mu\text{g l}^{-1}$ for tap and surface waters respectively.

Wok and Mai investigated the distribution and mobilisation of As and Sb species in the Coeur D'Alene River, Idaho⁽¹³⁶⁾. They utilised a pyrrolidine carbodithioate extraction procedure to extract Sb(III) and Sb(V) and then determined Sb by NAA. Although the authors do not refer to organoantimony they do point out the extraction procedure is for inorganic Sb species. Speciation of Sb(III) and Sb(V) is obtained by difference with the determination of total Sb and selective determination of Sb(III). The Sb(V) was determined by subtracting Sb(III) from the total. The details for Sb(V) reduction were not given. The concentrations of Sb in water samples was reported to range from $0.17 - 8.25 \mu\text{g l}^{-1}$ Sb with Sb(V) being the predominant species. The reported limit of detection was 1 ng l^{-1} .

Neutron activation analysis was used by Chwastowska *et al.*⁽¹³⁷⁾ for the determination of Sb(III) and Sb(V) in natural waters. Sb(III) is selectively retained on a thionalide loaded resin. Sb(V) in the effluent was reduced by 1% KI in 3M HCl and both species were determined directly on the sorbent. The limits of detection for Sb(III) and Sb(V) were 2.5 and 25 ng l^{-1} respectively. The concentrations observed ranged from $2.5 - 133 \text{ ng l}^{-1}$ with Sb(V) being at the higher concentrations.

Van der Hoek *et al.*⁽⁷⁴⁾ made use of hydride generation-NAA for the determination of Sb(III) and Sb(V) in coal fly-ash leachates. Such a technique means that one species, Sb(V), was determined by difference. Sb(III) is the preferred oxidation state for the production of SbH_3 and Sb(V) usually requires pre-reduction. KI/ascorbic acid was used to reduce Sb(V) to Sb(III). However, the authors concluded that total determinations were more reliable than species specific determinations.

1.4.2 UV/Vis Spectrophotometric Methods

In 1985 Sato⁽¹³⁸⁾ showed that Sb(V) and Sb(III) would complex with an α -hydroxyacid, mandelic acid ($C_6H_5CH(OH)COOH$). These complexes were extracted with malachite green into chloroform and determined at 628 nm, in the organic phase. Sato exploited the rate differences in complex formation for Sb(V) and Sb(III) with mandelic acid. Thus, no reducing agent was required in the sample preparation. Sato tried a range of complexing agents many of which had the hydroxy functionality. The method was linear over the range 0.15 - 6.10 $\mu g\ ml^{-1}$ of Sb(III) and 0.2 - 10 $\mu g\ ml^{-1}$ of Sb(V). The limit of detection was not reported.

Sharma and Patel⁽¹³⁹⁾ described the selective extraction of Sb(V) as the $[SbCl_6]$ -Brilliant Green ion pair in a toluene solution of N,N'-diphenylbenzamidine (DPBA). However, this is not an Sb(III) reaction. Sb(III) has to be pre-oxidised by ceric ammonium sulphate. The absorbance was measured at 640 nm. The limit of detection for this method was 10 $\mu g\ l^{-1}$. When applied to industrial waste waters from a steel plant the range of concentrations for Sb(III) was 11.1 - 62.2 $\mu g\ l^{-1}$ and Sb(V) was 55 - 64 $\mu g\ l^{-1}$. Speciation was achieved by difference.

In 1997 Rath *et al.*⁽¹⁴⁰⁾ determined Sb(III) and Sb(V) in Meglumina antimoniate (Glucantime), an antileishmanial drug. Bromopyrogallol red (BPR) will react with Sb(III) in neutral solution to form a complex Sb-BPR. The absorbance of BPR, at 560 nm, will decrease proportionally to the amount of Sb(III) in solution. Sb(V) needs to be pre-reduced and this was achieved in this study by iodide. The limit of detection was $1.65 \times 10^{-6}\ mol\ l^{-1}$. The Sb(V) content ranged from 75.4 - 94.5 $mg\ ml^{-1}$ and the Sb(III) content ranged from 5.19 - 10.5 $mg\ ml^{-1}$. The application of this method was primarily to monitor the toxic Sb(III) content.

X.Huang *et al.*⁽¹⁴¹⁾ also utilised BPR when spectrophotometrically determining Sb(III) in Sb(III)/(V) binary mixtures. They achieved a detection limit of $0.04 \mu\text{g ml}^{-1}$. 10 mg Sb(III) could be determined in the presence of 100 mg Sb(V). This method was not applied to real samples.

1.4.3 Hydride Generation - Atomic Absorption/Atomic Fluorescence Spectroscopy

Although the mechanisms for atomic absorption and atomic fluorescence are different, for the purposes of this review it is convenient to discuss the two techniques together. The mechanisms are, however, discussed in Chapter Two. The formation of stibine is also discussed in greater detail in subsequent chapters.

Holak⁽¹⁴²⁾ was the first to introduce the technique of HG-AAS in 1969 and many workers have utilised the technique for the speciation of Sb. Apte and Howard⁽¹⁴³⁾ used HG-AAS for the determination of Sb(V) and Sb(III) in natural waters. This paper reported the application of cryogenic preconcentration of the hydride followed by atomisation of the hydride in an electrically heated quartz tube furnace. This furnace was mounted in the light path of an AAS. They achieved speciation by careful attention to the pH dependence of the reduction step. For total Sb the sample aliquot was acidified to $[\text{H}^+] 1\text{M}$ with concentrated HCl and KI was added to reduce the Sb(V) to Sb(III). For Sb(III) determinations citric acid replaced HCl and KI. Under these conditions Sb(V) was not reduced to the hydride. The cryogenic trap was cooled in liquid N_2 for 60 s then NaBH_4 was added to the acidified solution. The hydride was carried by a N_2 gas flow to the trap. The trap was then allowed to warm to room temperature. The hydride re-volatilised and was carried to the atomiser. Sample throughput was around 7 h^{-1} . The linear range was 0 - 300 ng l^{-1} with detection limits of 10 ng l^{-1} total Sb and 1 ng l^{-1} as Sb(III). This type of analytical performance matched ICP-MS in terms of sensitivity and is more than satisfactory for analysis of Sb in natural waters.

This work showed that sample pH had a great effect on the hydride formation. By buffering the pH with citrate to pH 2 the hydride yield from Sb(V) was zero. The method was applied to waters from Scotland and the Tamar Estuary, S.W. England.

Up to 616 ng l^{-1} Sb was found but no more than 3% of this was determined as Sb(III).

In 1990 Mohammad *et al.*⁽¹⁴⁴⁾ determined Sb(V) and (III) in mine drainage and stream waters by HG-AAS. This study utilised citric acid for species discrimination and was based on continuous flow HG rather than a batch HG method in the previous study⁽¹⁴³⁾. The speciation was achieved at $\text{pH} < 1$ hence, not pH controlled. In the flow system citric acid (12% m/v) replaced KI (Sb(V) reductant). The suppression of Sb(V) hydride formation was attributed, by the authors, to complexation of Sb(V) with citrate. The limit of detection for this method was $1 \text{ } \mu\text{g l}^{-1}$ and the concentration range in the samples was $5.3 - 60.4 \text{ } \mu\text{g l}^{-1}$. Using an autoanalyser set-up this method was reported as being capable of a 40 h^{-1} sample throughput.

In the early 1990's Cámara's group in Spain, became very active in Sb research. In 1992 a series of papers were published on Sb(V) and Sb(III) speciation fundamentals covering pH-control using three inorganic acids⁽¹⁴⁵⁾, a stability study of total Sb, Sb(V) and (III)⁽¹⁴⁶⁾ and how interference from Sb and Se could be minimised by α -hydroxyacids and KI in the determination of As by HG-AAS⁽¹⁴⁷⁾.

These papers, in summary, found that; 1) in phosphoric acid medium Sb(III) could be determined at $\text{pH} < 2$ without interference from Sb(V) and without the requirement of added citric or tartaric acid to obtain optimum pH levels for speciation⁽¹⁴⁵⁾; 2) Organic acid (lactic, citric, ascorbic) additions to stabilise Sb in storage is not necessary and that storage at $0 - 4^\circ \text{C}$ is adequate, thus the oxidation of Sb(III) to Sb(V) is affected by factors such as temperature as well as the presence of oxidising agents in the sample⁽¹⁴⁶⁾; and 3) α -hydroxyacids such as lactic, citric and malic can suppress Sb(V) hydride formation and the further addition of KI will suppress Sb(III) hydride formation. This was hypothesised as

being due to complex formation. This modification was utilised to eliminate interference effects of Sb in the determination of As⁽¹⁴⁷⁾.

More recently, 1995, D'Ulivo *et al.*⁽¹⁴⁸⁾ analysed reference materials of sediments, riverine water and metallic copper by hydride generation/non-dispersive atomic fluorescence detection. They achieved a limit of detection of 22 ng l⁻¹ with linearity up to 1 mg l⁻¹. The concentration range determined was 0.14 µg g⁻¹ (water) to 9.38 µg g⁻¹ in the copper samples.

In 1997, Keenan *et al.*⁽¹⁴⁹⁾ investigated Sb concentration in the umbilical cord and infant hair by HG-AFS. This paper is another dealing with the implied connection between Sb and SIDS. The limits of detection were 3 ng g⁻¹(hair) and 1 ng g⁻¹(cord). An average of 27.7 ng g⁻¹ was determined in cord and 826 ng g⁻¹ in the hair samples. They reported the results as being indicative of low level contamination by Sb being common with hair possibly being the excretion mode.

1.4.4 Electrothermal Atomisation-AAS

De la Calle-Gutiñas *et al.*⁽¹⁵⁰⁾ exploited the reaction between lactic acid and Sb(III) that forms a charged complex which can be extracted from an aqueous solution containing Sb(V). The Sb(III)-lactic complex is extracted into chloroform with malachite green. The reaction was reported as being Sb(III) selective. Thus, speciation is achieved and Sb(III) is determined in the organic extract while Sb(V) can be determined in the aqueous phase. An electrothermal atomisation-AAS was used for Sb determinations. The limit of detection was 0.01 ng, although the method was not applied to real samples.

In 1993 the same group looked at how an enzyme, fructose-6-phosphate kinase immobilised on controlled-pore glass, would selectively retain Sb(III) thus separating this species from Sb(V) and allowing preconcentration of Sb(III)⁽¹⁵¹⁾. This preconcentration effect was important because of the typically low concentrations of Sb(III) in the environment. The

retained Sb(III) was eluted with a lactic acid solution (3% v/v). Analysis of waters was carried out using this method with determination by ET-AAS. The Sb(III) species were believed to covalently bond to the thiol groups of the enzyme. The limit of detection was $4 \mu\text{g l}^{-1}$ and had a linear range of 20 - 180 $\mu\text{g l}^{-1}$. This method was not sufficiently sensitive for the determination of Sb in the environmental samples but the authors acknowledged there was substantial room for improvements to this method.

Speciation and preconcentration of Sb(III) and Sb(V) on a alumina substrate was achieved by Smichowski *et al.*⁽¹⁵²⁾. This was most effectively achieved with phosphoric acid. The authors found that Sb(V) was retained at less than 1% at pH 9.5 while Sb(III) was retained and then eluted with 4M HCl. Whereas both species were retained at pH 7.5. Using ET-AAS determination the limits of detection were preconcentration factor dependent between 4 - 26 pg. The linear range was 5 - 90 ng ml^{-1} . These workers used spiked sea-water samples for method validation and found it to be useful giving close to 100% recoveries for Sb(III) and Sb(V).

Although Smith *et al.*⁽¹⁵³⁾ did not report concentrations of Sb(V) and Sb(III) in urine, they did discuss the pH dependence in the extraction efficiency for the two oxidation states when developing the solvent extraction method in this paper. The Sb(III) present was chelated with ammonium N-nitrosophenyl hydroxylamine (cupferron), which was then extracted into isobutyl methyl ketone. The authors found that Sb(V) was not extracted between pH 2 - 6 yet Sb(III) was most efficiently extracted between pH <1 and 5. Based upon this the authors reduced Sb(V) to Sb(III) by heating the sample at 90° C for 30 - 40 minutes after acidification with concentrated HCl. The limit of detection was calculated as $0.69 \mu\text{g l}^{-1}$ and while this was not sensitive enough for environmental analysis, the authors applied the method to urine analysis for Sb. The monitoring was carried out on urine obtained from workers who were occupationally exposed to antimony. Battery workers were found to

have upto five times more Sb in their urine than other workers (chemical industry, refinery, control group). This was probably due to heightened risk of exposure to volatile SbH_3 .

The complexation of Sb(III) with APDC was investigated by Yan *et al.*⁽¹⁵⁴⁾ Using a flow injection system the complex was absorbed onto the inner walls of a knotted reactor made from PTFE tubing. Quantitative elution was achieved with ethanol and determination was by ET-AAS. Although not strictly a speciation paper, emphasis was put on the application that Sb(III) could be quantitatively determined in the presence of upto 20 times more Sb(V). The method limit of detection was $0.021 \mu\text{g l}^{-1}$ and the method was applied to spiked water samples.

Another example of sorption preconcentration was demonstrated by Garbos *et al.*⁽¹⁵⁵⁾. The sorbent substrate was Polyorgs 31 which contains mainly amidoxime and amine functional groups. This would absorb the total Sb at pH 2 and Sb(III) only at pH 10. The limit of detection for Sb(V) at pH 2 was 31 ng l^{-1} and for Sb(III), 30 and 34 ng l^{-1} at pH 2 and 10 respectively. The method was applied to tapwater and snow samples. The concentrations observed for Sb(III) ranged between not detected (tapwater) and 38 ng l^{-1} (snow). Sb(V) ranged between 180 ng l^{-1} (tapwater) and 72 ng l^{-1} (snow).

1.4.5 Gas Chromatography

The following sections in this review concentrate on direct speciation methods for Sb compounds, i.e. methods where the determination of Sb(III) and Sb(V) is carried out on the same sample aliquot in one run. This is as opposed to the 'by difference' methods typified by batch hydride generation or oxidation state specific extraction methods. This first section covers examples of gas chromatographic (GC) methods.

The interest in biomethylated Sb species has attracted analysis by GC, particularly as GC has been applied to the analysis of methyl arsenic compounds. Dodd *et al.*⁽¹⁵⁶⁾ looked at pure samples of di-and tri-methylated 5-coordinate Sb species by GC-AAS. Prior to

analysis the hydrides of the species were formed using apparatus similar to that used for As. However, they found that single species injections would give four peaks relating to, they presumed, SbH_3 and mono-, di- and tri-methylstibine. This paper was one of the first to doubt the hydride generation methodology of the time, namely that based upon tetrahydroborate reduction in an acidic (HCl) medium, for Sb speciation. The reason being that molecular rearrangement clearly occurred.

At the same time, Yamamoto *et al.*⁽¹⁵⁷⁾ looked at the separation of Sb and As species by GC with photoionisation detection. The Sb species were inorganic Sb(V) and antimonyl(III) tartrate. As with the previous example the hydrides were produced and cold-trapped prior to GC analysis. The AsH_3 and SbH_3 species were separated on a packed GC column (Tenax GC). Sb(V) was calculated by difference following total Sb and Sb(III) determinations. The limit of detection for Sb was 9.4 ng l^{-1} and the method was applied to natural waters. Sb(III) was not determined in any samples, but Sb(V) was determined in the range 163 ng l^{-1} (rainwater) to 450 ng l^{-1} (seawater).

Four years after looking at synthetic methylated Sb compounds by HG-GC-AAS Dodd *et al.*⁽⁷⁸⁾ published an investigation of Sb speciation in freshwater plant extracts by HG-GC-MS. In this paper the samples were acidified with acetic acid to facilitate the analysis of methylantimony. The aforementioned molecular rearrangements⁽¹⁵⁶⁾ were eliminated when the HG reagents were introduced to the reaction coil for a few minutes prior to sample analysis whereas previously the reaction generator was rinsed with deionised water prior to sample analysis. No clear explanation was provided as to why such a difference should be made.

The plant samples (pondweed) were collected from lakes in Canada that had been influenced by mine effluent. The sample (50 g) was homogenised with 0.2 mol l^{-1} acetic acid, sonicated for 1 hour and left to stand overnight. These extracts were filtered and analysed. The generated stibines were cold-trapped before being thermally released to the

gas chromatograph. The column used was a Porapak-PS packed column. The limit of detection was reported as approximately 15 ng of Sb. Sample analysis showed the presence of SbH_3 , mono-, di- and tri-methylated antimony species. These were identified by comparison of chromatograms and mass spectra with those of synthetic standards. However, there were differences in chromatograms of extracts for pondweed from different lakes. This was thought to be due to the nature of anthropogenic input. This paper was important as it was the first to report structural evidence for the presence of methylated Sb species in biological systems. Importantly, though, the authors recognised the limitations of HG in that complex organoantimony compounds that cannot be reduced to stibines will not be determined in this way. Thus, they concluded, HPLC or similar techniques coupled with ICP-MS would have to be used to overcome this problem.

De la Calle-Guñtinas and Adams⁽¹⁵⁸⁾ derivatised Sb(III) with triphenylmagnesium bromide to form volatile triphenylstibine and determined this by GC coupled to a quartz furnace AAS. Thus Sb(III) was determined in the presence of Sb(V), albeit after being extracted into hexane with APDC at pH 4.5. The limit of detection was calculated as 0.26 ng and the method was applied to spiked tap waters.

1.4.6 Liquid Chromatography (LC) Methods

Unlike As speciation LC methods, tangible success for Sb speciation has only been achieved in the last couple of years.

In 1995 Smichowski *et al.*⁽¹⁵⁹⁾ reported the speciation of Sb(V) and Sb(III) in aqueous solutions by HPLC coupled to HG-AAS, ICP-MS and HG-ICP-MS. Separation of Sb(V) as $[\text{Sb}(\text{OH})_6]^-$ and Sb(III) as antimonyl(III) tartrate was achieved using an anion exchange column with a phthalic acid (2 mM) mobile phase. The retention times for the species were most significantly affected by pH changes with retention times decreasing with increasing pH. Sb(V) eluted easily, after approximately 1.5 minutes, and Sb(III) was more strongly

retained eluting after about 7 minutes. The Sb(V) species was believed to elute in the dead-time of the chromatographic system, although this does not appear to have been tested. The method had the following limits of detection:

Table 1.10 Limits of detection for methods utilised by Smichowski *et al.*⁽¹⁵⁹⁾

Technique	Limit of detection ($\mu\text{g l}^{-1}$)	
	Sb(V)	Sb(III)
HPLC-HG-AAS	6.0	50
HPLC-ICP-MS	0.9	7.5
HPLC-HG-ICP-MS	0.08	0.4

The methods were applied to spiked waters, waste waters from the metallurgical industry and municipal discharge, sea and river water.

Lintschinger *et al.*⁽¹⁶⁰⁾ investigated not only anion exchange but also cation and reversed-phase chromatography for the separation of Sb(V) and Sb(III) species as well as trimethylated Sb compounds, $(\text{CH}_3)_3\text{SbCl}_2$ and $(\text{CH}_3)_3\text{Sb}(\text{OH})_2$. A wide range of mobile phases were investigated throughout concentration and pH ranges. These workers found that by anion exchange Sb(V) eluted easily but Sb(III) would not elute. This was believed to be due to precipitation of SbCl_3 as the oxychloride (SbOCl) or, in the case of antimony(III) tartrate, because the retention of the dinegative ion was too strong for the mobile phases used. Good separation was achieved between the trimethyl Sb (TMSb) species and Sb(V). Only in the case of the phosphate buffer was TMSb not eluted on the solvent front. These separations were achieved at pH's neutral-alkaline. When the anion exchange column was used with complexing agents in the mobile phase, Sb(III) would elute and most effectively

in an EDTA:phthalate mobile phase. The observation of most note was that no difference in retention times were observed between Sb(III) species, SbCl_3 and antimonyl(III) tartrate. Hence the authors acknowledged that this separation would probably only receive application interest where just oxidation state information was required.

Neither cation exchange or reversed-phase chromatography yielded satisfactory separations. Nor did these workers obtain a separation of all three Sb species. The best limits of detection observed for the three species were $0.6 \mu\text{g l}^{-1}$ (TMSb), $0.5 \mu\text{g l}^{-1}$ (Sb(V)) and $0.8 \mu\text{g l}^{-1}$ (Sb(III)). The modes of separation, KOH mobile phase for TMSb, Sb(V) and EDTA:phthalate mobile phase for Sb(V),Sb(III) were applied to water samples from New Zealand and soil samples from Bavaria. The soil samples were extracted with deionised water and filtered prior to analysis. Sb(III) was not detected in any samples due to the poor $0.8 \mu\text{g l}^{-1}$ detection limit which was not sufficiently sensitive to determine Sb(III) in aqueous environmental samples. The authors did, however, claim the techniques were sufficiently sensitive to determine Sb in situations of toxicological interest.

In 1998 Nina Ulrich studied the ion chromatographic behaviour of Sb species with HPLC coupled to an ICP-MS⁽¹⁶¹⁾, and then applied HPLC-ICP-AES/MS to surface water and soil extract samples⁽¹⁶²⁾. In a similar manner to Lintschinger *et al.*⁽¹⁶⁰⁾, Ulrich assessed the separation of TMSb, Sb(V) as $[\text{Sb}(\text{OH})_6]^-$ and Sb(III) as antimonyl(III) tartrate. However, phthalic acid was the only mobile phase used. The influence of a range of complexing agents was investigated - tartrate, citrate and chloride. A separation of the three species was observed with 2 mM phthalic acid (pH 5) modified with 2% acetone. The retention order was Sb(V), TMSb followed by Sb(III). The detection limits for the species were 0.51, 0.59 and $3.1 \mu\text{g l}^{-1}$ respectively. The complexing agents had no observed effect on Sb(V), both tartrate and citrate increased the retention time of TMSb as the excess of complexing agent increased, and only citrate affected the Sb(III) retention time. The interaction defied chromatographic interpretation.

One of the more interesting conclusions drawn from the above study was with respect to future investigations of the complex formation of antimony with, for example, citrate. Ulrich stated, 'For further investigations of the complexing abilities of citrate and other species an eluent system has to be used which has only little complexing tendency with antimony species. Interesting mobile phases could consist of inorganic anions like nitrate, chloride or perchlorate which offer the desired characteristics'.

The last aspect of this particular paper⁽¹⁶¹⁾ worth discussing is the very poor sensitivity for Sb(III), the most toxicologically important species of Sb. Ulrich applied this method to real samples⁽¹⁶²⁾, soil extracts and surface water. An ICP-AES detector was coupled to the ion chromatograph system for method development, but ICP-MS was utilised for monitoring antimony at trace levels. Results for water samples indicated as much as 10% of the Sb in the form of Sb(III). The limit of detection for Sb(III) was reported as 0.311 ng/100 µl, yet Ulrich reported an Sb(III) concentration in one water sample as 0.2 ng/100 µl. In the chromatogram obtained from the polluted water sample a couple of unknown peaks were observed. In the soil sample extracts (MeOH:H₂O, acetic acid 0.2 mol l⁻¹) the ratio of Sb(V) to Sb(III) was very similar to that of the water samples, but TMSb was seen followed by three humps for species that were strongly retained but very poorly resolved. This was recognised by the authors as no tables of results for samples or spiked samples were presented.

1.4.7 Discussion

The steady progress of GC and LC applications is obvious. With the increasing level of understanding of the environmental chemistry of Sb, or at least what is highly probable or possible, the chromatographic separations have become better able to determine Sb on a molecular basis. However, the research to date has strongly concentrated upon anion exchange chromatography, with only occasional investigation of the alternatives - cation

and reversed-phase chromatography. The reasons behind why cation exchange is not used for environmental analysis is sound. The existence of Sb cations in solution is not thermodynamically favoured. However, recent understanding of the chemistry of Sb has shown a number of neutral organic complexes are possible, therefore it seems strange that reversed-phase chromatography has not been investigated more thoroughly.

Most recent analytical investigations have shown that Sb will form complexes in solution with some carboxylic acids. The literature review in Section 1.2.5 has shown that other organofunctional groups that may exist in environmental or biological systems will form quantifiable complexes with Sb(V) and Sb(III). Also, none of the studies utilising LC discuss optimisation of the HPLC coupling to the spectrometers. No chromatographic development or procedure should commence or be validated without addressing the problems associated with dead-volume and post-column dispersion⁽¹⁶³⁾.

1.5 Aims and Objectives of Study

The primary aim of this study was to develop methods for the speciation of antimony based on chromatographic separations and utilising plasma spectroscopic determination. The key areas of interest were :

- Fundamental studies : Utilisation of synthetic Sb species for method development and investigation of Sb complexes.
- Environmental : This includes surface water, soil and plant samples from an antimony contaminated site.
- Industrial : Analysis of polymer leachates in water, acetic acid and ethanol.

This broad aim covered many sub-areas that will now be described in greater detail.

1.5.1. Antimony Speciation

The preceding review of the literature has clearly shown the chemistry of antimony is varied. Careful reading of many of the publications will show that the authors make reference to comparable reactions for arsenic. However, unlike arsenic, biogeochemical studies of Sb have been limited. This, in part, has been due to the assumed similarities between Sb and As, for example workers have applied similar protocols for As speciation to Sb speciation, especially in LC methods. The minimal level of success to date clearly shows that although Sb reactivity is similar, the chromatographic properties of Sb are not. Thus, a novel approach to Sb speciation is required, i.e. an assessment of the chromatographic development without bias. As such the straightforward development of chromatographic separations of Sb compounds is a major aim of this project.

In addition, Sb speciation on a wide scale cannot be realistically achieved when just two Sb species are used for method development. Thus other potentially soluble Sb species need to be investigated and incorporated into the chromatographic methodology, i.e. the Sb, α -hydroxyacid complex system and methylated species of Sb. If Sb does form complexes with α -hydroxyacids then it is conceivable that they will have different chromatographic properties to the parent Sb compound under a given chromatographic protocol. Thus, if such an interaction can be identified and quantified then the number of Sb species available to characterise the separation methods increases, improving the robustness of the method.

1.5.1.1 Environmental Samples

The identification of a suitable site in which antimony was present and had been present for a great many years was required. This would hopefully provide an ecosystem in equilibrium, where for example, the flora had had sufficient time to establish metabolic pathways for the Sb if indeed it could be metabolised as has been described in the literature⁽⁷⁸⁾. Although clearly many plants will survive as a result of not being effected by the presence of Sb because their metabolic pathways have not been disrupted.

A number of mine sites in S.W. England were considered as ores were assayed for Sb. However, a mine approximately 5 miles and to the S.E. of Plymouth was selected. Further details are given in Chapter 4.

The aims of the analysis of the samples taken from this site were 1) to ascertain whether Sb could be speciated in these samples by the methods developed for synthetic Sb compounds; 2) to see whether unknown Sb species in speciated samples could at least be assigned an oxidation state by the use of HG in-line with the chromatography-ICP coupling; and 3) to see whether dissolved complexing agents in the matrices will coordinate with synthetic spikes, providing some data that may fall in line with the work on α -hydroxyacid complexes.

1.5.1.2 Industrial Samples

Because of the extensive usage of Sb for industrial purposes it was deemed that any analytical procedure utilised had to include the investigation of solutions exposed to Sb of anthropogenic origin. Thus, an aim of this study was to determine if Sb leached into food simulants - water, acetic acid (3% v/v) and ethanol (95% or 15%) - from food contact polymers such as poly(ethylene terephthalate) (PET) could be speciated, assuming it was leached in more than one form.

The most recent literature⁽¹⁶⁴⁾ suggests that reduction processes for Sb can occur in polymerisation of PET, as such the form of Sb in the polymer may well differ from the catalytic form in which it was added.

1.5.2 Fundamental Studies

This aspect of the aims and objectives is primarily served by analysis of Sb solutions by methods other than by exclusively using HPLC coupled to ICP instrumentation. Specifically it is the analysis of Sb in the presence of α -hydroxyacids by instruments that can provide structural or molecular information on any complexes that may be formed in solution. Thus nuclear magnetic resonance (NMR) and electrospray ionisation - mass spectrometry (ESI-MS) will be used to investigate the effects of complexation on the ligands (NMR) and to determine molecular weights for complexes formed in solution (ESI-MS).

The post-analytical column assembly will also be investigated. The nebuliser and spray-chamber assembly is of increasing concern for workers involved with coupling HPLC with plasma instruments.

The aim is to find the optimum coupling of nebuliser type and spray-chamber to minimise peak-broadening and thus providing the best possible set-up for sensitive separations. This will be achieved by studying the effects of different combinations of nebuliser and spray-

chamber upon the resolution of separations, the signal-to-noise ratios and the stability of the response when using low-flow of mobile phase, $<0.5 \text{ ml min}^{-1}$.

The number of techniques and types of instrumentation used throughout this project has meant that a detailed discussion of the state of the art developments in this chapter is impractical. However, where appropriate, more detailed information is provided when specific to the aims of the study.

2.1 Principles of Chromatography

2.1.1 Introduction

Chromatography as originally described by the Russian botanist Mikhail Tswett comes from the Greek *chroma* meaning 'colour' and *graphein* meaning 'to write'⁽¹⁶³⁾. Thus, when Tswett first developed column chromatography it was applied to the separation of plant pigments through a CaCO_3 packed glass column. The separated components appeared as coloured bands, hence his term for the method, although some might say he named the method after himself in a roundabout way as Tswett or tsvet means 'colour' in Russian⁽¹⁶⁵⁾. Indeed Tswett defined chromatography simply by stating that the method in which different components of a mixture are separated on an adsorbent column in a flowing system is a "chromatographic method". Thus, he was also stating colourless compounds could also be separated this way.

However, a more general definition arose from a special committee of the International Union of Pure and Applied Chemistry⁽¹⁶⁶⁾. Suffice to say chromatography should be viewed as a method of separation in which the components to be separated are distributed between two phases, the stationary and the mobile phase. It is the level of distribution which determines the effectiveness of the separation and the value of the information that can be obtained for qualitative and quantitative determinations.

The importance of chromatographic methods is clearly demonstrated by the statistic that between 1937 and 1997 at least 12 Nobel prizes were awarded for work where chromatography played a pivotal role.

2.1.2 Categories of Chromatography.

Table 2.1 gives a list of categories of column chromatographic methods covering not just liquid chromatography (LC) but gas chromatography (GC), supercritical-fluid chromatography (SFC) and capillary electrochromatography (CEC).

Table 2.1 Classifications of column chromatographic methods with some examples of applications

Classification	Mode of separation	Applications
Liquid Chromatography (LC)	Reversed-phase	Antibiotics, Proteins, Dyes, PCBs, narcotics and drug metabolites, protein-bound Cd.
	Ion-pair	Amines, carboxylic acids, sulphonic acids and dyes.
	Size-exclusion	High molecular weight natural products, polymers & molecular-weight distribution measurements
	Ion-exchange	A wide range of inorganic anions and metal cations, amino acids and some carboxylic acid applications.
Gas Chromatography (GC)	Gas-liquid	Hydrocarbons, steroids, fatty acid methyl esters, alkaloids, alcohols,.....
	Gas-solid	Atmospheric analysis of H ₂ S, CS ₂ , NO _x , CO, CO ₂ , and the rare gases.
Supercritical-Fluid Chromatography (SFC)		Hydroxy polycyclic aromatic hydrocarbons.
Capillary Electrochromatography	Electroosmotic flow, separation based upon charge of analyte.	Steroids, PAHs, diuretics.

GC, SFC, and CEC are not reviewed in this thesis but the application of GC in the determination of Sb is highlighted in Chapter 1, Section 1.4.5.

2.1.3 Separation Parameters

2.1.3.1 Retention

Figure 2.1 represents the chromatographic separation of two species.

The terms annotating this figure are as follows: t_M is the dead-time of the chromatographic system, any peak at this point will be unretained species or due to a perturbation of the detector as a result of the solvent front. The retained species are characterised by the terms t_{TA} and t_{TB} , their retention times. The peak width at the base of the peak is w . From such a chromatogram virtually all of the calculations required to characterise and optimise the separation can be made.

Rather than retention time, a more reliable factor by which to identify species according to retention is the capacity factor, k' :

$$k' = (t_r - t_M)/t_M \quad (2.1)$$

This is analogous to a partition coefficient. If k' is greater than 10 the analysis time tends to be too long and if it is less than 1 then the eluting species will most likely not be adequately resolved.

The selectivity factor, α , is a measure of the separation of two consecutive peaks:

$$\alpha = k'_B/k'_A \quad (2.2)$$

The degree of separation, resolution (R_s), is measured in terms of retention times and their peak widths:

$$R_s = 2(t_{RB} - t_{RA})/(W_A + W_B) \quad (2.3)$$

The components are baseline resolved when $R_s \approx 1.5$.

Column performance is measured in plate numbers (N) or plate height (H). They are defined:

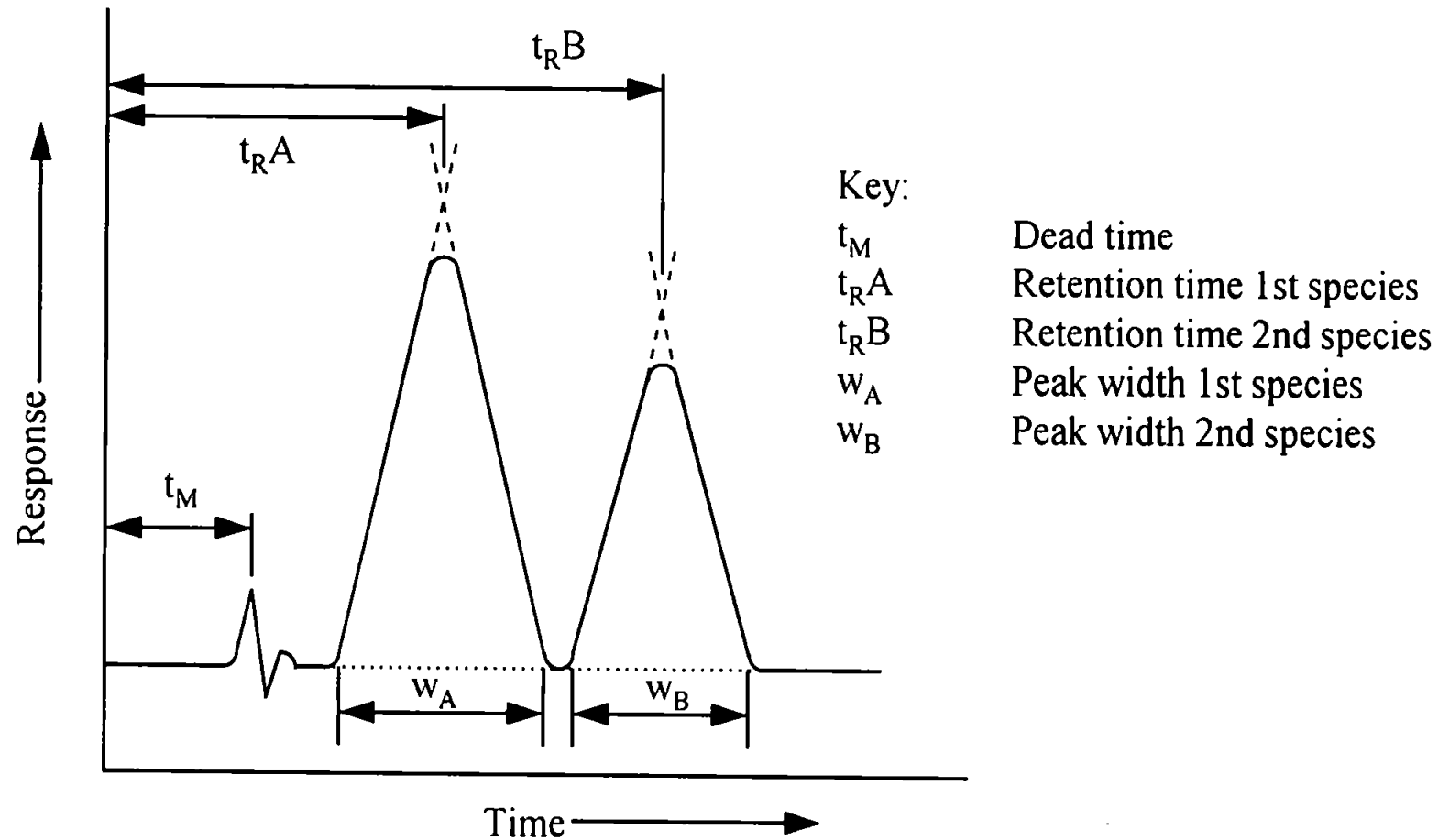


Figure 2.1. Representation of a Chromatographic Separation of Two Species

$$N = 16(t_R/w)^2 \quad \text{or} \quad 5.54(t_R/w_{1/2})^2 \quad (2.4)$$

$$\text{and } H = L/N, \text{ where } L = \text{column length} \quad (2.5)$$

Plate height is the more useful as it is a measure of the efficiency for unit column length.

The smaller the plate height the better.

All of the above factors can be related in the Resolution Equation :

$$R_s = 0.25(\alpha - 1/\alpha)(\bar{k}'/1 + \bar{k}')N^{1/2} \quad (2.6)$$

where \bar{k}' is the average capacity factor for the two species.

The capacity factor is controlled by stationary and mobile phase composition. Selectivity can be altered by stationary or mobile phase changes. Resolution is obviously heavily dependent upon the changes of both these factors but also plate number, N . Optimisation of an HPLC method tends to be a compromise process between analysis time and resolution sufficient for quantitative analysis of analytes.

2.1.3.2 Dispersion Mechanisms and Band Broadening

As the band of solute moves through the column there are three mechanisms that can cause dispersion and broadening of the band, observed in the chromatogram:

- 1) Eddy diffusion; A flow dispersion term. Arises from the different flowpaths that a solute takes through the column. The path differences are due to variable particle sizes and shape in the stationary phase. As such solute molecules travelling at the same speed but in different paths will travel different distances in a given time.
- 2) Longitudinal diffusion; Not an important factor in LC, but becomes more important the longer the analyte remains on column. This diffusion is in an axial direction to the column.

3) Mass Transfer;

This is related to the rate of the distribution process of the solute species between the mobile and stationary phases.

These factors can all be related in the van Deemter equation:

$$H = A + B/u + Cu \quad (2.7)$$

Where A is the flow dispersion term, B is longitudinal diffusion and C is the mass transfer term. The flow velocity (unit length s⁻¹) of the mobile phase is represented as u. Figure 2.2 gives the van Deemter plot which highlights how each term is related to each other and to flow velocity. The lowest point on the curve is where the optimum plate height conditions exist.

Extra-column dispersion, a factor which is dependent upon the connecting tubing pre- and post-column can also have a large effect upon band-broadening, however, this is discussed in greater detail in Chapter Five. A more detailed account of both the theory and practice of chromatography may be found elsewhere^(165,167-171).

2.1.4 Modes of Separation

The principal modes of LC are briefly described below with emphasis upon the modes utilised in this study. Table 2.2 gives the mode and separation characteristic for various forms of LC.

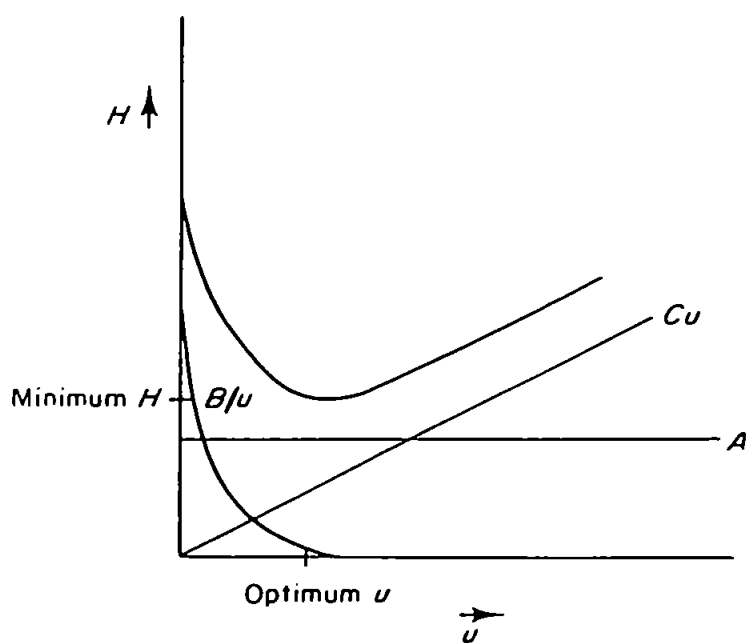


Figure 2.2. The van Deemter Plot

Table 2.2. Modes of LC separation and the general mechanism

Mode	Separation Mechanism
Reversed-Phase	Relatively non-polar stationary phase & variable polarity mobile phase. Separation based upon relative affinities of species for stationary phase. These columns can also be utilised for ion-suppression chromatography
Ion-Pair	Separation based upon formation of ion-pair between soluble sample ion and counter-ion in the mobile phase and their distributions in the stationary/mobile phases.
Ion-Exchange	The packing surface is functionalised such that sample ions bind in competition with exchanging ion in the mobile phase. Depending upon the extent of cross-linking these columns can demonstrate mixed mode characteristics where two separation mechanisms might be involved.
Size-Exclusion	Molecules separated by size during their migration through porous packing material.

Each mode of LC in Table 2.2 exploits some chemical or physical characteristic of the sample in such a way that the general working definitions for chromatography in Section 2.1.1 are met. Size-exclusion chromatography (sometimes described as gel filtration or gel permeation) is predominantly applied to high-molecular-weight samples such as proteins and synthetic polymers with a typical application being to measure molecular-weight-distributions. This method of separation is probably the simplest to characterise as it is not complicated by ionisation of the molecules or polarity.

Ion-pair chromatography is a mode of separation that typically is described as a hybrid of reversed-phase (RP) and ion-exchange chromatography. The stationary phase is often the same as for RP which is described in the next section, and the mobile phase is made up of an aqueous buffer and organic solvent and to this is added a counter-ion. The counter ion should be of opposite charge to the sample analytes, i.e. the analysis of carboxylic acids in

a mobile phase at a pH which maintains the compounds in the form RCOO^- , the counter-ion would be a cation such as tetrabutylammonium. The separation is thus achieved by distribution of the ion-pair which is retained on the non-polar stationary phase.

In ion-exchange chromatography the packing is functionalised with charge-bearing groups. Figure 2.3 gives an example of the type of packing typically utilised for ion-exchange columns. The core is chemically and mechanically inert and non-porous, and typically 5-15 μm in diameter. The surface of the particle is cross-linked and sulfonated. This permits the use of HPLC solvents. Figure 2.4 shows a structural representation of cross-linked polystyrene divinylbenzene copolymer with sulfonate groups. The outer layer consists of very much smaller (0.1 μm) ion-exchange beads. This is where the chromatography occurs. The pellicular configuration means that a high loading capacity is achieved while maintaining short diffusion paths allowing high efficiency and selectivity. The retention mechanism is determined by the functional group, if it is a cation then the sample ions to be separated will be anionic, the converse is true for cationic sample ions. Table 2.3 gives typical functional groups.

Table 2.3 Functional groups used in ion-exchange chromatography (IEC) and their ion exchange strength

Functional Group	Ion-exchange mode
Sulphonate, $-\text{SO}_3\text{H}^+$	Strong cation exchange
Carboxylate, $-\text{COOH}^+$	Weak cation exchange
Quarternary ammonium, $-\text{N}(\text{CH}_3)_3^+\text{OH}^-$	Strong anion exchange
Amine, $-\text{NH}_3^+\text{OH}^-$	Weak anion exchange

IonPac's Pellicular Anion Exchange Resin Bead

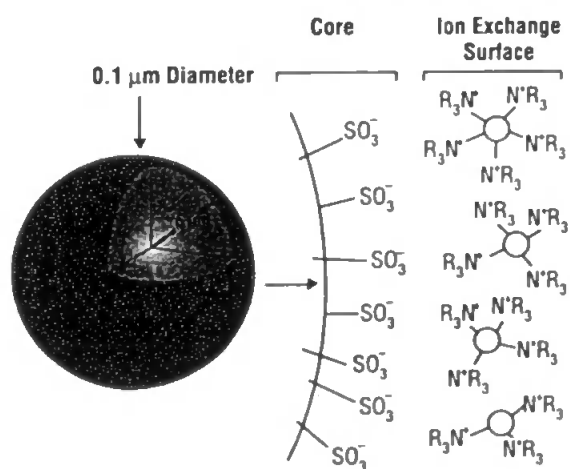


Figure 2.3 Diagram showing the make-up of IonPac packing material and functionalisation utilised by Dionex

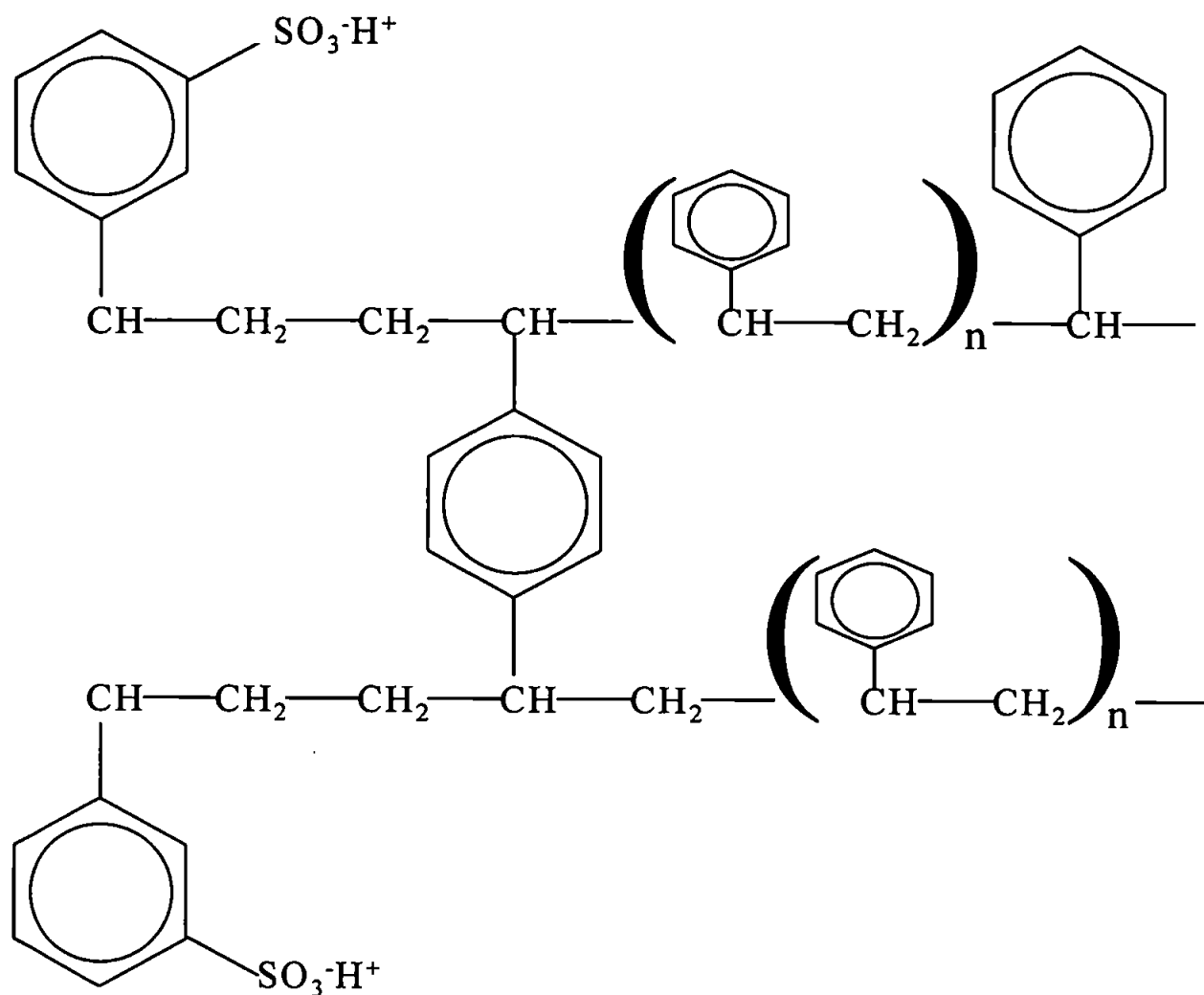


Figure 2.4 Structural representation of cross-linked polystyrene divinylbenzene copolymer with sulfonate groups.

The extent of cross-linking determines the rigidity of the polymer, low cross-linking percentage allows greater swelling in aqueous buffers and with larger pores larger sample molecules can undergo ion exchange. With a greater percentage of cross-linking comes increased rigidity and increased hydrophobicity. There is another effect of extensive cross-linking with a relatively non-polar aromatic polymer that needs to be considered. If there is an affinity of the analyte for such a polymer then there is a possibility that ion-exchange will not be the only mechanism by which these columns can operate. This possibility is

explored in more detail in Chapters 3, 4 and 5. Aqueous salt solutions are usually used as the mobile phase in IEC, it is often buffered, and sometimes contains an organic solvent (though this is column dependent). The pH, ionic strength and organic component associated with the mobile phase are the controlling factors in the efficiency of the separation and some predictions can be made as to retention characteristics of sample analytes, but, each system should be optimised for these parameters individually because column performance can vary widely.

Reversed-phase chromatography is utilised for separations that rely upon characteristics such as the polarity of the sample analytes. A relatively non-polar stationary phase is used such as C₈ or C₁₈ hydrocarbon. The mobile phase is usually aqueous (very-polar) solutions typically as the base solvent with varying concentrations of miscible organic solvents to adjust the polarity. The solutes are separated according to their affinity for the stationary phase. The more polar they are the more rapidly they elute. Typical organic modifiers used are methanol and acetonitrile.

A form of ion chromatography, ion-suppression chromatography can be carried out using both standard C₈ and C₁₈ columns or cross-linked columns. In, for example, the ion-suppression chromatographic separation of weak organic acids the eluent used would reduce the pH of the sample to a point at which the acids are not ionised (undissociated) and therefore are separated according to their adsorption and distribution behaviour with the stationary phase. The cross-linking polymers utilised in ion-exchange columns can also act as a relatively non-polar stationary phase for a similar separation. The Ionpac and Omnipac family of columns manufactured by Dionex have been recognised as having the ability to operate in a mixed-mode (ion-exchange and reversed-phase and, by definition, ion-suppression) by virtue of the packing construction. This makes the clear chromatographic interpretation open to debate.

2.2 Atomic Spectroscopy

2.2.1 Introduction

There are three principle forms of atomic optical spectroscopy; 1) atomic emission; 2) atomic absorption; and 3) atomic fluorescence spectroscopy. All three rely upon the absorption of energy by the atom either by heat, electrical, chemical or electromagnetic radiation energy. Figure 2.5 illustrates the process for each form of spectroscopy. Emission and fluorescence determinations are made by measuring the radiant energy after absorption whereas absorption determinations are made by measuring the amount of electromagnetic radiation that is absorbed, namely the attenuation of the beam⁽¹⁷²⁾.

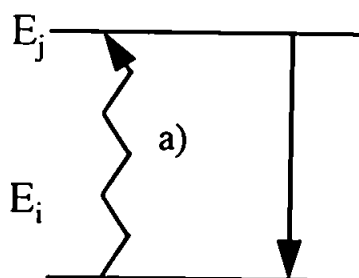
The processes by which line spectra for elements are formed and their measurement are very well explained by Skoog and Leary⁽¹⁶³⁾ or Ebdon *et al.*⁽¹⁷³⁾ and do not require exhaustive description here. However, an overview of atomic emission spectroscopy (AES) as used in this study is included with particular reference to the factors relevant to later discussion.

2.2.2 Inductively Coupled Plasma-Optical Emission Spectroscopy

2.2.2.1 The Inductively Coupled Plasma (ICP)

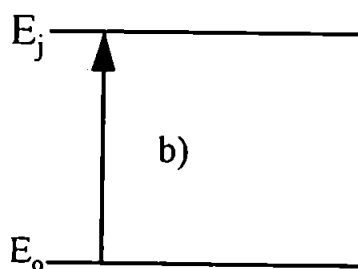
As has already been mentioned, S. Greenfield and V.A. Fassel developed the ICP as a source for AES. Figure 2.6 gives a schematic of a torch and the ICP. The torch consists of three concentric quartz tubes. Through the two outer tubes flows a tangential stream of gas, normally argon. Ebdon *et al.*⁽¹⁷³⁾ proposed a working definition for a plasma as '....a partially ionised gas with sufficiently high temperature to atomise, ionise and excite most of the elements in the Periodic Table'. Thus the tangential flow of gas needs to be ionised to form a plasma. This is achieved by coupling radio-frequency energy into the gas via an induced magnetic field. This is shown in Figure 2.6. The RF energy is supplied at

Atomic
Emission
Spectroscopy



Absorption Process
a) Heat or Chemical
b) $h\nu$
c) $h\nu$

Atomic
Absorption
Spectroscopy



Emission Process
a) $h\nu$
b) No-emission
c) $h\nu$

Atomic
Fluorescence
Spectroscopy

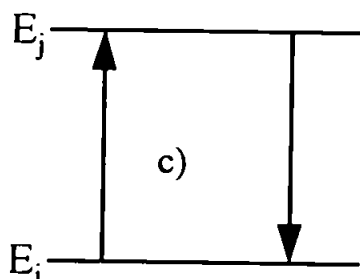


Figure 2.5. Processes of absorption/emission of energy in AES, AAS and AFS

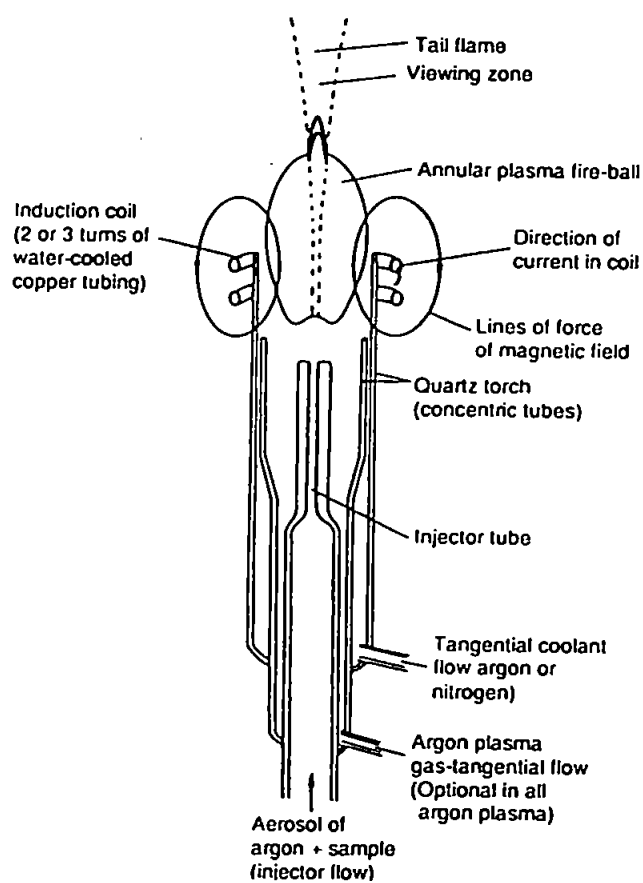


Figure 2.6. Schematic diagram of a torch and inductively coupled-plasma

frequencies between 27-40 MHz, delivering forward powers between 500-2000W. The current flow through the coil induces a magnetic field according to the right-hand rule⁽¹⁷⁴⁾.

The gas is then seeded with electrons, via a spark or tesla coil. These electrons accelerate in the magnetic field until they have enough energy to ionise the gaseous atoms in the magnetic field. Following further collisions with other gaseous atoms more ionisation occurs until the plasma becomes self-sustaining, this might be described as a 'cascade effect'. This process is almost instantaneous. The plasma fire-ball is generated by collisional energy exchange of the neutral argon by the electrons and ions in the magnetic field.

Because of the tangential flow of the outer gases, and the revolving nature of the plasma there is a 'weak spot' at the base in the centre which may be considered the eye of a very hot storm. As such the sample can be introduced in another gas flow through the third inner concentric tube. The hottest parts of the plasma can reach 8000-10000K, however the analytically useful part is in the tail-flame where the temperatures are around 5000-6000 K.

2.2.2.2 Sample Introduction

The sample introduction set-up for any ICP-AES is made up of three parts; i) the pump; ii) the nebuliser; and iii) the spray-chamber. The pump is typically a stand-alone or integrated peristaltic pump. This not only pumps sample to the instrument but also removes waste. The nebuliser acts to smash the solution into an aerosol with the nebuliser gas to form droplets small enough to be carried by this gas to the plasma. The spray-chamber serves to separate the small desired droplets from the large droplets with the latter being collected and pumped to waste. A typical arrangement is shown in Figure 2.7.

Obviously it is the nebuliser/spray-chamber set-up which is the most critical aspect of sample introduction to the plasma. When introducing solutions for analysis, the make-up of the matrix itself can affect the choice of nebuliser. The range of matrix types that can be analysed by this instrument is wide, from ultrapure waters or acid-solutions with a very low

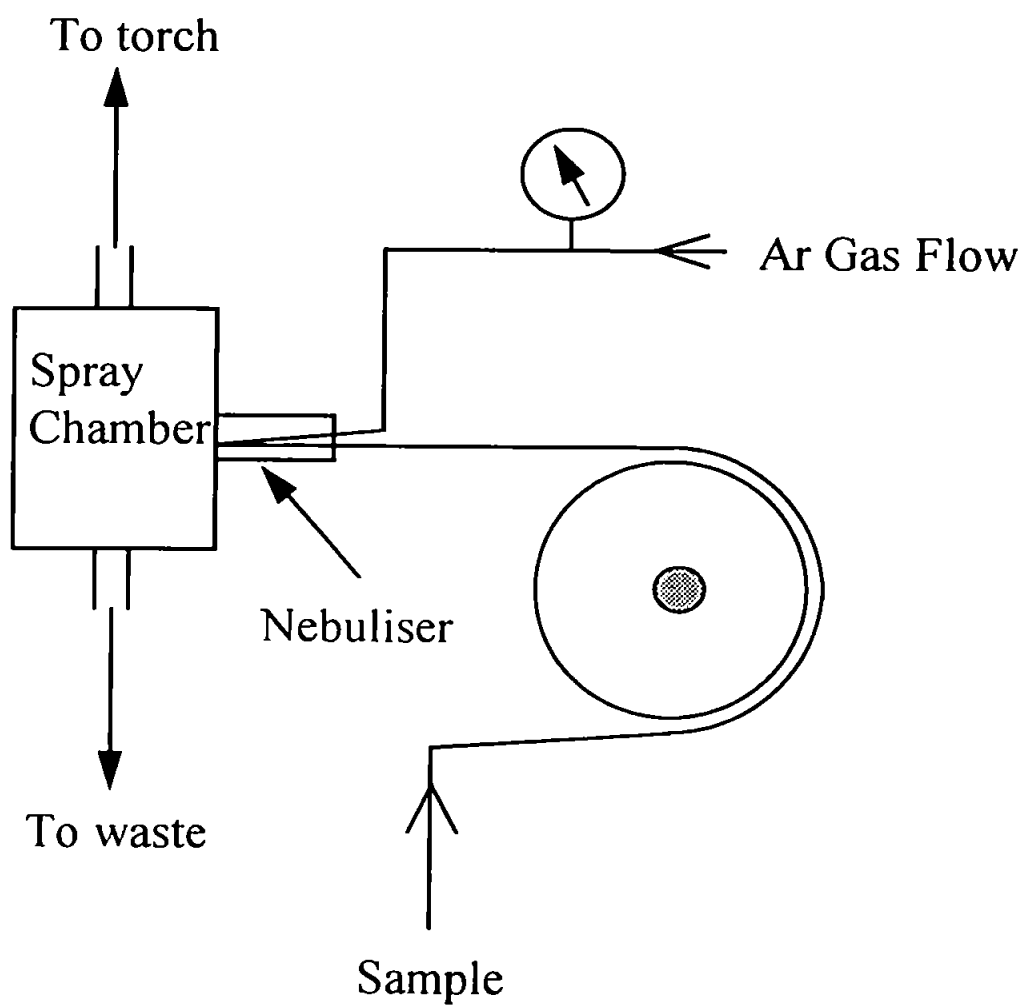


Figure 2.7 The components of a typical sample introduction arrangement for ICP

dissolved solid content up to slurried samples, where dissolved solids are considerably less important than suspended solids. Very high slurry concentrations, slurries or viscous matrices will not be analysed by an ICP instrument. However, the range of matrices that can be analysed means that no one nebuliser is ideal for all types of analysis. This is because some nebulisers have been designed for very low dissolved solid work and particulates would block such a nebuliser. The particulars of nebuliser design and primary role are given in Chapter Five.

There are several types of nebuliser available for ICP-AES that can meet the varying requirements for analytical methodology. They are:

- 1) Pneumatic nebulisers; concentric(Meinhard) and crossflow.
- 2) Glass frit/metal grid type.
- 3) Ultrasonic.
- 4) Babington-type; v-groove, de Galan and Burgener.
- 5) Direct Injection Nebulisers (DIN)
- 6) Micro-concentric Nebulisers (MCN)

Schematic diagrams for many of these types of nebuliser are given in Figure 2.8.

In pneumatic nebulisation the velocity of the gas creates a pressure-drop which sucks up, draws out and shatters the liquid into small droplets. This is known as the venturi-effect, and is shown in Figure 2.9. These types of nebulisers can only operate efficiently for solutions that contain less than 1% dissolved solids. Any suspended particles could block such a nebuliser. In the case of glass concentric (Meinhard type) nebulisers, such a blockage could render the nebuliser permanently unusable.

The glass frit and metal grid type nebulisers work by depositing sample onto the frit or grid and then shearing the sample with a high velocity nebuliser gas. These nebulisers have improved transport efficiency when compared to pneumatic nebulisers but can be affected by deposition if solutions contain high dissolved solids.

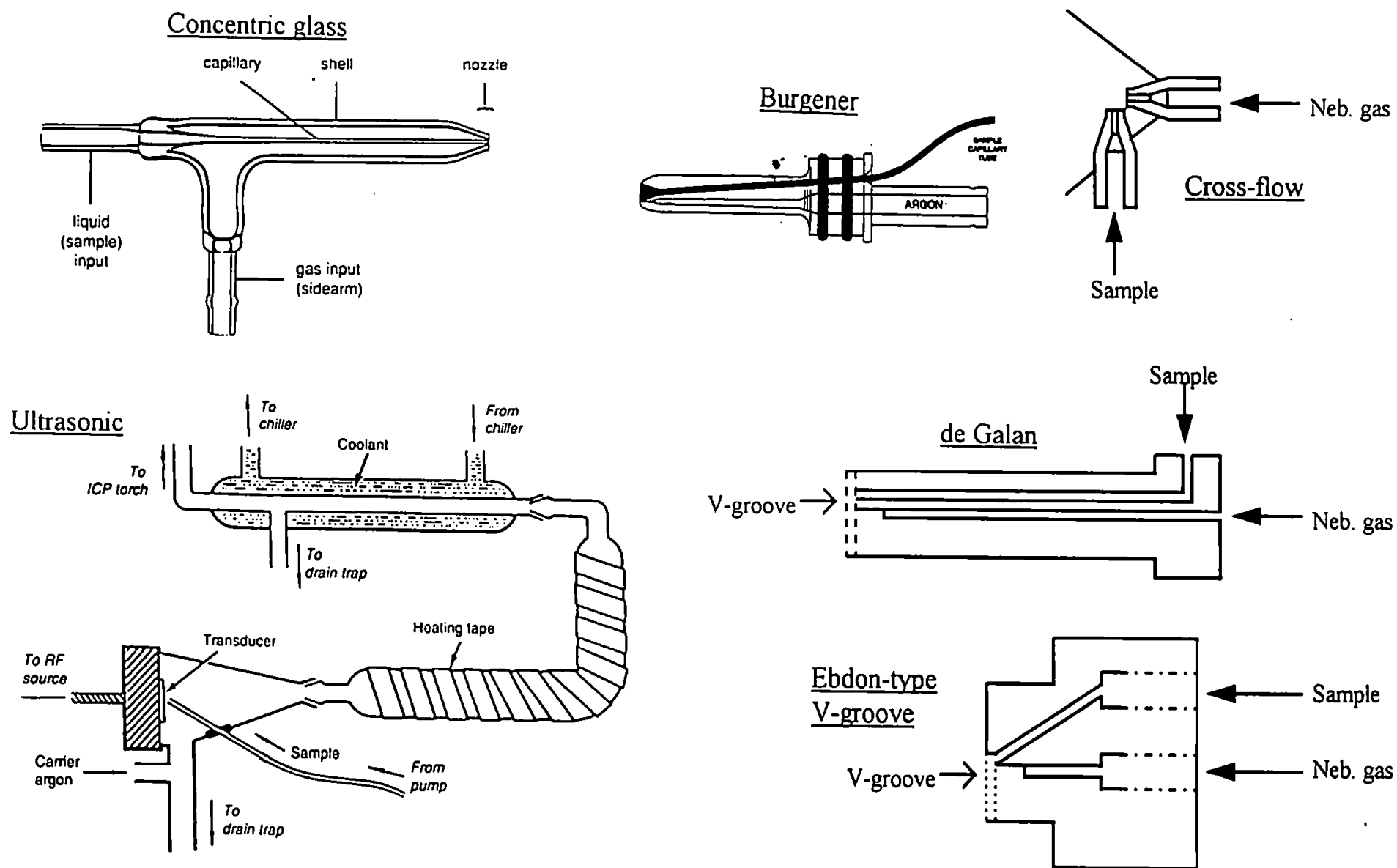


Figure 2.8 Nebulisers utilised for sample introduction to ICP-AES

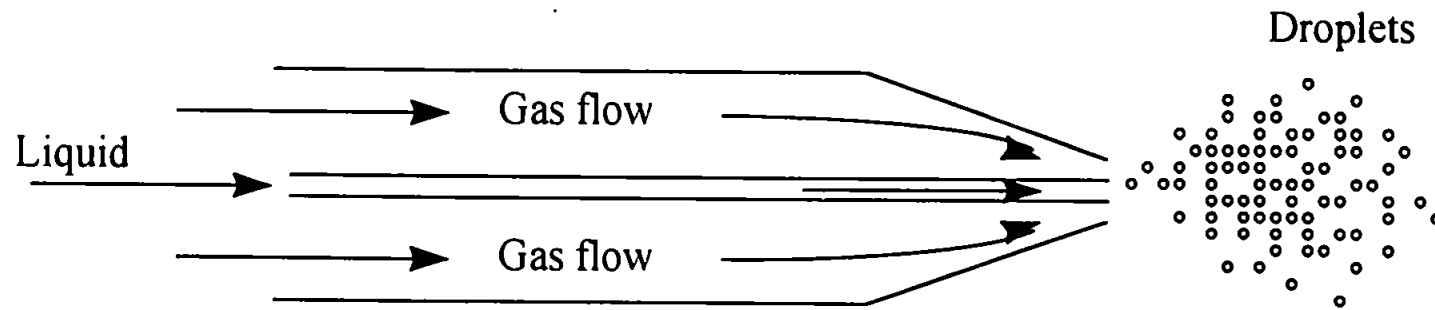


Figure 2.9 The Venturi effect

Ultrasonic nebulisers form an aerosol by rapid vibration of the sample solution. This vibration is achieved by the application of RF energy to a transducer plate onto which the sample is deposited. The sample transport can be as much as 15%⁽¹⁷³⁾, but such a large level of solvent vapour could impinge upon the plasma stability, as such desolvation of the vapour with a heater/condenser set-up is usually required.

With the requirement to analyse samples that have a high dissolved solids content or indeed slurried samples a different nebuliser is needed. For these purposes Babington-type nebulisers are used or variants of this nebuliser in principle. Essentially the sample is pumped through a large 'unblockable' orifice, runs down a groove over a tiny gas orifice. The high velocity of the emerging gas smashes the sample into droplets.

The spray-chamber is essential to remove large droplets from the gas carrier in order to prevent fluctuations in the plasma caused by these droplets. They can be made from glass or inert polymers.

There are fundamentally three types of spray-chamber in common use:

- 1) The double-pass (Scott-type);
- 2) Single-pass, with impact bead; and
- 3) The cyclonic spray-chamber.

Figure 2.10 a-c) gives diagrams for examples of each type. The first example, the double-pass, is probably the most common, but like the single-pass the design suffers from a very poor sample transport efficiency, approximately 1%⁽¹⁷⁵⁾. The cyclonic spray-chamber greatly improves the transport efficiency⁽¹⁷⁶⁾. This general design principle has been intensively researched since 1992⁽¹⁷⁶⁻¹⁸⁰⁾ in order to further improve transport efficiency and reduce washout times.

The most influential design change has been the introduction of a dimple in the main body of the chamber, illustrated in Figure 2.10 d). The general processes of the nebuliser and spray-chamber designs mentioned here are extensively reviewed by Sharp^(181,182), and the

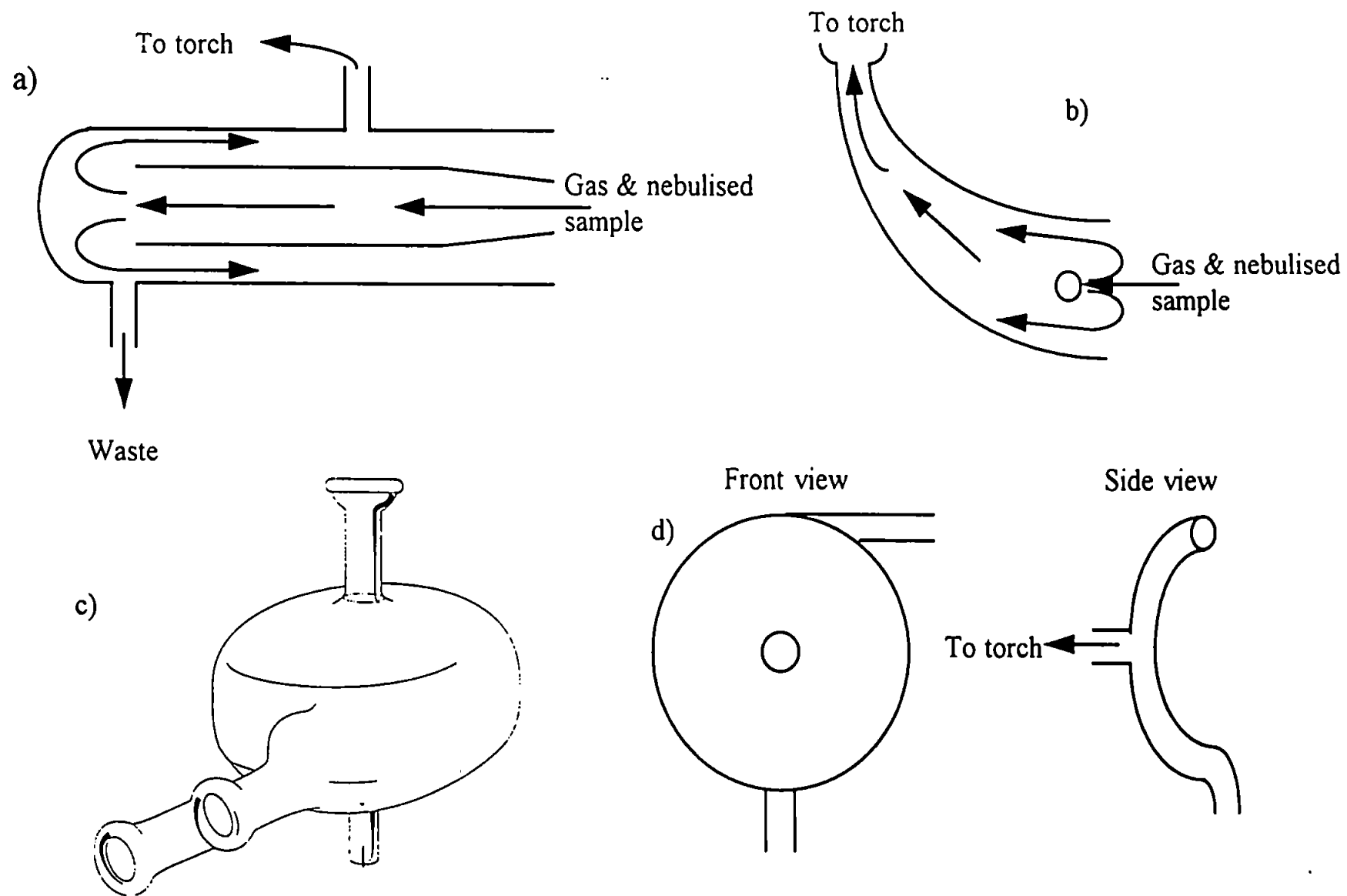


Figure 2.10 Spray chambers for ICP. a) The double pass; b) singlepass with impact bead; c) cyclonic spray chamber; and d) dimple modified cyclonic spray chamber

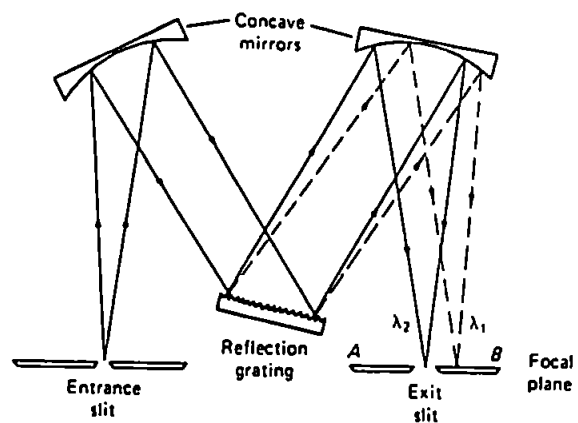
dimple-modified cyclonic spray-chamber is discussed in greater detail in Chapter Five with special reference to the impact of spray-chamber design and nebuliser selection on chromatographic separations with ICP-MS detection.

However, whatever the choice of nebuliser and spray-chamber, the aerosol is swept to the ICP torch by the nebuliser gas flow. Here the nebuliser gas punches the plasma giving its distinctive annular doughnut-shape. It is the passage through the plasma where rapid desolvation, decomposition and atomisation of the sample occurs. The sample is then in the required gaseous atom state where they are then ionised and excited by the collisional or charge-transfer processes in the plasma. The absorbed energy is then re-emitted and detected by the optical spectrometer.

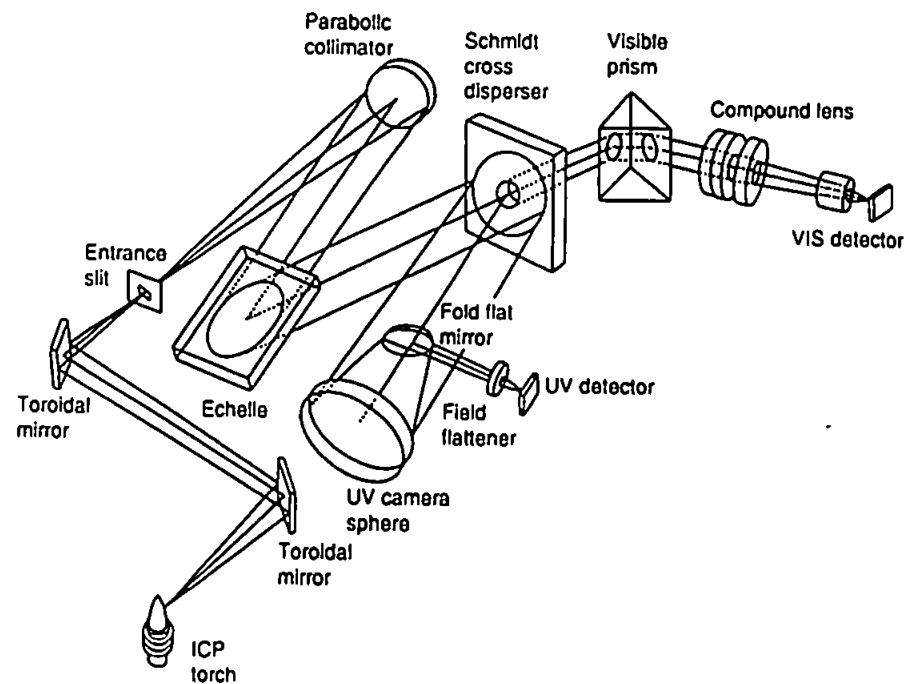
2.2.2.3 Optical Spectrometer

The atomic emission from the analytes in the plasma is focused by monochromator pre-optics through an entrance slit and into the monochromator. There are commonly two types of wavelength selector employed by instrument manufacturers. One is the grating monochromator often based on the Czerny-Turner geometry. The second is based upon the echelle monochromator with a cross dispersion system. The first type is typically employed in sequential instruments, i.e. where one wavelength is measured at a time, whereas the second type will allow analysis of most of the spectrum at once.

Figure 2.11 gives example schematics of both types of monochromators. From Figure 2.11 a) it can be seen that the emitted radiation coming through the entrance slit is incident upon the first concave mirror which collimates the radiation into a parallel beam to the grating. The grating then disperses the radiation into its component wavelengths. This dispersion is achieved by diffraction at the grating surface. Modern instruments using holographic grating have as many as 6000 lines/mm. Wavelength and diffraction are associated by the grating equation;



a) Czerny-Turner grating monochromator



b) Echelle-grating cross dispersion monochromator

Figure 2.11 Schematic diagrams for monochromator types used in ICP-AES

$$n\lambda = d\sin\theta \quad (2.8)$$

where λ is the wavelength, d is the distance between lines on the grating, n (an integer, 0, 1, 2...) is called the order of diffraction and θ is diffraction angle. However, for any given θ there will be several different wavelengths. The overlapping of orders and wavelengths can be reduced by blazing the grating, i.e. tilting the facets at an angle to the grating surface between rulings. These types of grating can be designed in such a way as to concentrate as much as 90% of the first-order diffraction (the most intense). So, now the blaze wavelength λ_b is related to the blaze angle ϕ ;

$$\lambda_b = d\sin 2\phi \quad (2.9)$$

Thus the incident light is diffracted to a lesser or greater degree depending upon its wavelength therefore achieving a spatial separation of wavelengths. Figure 2.11 a) shows the diffracted light incident upon a second mirror which focuses the selected wavelength on the exit slit. Rotation of the grating will focus different wavelengths on this exit slit.

An echelle grating has a blaze angle that is large and typically much less lines per millimetre (≈ 100). This results in a ruling a few hundred times wider than the average wavelength to be studied. The large blaze angle results in large angles of diffraction, i.e. the angle of refraction approaches that of the angle of incidence, so that the grating equation becomes;

$$n\lambda = 2d\sin\beta \quad (2.10)$$

where β is the diffraction angle. Echelle gratings work at high orders and as such are capable of high dispersion such that the variation of wavelength across the focal plane is significantly improved. Because of the high order there is again the problem of overlap. Figure 2.11 b) shows a cross-dispersion system. This effect introduces a second dimension to the dispersed radiation. As such a suitable detection system could take advantage of this effect and provide simultaneous detection of many elements at the same time.

2.2.2.4 Detection and Data Manipulation

There are two main methods of signal detection utilised by ICP-AES manufacturers. The first type is the photomultiplier tube (PMT). There are side-on and end-on configurations but the principle of operation is the same. The emitted radiation, of energy $h\nu$, is incident upon a photoemissive cathode which ejects electrons. These electrons are voltaically accelerated towards dynode 1. For every electron strike of the dynode approximately five are ejected. These ejected electrons then strike another dynode, ejecting yet more electrons and so on through yet more dynodes, between 9-16 depending upon the tube. At the last dynode stage is an anode and the current measured at this anode is directly proportional to the radiation reaching the PMT. A nine-dynode PMT ejects up to 10^7 electrons per photon striking the photoemissive cathode.

The other type of detector employed primarily with the spectrometer configuration in Figure 2.11 b) is the charge-transfer device. These are either charge-injection or charge-coupled devices (CID, CCD). These detectors can handle large parts of the spectrum and in many orders. It does this by taking an 'electronic photograph'⁽¹⁷³⁾.

These devices have linear arrays of photodetectors on a silicon chip. Each array is segmented with each segment able to detect 3 or 4 analytical lines. These sub-arrays are made up of photosensitive pixels and the positions on the chip correspond to the locations of the desired emission line. So, the emission is initially registered on the photosensitive arrays, this charge is then transferred to the storage register and then to the output register. The photosensitive arrays are then wiped electronically ready to receive a fresh signal.

The signals from these detectors are nearly always amplified and converted to a digital signal by an analogue-to-digital converter (ADC). This allows very rapid processing of the

emission into a form that can be utilised analytically, tied in with software that handles the analytical procedure, calibrations, calculations of concentrations in samples, check standards etc.

These types of instrument are primarily manufactured for the routine analysis of continuously nebulised samples rather than the analysis of a discrete volume of sample introduced chromatographically or by flow injection. Many instruments require modifications to the sample introduction assembly to accept a chromatographic flow and the software needs to be either modified or circumvented entirely. This study is primarily concerned with the coupling of chromatography to the plasma spectrometers. This means that any sample entering the plasma will have been in a discrete volume, i.e. the volume of the sample loop in the injection valve. Thus the instrument needs to be able to handle data on a temporally.

Of the two instruments used in this project one has software where a time display of up to 600s is incorporated. Typically this would be used to assess spray-chamber washout characteristics for a particular matrix, but can also be used to aid chromatographic development. Unfortunately, as is very common in such instruments, there is no provision in the software for peak integration. The second instrument has no such time display function, but data acquisition parameters can be programmed in such a way as to take data points at short time intervals thereby allowing the gathering of temporal data and the formation of a chromatogram. This instrument had no integration software. Software packages have been produced and marketed that could handle the output but were not available for this project. However, the sequential instrument that uses a PMT, an analogue detector, also has a direct output from the PMT. Via a high-low-ground connection a chromato-integrator can be interfaced directly with the PMT allowing peak integration to be carried out directly. The particulars of each instrument in terms of the data acquisition parameters are given in the relevant results chapters.

2.2.3 Inductively Coupled Plasma-Mass Spectrometry (ICP-MS)

The formation of the ICP is discussed in section 2.2.2.1. Sample introduction to an ICP-MS is essentially the same as for ICP-AES, except for the geometry. Figure 2.12 a&b) compares typical geometries of ICP-AES and ICP-MS set-ups. The effect of this difference is that for ICP-MS the plasma, and therefore the sample, is incident upon the analyser rather than at right angles to the analyser in the case of most ICP-AES instruments. As such ICP-MS tends not to be used for samples that may have a high dissolved salt content or organic content, although modifications are possible to overcome problems associated with these matrices. This aspect is discussed in more detail in later sections. It is important to state that some ICP-AES instruments are now being constructed with identical geometries to the ICP-MS so similar sampling considerations should be made for these instruments. The purpose for the modified geometry for ICP-AES is that by viewing the plasma axially (end-on), rather than radially (side-on) as is shown in Figure 2.12 a), more of the emission can be sampled.

2.2.3.1 Ion formation in the plasma.

Ionisation of atoms in the plasma can be caused by a range of processes:

- 1) Penning ionisation - caused by collisions between ground state atoms and Ar metastable species;
$$\text{Ar}^m + \text{X} \rightarrow \text{Ar} + \text{X}^+ + \text{e}^-$$
- 2) Charge transfer;
$$\text{Ar}^+ + \text{X} \rightarrow \text{Ar} + \text{X}^+$$
- 3) Ion-atom collision;
$$\text{Ar}^+ + \text{X} \rightarrow \text{Ar}^+ + \text{X}^+ + \text{e}^-$$
- 4) Atom-atom collision;
$$\text{Ar} + \text{X} \rightarrow \text{Ar} + \text{X}^+ + \text{e}^-$$
- 5) Electron impact;
$$\text{X} + \text{e}^- \rightarrow \text{X}^+ + 2\text{e}^-$$

As most elements are almost always singly ionised in the Ar ICP it is an ideal source for mass spectrometry, i.e. when the charge on a metal ion is +1 and is detected as a function of its mass/charge ratio (m/z) it can simply be handled as detecting its mass.

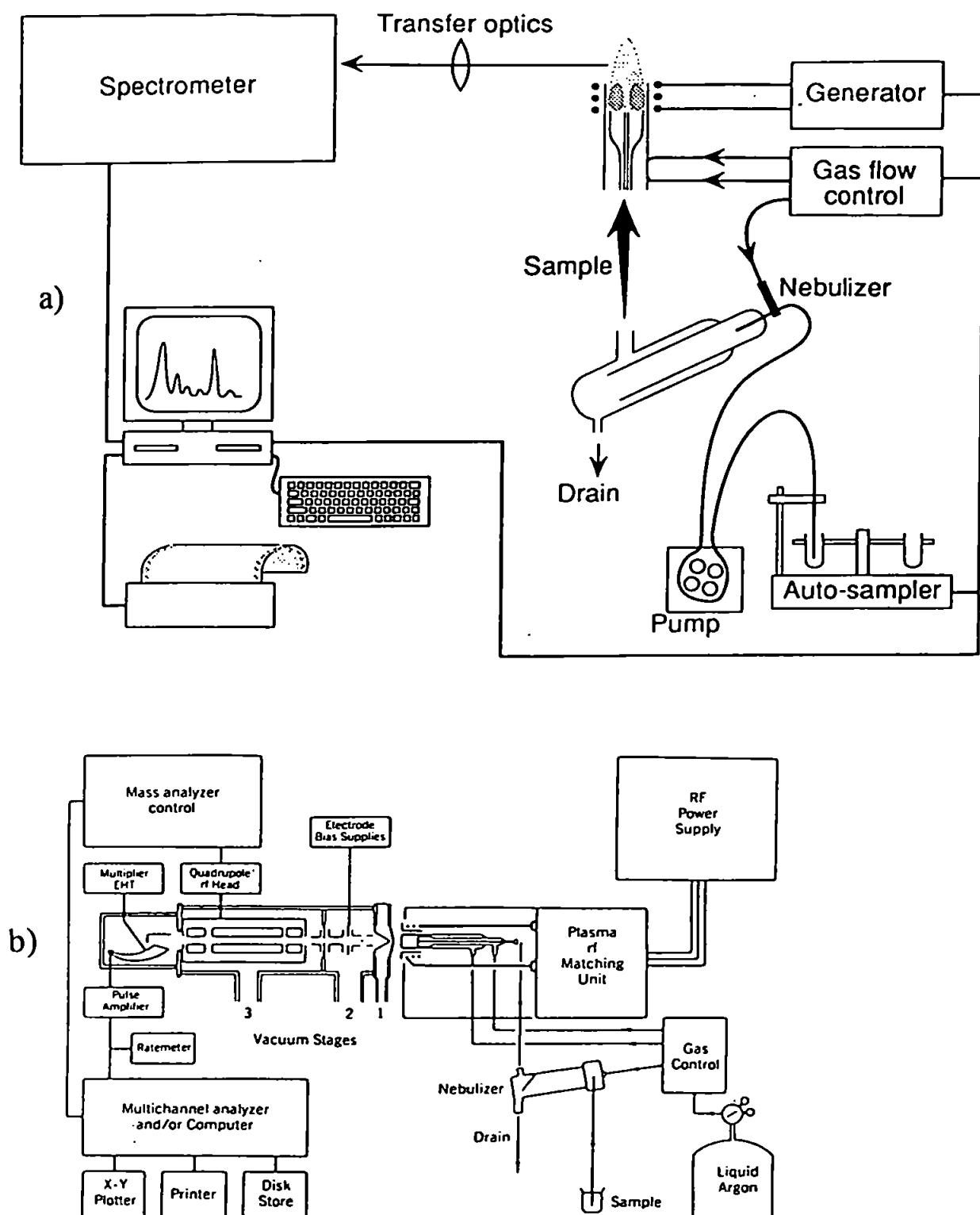


Figure 2.12 Schematic diagrams of typical arrangements for
a) ICP-AES and b) ICP-MS

2.2.3.2. ICP-Mass Analyser Interface.

The first successful construction of the ICP-mass analyser interface was achieved by Houk *et al.*⁽¹⁸³⁾ by placing the plasma source in direct contact with the sampling interface where the ions were extracted through a series of differentially pumped vacuum chambers. Figure 2.13 gives a typical schematic diagram of the interface and mass analyser arrangement.

The source is aligned with a sampling cone behind which the pressure is ca. 2×10^{-3} atm, this is the expansion chamber, and is named thus because the plasma gas and analyte ions expand through the sampling cone orifice. The skimmer cone protrudes into the expansion zone and analyte ions pass through the skimmer cone orifice into a second vacuum chamber where a series of ion lenses are in place to form the ion beam prior to entering the mass analyser. The photon stop is used to prevent photons from the plasma reaching the detector and contributing to the background.

The mass analyser is in almost all cases based upon a quadrupole although high resolution-ICP-MS instruments based upon magnetic sector arrangements are increasingly being used. For the purposes of this discussion only quadrupole mass analysers will be considered.

The quadrupole is made up of four metal rods, cylindrical or hyperbolic in cross-section. RF and DC voltages are applied to each pair of rods as shown in Figure 2.14. Thus an electric field is created in the region bounded by the rods. The RF/DC ratio determines which ions can pass through to the detector. By scanning this ratio, ions of consecutively higher m/z can be allowed to pass through with the others striking the rods where they are eliminated. Such scanning is done incrementally and very rapidly. A mass scan of 2-260 m/z can take less than 100 ms. If only a small number of m/z ratios are required then the RF/DC ratio can be adjusted to select those m/z values in turn, this is known as 'peak-hopping'.

For most ICP-MS instruments the resolution of a quadrupole mass analyser is between 12-350 with peak widths of approximately 0.8. However, a number of possibilities for

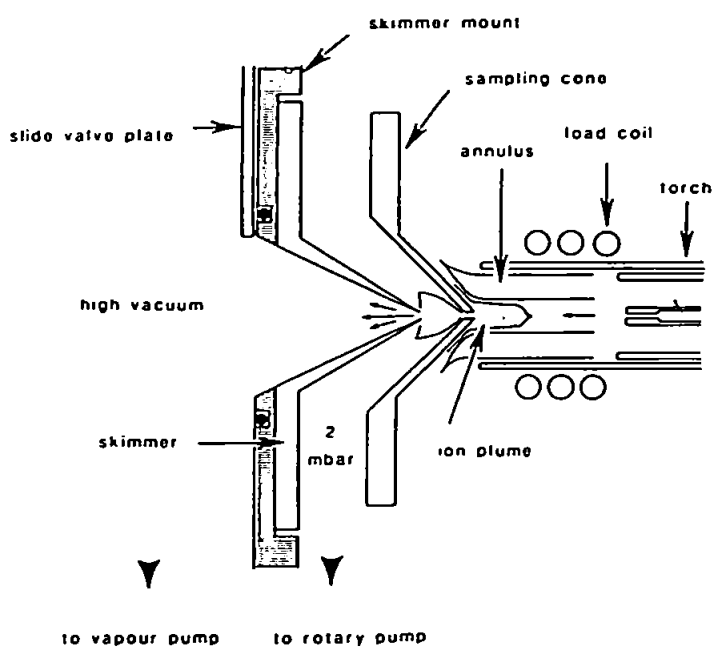


Figure 2.13 Schematic diagram of a typical ICP-MS interface

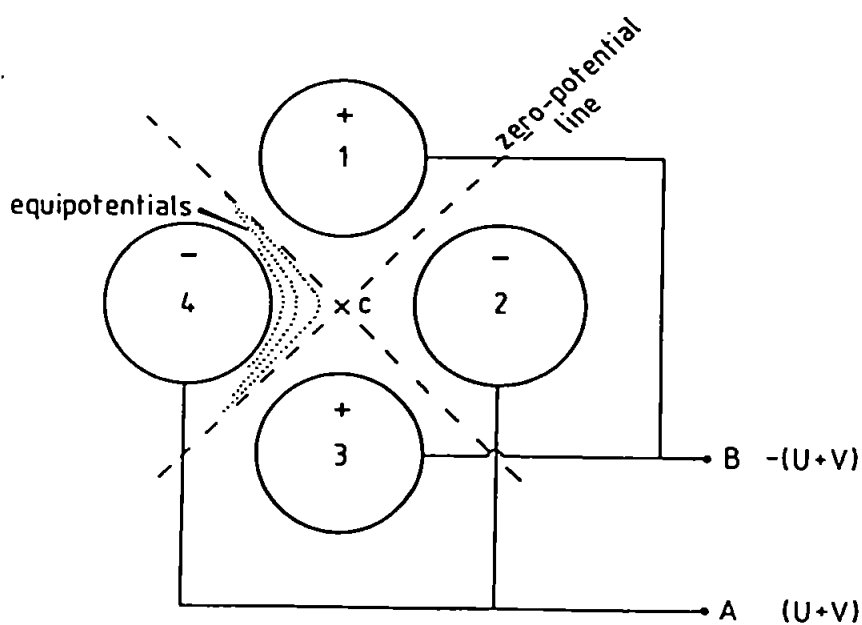
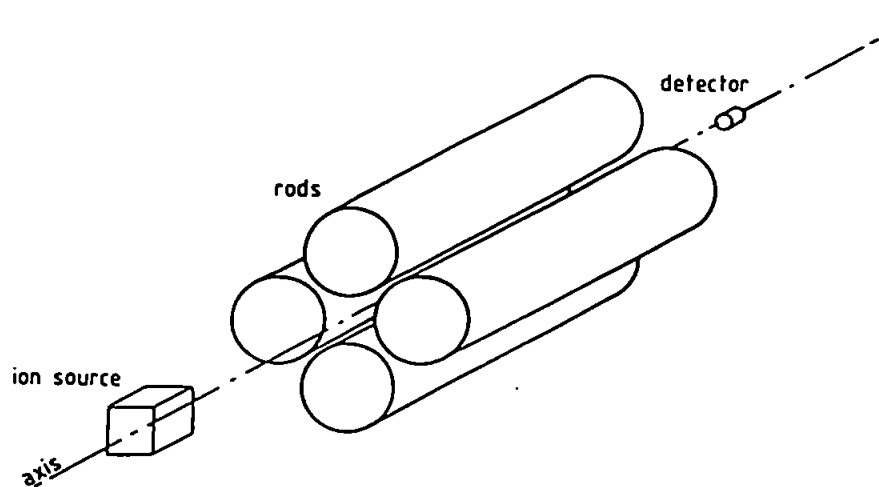


Figure 2.14 Schematic diagrams for a quadrupole mass analyser and potential arrangement

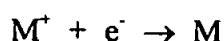
interference exist at these low resolution values. The most common interferences come from molecular ions such as those given in Table 2.4.

Table 2.4. Examples of interfering molecular ions for some elements in ICP-MS analysis

Ion affected	m/z	Probable Molecular ion
$^{56}\text{Fe}^+$	56	$^{40}\text{Ar}^{16}\text{O}^+$
$^{75}\text{As}^+$	75	$^{40}\text{Ar}^{35}\text{Cl}^+$
$^{80}\text{Se}^+$	80	$^{40}\text{Ar}^{40}\text{Ar}^+$

The resolution required to separate these isotopes is in excess of 2,500. These types of 'isobaric' interference decrease in importance the higher up the mass range you go for many types of analysis.

Another interference comes from the matrix in the form of suppression of the ion signal from the analyte of interest. This is most obviously seen when there is a high level of an 'easily ionisable element' (EIE) such as potassium in the matrix. If the concentration of the EIE is high then the ionisation of this element can be so extensive as to produce an electron sink which can reduce the number of analyte ions:



The last type of significant interference comes from salt deposition or carbon deposition on the sampler cone. This will come about if there are high levels of dissolved solids or the presence of organic solvents in solution. Such interference manifests itself as an attenuation (suppression) of the ion signal owing to a decrease in the diameter of the orifice in the sampler cone, thus reducing the number of ions passing through to the expansion chamber.

Most of these effects can be minimised or avoided altogether by either choosing alternative isotopes to overcome isobaric interferences (not always possible) or by careful sample preparation and optimisation of plasma operating conditions to deal with matrix interferences.

However, there is potential for a great many matrix dominated interferences when coupling LC to ICP-MS. The first and most obvious is the use of organic modifiers, next is the buffer choice. Ion exchange chromatography can utilise phosphate or sulphate buffers to facilitate separations, however, such buffers can have deleterious effects on the sensitivity and stability of the ICP-MS. The methods that have been used, where applicable, to minimise matrix effects from the mobile phase in this study are discussed in later chapters.

2.2.3.3. Detection and Data Manipulation.

The most common ion detector used would be the channel electron multiplier. An electron multiplier consists of a funnelled curved glass tube approximately 1 mm i.d. with an inner resistive coating. This is essentially a continuous dynode, rather than a multiplier based on discrete dynodes such as those described in Section 2.2.2.4. The detector has a potential of 1.8 to 3.5 kV applied to it and this attracts the positive ions. The ion strikes the surface and this ejects electrons from the surface. These electrons are accelerated down the tube colliding with the surface and ejecting more electrons creating a cascade of electrons.

In the very sensitive pulse count mode the pulse is read at the base of the multiplier with the gain being 10^7 - 10^8 that of the original collision. The multiplier can also be used in an analogue mode but this is generally less sensitive. The analogue mode becomes less saturated at higher levels of analyte than in pulse mode. The application of this dual-mode to analysis extends the linear dynamic range to as much as 10^9 . Computers handle the data acquisition. The details for the instrument used specifically in this study are given in later chapters.

2.2.4. ICP-AES/MS Analytical merits and applications

Table 2.5 gives the limits of detection for ICP-AES and ICP-MS instruments compared with other popular atomic spectroscopy instruments for some selected elements.

Table 2.5. Limits of detection for selected elements by a range of atomic spectroscopy instruments

Instrument	Element ($\mu\text{g l}^{-1}$)					
	Be	Fe	Mo	Sb	Eu	U
ICP-AES	0.2	1.5	4.0	18	0.3	18
FAAS	1.0	6.0	20.0	40	1.5	40,000
ETAAS	0.001	0.005	0.005	0.01	-	-
ICP-MS	<0.001	<0.1	<0.01	<0.01	<0.001	<0.001

This table shows that clearly ICP-MS and ETAAS are more sensitive atomic spectroscopy instruments than FAAS and ICP-AES. What the table does not show is that both of the ICP instruments are truly rapid multi-element detectors of good sensitivity across the range of elements. It is this coupling of attributes that ensures ICP spectroscopy will dominate routine analytical atomic spectroscopy for many years.

Table 2.6 gives examples of applications ICP-AES and MS have been used for together with the variations in sample introduction.

Table 2.6. Examples of the application base for plasma instruments. CN - Continuous Nebulisation, FI - Flow Injection, HPLC - High Performance Liquid Chromatography

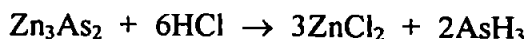
Instrument	Sample Introduction	Applications	References
ICP-AES	CN	Geological, sediment and soil extracts. Environmental waters (terrestrial, estuarine & marine). Plant extracts (tea analysis).	184, 185
	FI	Standard solutions for characterising spray chamber processes. Trace metal analysis following pre-concentration.	177, 186
	HPLC	Speciation developments for metal analysis.	187
ICP-MS	CN	As for ICP-AES	
	FI	"	
	HPLC	Arsenic, organotin, organolead and Pt speciation as well as other metals.	178, 188, 189, 190, 191

2.2.5 Hydride Generation (HG)

2.2.5.1 Introduction

Covalent hydrides can be formed with non-metals or weakly electropositive metals, e.g. PH_3 , CH_4 , SbH_3 , BiH_3 , SnH_4 , $\text{H}_2\text{Te}^{(192)}$ and AsH_3 . These hydrides are held together by weak van der Waals forces and as such are usually gases, liquids or solids with low melting and boiling points.

Arsine (AsH_3), stibine (SbH_3) and bismuthine (BiH_3) can be produced by reducing the trichlorides with zinc (Zn) and dilute hydrochloric acid (HCl) or by the action of HCl on compounds of the elements with Zn or magnesium ($\text{Mg}^{(192)}$).



All of these hydrides are gases, AsH_3 will decompose to elemental As upon gentle heating whereas SbH_3 and BiH_3 are both unstable at room temperature.

Since many of the elements that form hydrides are suspected or known to be highly toxic the ability to determine them at very low levels is very important. The analytical techniques discussed above may suffer problems related to analytical sensitivity for these elements. For instance As has an isobaric interference in the form of ArCl^+ in ICP-MS determinations and the detection limits for ICP-AES and FAAS for As, Sb, Pb, Sn and Ge are not sufficiently low for environmental analysis.

In 1969 hydride generation was first utilised with AAS determination for $\text{As}^{(142)}$. In fact HG-AAS determinations can improve sensitivity for hydride forming elements by as much as a factor of 100 compared to continuously aspirated liquid samples to FAAS. This improvement can be attributed to a number of reasons.

Firstly, the technique is highly efficient in terms of sample transport efficiency and in an optimal set-up the theoretical transport efficiency of the analyte to the source/atom cell is 100% compared to 10-15% for continuously aspirated samples in FAAS. Secondly, this method is effective in terms of matrix removal, i.e. the volatile hydride evolves from the matrix and the liquid sample is simply pumped to waste.

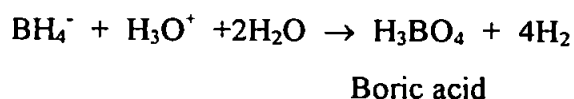
Thompson *et al.*⁽¹⁹³⁾ first reported the potential for HG coupled to an ICP. The increase in transport efficiency of the analyte in HG compared to a continuously nebulised sample in plasma spectroscopy is even greater than for FAAS, thus enhancing the potential for very low detection limits.

The following sections describe the action of HG reagents and considers experimental constraints, particularly when coupling an HG system to a plasma instrument.

2.2.5.2 Principles

Sodium tetrahydroborate(III), NaBH_4 , is used predominantly in HG studies today because it acts as both a rapid reducing agent and source of the hydride⁽¹⁹⁴⁾. Figure 2.15 shows a typical arrangement for a hydride generation system.

The NaBH_4 is stabilised in an alkaline solution to prevent spontaneous decomposition of the tetrahydroborate. A recent study⁽¹⁹⁴⁾ has shown that in NaOH concentrations of 0.05 mol l^{-1} the decrease in concentration of NaBH_4 was 16% in 4 days. At NaOH concentrations of 0.5 mol l^{-1} there was no observed decrease in NaBH_4 concentration after 4 days. HCl is added to NaBH_4 to lower pH and bring about decomposition:



If a hydride forming element is present in the sample and this is now added to the HCl carrier stream and reacted with the NaBH_4 the decomposition of the tetrahydroborate and the formation of the hydride occur almost simultaneously:



where A^{n+} is the analyte and AH_n is the analyte hydride. The volatile hydride is stripped from the solution and is then separated from the liquid phase in the gas-liquid separator before being carried to the source or atom cell. In the case of this study the carrier gas was Ar and the source was the ICP.

Since Holak's initial work many studies have been carried out on the hydride forming elements mentioned in this section and the use of HG as a form of sample matrix removal. It has been utilised as the major method for Sb analysis in a wide range of matrices for the last two decades. These have already been reviewed in Chapter 1, Sections 1.3 and 1.4.

For many of the hydride forming elements the oxidation state of the element in solution can affect whether a hydride is formed rapidly or at all. In the case of Sb the +III oxidation state

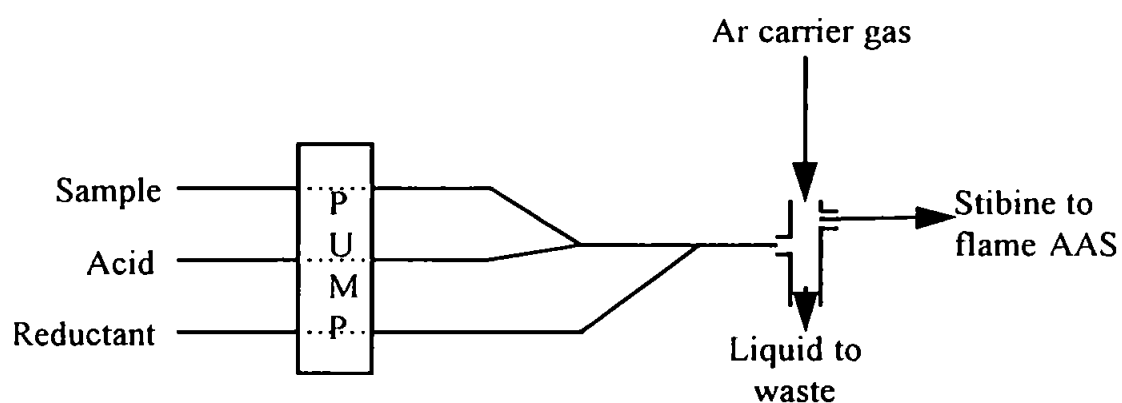


Figure 2.15 Typical hydride generation arrangement.

is the preferred state for hydride formation. The +V oxidation state has a very low propensity towards hydride generation, although with high acid and reductant concentration this low reduction problem can be overcome. What is preferred however is the use of a pre-reductant such as potassium iodide, KI, or L-cysteine to ensure all the analyte present is in the desired oxidation state. As has already been stated in Chapter 1, the oxidation state dependence in HG has been utilised to facilitate speciation studies, to determine the levels of the more toxic Sb(III) in the presence of Sb(V) without actually determining Sb(V).

The overall effectiveness of HG as a speciation tool is ultimately limited because there sometimes exist situations where the analyte is present in a form that will not form a hydride at all or with great difficulty, and as such the chemical transitions required could well contribute to analytical error. Also, HG on its own cannot provide molecular speciation information. However, in the determination of inorganic Sb species the coupling of HG to ICP instruments can greatly improve the sensitivity and detection limits of these instruments by the improvement in transport efficiency.

2.3 Nuclear Magnetic Resonance

2.3.1 Principles of Nuclear Magnetic Resonance (N.M.R.)

In N.M.R., it is the absorption of electromagnetic radiation in the radio-frequency (RF) region by a nucleus placed in a magnetic field that is measured. Kemp⁽¹⁹⁵⁾ breaks down the N.M.R. function using the hydrogen nucleus (proton, ^1H) as the example nucleus.

The proton, possessing both electric charge and mechanical spin, acts as a spinning bar magnet. As such it will respond to the influence of an external magnetic field and tend to alignment with the field. Only two orientations, aligned with or opposed to the field, can be adopted. In terms of energy states the aligned orientation is the lower in energy. The proton

has a spinning moment somewhat analogous to a spinning top under the influence of the earth's gravitational force, it will *precess*. This precessional motion means the top moves slowly around the vertical. Figure 2.16 shows both orientations and precessional motion for nuclei under the influence of an external magnetic field B_0 . The precessional frequency is directly proportional to the strength of B_0 . If a proton is precessing in the aligned orientation it can absorb energy and pass into the opposed orientation but only if the RF is the same as the precessing frequency of the nuclei. It will absorb this energy and go to a higher energy state and then relax. 'When this occurs the nucleus and the RF beam are said to be in resonance; hence the term N.M.R.'⁽¹⁹⁵⁾.

The property a nucleus must have to be N.M.R. active is that the spin quantum number, I , is greater than zero. The relationship between mass and atomic numbers of nuclei and the spin quantum number is shown in Table 2.7.

Table 2.7 Relationship between mass/atomic numbers and spin quantum number

Mass Number	Atomic Number	Spin Quantum Number, I
odd	odd or even	$1/2, 3/2, 5/2, \dots$
even	even	0
even	odd	1, 2, 3,

The nucleus of ^1H has $I = 1/2$, ^{12}C and ^{16}O have $I = 0$. ^1H is N.M.R. active, ^{12}C and ^{16}O are not. ^{13}C is N.M.R. active.

The precessional frequencies of the protons in an applied external magnetic field are not necessarily the same. The frequency depends upon the chemical and magnetic environment in which the proton is precessing, e.g. the precessing frequency of the protons in ethanol ($\text{CH}_3\text{CH}_2\text{OH}$) will be different, namely the signals for the CH_3 , CH_2 and OH protons will

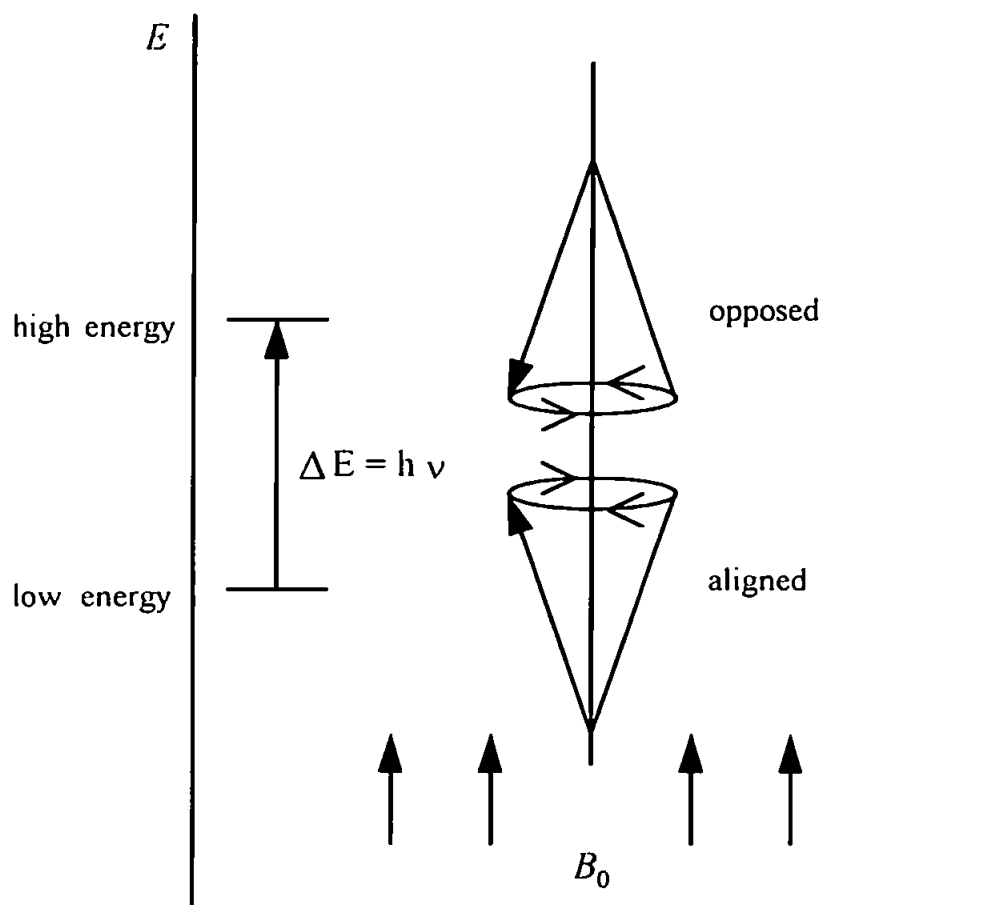


Figure 2.16 Representation of precessing nuclei under the influence of an external magnetic field B_0

appear at different frequencies. Figure 2.17 gives the ^1H N.M.R. spectrum for ethanol. The differences in frequency are quoted as chemical shifts.

So, what factors can affect chemical shift? Protons bonded to a carbon which is bonded to an electronegative atom or group, i.e. halogens, will undergo chemical shift. For the applied field, B_0 , to bring a hydrogen nuclei to resonance it must first overcome the surrounding electronic charge which partially shields the nucleus. An electronegative group or atom withdraws electron density from the C-H environment(inductive effect). The proton becomes de-shielded and the magnetic field needed to bring the protons to resonance is lower. Any attached groups that has a +I inductive effect will shield the protons so that they will come to resonance at a higher B_0 . There are many other effects upon the chemical shift that have been characterised and can be found in a large range of specialist N.M.R. texts⁽¹⁹⁶⁾.

In Figure 2.17 the N.M.R. signals not only appear at different places but there are multiple signals for each type of proton. This phenomenon is called spin-spin splitting or spin-coupling.

The number of lines observed for a group of protons is related to the number of protons on a neighbouring group. This is simplified by the (n+1) rule, which states; to find the multiplicity of the signal from a group of protons, count the number of neighbours (n) and add 1⁽¹⁹⁵⁾.

As has already been stated it is the chemical and magnetic environment of a proton H_A that determines its precessional frequency. Thus a neighbouring proton H_X will be a part of H_A magnetic environment. H_X can align with or be opposed to H_A thereby increasing or decreasing the net magnetic field experienced by H_A . The effect is of course reciprocal. So, if there are two possible different magnetic fields then there are two possible resonance frequencies per proton giving rise to doublets on the N.M.R. This influence is transmitted

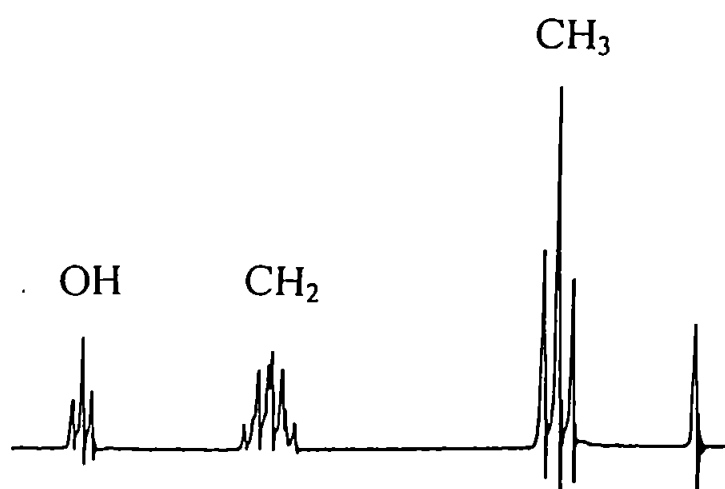


Figure 2.17 ^1H N.M.R. of ethanol, $\text{CH}_3\text{CH}_2\text{OH}$

via electrons in the intervening bonds. The further away the neighbouring protons the less the influence they can exert upon each other.

The magnitude of the coupling is expressed as the coupling constant J , and is related to the energy of the interaction of the nuclei. As with chemical shift properties, organic spectroscopy textbooks deal with this subject in much greater detail than is relevant to this thesis^(195,196). It is this interaction however, that was the basis for the N.M.R. experiments carried out in this study. The experiments and their foundation in theory are discussed in Chapter 3.

2.3.2 Sampling

Sample preparation for N.M.R. analysis is straightforward. For ^1H N.M.R. non-protonic solvents are preferred hence the extensive use of readily available deuterated solvents such as deuteriochloroform, CDCl_3 . However, for the most commonly used solvents the ^1H and ^{13}C chemical shifts are well characterised should protonated solvents be required.

Owing to the poor sensitivity of N.M.R. as a technique the concentration of sample in solution is quite high in analytical terms (2-15%). The sensitivity is related to the energy difference between ground and excited states of the nuclei. This ΔE is very small and the population excess in the lower state is only about 0.001%. It is this excess which determines the probability of transition and consequently the sensitivity of the experiment. Thus, N.M.R. spectroscopy relies upon detecting very weak signals.

2.3.3 Applications

In the relatively short time N.M.R. has been available, there have been numerous applications reported for the analysis of organic, organometallic and biochemical compounds. N.M.R. is a major tool in the characterisation of pure compounds, but as this

study attempts to show, it can also be used to identify ligand behaviour in the formation of complexes.

2.4 Electrospray Ionisation-Mass Spectrometry (& LC-MS)

2.4.1 Principles

Although the behaviour of ions in magnetic fields was first described by 1920, it was not until 1950 that a commercial mass spectrometer was available⁽¹⁹⁷⁾.

A mass spectrum is obtained by converting components of a sample into rapidly moving gaseous ions and separating them on the basis of their mass-to-charge ratios.

The use and applications of mass spectrometers are widely reported⁽¹⁹⁸⁻²⁰¹⁾ and do not need exhaustive description here, but one area that has provided a taxing and intensive research problem in mass spectrometry over the last 20 years, is the coupling of LC to MS.

A gas chromatograph was first interfaced with a mass spectrometer in 1957⁽²⁰²⁾. Post GC separation, the compounds to be analysed were in the required gaseous state prior to ion formation. However, liquid chromatographic methods present an altogether different problem. The major difficulties result from the need to produce gaseous ions from involatile samples and removing these from involatile buffers. The high flow rates in LC techniques also create complications.

In order to overcome the problem of high flow levels, microbore or HPLC with low flow rates have been developed, but this is a compromise measure and cannot be applied across the board. Thus the ionisation source has received a great deal of attention. Electrospray ionisation is one such method. Zeleny demonstrated the first production of a fine mist of charged droplets by electrospray in 1917, but the first applications of ESI-MS did not start to appear until the mid-1980's. This ionisation method has three main features : an

atmospheric pressure ion source, a low temperature ionisation process and the direct emission of ions from electrically charged liquid.

The sample, in solution, typically flows between 5-300 $\mu\text{l min}^{-1}$ through a stainless steel capillary. Solutions can range from 100% organic to 100% aqueous but a common make-up is 1:1 (v/v) $\text{H}_2\text{O/MeOH}$. For a full spectrum to be produced for a sample upto 1000 Da molecular mass the concentration needed would have a range of 1-50 $\text{ng } \mu\text{l}^{-1}$ depending upon the instrument and the samples suitability to electrospray.

In electrospray, a voltage is directly applied to the spraying capillary and a counter electrode is located a short distance away. This generates a strong electric field, and the solution emerges as an aerosol of charged droplets. These droplets evaporate until the increased surface charge density makes the droplet unstable. The surface charge electrical forces approach equality with the forces due to surface tension and the droplet disintegrates to produce smaller charged droplets. With continued evaporation and reduction in droplet size, eventually charged sample ions are ejected from the droplets. A counter current of warm nitrogen gas is introduced between the spraying tip and sampling orifice to aid desolvation and minimise the flow of neutral solvent molecules into the vacuum chamber.

The sample ions pass through a sampler cone into a pumped intermediate vacuum region (ca. 1 mbar), then through a skimmer and into the analyser for the mass spectrometer. In the case of the Finnigan Mat LCQ used in this study the mass analyser is an ion-trap. The MS then measures the m/z ratios for the sample ions.

2.4.2 Sampling

Electrospray ionisation relies on the prior formation of sample ions in solution. Thus, if the compounds in solution are not ionic then dissolution in a protonating solvent could be an appropriate measure for positive ion determinations. Adduct formation owing to the matrix also affects results because more complex spectra are observed and the sensitivity is

reduced because the ion current is distributed between a larger number of mass values. Electrolyte concentrations in excess of 10^{-5} M can reduce sample ion intensity and higher concentrations resulting in increased solution conductivity can produce unstable sprays.

Thus, sensitivity is higher in organic phases than aqueous phases, however, a dilution of the flow with a miscible organic solvent just prior to spraying could improve the analysis of highly aqueous solutions.

The key with any analysis where the matrix is predominantly aqueous in nature is to attempt the production of a mass spectrum for the samples then make necessary adjustments where appropriate.

2.4.3 Spectra and Applications

One of the features of ESI is that for analytes with molecular weights greater than 1000, multiply charged molecular ions can be formed. This phenomenon effectively increases the range of the mass spectrometer up to as much as 100-200 kDa molecular weight, even with limited m/z range analysers such as quadrupoles.

Typically, for samples with low molecular weights, up to 1000, ions such as MH^+ are formed in positive ion mode for basic compounds and $(M-H)^-$ in negative ion mode for acidic compounds. Adducts formed from the presence of ammonium ($M+18$), sodium ($M+23$) or potassium ($M+39$) in positive ion mode can be observed. Fragments are seldom seen as the ionisation is described as 'soft'. If the instrument has collision cell capabilities then fragmentation can be achieved. The collision cell is situated after the first analyser and has an inert gas such as Ar, He or Xe admitted to it. If they have sufficient energy they will bombard the sample ions and cause fragmentation. Thus, ESI-MS can be very applicable to the determination of molecular masses of low molecular mass samples and the determination of drugs, pesticides, small peptides, sugars and organometallics.

3.1 Introduction

The chemistry of Sb has been reviewed in Chapter One highlighting the dominance, in terms of variety, of Sb(III) reactivity. Chapter One also described the methods that have been adopted or developed for the speciation of Sb in specific applications, i.e. 1) aqueous environmental samples, 2) contaminated industrial waste and 3) solid material digests.

However, there is a group of chemicals, the α -hydroxyacids, that have been used in reactions with both Sb(V) and (III) in order to study the chemistry of this reaction directly or to aid determination of these compounds. Examples of this include Sato⁽¹³⁸⁾ in 1985 where Sb(V) and (III) were complexed with mandelic acid (Figure 3.1 a.) and extracted with Malachite Green. The aim was to speciate Sb(V) and (III) by exploiting the rate of reaction between the two species and mandelic acid, with Sb(III) reacting quickly at room temperature and Sb(V) only quickly forming a complex completely with heating. This paper is important because although Sb(V) compounds have been reported as being able to form complexes with a variety of oxygen donors⁽¹⁾, the donor ligands in question were in an inorganic form. Sato confidently reported the complexation of Sb(III) and (V) with an α -hydroxyacid. The composition of the complexes were hypothesised as $[\text{Sb}(\text{MA})_2(\text{OH})_2]^-$ for Sb(V) and $[\text{Sb}(\text{MA})_2]^-$ for Sb(III) but this could not be determined by the continuous variations and mole-ratio methods because of the large excess of complexing agent and dyestuff required for their formation.

Other examples of α -hydroxyacids are given in Figure 3.1. Lactic, DL-malic and citric acid have all been used by a host of workers since Sato's study for reasons ranging from stability studies for long term storage of standards⁽¹⁴⁶⁾ to aiding speciation in hydride generation techniques^(144,143).

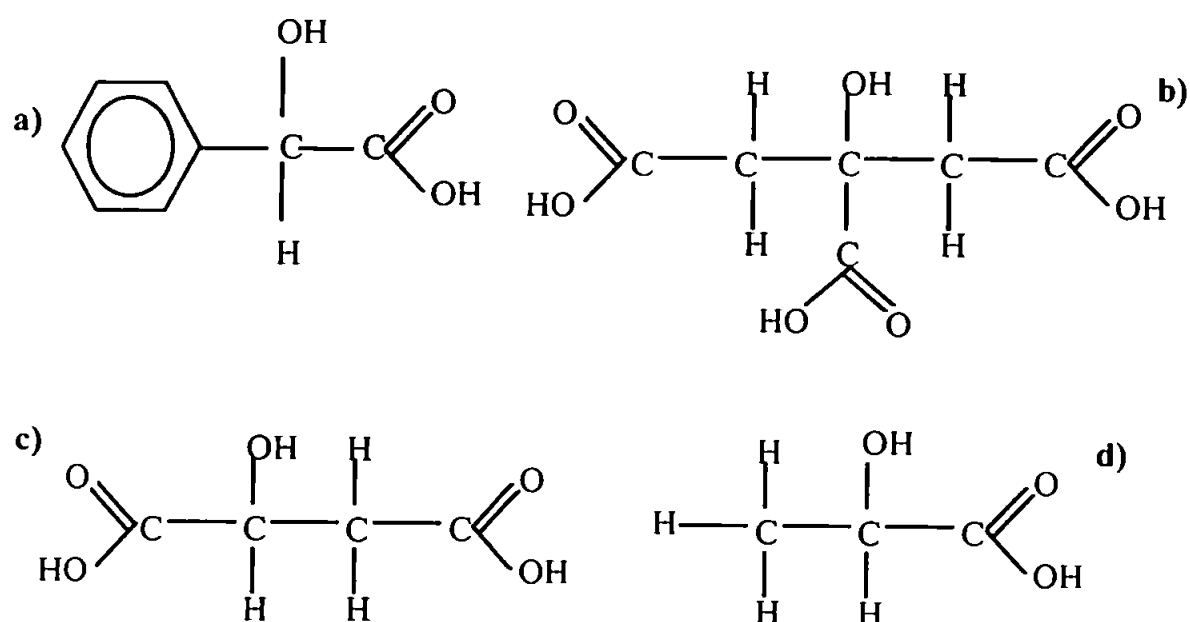


Fig. 3.1 Structures of selected hydroxyacids. a) Mandelic acid; b) Citric acid; c) Malic acid; and d) Lactic acid

In 1991 de la Calle-Gutiñas *et al.*⁽¹⁵⁰⁾ reported speciation of Sb(III) and (V) in water by an extraction method utilising the formation of a complex of Sb(III) and lactic acid. This complex was extractable into chloroform as an ion-pair with malachite green. The Sb(V) remained in the aqueous phase. Sb(V) was reported as not reacting with lactic acid although the authors did not discount the theory that reactions between Sb(V) as $[\text{Sb}(\text{OH})_6]^-$ do occur, with difficulty. However, this paper is not totally conclusive. It is entirely possible that Sb(V) does react with lactic acid quickly but simply does not extract into the organic phase. In addition, the paper does not offer an alternative theory in that it is possible the antimonyl(III) tartrate used in the study simply extracted as an ion-pair with malachite green without any help from lactic acid. In 1992 the same group conducted a stability study of Sb species in a range of matrices including lactic and citric acid. The determination of Sb(III) and (V) was carried out using HG-AAS. In the α -hydroxyacid matrix it was observed that Sb(V) determination was not possible under the HG conditions of choice. However, 6%(w/v) citric acid was used with sodium tetrahydroborate (3%) to produce the hydrides.

In the same year, de la Calle-Gutiñas *et al.*⁽¹⁴⁷⁾ conducted a further study reducing Sb and Se interferences in As determination by hydride generation-AAS. Their results demonstrated that lactic, citric and malic acid addition to a solution of Sb(V) caused the AAS signal to be reduced to 'negligible' levels, "without the need to control pH, as a result of the formation of a complex". This statement in respect of lactic acid is directly contradictory to those made in previous work⁽¹⁵⁰⁾. This paper also indicates complex formation between Sb(III)-lactic acid and very slow formation of a complex between Sb(III) and citric/malic acid.

In both of these papers two groups of workers were not cited, Mohammed *et al.*⁽¹⁴⁴⁾ and Apte and Howard⁽¹⁴³⁾, yet their work spanned 1986 to 1990. In the case of Apte and Howard, citric acid was used to suppress hydride formation from Sb(V) by pH control and Mohammed and co-workers used citric acid as complexing agent to suppress hydride

formation. They also assumed citrate complexation was involved with suppression of the Sb(V) signal based on a reference "antimony salts readily form complexes with various acids in which antimony forms the nucleus of an anion"⁽²⁾. This concluded their reference to complexation and no further elucidation of the interaction was provided.

Following this a couple of papers were published by Smith's group in Australia⁽²⁴⁻²⁶⁾ relating to the preparation and crystal structures of Sb(III) complexes with carboxylic acids, and more specifically the citrate complex. Figure 3.2 gives the structure of one such complex. The co-ordination with Sb was reported as being through the hydroxo- and iso-carboxylic oxygens denoted a) and b) respectively. This complex, $[\text{SbNa}(\text{C}_6\text{H}_6\text{O}_7)_2(\text{H}_2\text{O})_2] \cdot \text{H}_2\text{O}$, was prepared by digesting Sb_2O_3 at 90° C with 5% aqueous citric acid followed by the addition of NaNO_3 . This group discussed the versatility of the α -hydroxycarboxylate residue of the citrate ligand as a chelating agent for the stabilisation of water-soluble antimony(III) complexes. They did not report any work regarding Sb(V) and as such no direct comparison with this present study can be made, but the precedent for investigating the interaction of α -hydroxyacids with Sb is made by this paper.

Thus, with respect to Sb(V), only Sato⁽¹³⁸⁾ has attempted to tackle the question of formulae of α -hydroxyacid complexes, and then only hypothetically.

As has already been discussed, speciation studies regarding Sb have suffered from the lack of a sufficient number of characterised soluble Sb compounds. In order to further enhance the knowledge of Sb chemistry and aid the robustness of chromatographic development for speciation the Sb(V)/ α -hydroxyacid interaction was further investigated. This was regarded as particularly useful since these acids are present in a number of environmental/biological systems⁽²⁰³⁻²⁰⁵⁾, and so if they can be shown to interact with Sb(III) and Sb(V), methods need to be developed to identify and quantify these compounds.

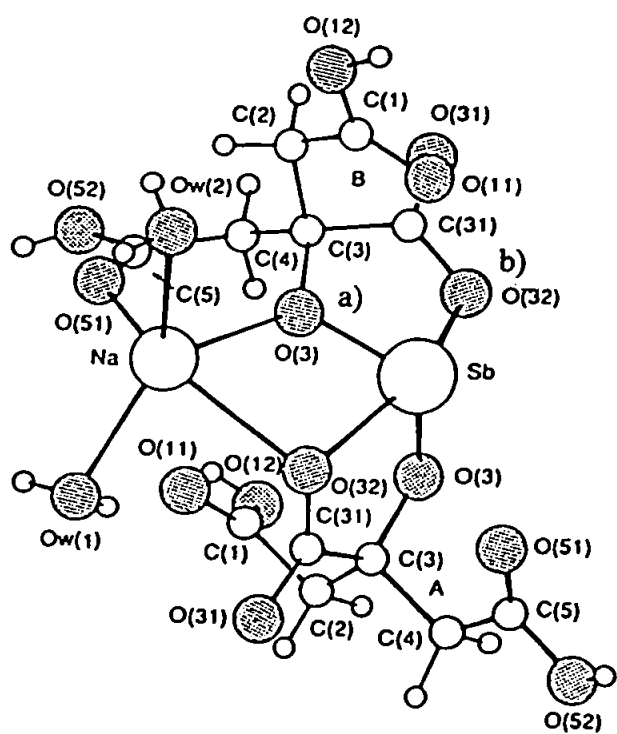


Fig. 3.2 Molecular configuration for the complex $[\text{SbNa}(\text{C}_6\text{H}_6\text{O}_7)_2(\text{H}_2\text{O})] \cdot \text{H}_2\text{O}$.

3.2 Experimental

3.2.1 Instrumentation

For HPLC separations a ConstaMetric 3200 solvent delivery system (LDC Analytical, Florida, USA) and an isocratic pump 305 with 805 Manometric module (Gilson, Villiers le Bel, France) was employed at 1.0 ml min^{-1} . The chromatographic columns used were the IonPac AS4A (25cm x 4 mm) and AS11-SC (25 cm x 2 mm) anion exchange columns (Dionex, Calif., USA). Sample introduction was via a six-port Rheodyne type 7125 injection valve with a 100 or 20 μl stainless steel sample loop. The ICP-AES instruments were the Liberty 200 (Varian, Australia) and the Optima 3000 DV (Perkin-Elmer, Beaconsfield, UK). The operating conditions were typically 1300W forward power, 15.0 - 16.5 l min^{-1} coolant gas flow rate, 0.4 - 1.5 l min^{-1} auxiliary gas flow rate and a nebuliser gas flow rate of 0.8 l min^{-1} . A Merck-Hitachi D2500 chromato-integrator was used to record peak areas and relative peak areas. The ICP-MS instrument was the VGPQ2+ turbo (VG Elemental, Winsford, Cheshire). The operating conditions were 1350W forward power, 15.0 l min^{-1} coolant gas flow rate, 1.0 l min^{-1} auxiliary gas flow rate and a nebuliser gas flow rate of 0.8 l min^{-1} . The ESI-MS instrument was a LCQ Mass Spectrometer (Finnigan MAT, San Jose, USA) with the following operating conditions: syringe pump flow rate, 5 $\mu\text{l min}^{-1}$; spray voltage, 3.43 kV; spray current, 1.02 μA ; capillary voltage, 28.25 V; and capillary temp., 210° C. The analysis commenced 2 mins after the start of infusion to allow for stabilisation. The NMR instrument used was a EX270 FT-NMR (Jeol, Welwyn Garden City, Herts, UK).

3.2.2 Reagents

All reagents used were of analytical grade unless otherwise stated. All working solutions of Sb(V) were made by dissolving the required weight of potassium hexahydroxyantimonate(V) (Aldrich, Gillingham, Kent, UK) in the appropriate matrix. All working solutions of citric acid (Aldrich), DL-malic (Aldrich, Gillingham, Kent, UK), lactic (Aldrich, Gillingham, Kent, UK) and (±)mandelic acid (Aldrich, Gillingham, Kent, UK) solutions were made by dissolving the required amount of each acid in the appropriate matrix. 10-20 mM NH_4Cl (BDH, Poole, Dorset, UK) was made up by dissolving 0.5349-1.0698 g of solid in 1000 ml of water. The pH of the mobile phase was adjusted with 0.05 M HNO_3 (BDH, Poole, Dorset, UK). 10 mM H_2SO_4 (BDH, Poole, Dorset, UK) was made up by adding 0.56 ml of the acid to a 1000 ml volumetric flask and making up to volume with water. Deionised water (Millipore, Mollsheim, France) was used in all cases.

3.3 Method Development

In order to investigate the interaction between Sb and α -hydroxyacids the techniques employed needed to be element specific and/or offer structural or molecular information on all or part of the reagents involved.

Nuclear magnetic resonance spectroscopy provides an excellent means by which to investigate the organic acids and to assess what affect addition of Sb had to the spectra of the acid. This, in turn, would tell us if the electronic environment of the atoms in the acid had changed, indicating that it may have bonded to the Sb in solution. The practical limitation imposed was the sensitivity of the instrument for ^{13}C analysis at approximately >1% w/v concentrations, so very concentrated solutions of Sb and acids were required for analysis.

As described in Section 3.1 it is hypothesised that antimony salts form complexes with α -hydroxyacids, and that the antimony forms the nucleus of an anion. Hence ion chromatography should be able to separate these complexes from the parent Sb salt and from each other. For this reason a high-performance liquid chromatography - inductively coupled plasma - atomic emission spectroscopy (HPLC-ICP-AES) method was investigated to try to achieve this separation and to also try to quantify the level of interaction, i.e. to try and establish stoichiometries for the Sb: α -hydroxyacid complexes. ICP-AES is an element specific technique and as such the C in the organic acid can be monitored as well as the Sb. Using the simultaneous ICP-AES instrument the Sb and C emissions at 204.597 and 193.026 nm respectively could be monitored together. In this way real-time chromatograms for both compounds could be obtained and any co-elution profiles could be assessed for exchange characteristics. Thus, the analysis was to be designed in such a way that quantification of the species was possible. This could only be achieved by a method akin to mole-ratio⁽²⁰⁶⁾ methodology married to a continuous variation⁽²⁰⁷⁾ approach.

The model used is based on the premise that if the concentration of each component is known then the resulting peaks in the chromatograms could be identified and integrated. From the integrated areas, peak area ratios can allow us to assign molar concentration values to each peak. Table 3.1 gives the molar ratios of Sb: α -hydroxyacid investigated.

Table 3.1. Molar ratios of Sb:α-hydroxyacid used in HPLC-ICP-AES investigation

Sb:α	Sb (mol dm ⁻³)	α-HA (mol dm ⁻³)
1:1	0.005	0.005
1:2	0.0033	0.0066
1:3	0.0025	0.0075
1:4	0.002	0.008
2:1	0.0066	0.0033
3:1	0.0075	0.0025
0:1	0	0.01
1:0	0.01	0

Aliquots of each of these solutions were injected onto the Dionex AS4A anion exchange column and determined by ICP-AES at 217.581, 187.115 or 204.597 nm for Sb and 193.026 nm for C. The peak areas were integrated and applied to the model.

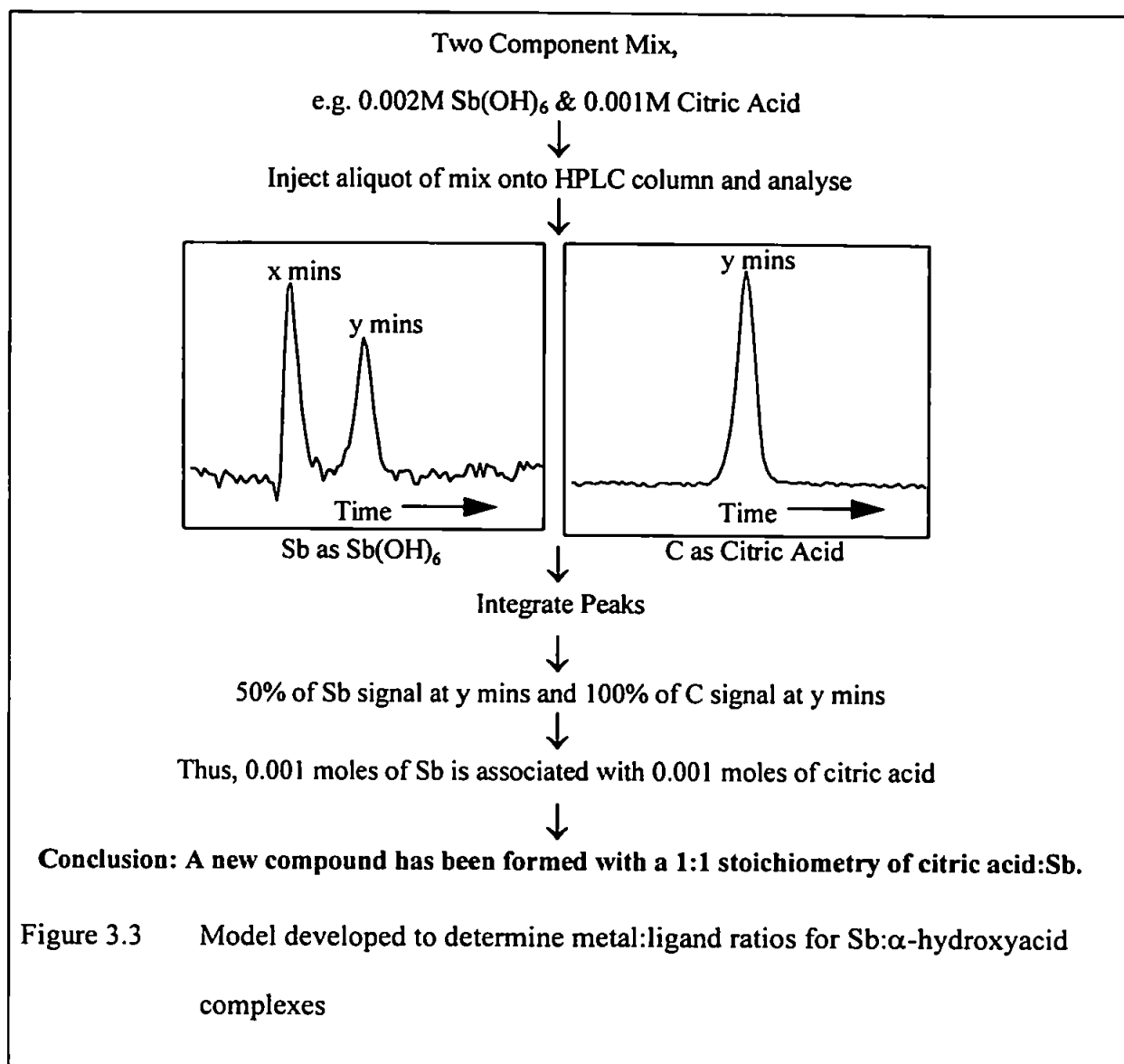


Figure 3.3 Model developed to determine metal:ligand ratios for Sb:α-hydroxyacid complexes

The assessment of association is based upon retention data. Associated elements in a complex will have exactly overlapping peak profiles and identical retention times. As such they are highly unlikely to be merely co-eluting.

Jayaprakasha and Sakariah⁽²⁰⁸⁾ reported the determination of organic acids in *Garcinia cambogia* (Malabar tamarind) by HPLC using a 10 mM H₂SO₄ eluent and a C₁₈ column. In this paper they achieved a separation of (-)-hydroxycitric acid, citric acid and malic acid. A similar method was attempted using the AS11 column as this has an ethylvinylbenzene substrate cross-linked with 55% divinylbenzene and as such could also act as a relatively non-polar substrate for reversed phase and ion-suppression as well as ion-exchange

chromatography. The determination was by ICP-MS. If such a separation could be achieved with complexes of Sb with citric, malic or mandelic acid then this would demonstrate that a suitable elution protocol for the determination of these compounds by HPLC-ESI-MS might be found.

This method was also used to determine which of the complexes was the most stable. For this experiment a mixture of each acid of known concentrations was made up. To this was added a known concentration of $[\text{Sb}(\text{OH})_6]^-$. The concentration of Sb in this experiment was lower than for any single acid. The complexes were determined against single standard calibrations for each acid complex.

The use of mass spectrometry is the final stage in the instrumental analysis of these complexes. If there is a complex in solution ESI-MS should be able to provide evidence of its existence, giving information about the molecular weight and whether it contains Sb. This can be found by the fact that there are two isotopes of Sb, 121 and 123. All of the hypothesised complexes should exhibit doublets of almost equal intensity as the isotopic abundances are 57 and 43% respectively. Another key use of this instrument is that it allows the determination of the molecular weights of the species as they come off the column during a chromatographic separation. Thus, a consideration as to whether any on-column reactions occurred could be evaluated to eliminate the perceived risk for on-column re-arrangements and reactions with mobile-phase reagents.

The solutions were made up based upon the findings of the HPLC-ICP-AES model results.

3.4 Results

3.4.1 NMR Interpretation

3.4.1.1 Sb: Citric Acid

The ^1H NMR for citric acid (2% w/v) is shown in Figure 3.4 along with its structure. The signals observed are for the protons attached to the starred(*) carbons. These protons are indistinguishable because they are equivalent enantiotopic hydrogens, but they do exhibit splitting due to the prochirality of the compound. Prochiral⁽²⁰⁹⁾ is a term which can be applied to a compound or group that has two enantiotopic groups or atoms, e.g., CX_2WY , of which citric acid is a good example. Replacement of, or addition to, one of the X groups ($-\text{CH}_2\text{COOH}$) would result in enantiomers. This would also lead to a loss of symmetry in the molecule and the hydrogens would no longer be equivalent. This is demonstrated in Figure 3.5, the ^1H NMR for citric acid in the presence of Sb(V). The peaks can now be assigned according to coupling constants, i) 16.83 Hz and ii) 20.28 Hz. This effect is thought to be due to bonding of the citric acid to Sb through a C^4 or C^6 carboxylate oxygen. This type of bond would create a chiral centre at the $\alpha\text{-C}$ and produce differences in chemical shifts for the protons.

The ^{13}C NMR for citric acid (2% w/v) is given in Figure 3.6. The four distinct C environments expected are easily distinguished: $-\text{CH}_2$, 43.995 ppm; C-OH , 73.985 ppm; terminal- COOH , 174.163 ppm; and iso- COOH , 177.577 ppm. If citric acid were to bond through a terminal carboxylate, the loss of symmetry would result in six C environments. Figure 3.7 shows this to be the case.

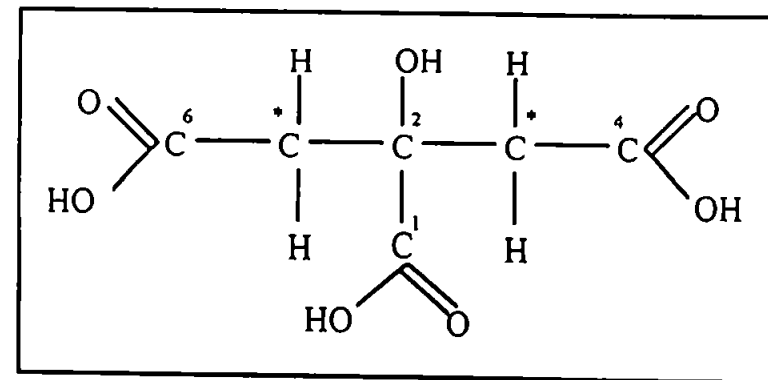
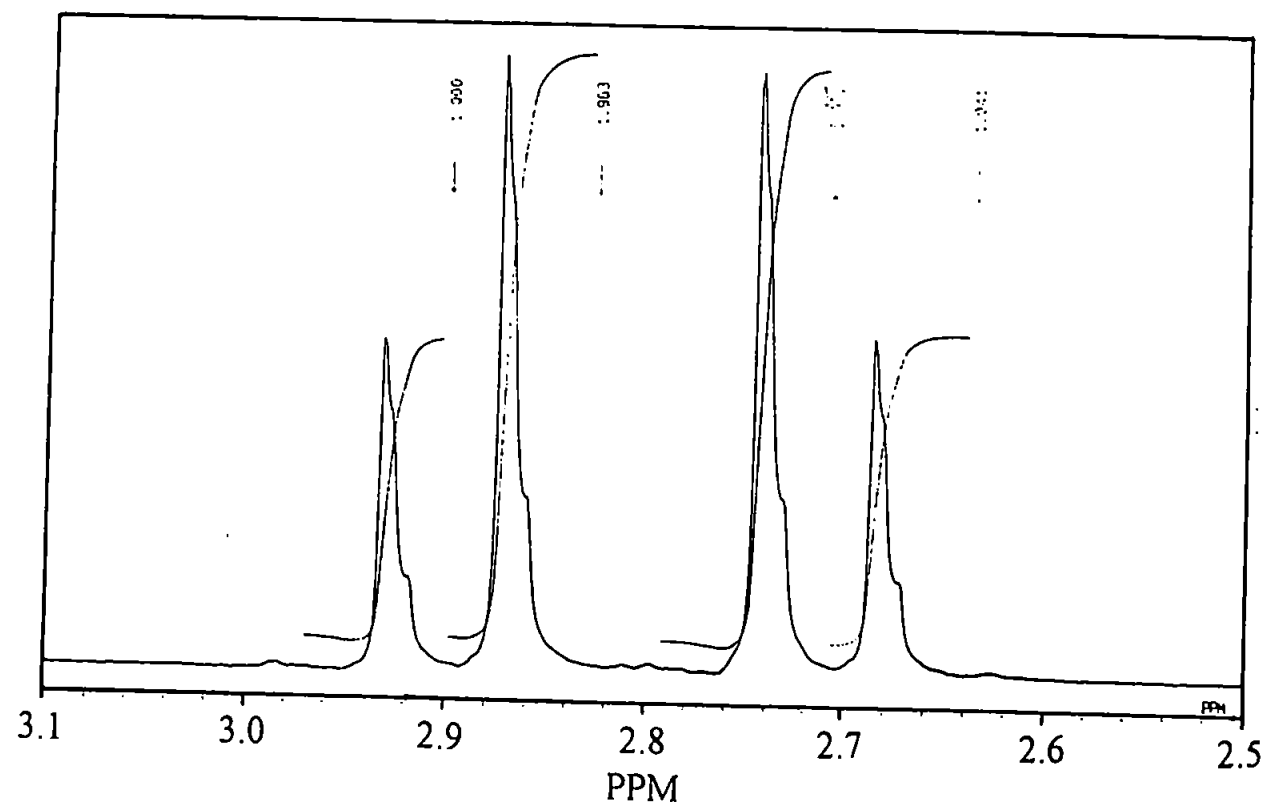


Fig. 3.4 ^1H NMR for 2% (w/v) citric acid in MilliQ. Inset is structure and annotation.

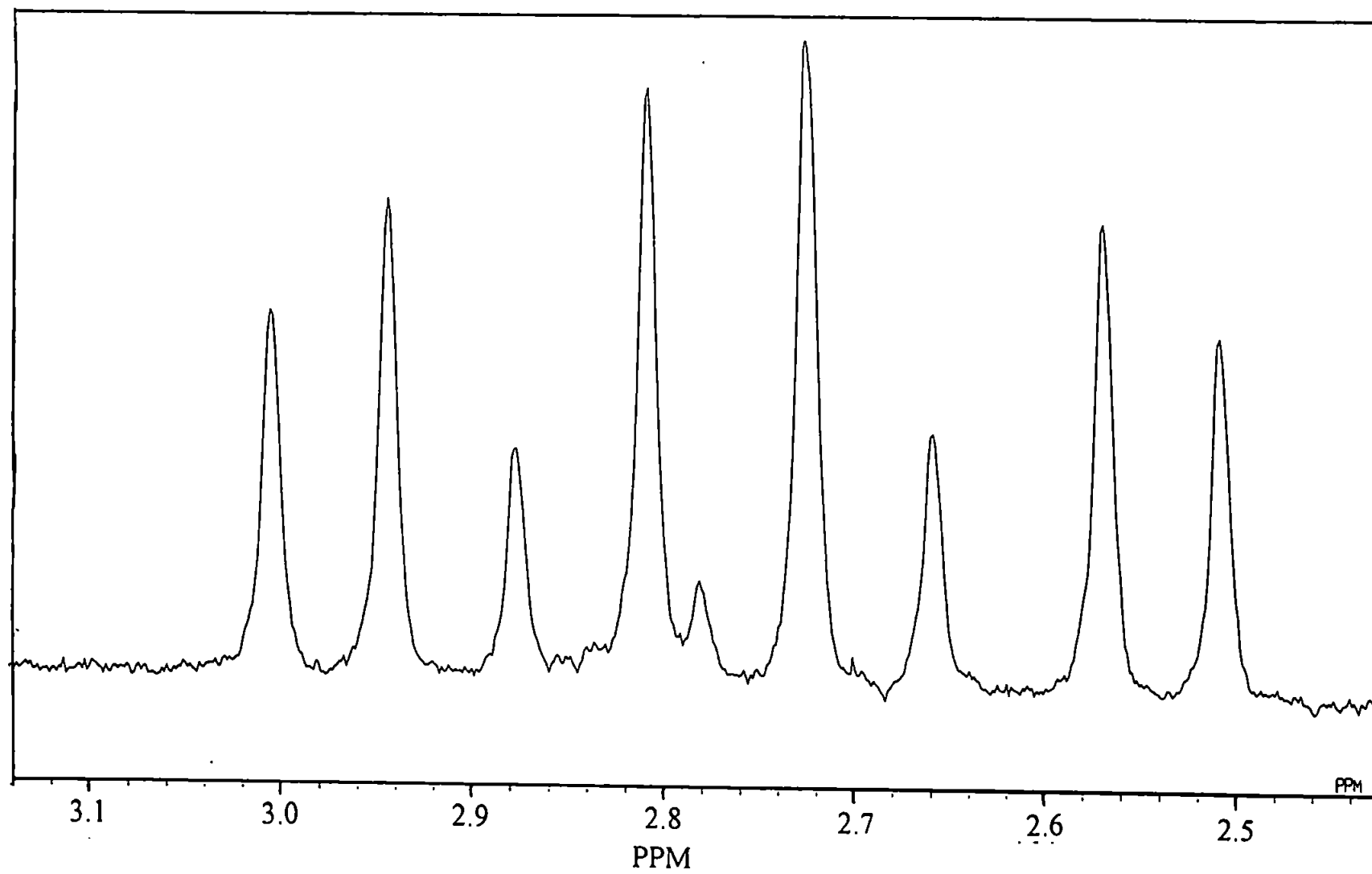


Figure 3.5. ^1H NMR for an equimolar solution of Sb(V) and citric acid in MilliQ.

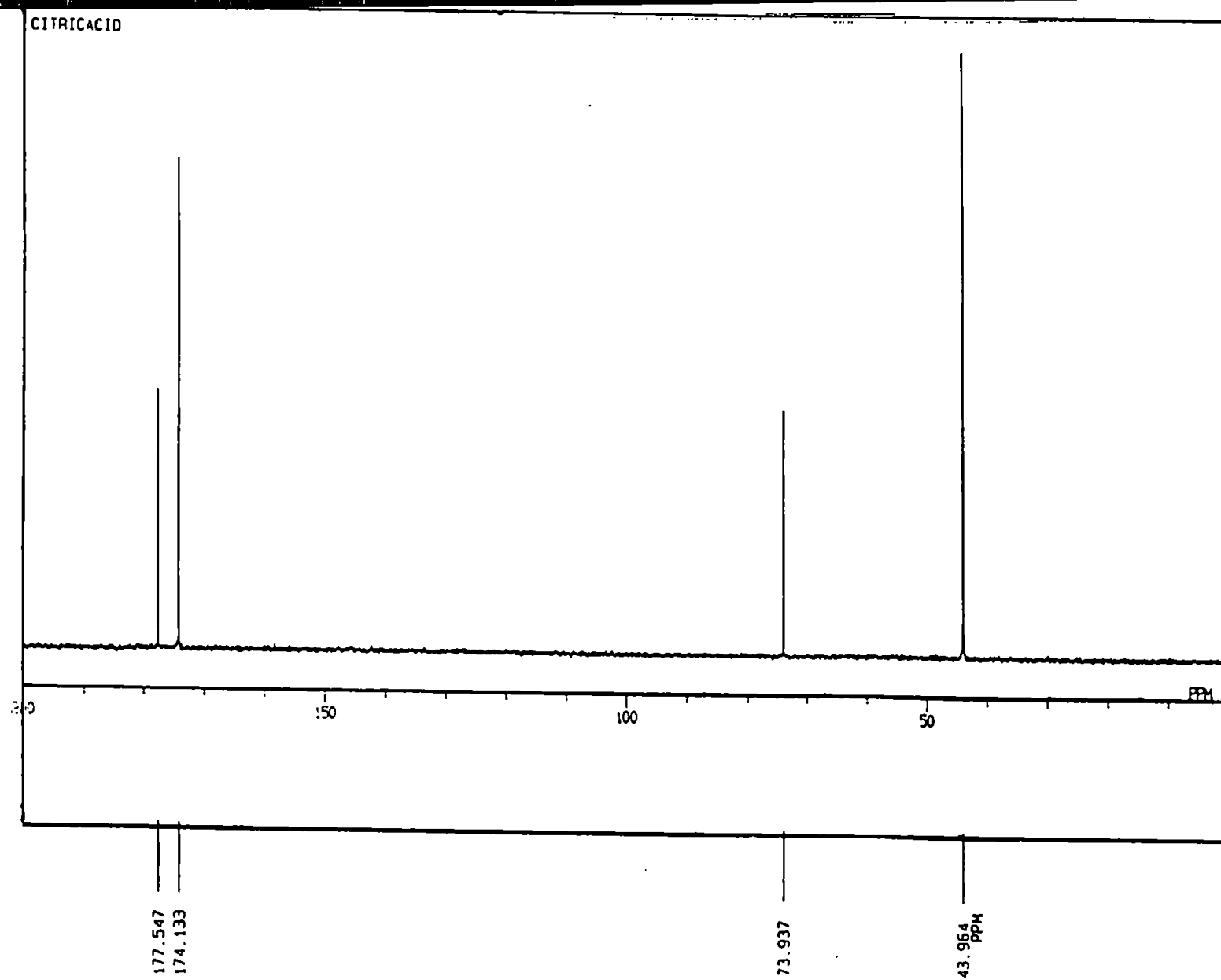


Figure 3.6 ^{13}C NMR for 2% (w/v) citric acid in MilliQ

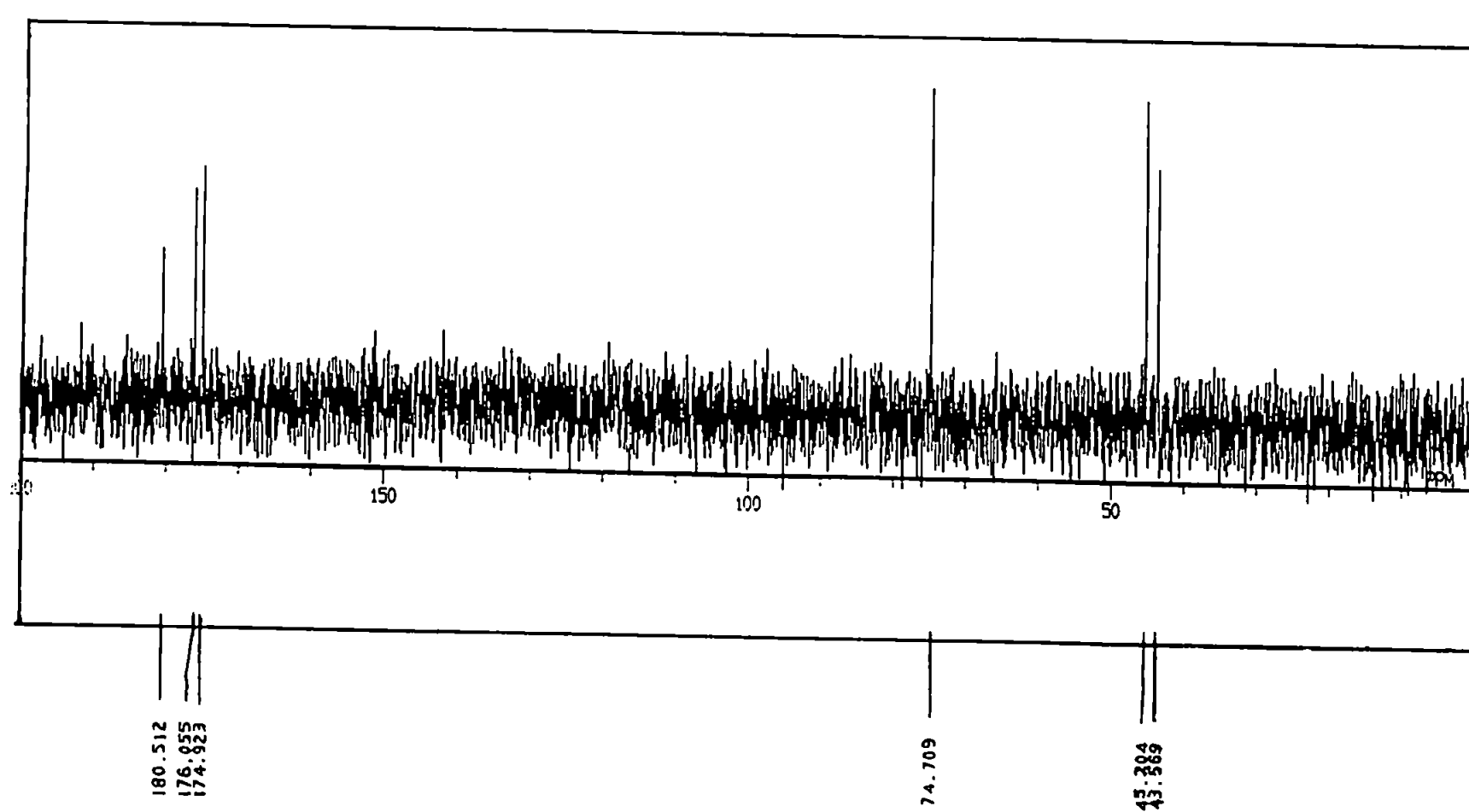


Figure 3.7. ^{13}C NMR for an equimolar solution of Sb(V) and citric acid in MilliQ.

3.4.1.2 Sb:malic acid

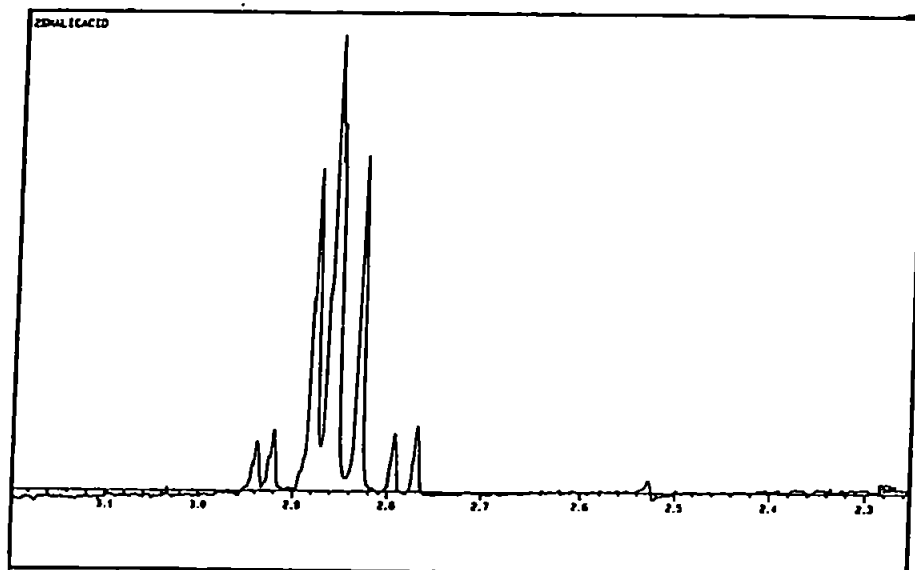
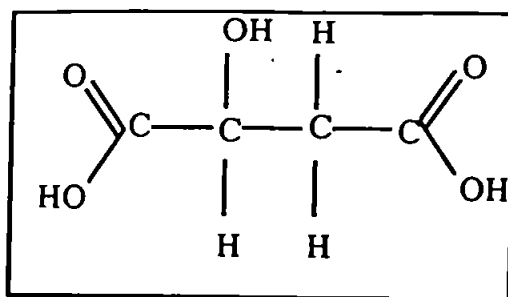
Figure 3.8 gives the ^1H NMR for a) DL-malic acid (2% w/v), including structure, and b) DL-malic acid in the presence of an equimolar quantity of Sb(V). The obvious differences in these spectra indicate that a major change has occurred in the compound. Although it is not impossible to tentatively associate signals by coupling constants the only real observation that can be made is that the two spectra are strikingly different. The ^{13}C experiment is more helpful. For the 2% (w/v) solution of DL-malic acid 4 C signals are observed : $-\text{CH}_2$, 39.269 ppm; C-OH, 67.642 ppm; and the terminal $-\text{COOH}$ groups at 175.295 and 177.416 ppm. With the addition of Sb, 6 signals are observed, Figure 3.9. It is highly unlikely that this is due to peak splitting but instead probably due to bonding of the DL-malic acid to Sb via either carboxylate group. Thus spectra for both possibilities are observed on the same spectrum. The differences in signal intensity for the $-\text{CH}_2$ and C-OH might indicate a preferred complex, but this is not certain.

3.4.1.3 Sb:mandelic acid

The ^1H NMR for the 2% (w/v) solution of mandelic acid, and its structure, illustrates the aromatic portion of this compound with the signal clear at 7.4273 ppm, Figure 3.10. The Sb:mandelic acid solution shows a striking effect upon the aromatic protons. Only one carboxylic group is available for bonding, and it is clear the addition of Sb to the solution has had a significant effect, however, it is unclear if the C-OH functionality is involved in the bond.

Figure 3.11 is the ^{13}C NMR for mandelic acid. The different carbons can be assigned as follows: CHOH, 73.608 ppm; *o,m,p*-aromatic C at 127.677 to 129.690 ppm; ipso-C, 138.710 ppm; and $-\text{COOH}$ at 176.984 ppm. The identity of these carbons is confirmed by the ^{13}C DEPT experiment, Figure 3.11.

a)



b)

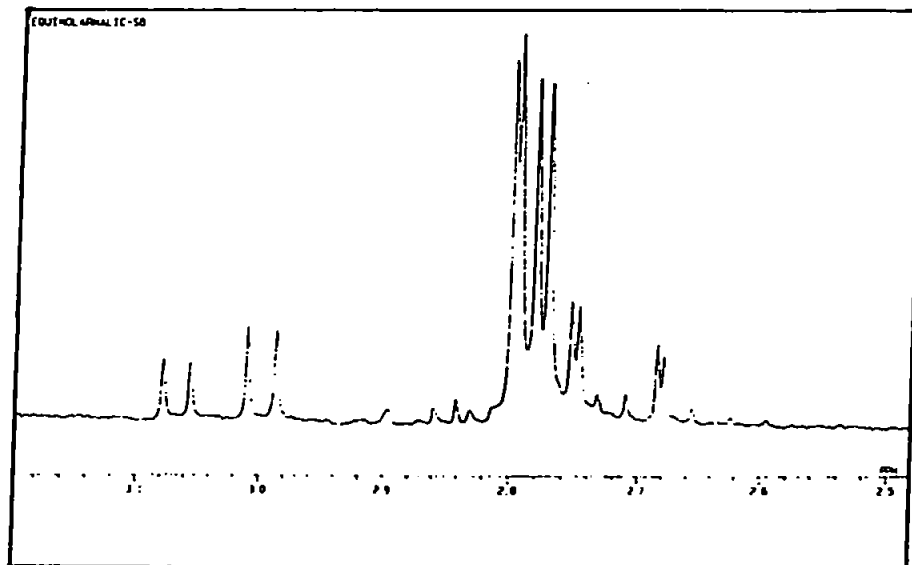


Figure. 3.8 ^1H NMR for a) 2% (w/v) DL-malic acid and b) equimolar solution of Sb(V) and DL-malic acid in MilliQ. Inset is structure.

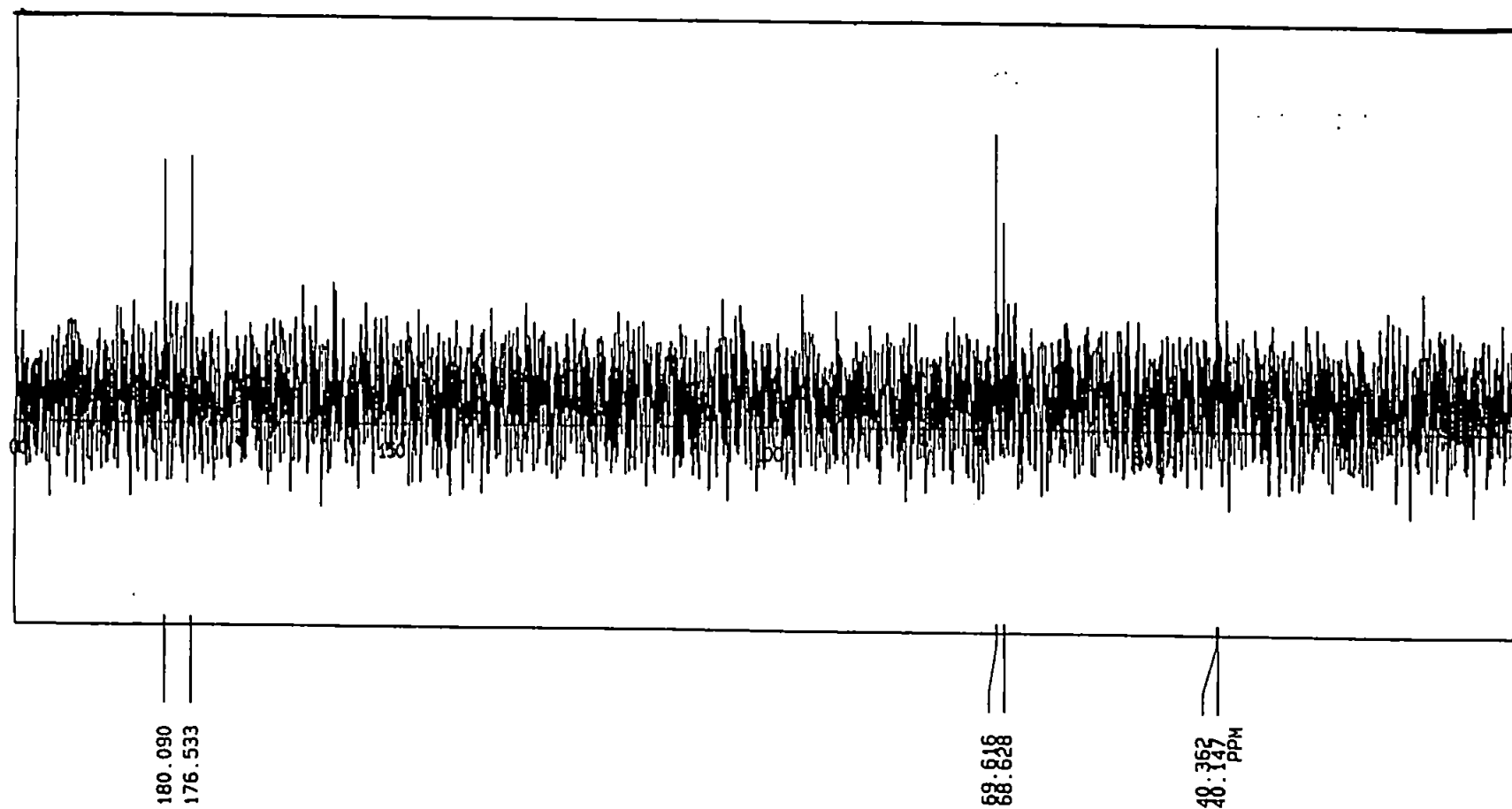
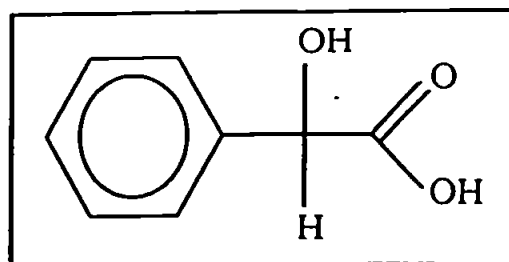
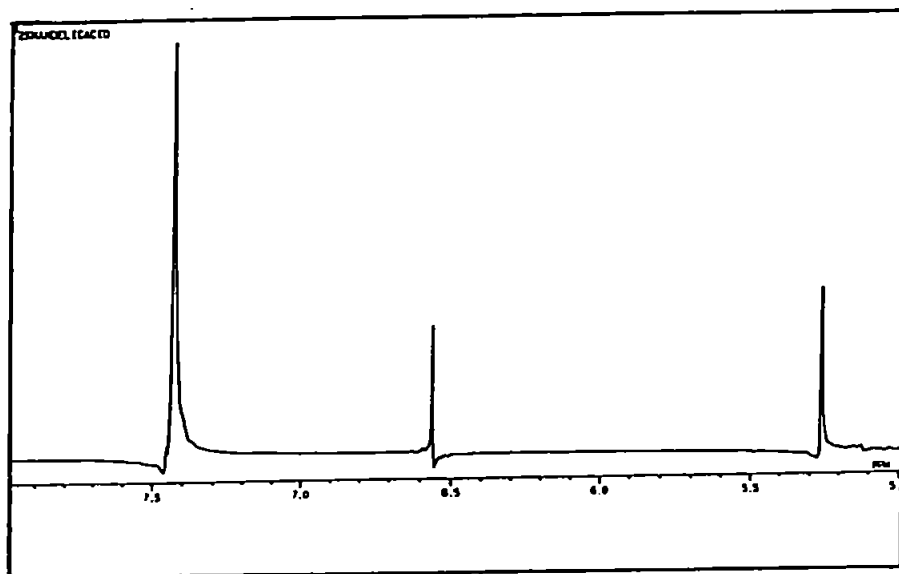


Figure 3.9 ^{13}C NMR for an equimolar solution of Sb(V) and DL-malic acid in MilliQ.



a)



b)

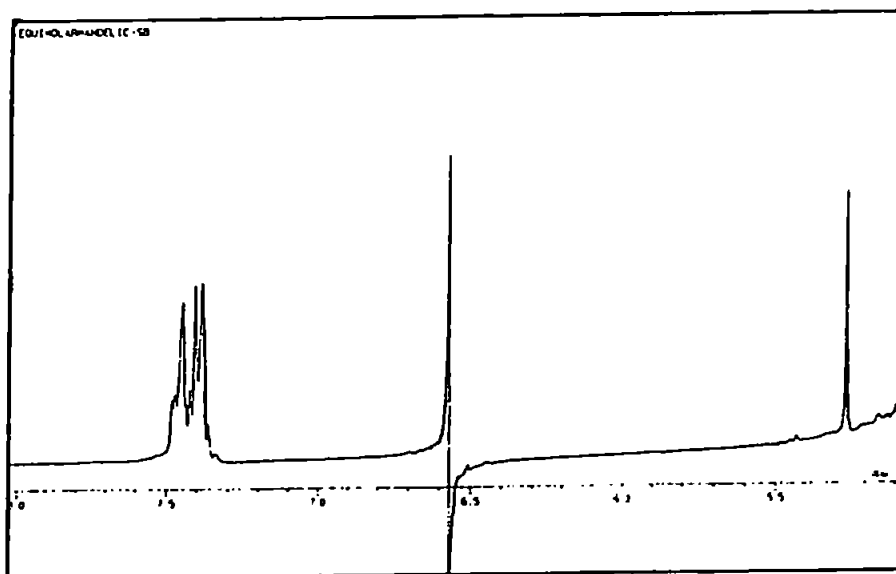
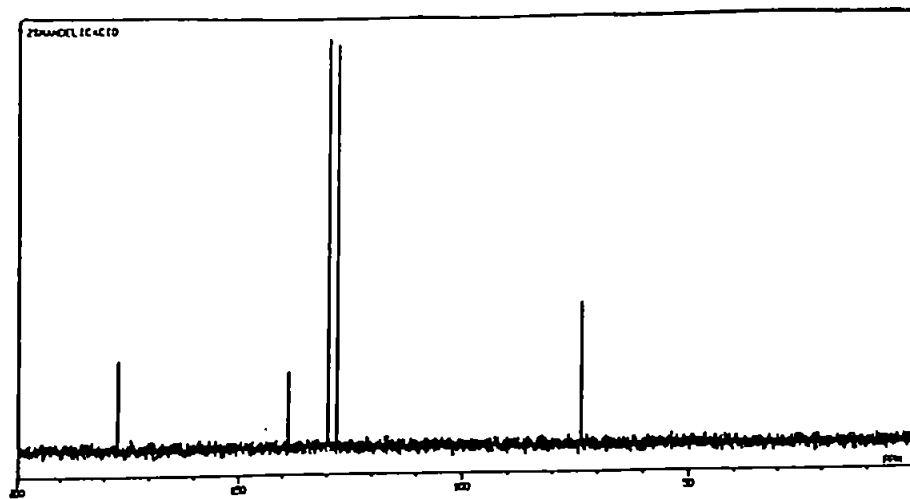
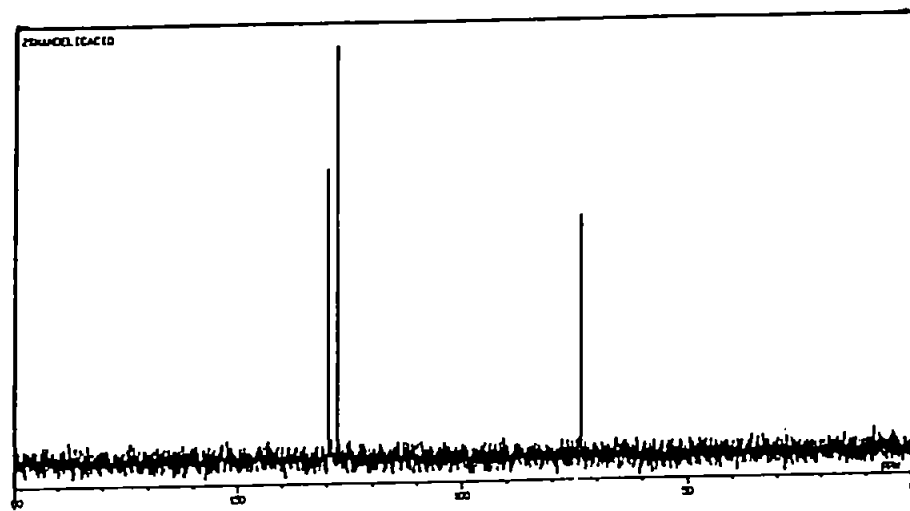


Figure 3.10. ^1H NMR for a) 2% (w/v) mandelic acid and b) equimolar solution of Sb(V) and mandelic acid in MilliQ. Inset is structure.

a)



b)



c)

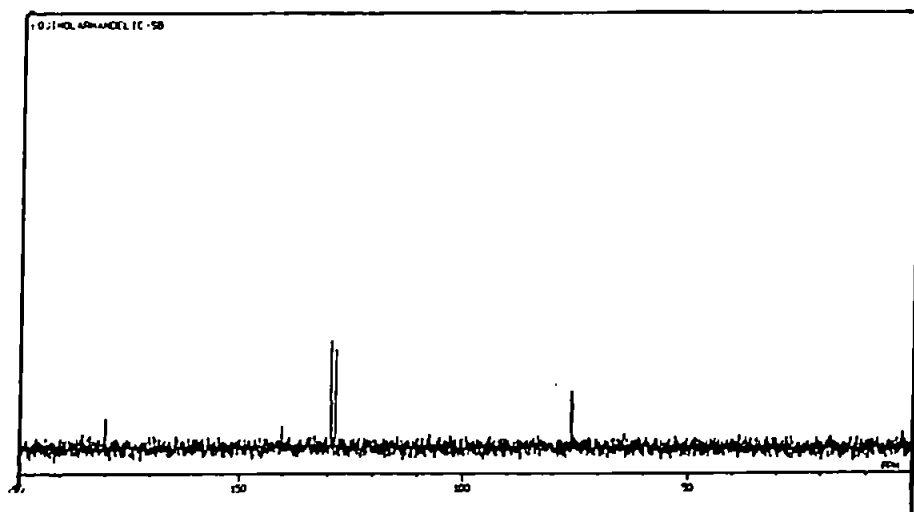


Figure 3.11. ^{13}C NMR for a) 2% (w/v) mandelic acid and b) as a ^{13}C DEPT experiment, and c) an equimolar solution of Sb(V) and mandelic acid in MilliQ.

The changes to this spectra brought about by the addition of Sb are small but observable, i.e. there is a small chemical shift in all the signals and the aromatic carbon peaks are better resolved, Figure 3.11.

3.4.2 Determination of Complexes by IC-ICP-AES

The initial ion chromatography studies of Sb, α -hydroxyacid complexes were performed at the same time as the NMR investigation of these systems. The studies used previously established aqueous separation protocols for the speciation of Sb(V) and Sb(III) compounds. These protocols are discussed in Chapter 4.

In the study of Mohammad *et al.*⁽¹⁴⁴⁾ only the suppression of the Sb(V) signal in hydride generation was observed, the chemistry of the citrate interaction with Sb(V) was not investigated, probably as a result of the vast excess of citric acid used in comparison to the levels of Sb in solution. A previous paper⁽¹⁴³⁾ also reported the suppression effect as being a result of pH control by citric acid. Hence the need for this investigation

3.4.2.1 Preliminary Results

Figure 3.12 shows preliminary results obtained from a 5 mg l⁻¹ mix of [Sb(OH)₆]⁻ and [Sb(OH)_x(citrate)_n] where the citric acid was in 2x molar excess of Sb. The mobile phase was 10 mM KNO₃ at pH3. The pH was adjusted with HNO₃. At a pH higher than 4.5 the peak for the Sb with citrate did not elute, although at pH 4.5 the observed peak was very broad. Lower pH levels for the mobile phase reduced retention times for this species and drastically reduced elution times. Figure 3.13 shows a chromatogram for two consecutive injections of [Sb(OH)₆]⁻ in malic acid (3x molar excess) together with an injection of an aliquot of [Sb(OH)₆]⁻. It was unclear at that time why the peak split, however, the NMR results could well point to this being

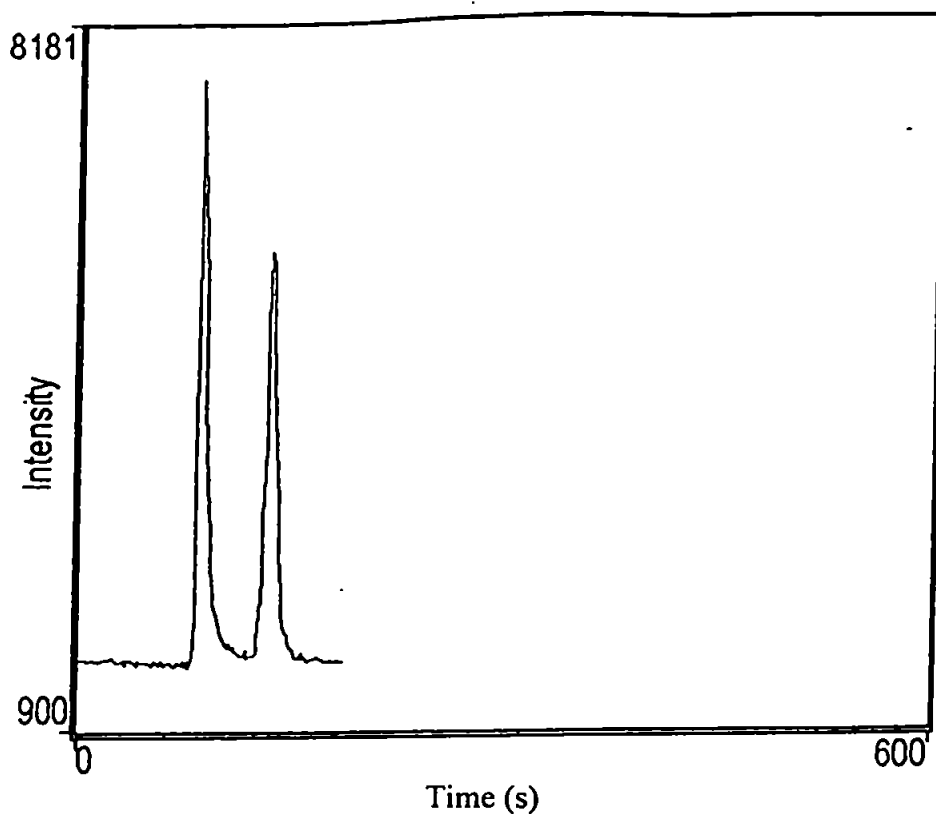


Figure 3.12 Separation of 5 mg l⁻¹ Sb(V) and Sb(V)citrate. 10 mM KNO₃ eluent at pH3. Flow rate 1 ml min⁻¹. AS4A column. ICP-AES detection @217.581 nm.

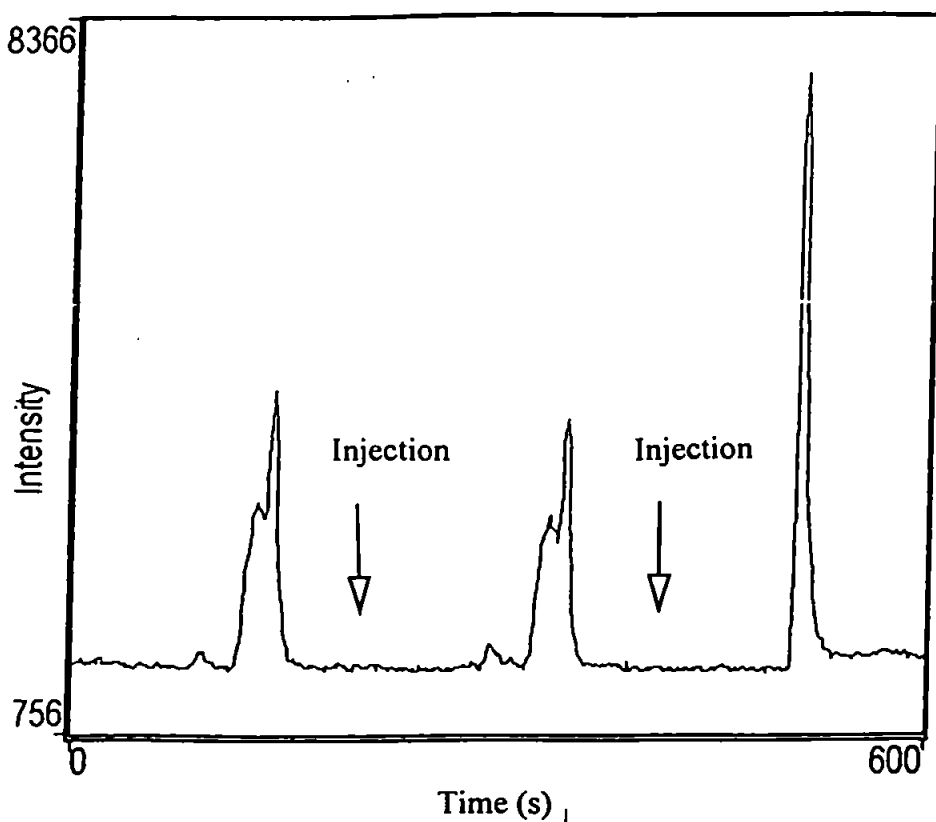


Figure 3.13 Injections of 5 mg l⁻¹ Sb(V) in excess DL-malic acid followed by an aliquot of Sb(V). 10 mM KNO₃ eluent at pH3. Flow rate 1 ml min⁻¹. AS4A column. ICP-AES detection @217.581 nm.

due to bonding of the malic acid group to Sb through either carboxylic group. This could well result in a mixture of complexes and thus slightly different chromatographic characteristics.

Figure 3.14 shows a chromatogram obtained for three repeat injections of a 10 mg l^{-1} mix of $[\text{Sb}(\text{OH})_6]^-$, $[\text{Sb}(\text{OH})_x(\text{malate})_n]$ and $[\text{Sb}(\text{OH})_x(\text{citrate})_n]$. The peak areas were observed to decrease in almost equal proportion with time. This was due to instrumental drift. If the peak areas are normalised for the largest peak, in each case the citrate peak, the proportions for each mix are approximately the same with $[\text{Sb}(\text{OH})_6]^-$ being 50-58% of Sb(citrate) and Sb(malate) being 67-74% that of the citrate peak. There was less variation if the peaks are normalised for peak height. The disproportionation of peak areas in favour of the citrate peak was believed to be due to the excess of citric acid in solution from the $[\text{Sb}(\text{OH})_x(\text{citrate})_n]$ standard. Free citrate molecules could be complexing with $[\text{Sb}(\text{OH})_6]^-$ in the mixture thus enhancing the citrate peak. The analytical and chromatographic figures of significance are summarised in Table 3.2.

Following this initial set of results it was decided that a study of the level of association of each acid with Sb was required, hence the development of the model in Section 3.3.

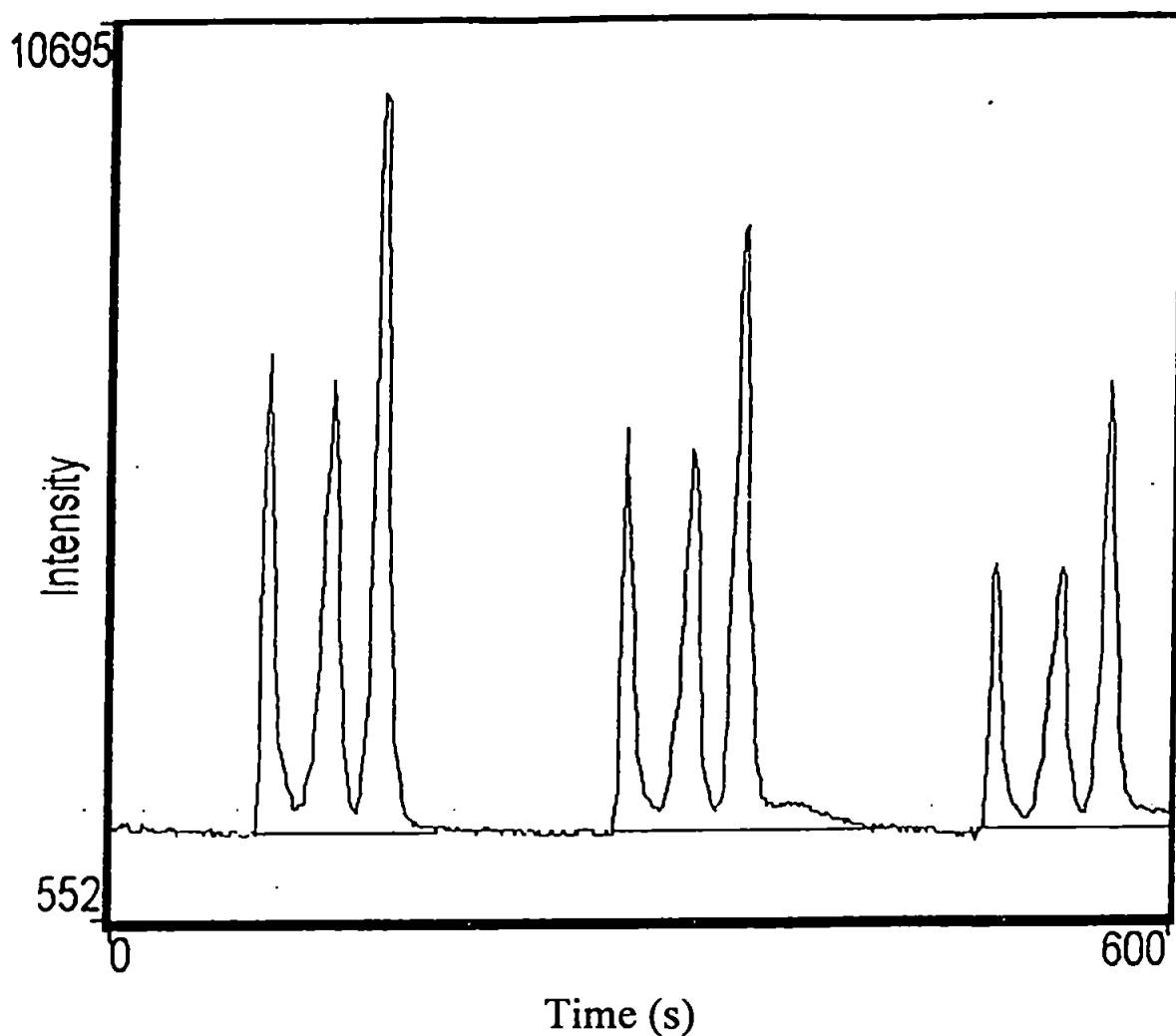


Figure 3.14 Chromatogram for three repeat injections of a 10 mg l⁻¹ as Sb mixture of $[\text{Sb}(\text{OH})_6]^-$, $\text{Sb}(\text{OH})_x(\text{malate})_n$ and $\text{Sb}(\text{OH})_x(\text{citrate})_n$. 10 mM KNO_3 eluent at pH3. Flow rate 1 ml min⁻¹. AS4A column. ICP-AES detection @217.581 nm.

Table 3.2 Figures of significance for preliminary separations of Sb, α -hydroxyacids

Species	Retention time (s)	Capacity Factor (k')	Selectivity factor (α) ^a	^b Plates m ⁻¹
[Sb(OH) ₆] ⁻	90 (t _m)	-		
[Sb(OH) _x (malate) _n] ⁻	126 (t _x)	0.4	1.775	1,698
[Sb(OH) _x (citrate) _n] ⁻	153.5 (t _y)	0.71		6,549

^a calculated as $k't_y/k't_x$

^b calculated as $16(t_R/W)^2$, corrected for t_m

The selectivity factor for the two Sb, α -hydroxyacid compounds confirms the virtually baseline resolution between the species and the number of plates for this separation is very good.

3.4.2.2 Detailed investigation and application of stoichiometric model.

3.4.2.2.1 [Sb(OH)_x(citrate)_n]

The elution profiles for citric acid only and [Sb(OH)₆]⁻ only were not identical even if the retention times were very similar. The 1:1 mixture, when analysing for Sb at 187.115 nm resulted in two peaks on the chromatogram, Figure 3.15. The relative peak areas for each were as follows : 1) 83.4 s, 14%; 2) 175.2 s, 86%. Thus with the addition of citric acid to the [Sb(OH)₆]⁻ in equimolar proportions a significant change occurred in the retention of Sb on the column. Carbon analysis at 193.026 nm gave just one peak at 176.4 s. The carbon analysis was carried out some 90 minutes after the Sb analysis for this solution. It seems likely therefore that a more complete complexation of Sb had occurred by this time. Importantly, the retention times and peak shapes for the associated peaks at 176 seconds were identical. The shape of the peak in Figure 3.16, which demonstrates a degree of

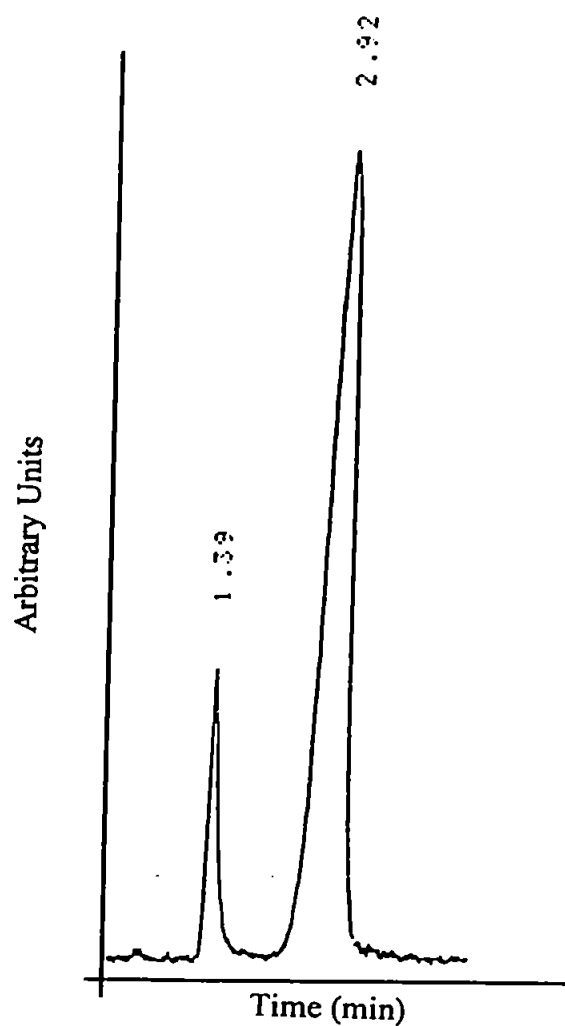


Figure 3.15 Injection of 1:1 solution of Sb(V):citric acid. 20 mM NH_4Cl eluent at $< \text{pH}3$. Flow rate 1 ml min^{-1} . ICP-AES detection @187.115 nm.

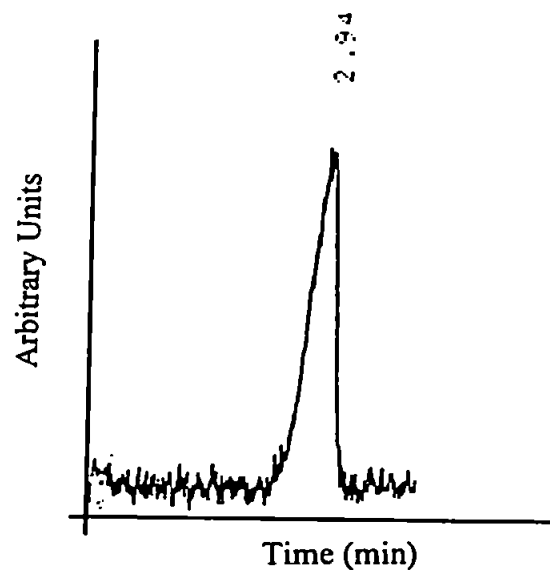


Figure 3.16 Injection of 1:1 solution of Sb(V):citric acid. 20 mM NH_4Cl eluent at $< \text{pH}3$. Flow rate 1 ml min^{-1} . ICP-AES detection @193.026 nm.

fronting with the unusual sloping leading edge and the almost vertical return to baseline confirms the association of Sb and citric acid in solution.

The 2:1 ratio solution gave one peak for the Sb analysis at 177 s. The carbon analysis gave two peaks at 95 s and 175s, with relative peak area ratios of 40:60, indicating approximately 60% of the total citric acid was associated with all of the Sb in the solution.

Table 3.3 summarises the results for these mixtures and the remaining Sb-citric acid mixtures.

To truly establish the association of citric acid with the Sb in solution the different parts of the new molecule had to be analysed simultaneously by HPLC. For this purpose a simultaneous ICP-AES was utilised as a detector for the HPLC separation.

Figure 3.17 shows the results obtained for this analysis. The peak retention profiles of $[\text{Sb}(\text{OH})_6]^-$ and citric acid injected separately are not identical and as such do not demonstrate identical exchange characteristics on-column. However Figures 3.17 b-e show that associated Sb-citrate peaks have identical elution profiles and retention times for peak maxima. This was taken as good evidence to support the theory that the Sb and citric acid were components of one compound. This result supported the NMR results indicating a reaction had taken place in solution and a new compound formed. Integration of these peaks and the application of the model described in the Experimental section showed a firm 1:1 relationship of citric acid with Sb. Table 3.3 shows this more clearly.

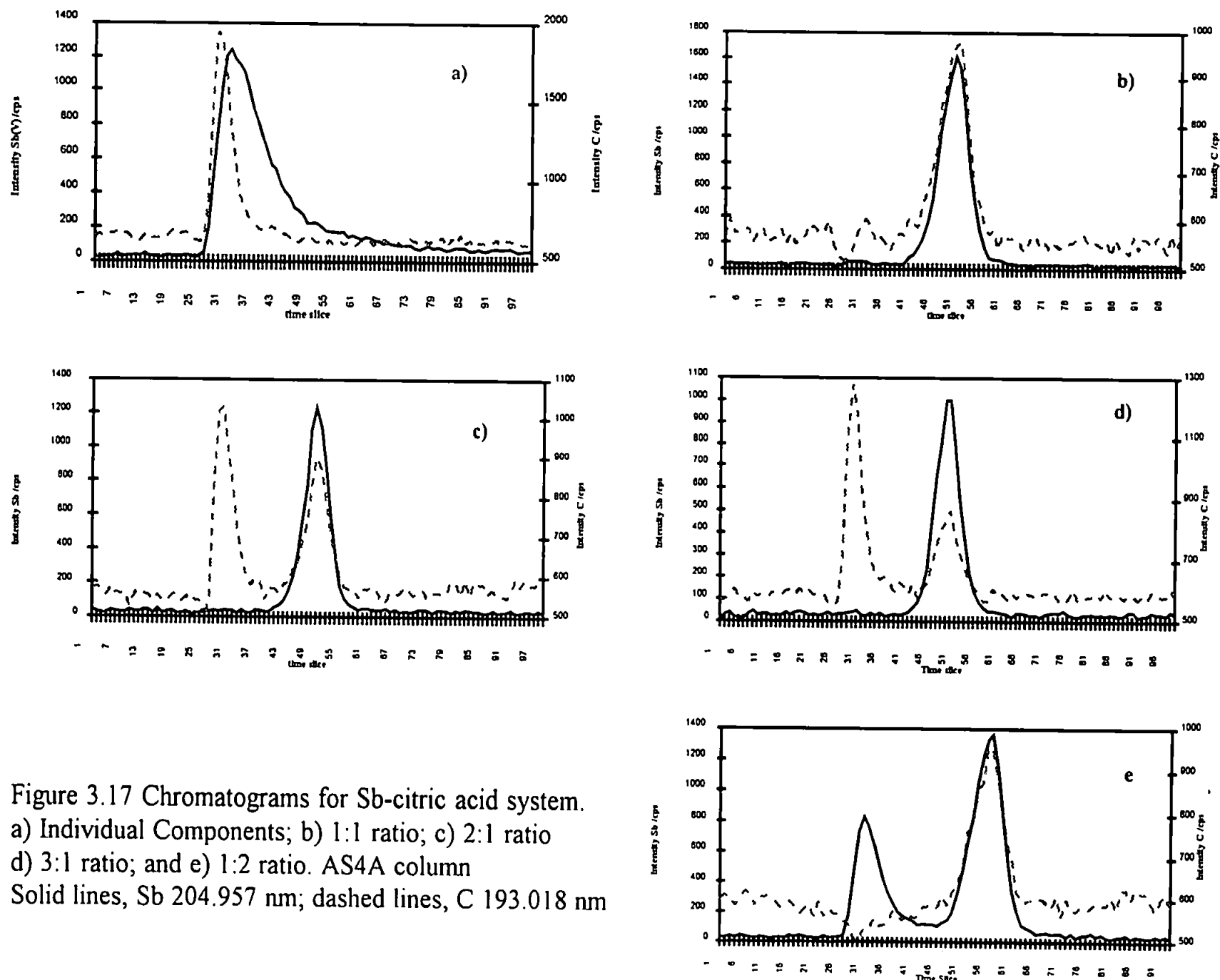


Figure 3.17 Chromatograms for Sb-citric acid system.
a) Individual Components; b) 1:1 ratio; c) 2:1 ratio
d) 3:1 ratio; and e) 1:2 ratio. AS4A column
Solid lines, Sb 204.957 nm; dashed lines, C 193.018 nm

Table 3.3 Summary of results for Sb: citric acid system including the calculated levels of association

Citric acid:Sb ratio	C determination @ 193.026 nm		Sb determination @ 187.115 nm		Level of Association (mol dm ⁻³)
	No. of peaks	Retention time (Relative Peak Areas)	No. of Peaks	Retention time (Relative Peak Areas)	
1:1	1	176.4s (100%)	2	83.4s (14%); 175.2s (86%)	0.005:0.0043
2:1	2	95s (40%); 175s (60%)	1	177s (100%)	0.0040:0.0033
3:1	2	92.4s (56%); 174s (44%)	1	173.4s (100%)	0.0033:0.0025
4:1	2	93s (77%); 171s (23%)	1	171s (100%)	0.0018:0.002
1:2	1	176.4s (100%)	2	85.2s (60%); 176.4s (40%)	0.0033:0.0040
1:3	1	175s (100%)	2	85s (75%); 174s (25%)	0.0025:0.0019

3.4.2.2.2 [Sb(OH)_x(malate)_n]

The malic acid only peak eluted at 89s and did not elute to baseline as quickly as did the [Sb(OH)₆]⁻ peak. The addition of malic acid to Sb(V) brought about an expected change in the retention times but the elution profile was unexpected, as will be discussed in the following sections.

In the 1:1 mix the Sb analysis produced chromatograms with two peaks at 88.2s and 126s. The second peak had a distinctive shape with a steep leading edge and a long, plateau-like, tail. This might be indicative of a deterioration of the complex on-column. The level of this plateau represented approximately 20% of the peak maximum. About 150s after the peak retention time the plateau rapidly dropped to baseline (see Figure 3.18). This peak profile was very distinctive but it was not possible to draw any conclusions from this even if the C analysis showed the same profile.

Indeed, the C analysis at 193.026 nm showed a chromatogram that had one peak at 126s (retention time). This peak had the same plateau-like tail, Figure 3.19.

With increases in molar ratio in favour of malic acid the Sb analysis showed complete association with malic acid with the C analysis producing two peaks for the free acid and associated acid molecules. With the reverse molar ratios, i.e. Sb in excess, two peaks were observed in the Sb chromatograms and one peak for the C analysis. All of the C was observed to be associated with the second Sb peak. Table 3.4 summarises the results for the malate system in the same way to that of Table 3.3 does for the citrate system.

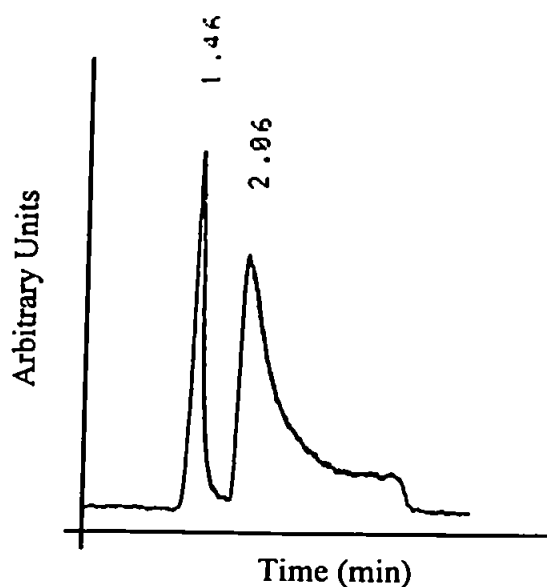


Figure 3.18 Injection of 1:1 solution of Sb(V):DL-malic acid. 20 mM NH_4Cl eluent at $< \text{pH}3$. Flow rate 1 ml min^{-1} . ICP-AES detection @187.115 nm.

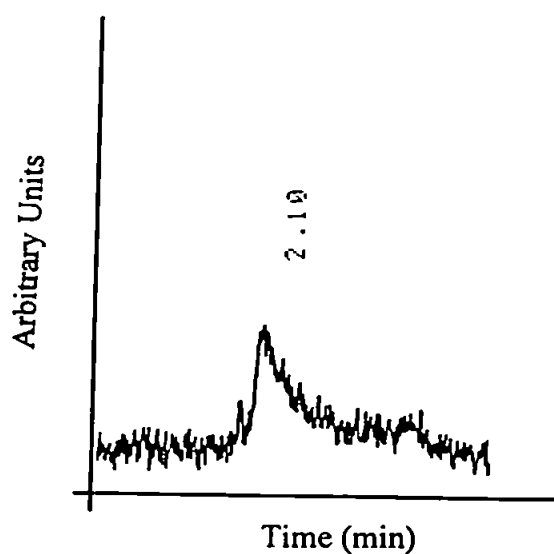


Figure 3.19 Injection of 1:1 solution of Sb(V):DL-malic acid. 20 mM NH_4Cl eluent at $< \text{pH}3$. Flow rate 1 ml min^{-1} . ICP-AES detection @193.026 nm.

Table 3.4 Summary of results for Sb:DL-malic acid system including the calculated levels of association

DL-malic acid:Sb ratio	C determination @ 193.026 nm		Sb determination @ 187.115 nm		Level of Association (mol dm ⁻³)
	No. of peaks	Retention time (Relative Peak Areas)	No. of Peaks	Retention time (Relative Peak Areas)	
1:1	1	126s (100%)	2	87.6s (31.4%); 123.6s (68.6%)	0.005:0.0034
2:1	2	96s (58%); 126s (42%)	2	87.6s (3%); 126s (97%)	0.0028:0.0032
3:1	2	93.6s (82%); 134s (18%)	1	132s (100%)	0.0014:0.0025
4:1	2	93.6s (70%); 132s (30%)	1	134s (100%)	0.0024:0.002
1:2	1	133.2s (100%)	2	88.8s (65%); 128.4s (35%)	0.0033:0.0023
1:3	1	129.6s (100%)	2	88.8s (75%); 132s (25%)	0.0025:0.0019

3.4.2.2.3 [Sb(OH)_x(mandelate)_n]

Mandelic acid eluted with a retention time of 106s, well after the retention time of Sb(V). This compound was therefore quite strongly retained on the column. This could be due to the aromatic part of this compound interacting more strongly with the resin backbone of the column than the aliphatic part of the other acids.

Table 3.5 summarises the results from this study in the same format as Tables 3.3 and 3.4. However, gaps appear in the calculations owing to the features observed in the chromatograms when mandelic acid was in excess. In the carbon analysis of the 2:1 mixture, what appears to unassociated mandelic acid partially co-eluted with associated mandelic acid. Figures 3.20 a-d show chromatograms for the remaining solutions with appropriate annotation.

Where Sb was in excess the associated Sb and mandelic acid were clearly observed, Figure 3.21 a) & b). From the results for all of the acids with Sb, formulae and relative molecular weights were hypothesised to aid identification by mass spectrometry. These can be found in Table 3.6.

Table 3.6 Hypothesised m/z values and formulae for the complexes

	m/z	Formula
1	265	KSb(OH) ₆
2	381	K[Sb(OH) ₅ (malate)]
3	439	K[Sb(OH) ₅ (citrate)]
4	398	K[Sb(OH) ₅ (mandelate)]
5	533	K[Sb(OH) ₄ (mandelate) ₂]

Table 3.5 Summary of results for Sb: (±)-mandelic acid system including the calculated levels of association

(±)-mandelic acid:Sb ratio	C determination @ 193.026 nm		Sb determination @ 187.115 nm		Level of Association (mol dm ⁻³)
	No. of peaks	Retention time (Relative Peak Areas)	No. of Peaks	Retention time (Relative Peak Areas)	
1:1	1	135.6s (100%)	2	88.2s (24%); 134.4s (76%)	0.005:0.0038
2:1	1	135.6s (Shoulder)	2	87.6s (5%); 134.4s (95%)	-
3:1	2	121s (40%); 136.8s (60%)	1	133.8s (100%)	0.0045:0.0025
4:1	2	111.6s (50%); 132s (50%)	1	135s (100%)	0.004:0.002
1:2	1	134.4s (100%)	2	88.8s (60%); 134.4s (40%)	0.0033:0.0026
1:3	1	134.4s (100%)	2	90s (72%); 135s (28%)	0.0025:0.0021

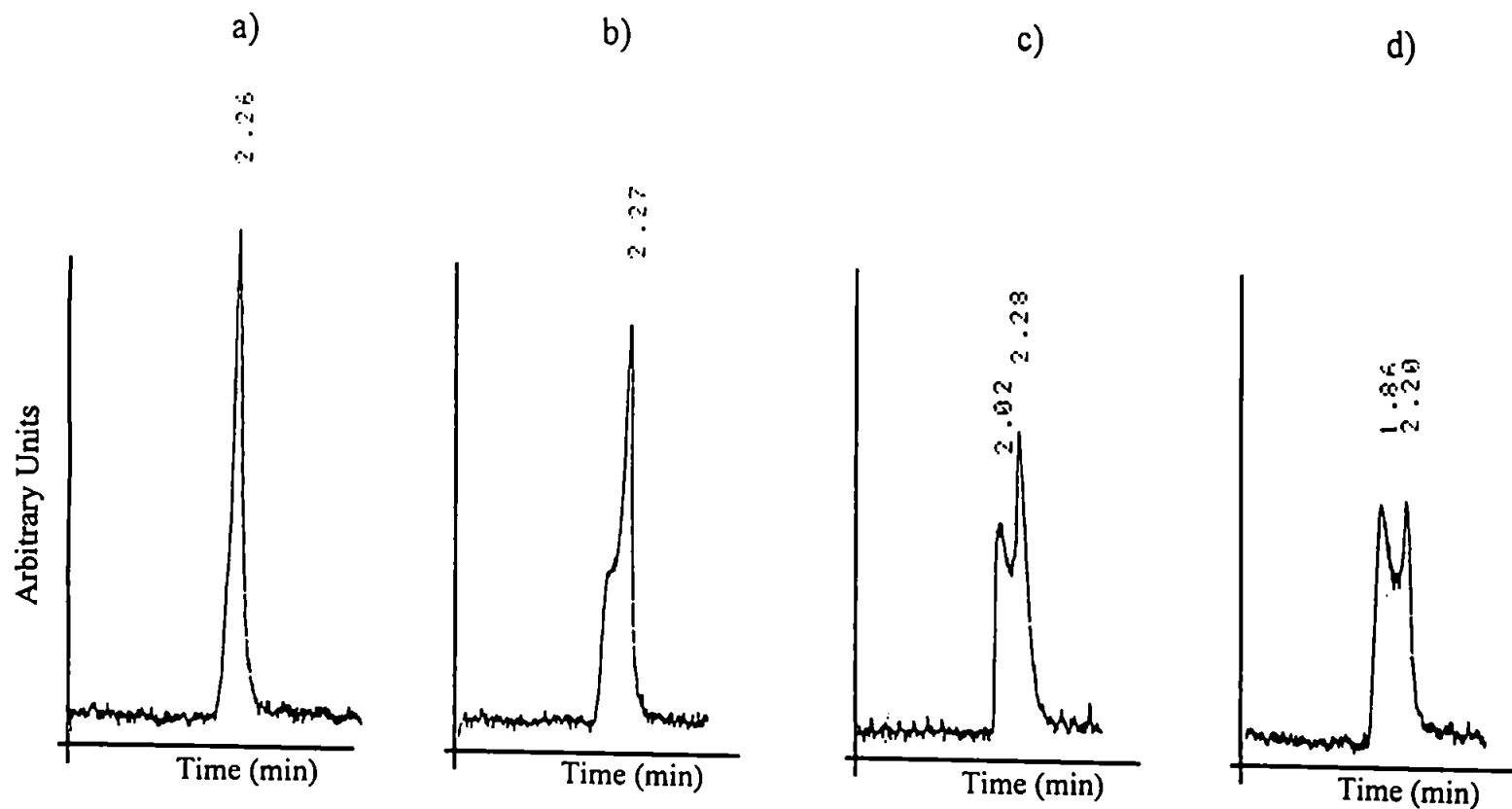


Figure 3.20 Chromatograms for C analysis @ 193.026 nm. a) 1:1 Sb:mandelic acid; b) 1:2 Sb:mandelic acid; c) 1:3 Sb:mandelic acid; and d) 1:4 Sb:mandelic acid. 20 mM NH_4Cl eluent at $\text{pH} < 3$. Flow rate 1 ml min^{-1} .

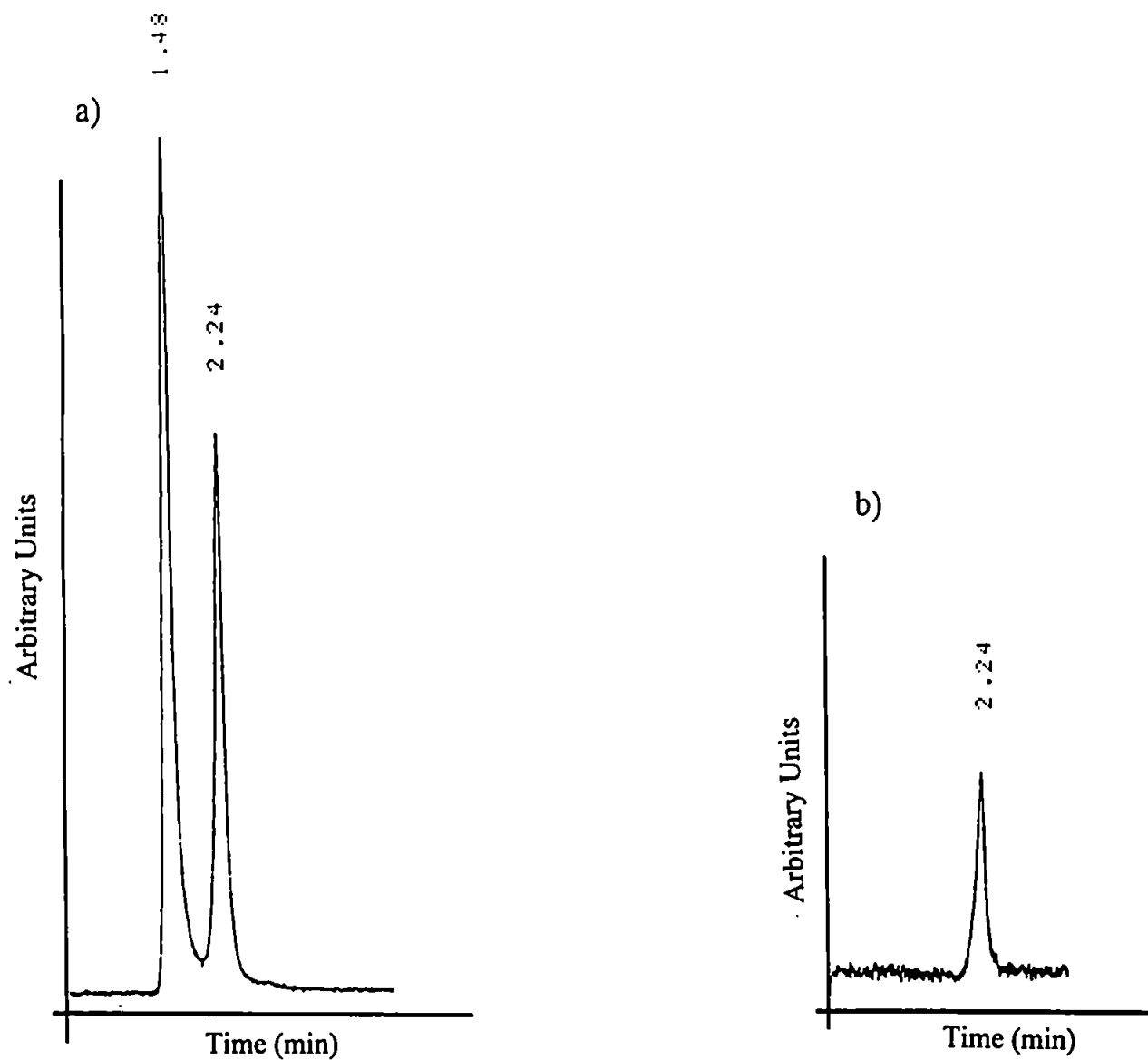


Figure 3.21 Chromatograms for Sb analysis @ 187.115 nm. a) 2:1 Sb:mandelic acid; and b) 3:1 Sb:mandelic acid. 20 mM NH_4Cl eluent at $\text{pH} 3$. Flow rate 1 ml min^{-1} .

3.4.3 Electrospray Ionisation-Mass Spectrometry (ESI-MS)

As previously described this aspect of the study was investigated in order to confirm the findings of the NMR study, but also importantly to corroborate the results of the HPLC analysis. Complexes were hypothesised from the HPLC results and as such relative molecular weights (RMW) were approximated. From these calculations the m/z range for the mass spectrometric analysis was selected and the solutions (as described in Section 3.2) were then analysed by ESI-MS.

3.4.3.1 Spectra Interpretation

$K^+[Sb(OH)_6]^-$ has a RMM of 265g, Figure 3.22 shows that mass spectrum for a solution of this compound. Although the base peak is not at m/z 265 the cluster of peaks does start with a pair of peaks at m/z 265. The range of this cluster is m/z 264-345. All of the signals observed in this cluster appear to result from the Sb adducts as indicated by the doublets observed. This reflects very closely the relative abundances of the two isotopes of Sb (^{121}Sb , ^{123}Sb) at 57 and 43 %.

$K^+[Sb(OH)_5(citrate)]^-$ was the hypothesised compound in the citric acid system. As can be seen in Figure 3.23 the mass spectrum for this solution shows two very clear features. Firstly the ion observed at m/z 231 due to $K(C_6H_7O_7)$ and secondly the major ion peak at m/z 439-441 (base peak). This peak has the same m/z value hypothesised for the compound believed to be formed between the Sb(V) and citric acid in solution. Just as importantly, however, the cluster observed for $K^+[Sb(OH)_6]^-$ has completely disappeared, indicating that the original compound has been transformed in solution by the addition of citric acid. This could have been due to some inhibition of ion formation by the α -hydroxyacid, but this seems unlikely considering the presence of ions at the m/z predicted for this compound. The cluster for this base peak is much reduced compared with that of the parent Sb compound.

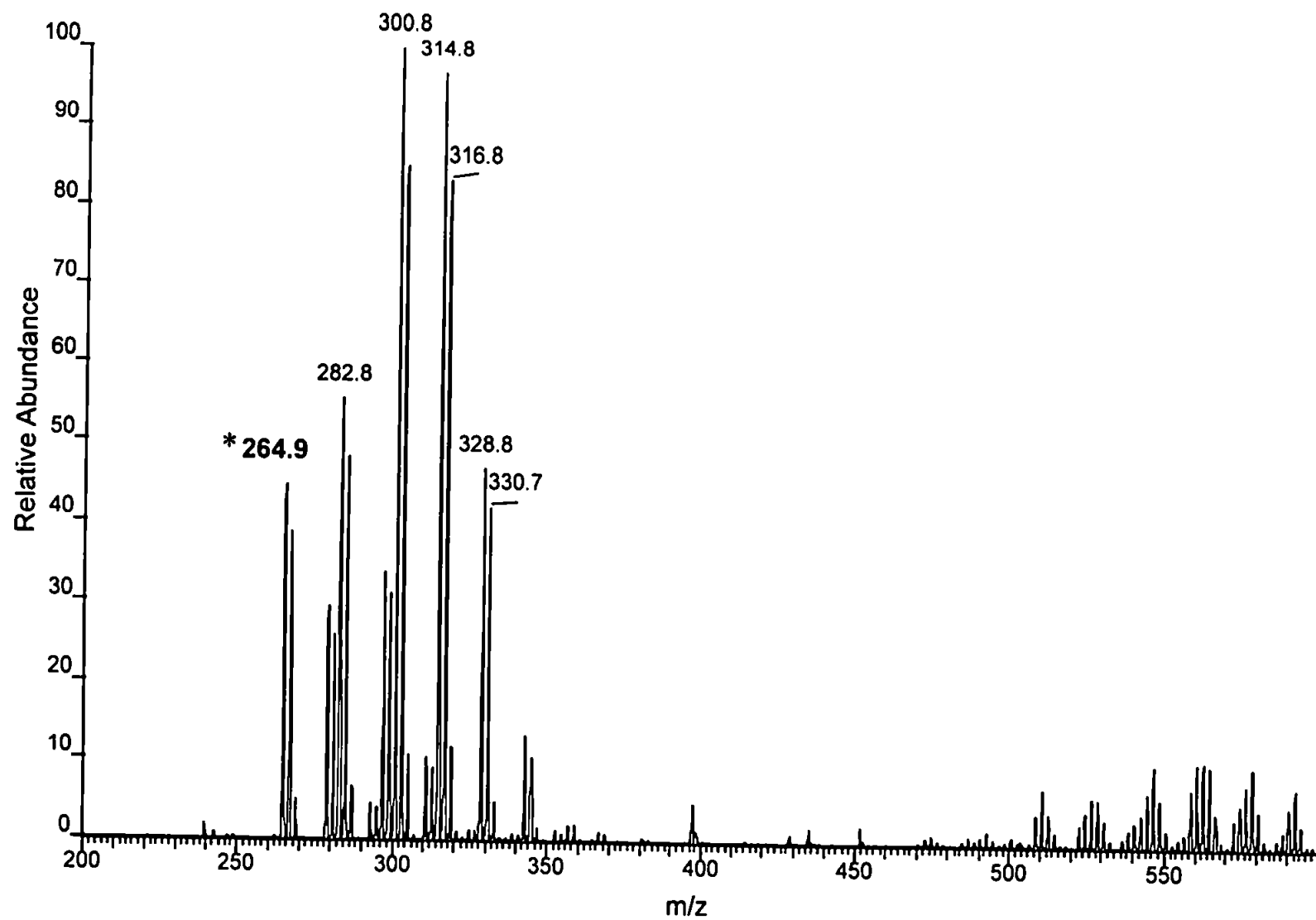


Fig. 3.22 Electrospray ionisation-mass spectrum for solution of KSb(OH)_6

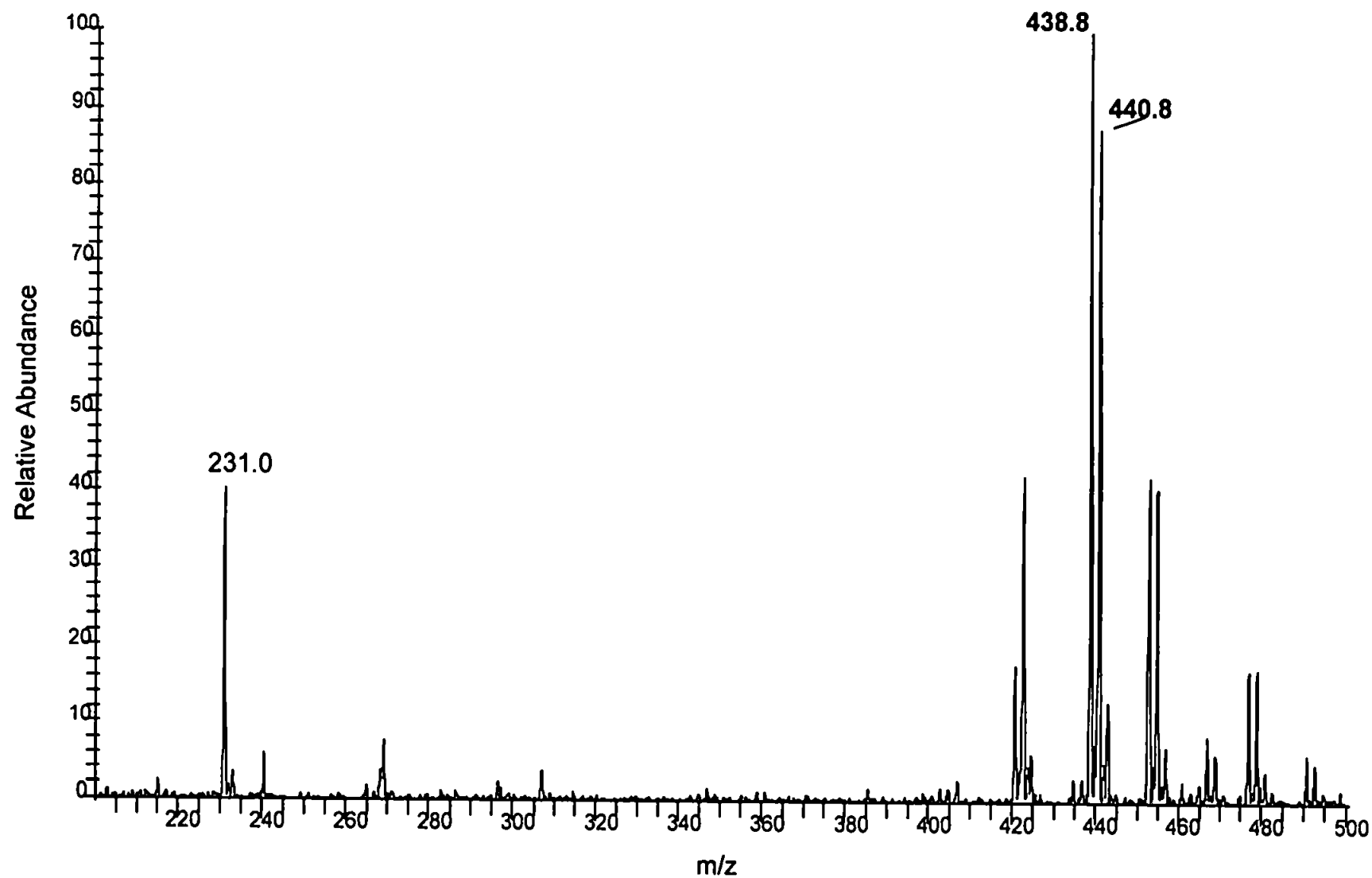


Fig. 3.23 Electrospray ionisation-mass spectrum for solution of $[\text{Sb}(\text{OH})_6]^-$ with citric acid

From Table 3.6 it can be seen that $K^+[Sb(OH)_5(malate)]^-$ is the most likely compound in the malic acid:Sb system. A major ion at m/z 381-383 (Figure 3.24) indicates the presence of an ion that agrees with our predicted compound. The peaks at m/z 211-213 and m/z 249-251 could be indicative of successive fragmentation of $(C_4H_6O_5)$ followed by K^+ . Once again the complete lack of a $K^+[Sb(OH)_6]^-$ cluster indicates a transformation of the original compound upon addition of malic acid.

As can be seen in Table 3.6 two compounds were hypothesised for the mandelic acid:Sb system, $K^+[Sb(OH)_5(mandelate)]^-$ and $K^+[Sb(OH)_4(mandelate)_2]^-$. Figure 3.25 gives the mass spectrum for this solution. Major ions appear at both the predicted m/z values, 397-399 and 533-535. There appears to be no evidence of Sato's original complex of $[Sb(OH)_2(mandelate)_2]$. As with the other solutions there is no $K^+[Sb(OH)_6]^-$ cluster.

3.4.4 Further Complex Determinations by HPLC

This study utilised a weak H_2SO_4 mobile phase to separate the Sb: α -hydroxyacid complexes using the AS-11 column. This is the heavily cross-linked column and as such a mixed-mode of ion-suppression and ion-exchange is hypothesised. However, bearing in mind that SO_4^{2-} is a strong ion-exchange candidate, the likelihood is that ion-exchange is a dominant mechanism.

Figure 3.26 presents the results obtained for separate injections of standards of Sb(V) in citric acid with decreasing eluent concentration. Reducing the eluent strength had the effect of increasing the retention time of the species. The same effect was observed for DL-malic and (\pm)mandelic. However, as Figure 3.27 shows for both of these systems double peaks were observed. This supports the possibility that for malic acid the complexation is through either carboxylate group and that the difference in polarity of the two types of complex affects the retention of the species. For mandelic acid the bond only goes through the lone carboxylate group.

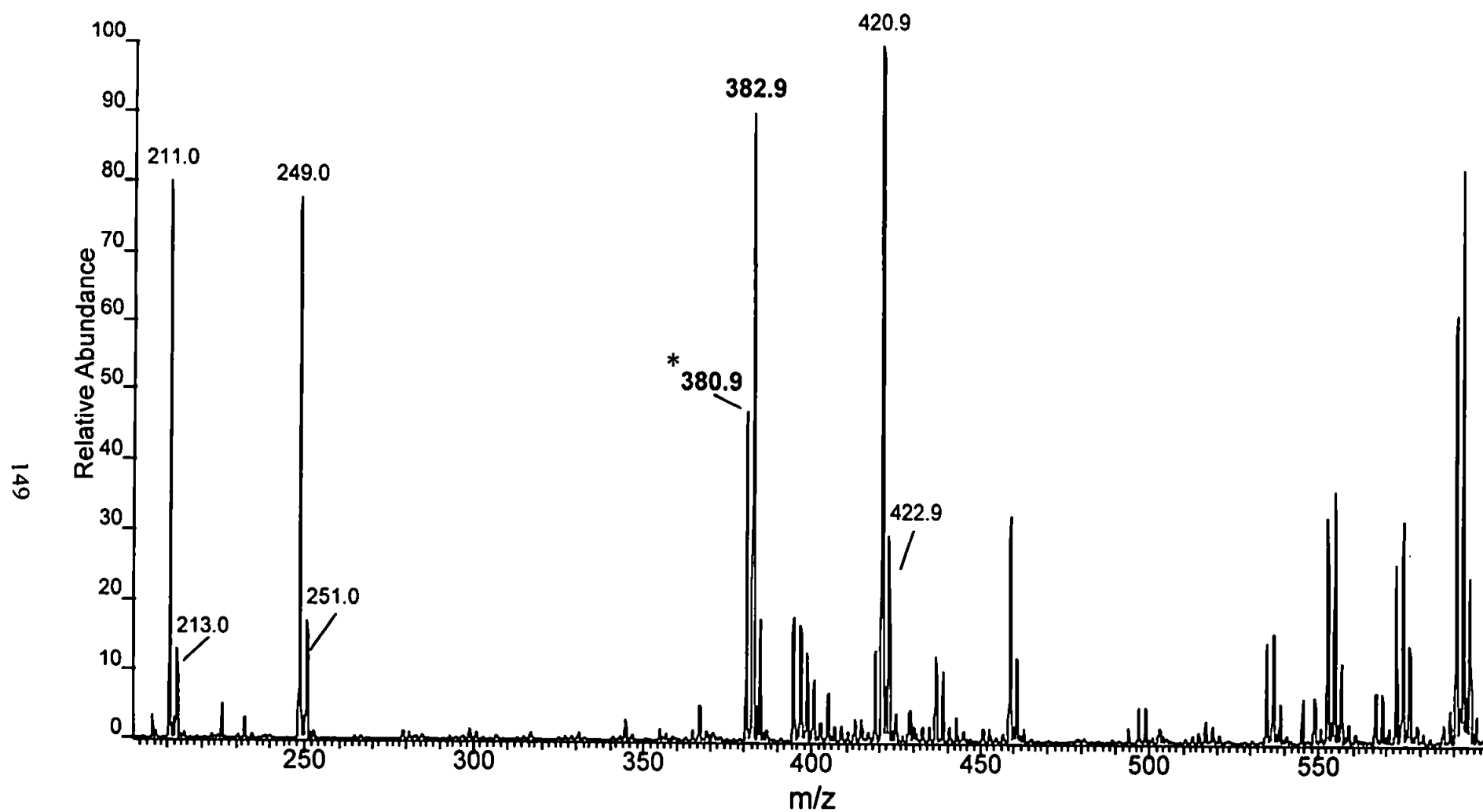


Fig. 3.24 Electrospray ionisation-mass spectrum for solution of $[\text{Sb}(\text{OH})_6]^-$ with malic acid

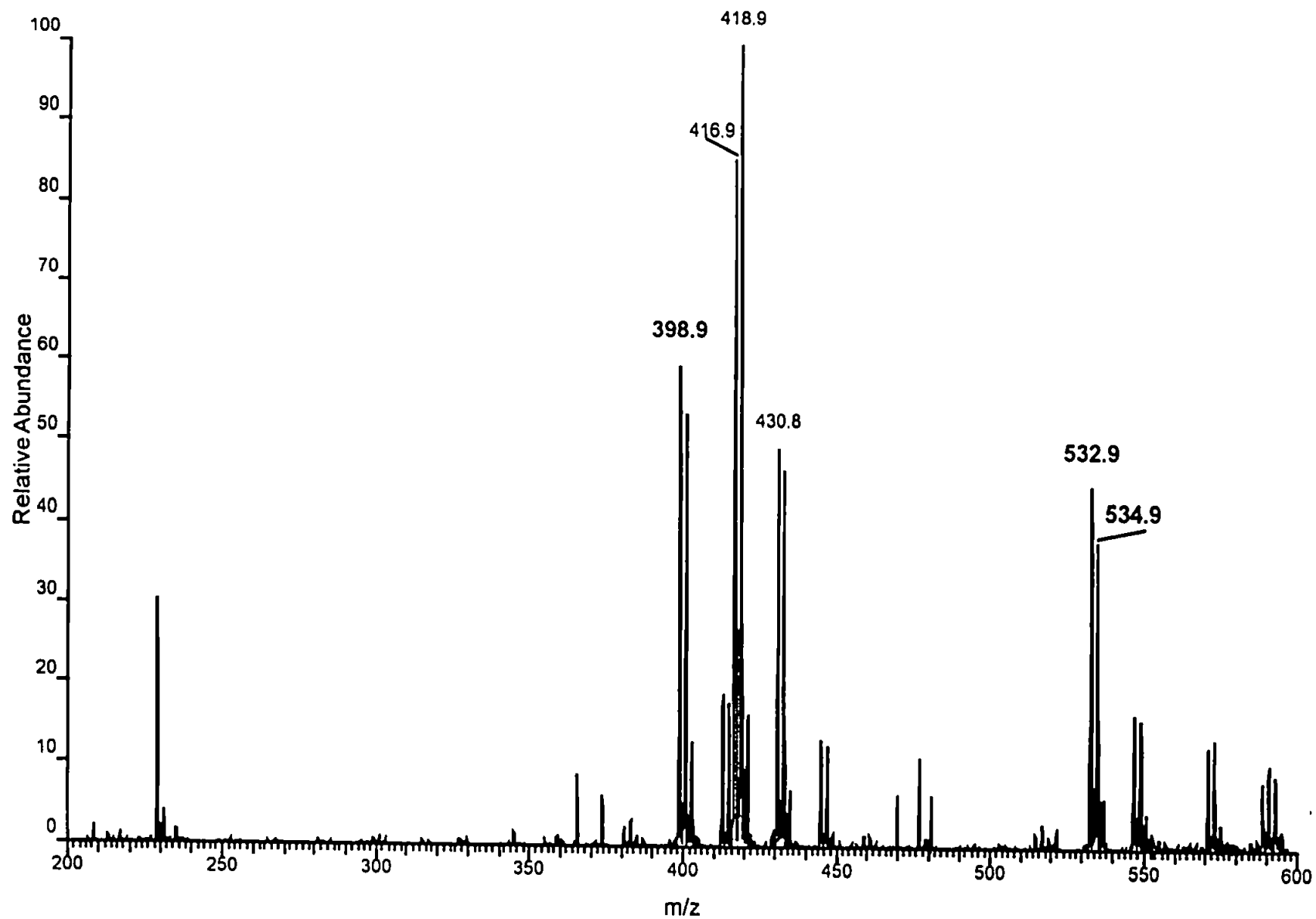


Fig. 3.25 Electrospray ionisation-mass spectrum for solution of $[Sb(OH)_6]^-$ with mandelic acid

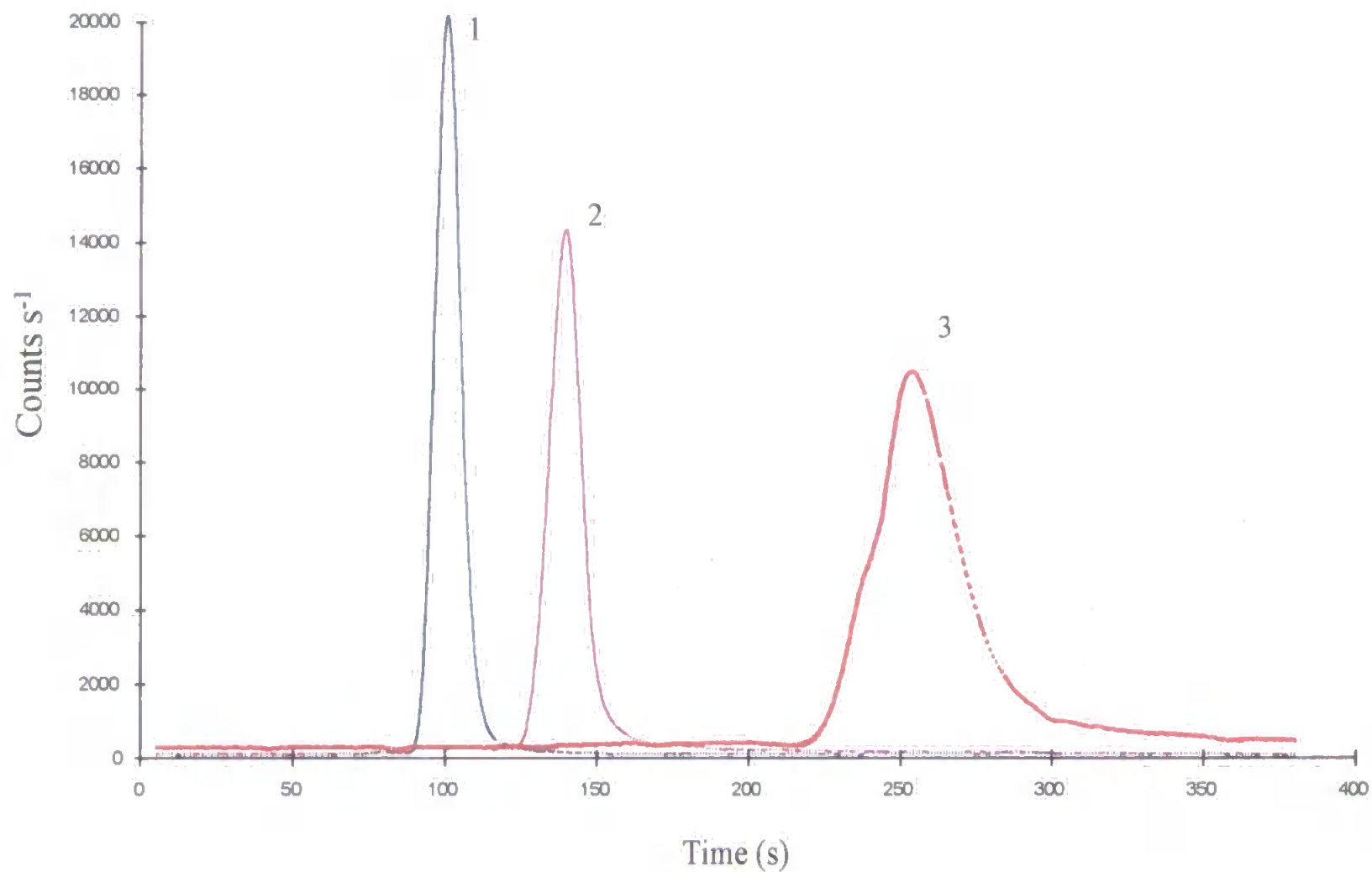


Figure 3.26 Chromatograms obtained for injections of $250 \mu\text{g l}^{-1}$ Sb(V) with citric acid. 1) 5 mM H_2SO_4 eluent; 2) 1 mM; and 3) 0.2 mM. Flow rate 0.35 ml min^{-1} . AS11 column

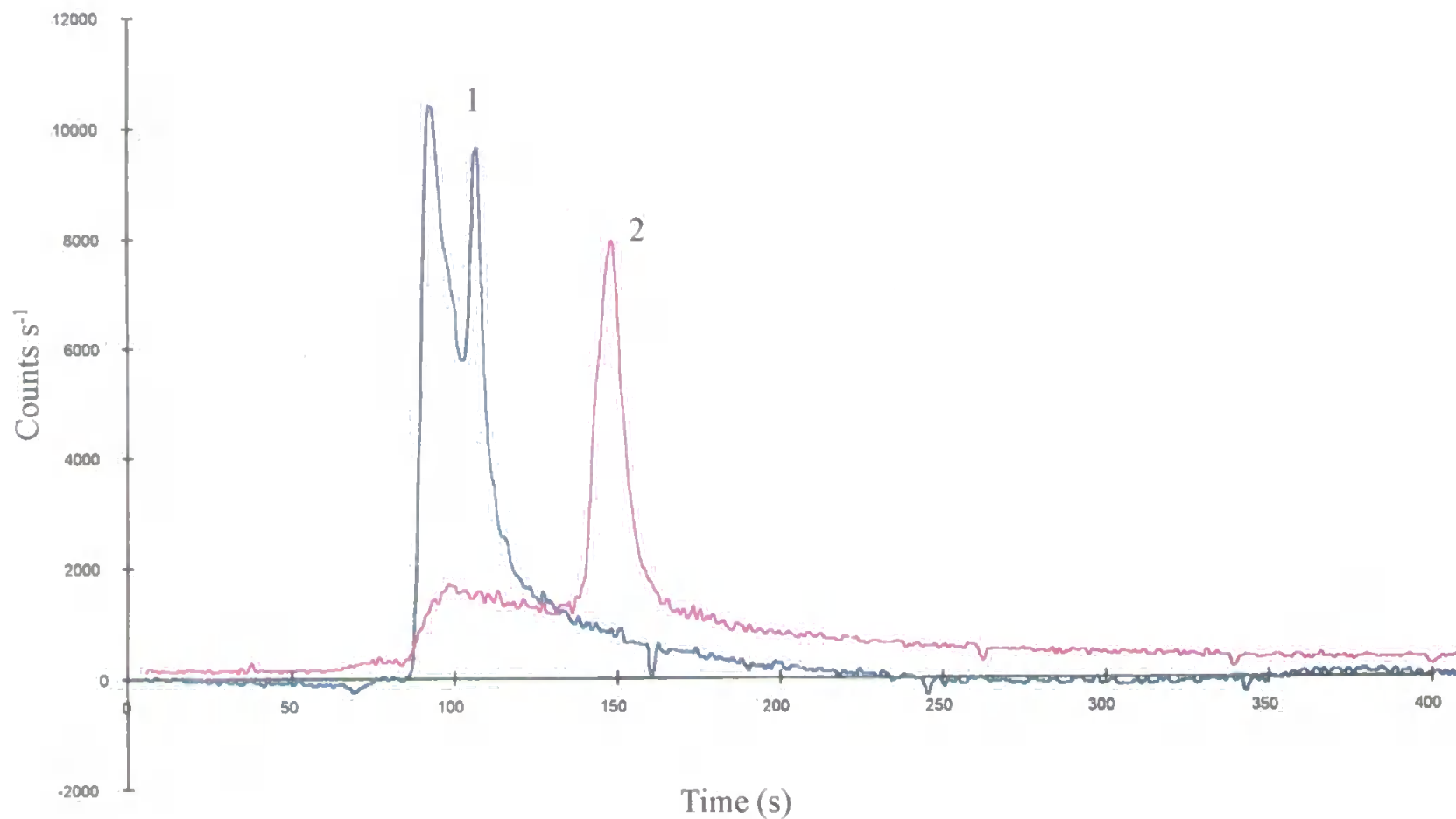


Figure 3.27 Chromatograms obtained for injections of $250 \mu\text{g l}^{-1}$ Sb(V) with 1) DL-malic acid; and 2) mandelic acid. $1 \text{ mM H}_2\text{SO}_4$ eluent @ 0.35 ml min^{-1} . AS11 column

The double peak could result from the formation of a complex with more than one mandelic acid molecule attached to the Sb atom. This was supported by the mass spectrum for this complex obtained by the ESI-MS analysis. This interaction could only be confirmed in solution by mass spectrometric analysis.

Figure 3.28 shows a chromatogram for a mixture of the Sb:acid systems. The peaks are sufficiently separated for the next phase of the study, i.e. to investigate the formation of the complexes in terms of stability/preferred formation. Figure 3.29 shows the result of the addition of Sb(V) to an excess of each acid in a mixture and comparing it with standards for each system. This result appears to suggest that the mandelic acid and malic acid complex faster than citric acid and that the mandelic is the most stable of the three systems. The appearance of the peak for mandelic acid in Figure 3.29 supports the high mass fraction of this complex compared with the other complexes.

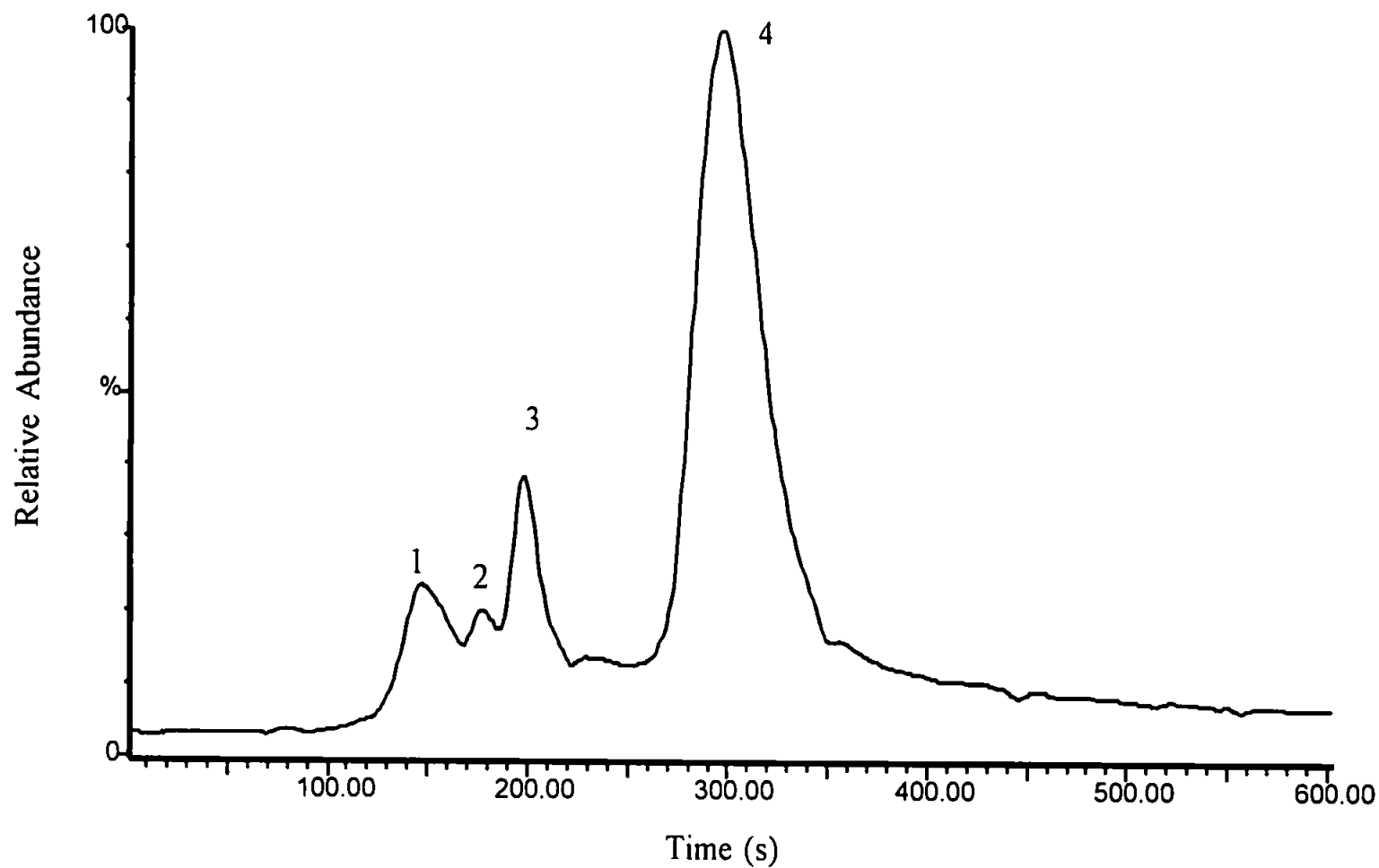


Figure 3.28 Chromatogram for injection of $250 \mu\text{g l}^{-1}$ Sb(V): α -hydroxyacid mixture. 1) DL-malic acid; 2) DL-malic; 3) mandelic; and 4) citric acid. $0.2 \text{ mM H}_2\text{SO}_4$ eluent @ 0.35 ml min^{-1} . AS11 column

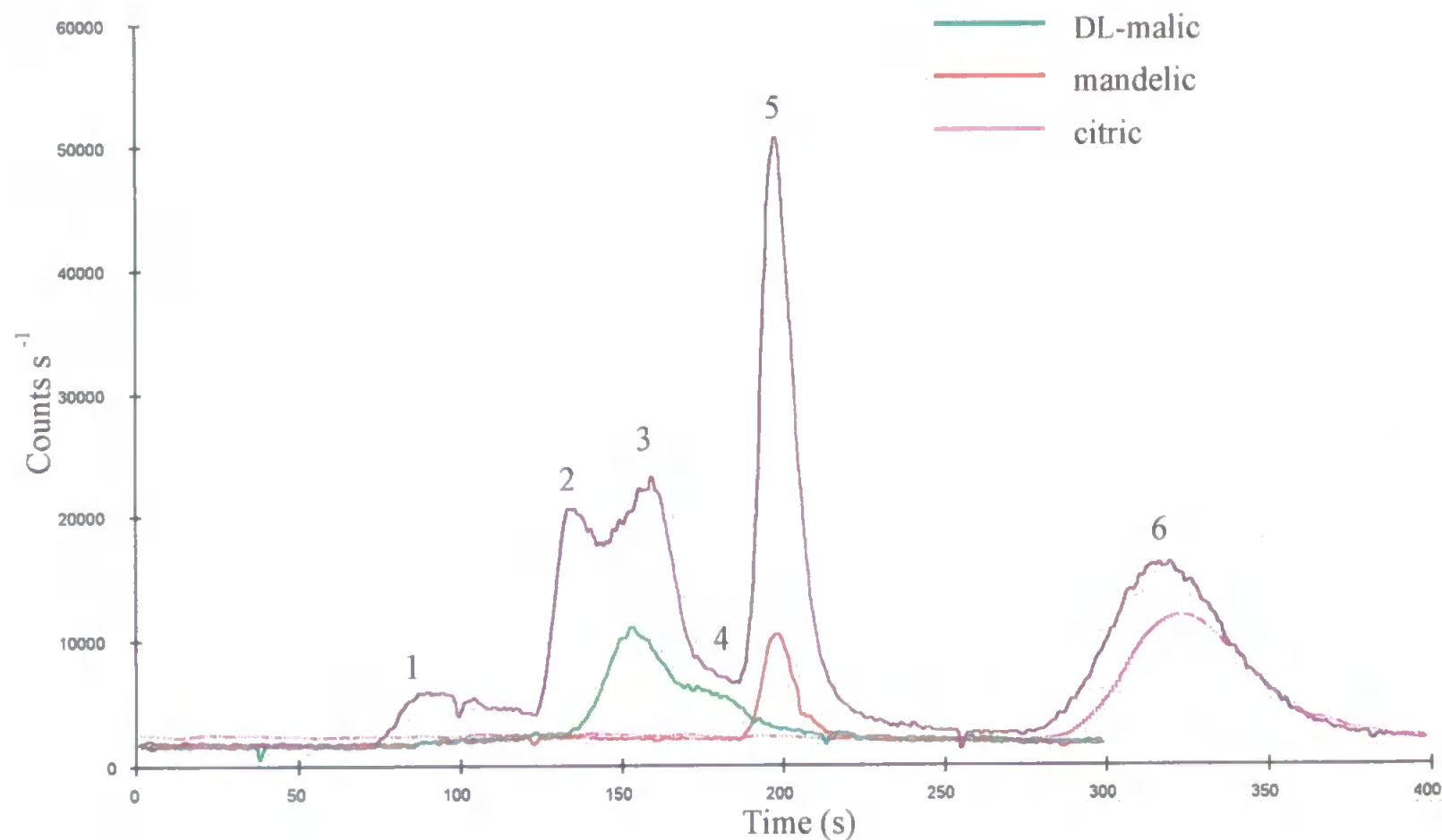


Figure 3.29 Chromatograms for injection of 4×10^{-6} M Sb(V) added to 1.33×10^{-4} M mixture of α -hydroxyacid; and separate standards of $63 \mu\text{g l}^{-1}$ Sb(V) in each acid. 1) Uncomplexed Sb(V); 2) mandelic; 3) DL-malic; 4) DL-malic; 5) mandelic; and 6) citric acid. 0.2 mM H₂SO₄ eluent @ 0.35 ml min⁻¹. AS11 column

3.5 Discussion

3.5.1 Structural Evaluation of Sb, α -hydroxyacid Compounds

The NMR, HPLC-ICP-AES, HPLC-ICP-MS and ESI-MS measurements and determinations all provided valuable evidence to support the theory that Sb(V) can form compounds with this group of carboxylic acids. The structural identification would be better achieved if these compounds could be isolated in solid form so as to obtain crystallographic data. However, their existence in solution over a large concentration range, $\mu\text{g l}^{-1}$ to % (w/v), is well supported by the data obtained.

The possibility that the addition of the acids merely affects the elution of Sb owing to competition for ion-exchange sites is unlikely, indeed improbable when one considers that some of the solutions contained an excess of Sb and that the ion-exchange sites would be in vast excess of any injected species at the concentrations used. Two distinct peaks are clearly observed in all cases, and not one single peak which would be the case if the former statement on ion-exchange competition was true.

It would seem sensible to assume that the (OH) groups around the Sb are exchanging for the acids and that probably the structure will be retained in an octahedral geometry. This assumption for the exchange of groups is supported by the MS results.

Only citric acid and mandelic acid gave evidence as to which part of the acid molecule formed a bond with Sb, (i.e. via NMR measurements). As such this discussion is limited in terms of structural evaluation. However, the reaction between Sb(V) and α -hydroxyacids has a useful number of possible applications, which will now be discussed.

3.5.2 Application of Sb:α-hydroxyacid complexation to separation methodology and determination of Sb compounds in real samples.

The uses of these reactions to date have already been discussed in Section 3.1. However, this study has shown that there is a possibility of utilising these reactions for chromatographic applications.

One of the major obstacles to the development of a robust HPLC separation protocol for Sb species has been the lack of suitably soluble Sb compounds to ensure the robustness and applicability of such a separation. Only two compounds are commonly used, potassium hexahydroxyantimonate(V) and potassium antimonyl(III) oxide tartrate hemihydrate. A further problem has been the low levels of Sb in the natural environment, the subject area of interest to many workers, which when coupled with the poor understanding of this elements biogeochemistry has proved problematic. Only when the chromatography has been sufficiently developed to handle more than two species of Sb will this knowledge develop.

The α-hydroxyacids as a group of compounds exist in a range of biological and environmental matrices^(203-205,208) and as such may react with Sb in these matrices, but more importantly the functionality involved in the bonding could exist in humic and fulvic materials in the environment⁽¹²⁷⁾. Thus, understanding this reaction could help with the development of pathways for Sb metabolism in the environment. Also, there is the potential for the use of these reactions in a model to determine the form of Sb(V) in solutions such as surface waters where the thermodynamically preferred or expected compound would be $[\text{Sb}(\text{OH})_6]^-$. If the Sb was in this form and was subjected to an addition of citric acid then it would be expected to react with the acid and elute with the same retention time as the synthetic Sb(citrate) compound. This would be distinct from Sb(III) in the form (SbO)tartrate as this compound was not observed to react with citric acid. The application of this reaction to environmental samples discussed in more detail in Chapter 4.

3.6 Conclusions

The methods of HPLC-ICP-AES, HPLC-ICP-MS, NMR and ESI-MS have proven to be complementary in the determination and identification of a group of Sb, α -hydroxyacid compounds. The interaction between Sb and this group of carboxylic acids had been previously hypothesised, but has now been characterised for the first time in this study.

Although the applications and significance of this work are highlighted elsewhere in this thesis, this study is important in its own right since it adds to the knowledge of Sb(V) chemistry in aqueous solutions at trace levels.

Initial work with HPLC separations of these compounds has shown that these compounds can co-exist in solution, although these studies have also shown that Sb(V) preferentially forms a compound with mandelic acid. The Sb(V) is taken up by these acids which can then be separated from each other using highly cross-linked anion exchange columns. The HPLC study has led to the development of a model that was applied to the calculation of the stoichiometric ratios of Sb to acid in these compounds.

Using the results from NMR studies the citric acid molecule is believed to bond to Sb through either of the terminal carboxylic acid groups in a 1:1 stoichiometric ratio forming a compound $K[Sb(OH)_5(C_6O_7H_7)]$. This was confirmed using ESI-MS. For DL-malic and (\pm)-mandelic acid the existence of a bond between the acid and Sb was confirmed with the compounds $K[Sb(OH)_5(C_4O_5H_5)]$, $K[Sb(OH)_5(C_8O_3H_6)]$ and $K[Sb(OH)_4(C_8O_3H_6)_2]$ identified by ESI-MS.

Importantly, Sb(III) in the form potassium antimonyl tartrate was not found to react in such a way as to be observed by HPLC methodology in the same way that Sb(V) could.

Chapter 4. Speciation of Antimony in Environmental Samples

4.1 Introduction

When completing the literature review prior to the final writing of this thesis a comparison was drawn between the number of publications that included Sb and those that included As. However, no distinction was made between the applications of the papers, for example, in terms of whether the samples were environmental or industrial in origin. Such an exhaustive review would not have been appropriate in the context of this study.

However, the authors of many of these publications do refer to the anthropogenic release of Sb into the environment and the fact that this release is the major cause of interest in this element, allied to the element's known toxicity.

This chapter describes the development of chromatographic methods for the separation of Sb species in environmental samples and the application of these methods to real samples. Various modifications to the basic method will also be described and the results obtained with these will be used to highlight the increasing number of problems associated with speciation methods as analytical instruments become more sensitive and the separation methods become more effective.

4.1.1 Antimony in the Environment

Table 4.1 gives a summary of the types of sample - along with the detection method, typical concentration range and method detection limits - that have been analysed over the last 20 years. Some of these are repeated from Chapter One.

Table 4.1 Summary of sample types, detection method, typical concentration range and limits of detection for Sb reported in the literature over the last 20 years

Sample type	Method of detection	Speciation (s) or total (t)	Conc. range	I.o.d.	Ref.
Contaminated Soil	LC-ICP-MS (Aqueous extract)	s	1 - mg kg ⁻¹	0.5 µg l ⁻¹	160
Geothermal Spring	LC-ICP-MS	s	10-440 µg l ⁻¹	"	160
Spiked Sea-water	pH controlled LC-ETAAS	s	<4 pg	4-26 pg	152
Fly-ash	HG/NAA	s	upto 82 µg l ⁻¹ Sb(V)	n.r.	74
Wine	HG-ETAAS	t	0.6-5.7 µg l ⁻¹	0.13 µg l ⁻¹	210
Sediments & Refs.	HG-ICP-AES	t	1.4-5.9 mg kg ⁻¹	0.3 µg l ⁻¹	107
Waters	HG-ICP-MS	t	2.7-8.5 µg kg ⁻¹	0.06 µg kg ⁻¹	114
Human tissue and Hair	HG-AFS	t	<3 µg kg ⁻¹ -3750 µg kg ⁻¹	3 µg kg ⁻¹	149
Mine water	HG-AAS	s	2.2 - 58.2 µg l ⁻¹	1 µg l ⁻¹	144
Pondweed	HG-GC-MS	s	5.5 - 25 µg l ⁻¹	15 ng	78
Waters	FI-HG-ICP-MS	t	upto 1 µg l ⁻¹	0.017 µg l ⁻¹	115
Sediments & waters	HG-AFS	t	0.12 - 0.6 µg g ⁻¹	0.02 µg l ⁻¹	148
Sea-water	HG-ICP-MS	t	upto 0.26 µg l ⁻¹	0.0022 µg l ⁻¹	116
Waters	HG-GC	s	upto 0.45 µg l ⁻¹	0.94 ng	195

Table 4.1 Continued

Sample type	Method of detection	Speciation (s) or total (t)	Conc. range	I.o.d.	Ref.
Sediments & waters	HG-ICP-AES	t	upto 50 $\mu\text{g g}^{-1}$	0.41 $\mu\text{g l}^{-1}$	106
Bovine liver tissue	HG-ICP-AES	t	upto 50 $\mu\text{g g}^{-1}$	0.41 $\mu\text{g l}^{-1}$	106
Sediments & rocks	HG-ICP-MS	t	upto 25 mg kg^{-1}	6 $\mu\text{g kg}^{-1}$	117
Waters	HG-AAS	s	upto 0.616 $\mu\text{g l}^{-1}$	0.001 $\mu\text{g l}^{-1}$	143
Water and biol. fluids	THETAAS	t	upto 237 $\mu\text{g l}^{-1}$	2.6 $\mu\text{g l}^{-1}$	90
NIST 1575 & pondweed	ETAAS	t	upto 40 mg kg^{-1}	n.r.	92
Tap water & snow	Resin sorption, THETAAS	s	0.18 - 0.58 $\mu\text{g l}^{-1}$	30 - 34 ng l^{-1}	155
Sediments, soils & refs.	Slurry ETAAS	t	0.61 - 20.1 $\mu\text{g g}^{-1}$	0.03 $\mu\text{g g}^{-1}$	93
Geological refs.	SE-ETAAS	t	2.2 - 480 $\mu\text{g g}^{-1}$	1 - 5 $\mu\text{g l}^{-1}$	94
Urine	SE-ETAAS	t	upto 220 $\mu\text{g l}^{-1}$	n.r.	211
Biol. fluids	ETAAS	t	n.r.	n.r.	212
Waters & refs.	Laser-induced fluorescence with ETAAS	t	upto 15 $\mu\text{g l}^{-1}$	0.005 pg	89
Urine	Pre-concentration, SE-ETAAS	t	0.08 - 149.2 $\mu\text{g l}^{-1}$	0.69 $\mu\text{g l}^{-1}$	153

Table 4.1 Continued

Sample type	Method of detection	Speciation (s) or total (t)	Conc. range	I.o.d.	Ref.
Rainwater	SE-spectrophotometry	t	upto 25 $\mu\text{g l}^{-1}$	3 $\mu\text{g l}^{-1}$	86
Wastewater	SE-spectrophotometry	t	upto 75 $\mu\text{g l}^{-1}$	10 $\mu\text{g l}^{-1}$	139
Sea/tap water	SE-spectrophotometry	t	upto - 0.240 $\mu\text{g l}^{-1}$	n.r.	87
Wastewater	FI-spectrophotometry	t	upto - 0.33 mg l^{-1}	0.014 mg l^{-1}	88
Hair & Soil	Differential ASV	Sb(III)	upto 7.2 $\mu\text{g g}^{-1}$	$8.9 \times 10^{-9} \text{ mol l}^{-1}$	129
Estuarine water	Voltammetry	t	upto 2.25 nM	n.r.	130
Wastewaters	Voltammetry	t	0.052 - 0.085 mg l^{-1}	0.020 mg l^{-1}	128
Tap & surface waters	Voltammetry	s	0.1 - 0.9 $\mu\text{g l}^{-1}$	0.1 $\mu\text{g l}^{-1}$	135
Snake venom	INAA/AAS	t	13.5 - 24.61 ng g^{-1}	n.r.	123
Brackish water coals	INAA	t	0.07 - 1.49 mg l^{-1}	n.r.	124
Waters	INAA	t	0.046 - 0.21 $\mu\text{g l}^{-1}$	0.023 $\mu\text{g l}^{-1}$	121
Waters	INAA	s	3.1 - 133 ng l^{-1}	2.5 + 25 ng l^{-1}	137

Table 4.1 shows the wide range of analytical techniques utilised for Sb determinations encountered in the literature. It also highlights the matrices in which total Sb has been determined or in which the two main oxidation states of Sb, (III) and (V), have been determined. However, by comparison relatively few workers have used speciation techniques to determine Sb species other than in aqueous samples or aqueous extracts of plant or geological samples.

The situation with antimony contrasts sharply with arsenic, the element which antimony is most often compared to in terms of reactivity. Indeed it seems somewhat strange that with the extensive use of chromatographic techniques for the speciation of As, allied with the often assumed similarity in the chemistry of the two elements, that so few chromatographic applications for the determination of Sb species have been achieved. This is especially so when one considers that the toxic nature of some Sb compounds is well known.

One example of a comparison between As and Sb has been made by Cullen's group in British Columbia. In 1992 Dodd *et al.*⁽¹⁵⁶⁾ published a paper on methylated Sb(V) compounds, their hydride generation properties and the implications for aquatic speciation. However, when the synthesised trimethyl Sb compounds were analysed by HG-GC-AA, four peaks were observed for one compound, thereby showing the compounds undergo decomposition or rearrangement in the HG-GC stage. At the time of this study these workers quoted previous literature that suggested that antimony speciation in the aquatic environment was similar to that exhibited by arsenic. However this experiment demonstrated that the behaviour of methylated Sb compounds to hydride generation was entirely different and that it is unrealistic to assume that simple extrapolation from one element to another is possible. Yet, in 1997 Lintschinger *et al.*⁽¹⁶⁰⁾ (this included Cullen) contradicted this statement stating 'because of the chemical similarity between As and Sb the commonly used HPLC methods developed for the separation of As compounds (anion and cation exchange, and RP HPLC) were investigated'. It could be argued that such an

approach is necessary in terms of the mechanism of separation and columns, but the comparison with arsenic is directly contradictory with their previous work.

When Andreae *et al.*⁽²¹³⁾ determined methylstibonic acid in natural waters the requirement to determine Sb by means other than the selective formation of hydrides (i.e. the reducing action of sodium tetrahydroborate) became obvious. Again, however, little has been achieved in terms of the development of sufficiently sensitive chromatographic separations of environmental Sb since Andreae's observations in 1981.

The most recent attempts at chromatographic analysis of substances other than waters have been by Lintschinger *et al.*⁽¹⁶⁰⁾ and Ulrich⁽¹⁶²⁾. The Lintschinger *et al.*⁽¹⁶⁰⁾ paper discussed aqueous extracts from contaminated soil samples in Germany. The extracts however, only showed the presence of Sb(V). The Sb(V) standard used in this work was KSb(OH)_6 . No Sb(III) was found in the samples. This supported the prediction that the predominant species in aqueous matrices will be the thermodynamically preferred Sb(V), most likely in the hydrolysed $[\text{Sb(OH)}_6]^-$ form. Ulrich looked at samples extracted with a 50:50 methanol:water solution. The samples were soils from a contaminated site. In a comparison with standards there appeared to be Sb(III) present in the extract. However, two peaks appeared on the chromatogram that could not be explained. These co-eluted with the Sb(III) species. Sb(V) and trimethyl antimony were also observed in these samples.

None of the uptake pathways by plants have been elucidated and the mechanisms for biomethylation are only now being studied with the fungal biomethylation of inorganic Sb compounds⁽⁷⁷⁾. Thus, although there is plenty of evidence to suggest there are methylated compounds of Sb in environmental samples the methodology developed so far has favoured the determination of Sb compounds that form volatile species. Mohammad *et al.*⁽¹⁴⁴⁾ and Dodd *et al.*⁽⁷⁸⁾ showed that the chemical form of the Sb could significantly affect the formation of a volatile hydride even in the presence of a pre-reductant such as KI. The work of Pilarski *et al.*⁽¹²⁷⁾ discussed in Chapter 3 has shown that Sb could well

associate with functionalities in complex organic molecules such as humic and fulvic materials. Indeed the study described in Chapter 3 tends to support the reported theory⁽¹²⁷⁾ very strongly. As such the chromatographic methodology should be developed in order to determine such species if they exist.

This chapter describes how an approach to Sb speciation was developed that disregarded the proposed analogy between As and Sb speciation and concentrated solely on what was known about Sb chemistry in environmental samples.

4.2 Experimental

4.2.1 Instrumentation

The HPLC system employed an inert pump (Model 9010, Varian, Australia). The chromatographic columns used were the Omnipac PAX-500, IonPac AS4A and AS11-SC anion exchange columns (Dionex, Calif., USA), the PRP-1(Hamilton,) and a C₁₈ column (Jones Chromatography). Sample introduction was via a six-port Rheodyne type 7125 injection valve with a 20 µl stainless steel sample loop. The ICP-AES instrument used was a Liberty 200 (Varian, Australia). The operating conditions were typically 1000W Forward Power, 15.0 l min⁻¹ coolant gas flow rate and 1.5 l min⁻¹ auxiliary gas flow rate. The ICP-MS instrument was a VGPQ2+ turbo (VG Elemental). The operating conditions were typically 1350W Forward Power, 15.0 l min⁻¹ coolant gas flow rate, 1.0 l min⁻¹ auxiliary gas flow rate and a nebuliser gas flow rate of 0.8 l min⁻¹.

4.2.2 Reagents

All reagents used were of analytical grade unless otherwise stated. All working solutions of Sb(V), TMSb and Sb(III) were made by dissolving the required weight of potassium hexahydroxyantimonate(V)(Aldrich, Gillingham, Kent, UK), trimethylantimony

dibromide(de Montfort University) or potassium antimonyl(III) oxide tartrate hemihydrate in the appropriate matrix. All working solutions of citric acid(Aldrich), DL-malic(Aldrich, Gillingham, Kent, UK), lactic(Aldrich, Gillingham, Kent, UK) and (\pm)mandelic acid(Aldrich, Gillingham, Kent, UK) solutions were made by dissolving the required amount of each acid in the appropriate matrix.

4.2.3 Method Development

ICP-AES was the detector of choice for method development. The coupling of HPLC with flows of up to 2 ml min^{-1} is much simpler for ICP-AES than for example flame atomic absorption spectrometers (FAAS). For the purposes of this study FAAS was deemed to lack sufficient sensitivity for future method development.

An ICP-AES typically has detection limits of $<20 \text{ } \mu\text{g l}^{-1}$ for Sb by continuous nebulisation, so when using a discrete sample volume of $100 \text{ } \mu\text{l}$, concentrations of $<1 \text{ mg l}^{-1}$ Sb should be observed.

Prior to coupling the HPLC to the ICP-AES a conventional HPLC system was set-up using a conductivity detector to quickly establish whether the Omnipac PAX-500 column would separate the Sb standards. The mobile phase was $40 \text{ mM NaOH}/5 \text{ } \%$ MeOH in deionised water.

After the instrument response was optimised for signal-to-background ratio by continuously nebulising a solution of Sb, usually 10 mg l^{-1} , the Omnipac PAX-500 column was coupled to the ICP-AES as shown in Figure 4.1.

The relative merits of each eluent are discussed in the appropriate results sections. However, in each case the performance was evaluated according to the effects of the eluent concentration, pH and organic solvent. Flow rate investigations were carried out when deemed necessary, i.e. if the species were strongly retained throughout the concentration and pH range.

Initial chromatographic separations started with the use of phthalic acid eluent according to a method used previously by Smichowski *et al.*⁽¹⁵⁹⁾. From this point on other mobile phase compositions were studied.

A hydride generation system was coupled to the ICP-AES as shown in Figure 4.2. The method of hydride formation was based loosely on methods previously developed^(106,107,144,159). The methods utilised by the references previously quoted were based upon HCl/NaBH₄ reagent systems but of slightly differing composition. However, the results did not differ with enough significance to favour one particular set of reagent compositions. The analytical performance was determined for this system with respect to a range of Sb compounds. Water samples collected from the site selected for study were then analysed for reducible Sb(III) and Sb(V) as were spiked samples. These results were compared with total Sb determinations made by ICP-MS.

At the point where the chromatography was transferred to the ICP-MS the emphasis was shifted to actual samples and the response to spiking with standards and pre-column reactions with complexing agents, α -hydroxyacids, as well as matrix effects. In each case the operating and chemical reagent conditions are described with the results.

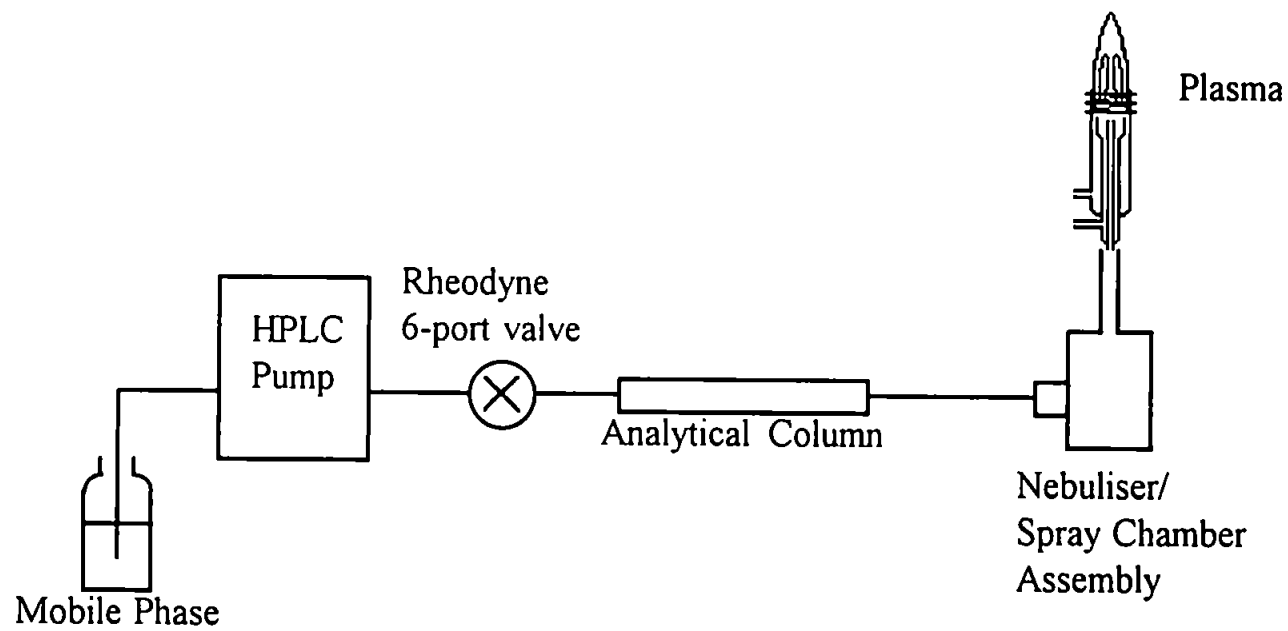


Figure 4.1. Schematic diagram of the HPLC-ICP-AES system

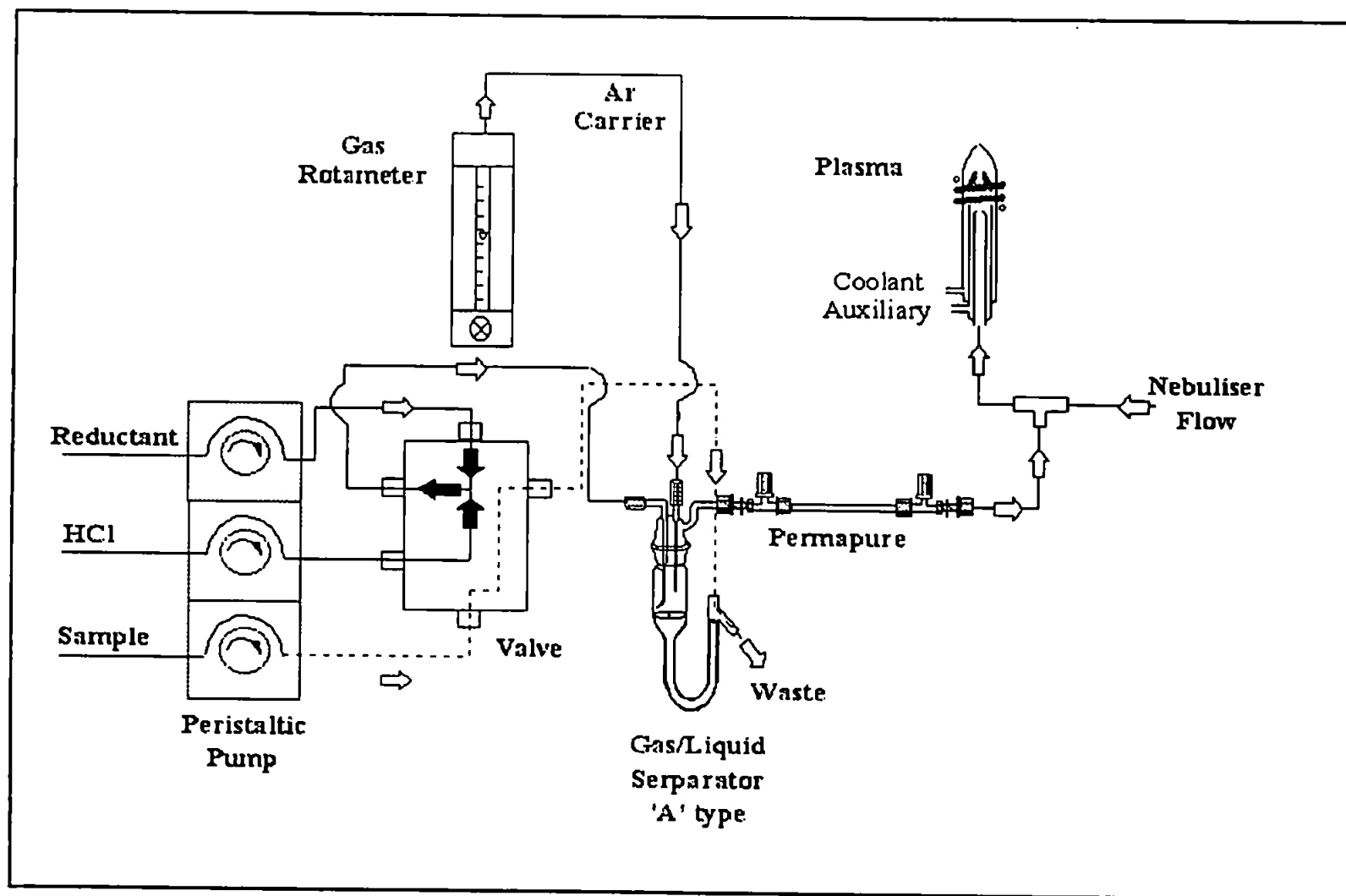


Figure 4.2 Schematic diagram showing the coupling of hydride generation system to the ICP-AES

The samples analysed were from a known antimony mine (disused), the Wheal Emily Mine at Knighton, South Devon. Figure 4.3 gives the location and map of the site. According to a report from 1922 by Toll & Barclay, this mine was worked in the early part of the 19th century but had been closed for many years prior to their survey⁽⁵³⁾.

The main adit (Point No. 1, Figure 4.3) has been reopened recently and there is evidence of some restoration of the adit although access to the adit was not permitted. There was a constant flow of water from the adit which initially flows over natural rocks before being diverted through a wooden trough to point No.2 above the valley. The spoil heap described by Toll and Barclay is clearly visible although overgrown with mosses, ferns and assorted other flora (No.3, Figure 4.3). The water from the adit drains onto and to the side of this spoil heap. Water and sediment samples were taken from the drainage point No.4 just above the stream which runs through the valley to the River Yealm. Further samples of water and sediments were taken from the stream at points indicated on the map, Figure 4.3. A control sample of water was taken from the point where the stream rises to the surface at the head of the valley. Dissolved oxygen and pH readings were also taken at these sampling sites. Plant samples were collected from a number of these sites.

The water samples were collected in triplicate in pre-washed polyethylene bottles. Sediment and plant samples were collected in Kraft sample bags. The water samples were then either filtered or left unfiltered, acidified with a few drops of 10% HNO₃ or left unacidified. The water bottles were then stored in a cool dark place until required for analysis. This was done to study the effects of such sample preparation. The sediment samples were dried and filtered through a 2 mm sieve and stored in glass sample bottles. The plant samples were washed and dried at ambient temperature. Again these were stored in glass sample bottles.

There is also a deeper adit at the high-tide mark on the bank of the Yealm. Water and sediment samples were taken from points in and around this adit entrance. Again access

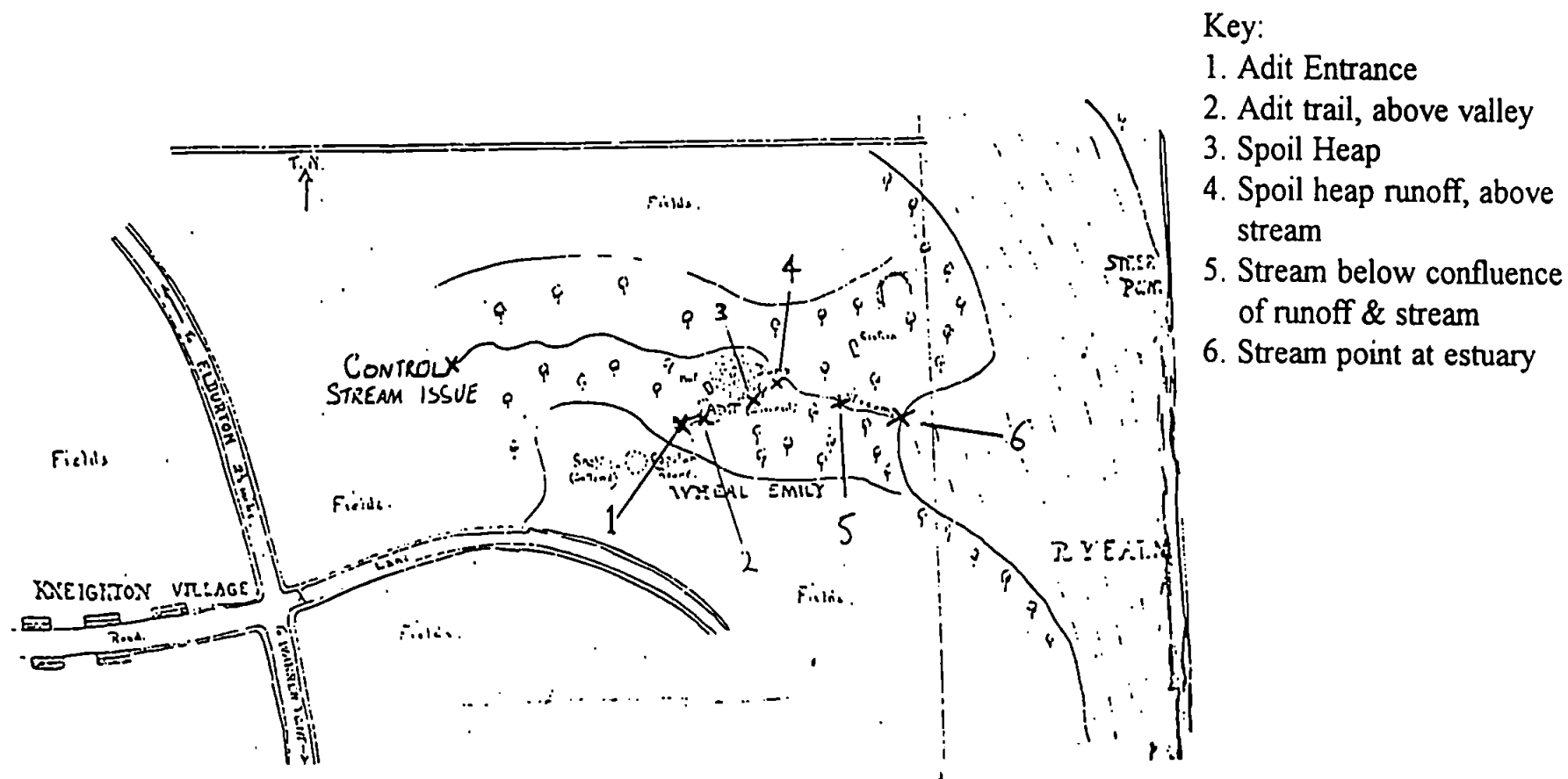


Figure 4.3 A map of the Wheal Emily antimony mine site showing the positions of the sampling points. A scale map is available, Ordnance Survey 1866 Edition, Devonshire Sheet 130.3.

to this adit was not permitted. This adit is some distance from the mine site itself and was not accurately located on the available maps.

4.3 Results

4.3.1 Ion-exchange chromatography and conductivity detection (CD)

Figure 4.4 shows chromatograms obtained for the initial ion-exchange experiments to test the Omnipac PAX-500 anion exchange column. Figure 4.5 shows the calibration graphs for KSb(OH)_6 and antimonyl(III) tartrate. These results showed that ionic species present in the standard solutions were separated by this analytical column. The retention time of the most retained peak, attributed to Sb(III) was also affected by NaOH concentration. However, this separation method needed to be coupled to an element specific detector before optimisation of the procedure could begin.

4.3.2 ICP-AES

The ICP-AES was optimised for best signal-to-background ratio for a solution of Sb at 10 mg l^{-1} . The individual parameters optimised were gas flow rates (nebuliser, coolant and auxiliary), RF power and viewing height. Following this a set of standards was made up in the range 0.001 to 100 mg l^{-1} . These standards were introduced to the ICP-AES and the response was measured at two wavelengths, 217.581 and 259.805 nm . The calculated limit of detection based upon $3s$ of the lowest standard signal was $31.5 \text{ } \mu\text{g l}^{-1}$. The instrument manufacturers quoted limit of detection was $18 \text{ } \mu\text{g l}^{-1}$.

4.3.2.1 Initial coupling of HPLC with ICP-AES

The HPLC was then coupled to the ICP-AES. The outlet of the column was connected to the sample introduction tube on the nebuliser with a small section of pump tubing. Utilising the ICP-AES timedisplay facility to observe the response, chromatographic runs were made using the same protocols as for the CD experiments. Figure 4.6a) shows the first observation of $[\text{Sb(OH)}_6]^-$ by this method. The injection volume was $200 \text{ } \mu\text{l}$.

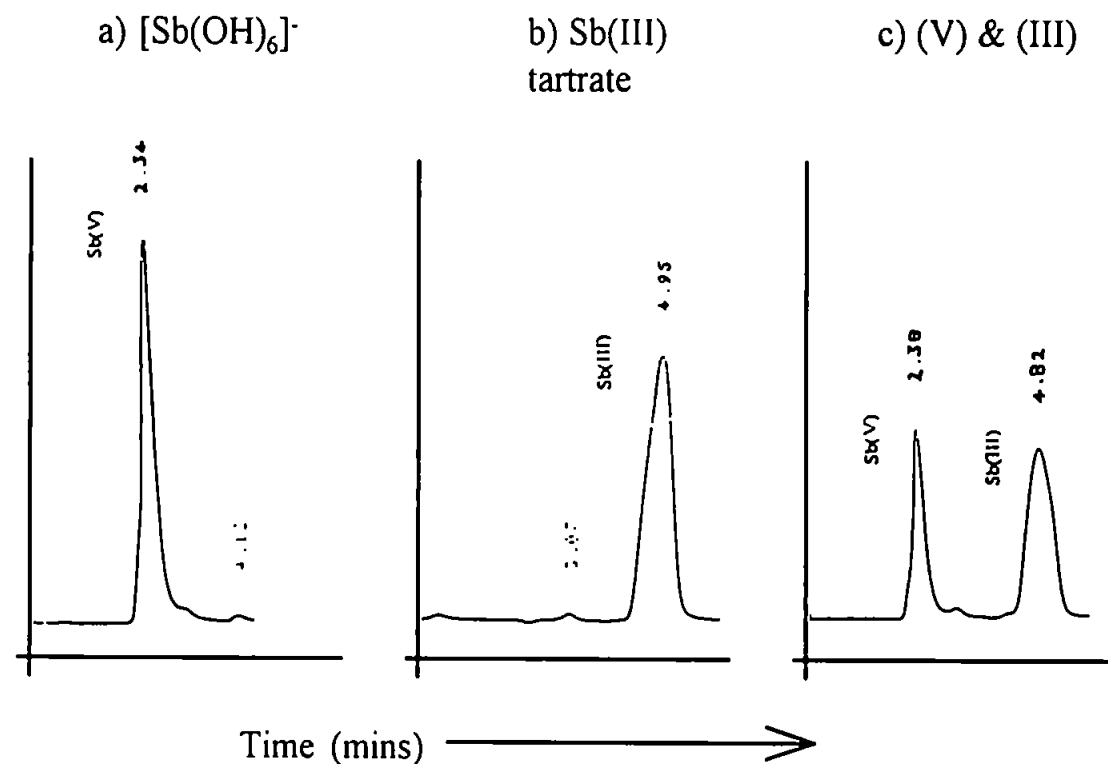


Figure 4.4 Chromatograms for the separation of Sb(V) from Sb(III) by HPLC-CD. (a) 50 mg l⁻¹ Sb(V); (b) 50 mg l⁻¹ Sb(III); and (c) 25 mg l⁻¹ mixed standard. Omnipac PAX-500 anion exchange column. 40 mM NaOH/5%MeOH mobile phase at 0.9 ml min⁻¹. 20 mN H₂SO₄ regenerant in anion micromembrane conductivity suppressor.

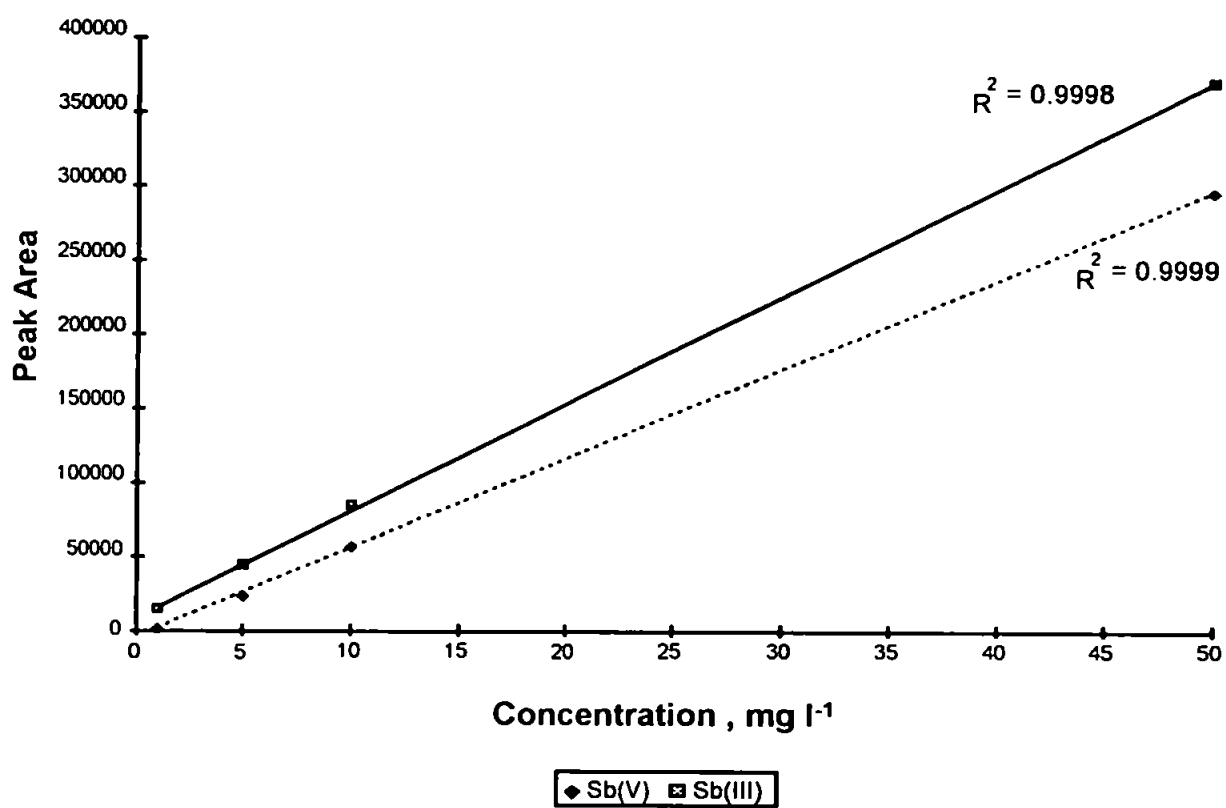


Figure 4.5 Calibration data for Sb(V) and Sb(III) by HPLC-CD.

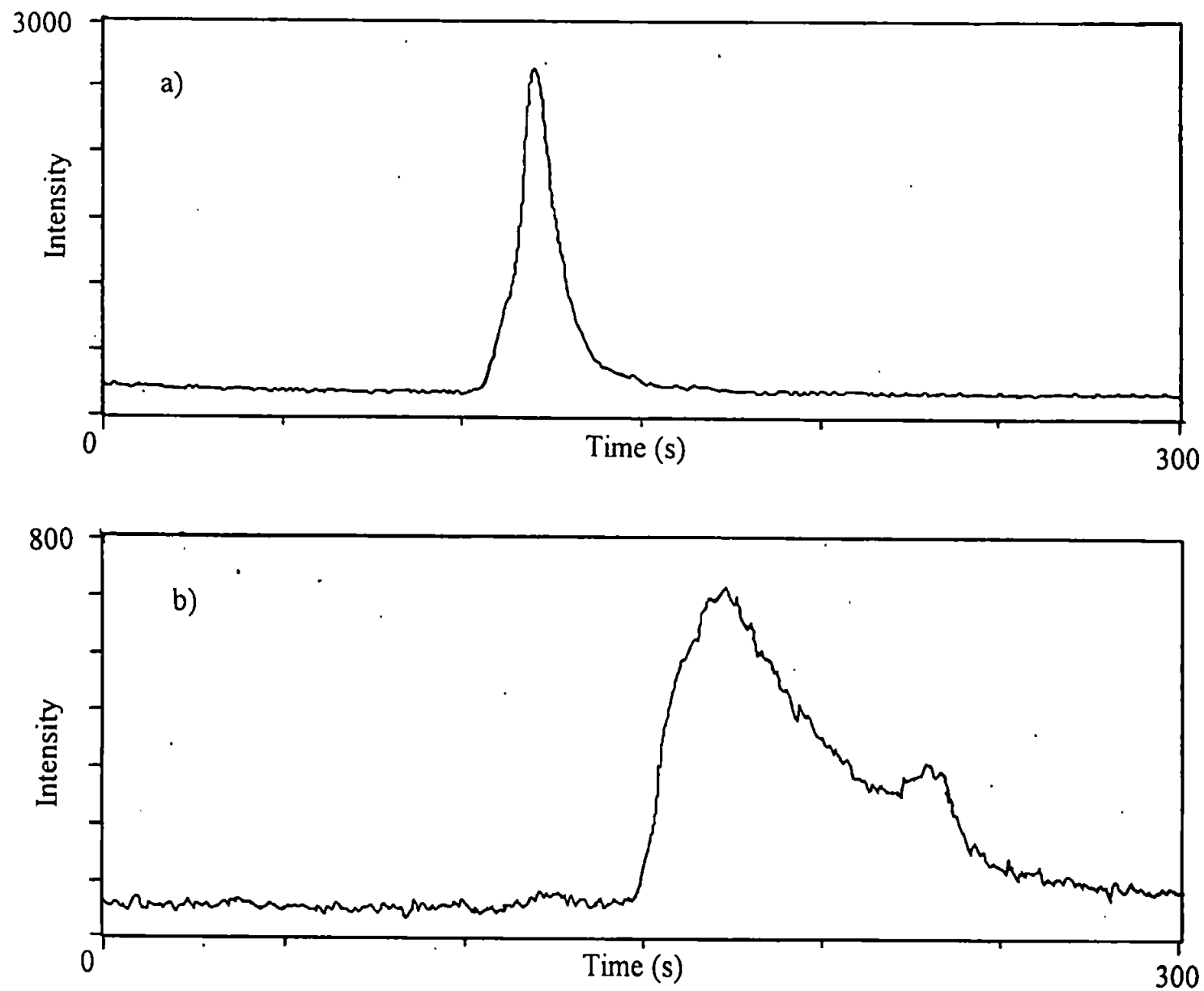


Figure 4.6 a) Chromatogram for $10 \text{ mg l}^{-1} \text{ Sb(V)}$; & b) chromatogram for $10 \text{ mg l}^{-1} \text{ Sb(III)}$. Elution protocol as for conductivity detection. Omnipac PAX-500 column

at a concentration of 10 mg l^{-1} as Sb, or $2 \text{ }\mu\text{g}$ on column. Figure 4.6 b) shows the result for an injection of 10 mg l^{-1} Sb(III) in the form of antimonyl tartrate. The retention order was the same as for that observed by conductivity detection, but the apparent retention time at peak maximum for antimonyl tartrate was much shorter than observed by conductivity. It is unclear why this should be except that there could be compound decomposition on-column with the Sb eluting as a neutral species that would not be picked up by conductivity detection. Figure 4.6 c) shows a mixed species chromatogram, Sb concentration was 5 mg l^{-1} per species.

At this point other eluents were tested, phosphate and phthalic acid⁽¹⁵⁹⁾. Separation of the Sb(V) and Sb(III) compounds were obtained with these eluents also, but the phthalic acid eluent was chosen for further investigation because the NaOH elution protocol did not provide a suitable determination of Sb(III) and the phosphate buffer was considered potentially problematic when transferring the chromatography to ICP-MS, owing to condensation of phosphate on the sampling cones.

Thus, using phthalic acid as the eluent, the separation was investigated with respect to changing pH, eluent concentration and organic solvent selection as well as investigating the effect of column temperature. Two antimony trihalide (SbX_3) compounds were also introduced in to the study, SbCl_3 and SbF_3 . The SbCl_3 was obtained as a spectroscopic standard of 1000 mg l^{-1} stabilised in 5M HCl. SbF_3 was obtained as the solid but was soluble in H_2O . Figure 4.7 shows an early separation of Sb(V) and SbCl_3 . Unfortunately the ICP-AES did not have a peak integration option in the operating software. To collect data for quantitative analysis a chromato-integrator was connected to the direct output from the PMT at the rear of the instrument.

When variation of the eluent concentration was investigated the most striking result was the separation of the SbX_3 compounds from antimonyl tartrate (Figure 4.8), despite both compounds being in the +III oxidation state. During the pH and eluent concentration

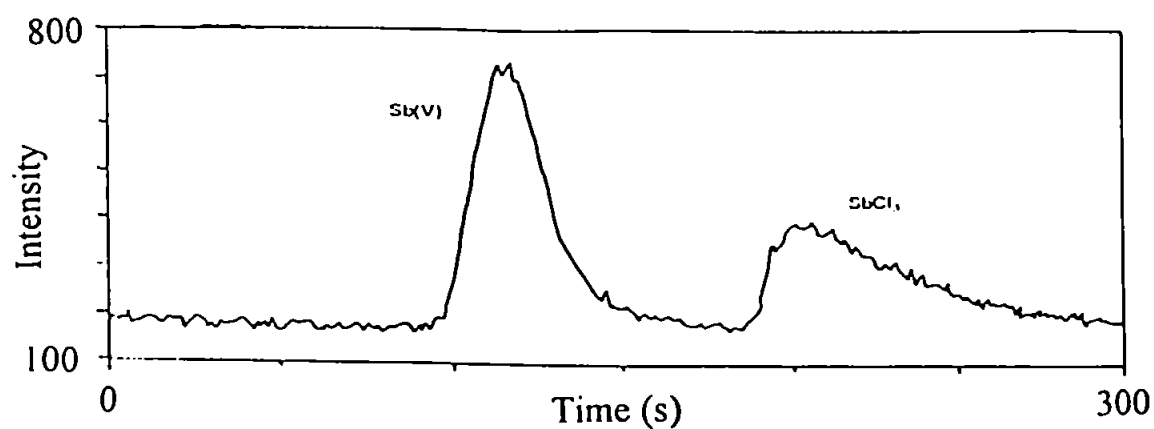


Figure 4.7 Chromatogram showing the separation of Sb(V) as $[\text{Sb}(\text{OH})_6]^-$ and SbCl_3 . 5 mM phthalic acid/1% MeCN mobile phase at 1.0 ml min^{-1} ; pH 4.45. Omnipac PAX-500 column.

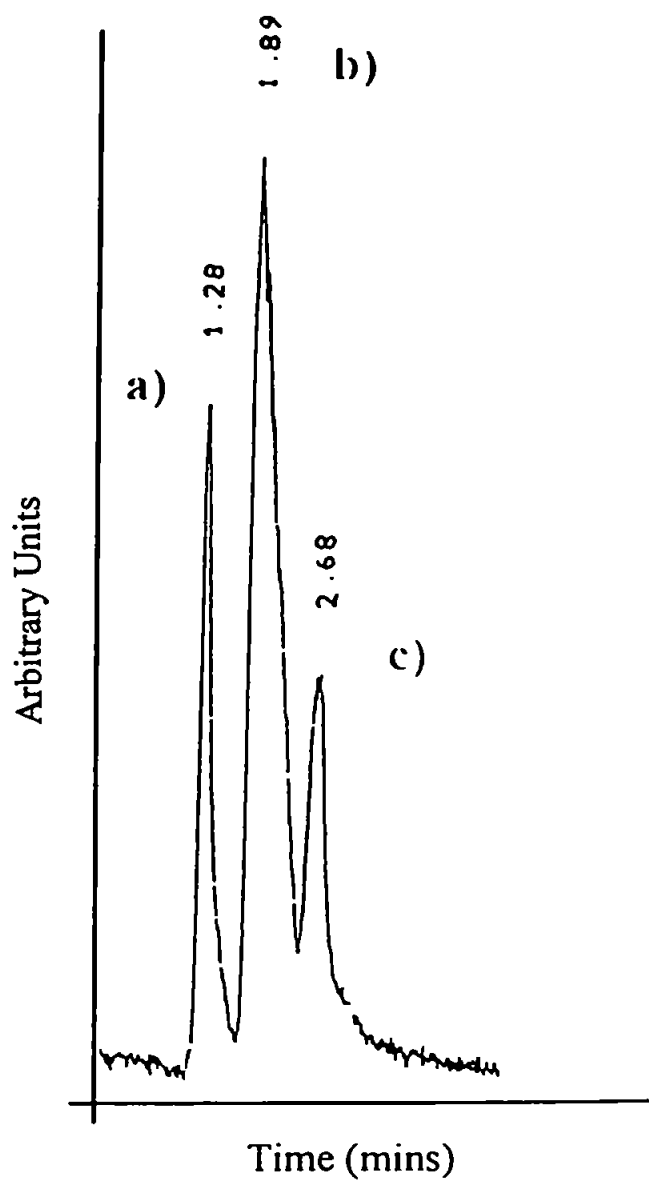


Figure 4.8 Chromatogram of Sb species at 10 mg l⁻¹. a) [Sb(OH)₆]⁻; b) SbF₃ and SbCl₃; and c) potassium antimonyl(III) tartrate. 10 mM phthalic acid mobile phase at 1.0 ml min⁻¹, pH 4.7. Ionpac AS4A column.

optimisation it became apparent that this separation was extremely sensitive to small changes in the pH/eluent ratio and as such was very difficult to reproduce. As such a change in pH from 4.7 to 5.0 would lose the resolution between the Sb(III) compounds.

The other feature of this protocol was that with the HCl stabilised SbCl_3 in a solution containing $[\text{Sb}(\text{OH})_6]^-$ the chromatogram for this mixture would show that the Sb(V) peak would be decreased in intensity and the SbCl_3 peak would be increased in intensity compared with the single species standards. This was thought to be due to the HCl and as such was investigated by injecting a solution of Sb(V) in HCl onto the column. However, the peak area difference between Sb(V) in HCl and Sb(V) in H_2O was only -2%. This was against -46% when in the presence of HCl stabilised SbCl_3 . This result together with the already described sensitivity to pH described above and the eluent concentration changes affecting the separation resolution meant that other eluents needed to be investigated. However, the speciation of the Sb(III) compounds was seen to be significant and this suggested that molecular speciation was possible for Sb compounds.

The next eluents studied were KNO_3 , NH_4NO_3 and NH_4Cl . These eluents were chosen because they were not suspected to have a possible complexing effect.

Figure 4.9 a) shows how NO_3^- concentration affected the retention times for the Sb species, while Figure 4.9 b) gives the result for retention time of Sb(V) with concentration of Cl^- . Decreasing pH showed a similar pattern for $[\text{Sb}(\text{OH})_6]^-$ and SbCl_3 when using a NO_3^- eluent but the retention time for antimonyl tartrate increased with decreasing pH. Using the nitrate eluent the optimum conditions for separation of Sb(V) and Sb(III) was 20 mM NO_3^- at pH3. Figure 4.10 shows chromatograms for two consecutive injections of a 10 mg l^{-1} mix of Sb species : a) $[\text{Sb}(\text{OH})_6]^-$, antimonyl tartrate and SbCl_3 , Sb(V)citrate; b) as a) but including antimonyl tartrate in the presence of citric acid.

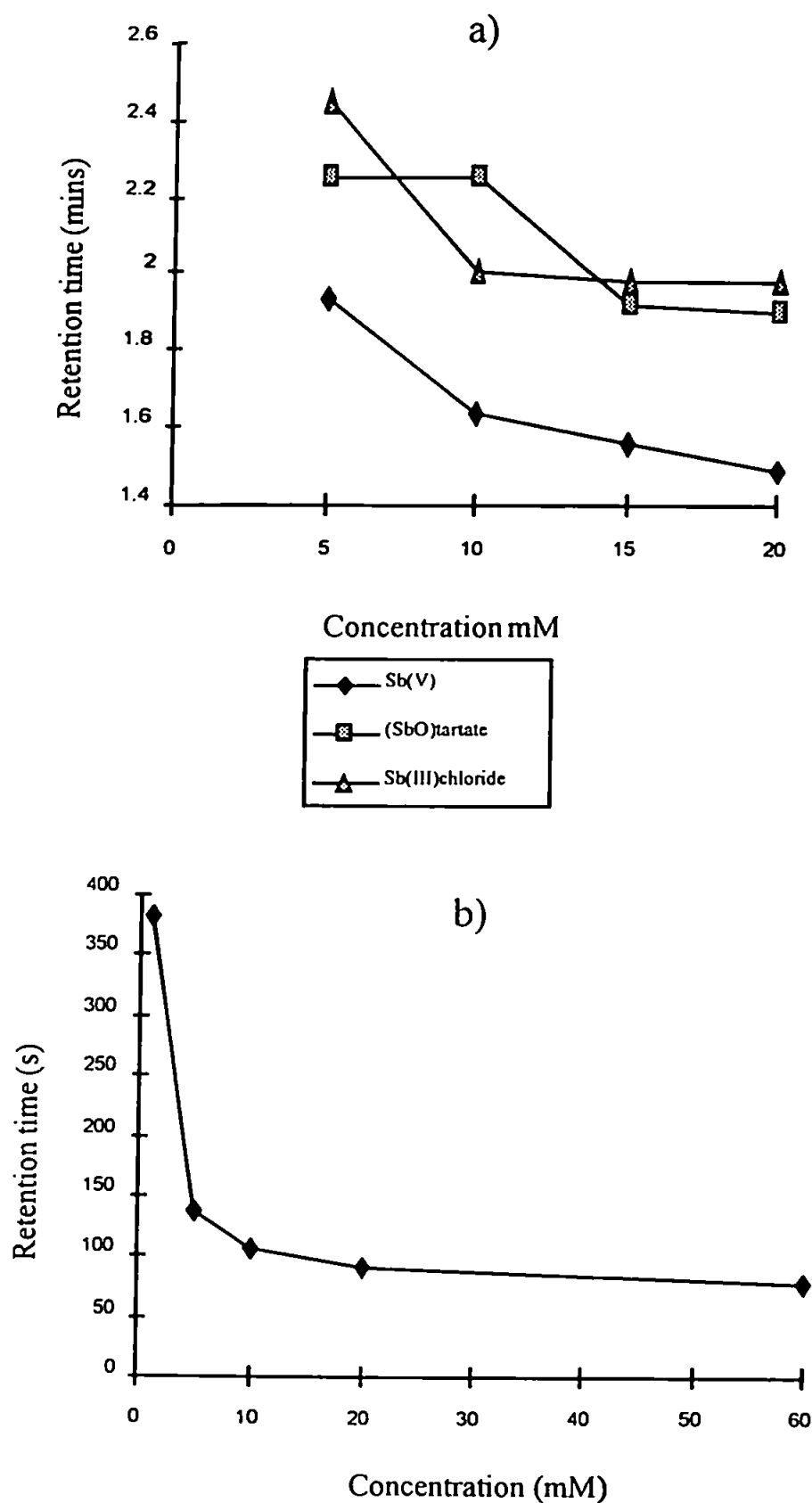


Figure 4.9 a) Effect of NO_3^- concentration on retention time of Sb species. b) Effect of Cl^- concentration on retention time of Sb(V).

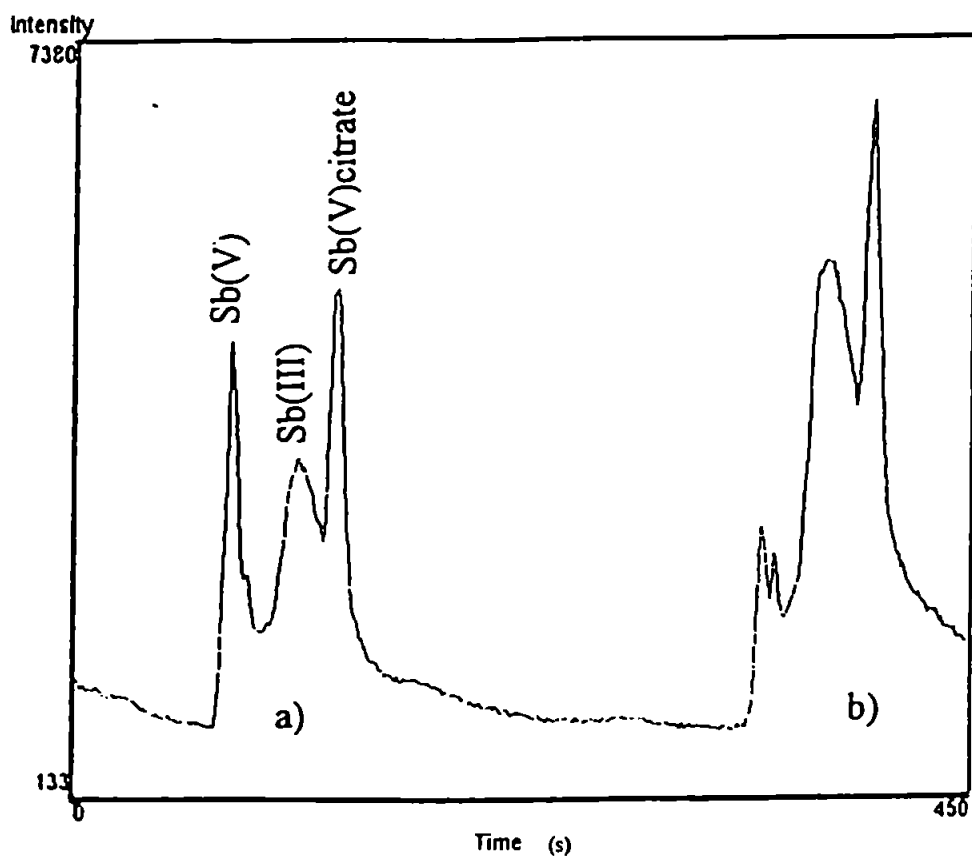


Figure 4.10 Chromatogram showing two consecutive injections of 10 mg l^{-1} mixed species. a) $[\text{Sb}(\text{OH})_6]^-$, antimonyl(III) tartrate and SbCl_3 and Sb(V)citrate ; & b) as a) but including Sb(III) with citric acid. AS4A column

The Sb(V) citrate peak was not observed at pH >4. Figure 4.10 also shows that the addition of a citric acid solution to an Sb(III) solution brought about no change to the retention time for all or part of the Sb(III) peak. This indicated the interaction, if any, of Sb(III) with citric acid was very limited and most likely not occurring. However, in Figure 4.10 b) the Sb(V) citrate peak clearly increases while the Sb(V) peak decreases in size. This is believed to be due to the unreacted citric acid from the Sb(III)/citric acid solution complexing with Sb(V). Using the NH₄Cl eluent the Sb(V) could be separated from antimonyl tartrate but the sensitivity of this method for Sb(III) was very poor. An alternative application was investigated however, the study of the Sb(V), α -hydroxyacid complexes. This separation was optimised in the same way as for the Sb(V) and Sb(III) species and the optimum conditions for the separation found to be 20 mM Cl⁻ at pH \leq 3. Figure 4.11 gives an example of this separation. Chapter 3 describes this aspect of the study in detail and it will not be repeated.

The separation process once developed was then transferred to an ICP-MS in order to provide the sensitivity required for environmental samples. ICP-AES was still utilised for totals analysis employing hydride generation.

4.3.2.2 Determination of Antimony by HG-ICP-AES

The determination of Sb by hydride generation of stibine, SbH₃, followed by detection using atomic absorption or emission spectroscopy has been long established and oft utilised^(106,107, 143&144). Thus operating conditions from the literature could provide the basis for the analysis of the samples in this study.

Figure 4.2 shows a schematic diagram of the general HG-ICP-AES arrangement. The reductant and acidified sample was pumped separately to a T-piece where the two flows converge. The hydride is stripped from the liquid flow and separated from this flow by the gas-liquid separator. From here the SbH₃ is swept to the plasma by an Ar carrier gas.

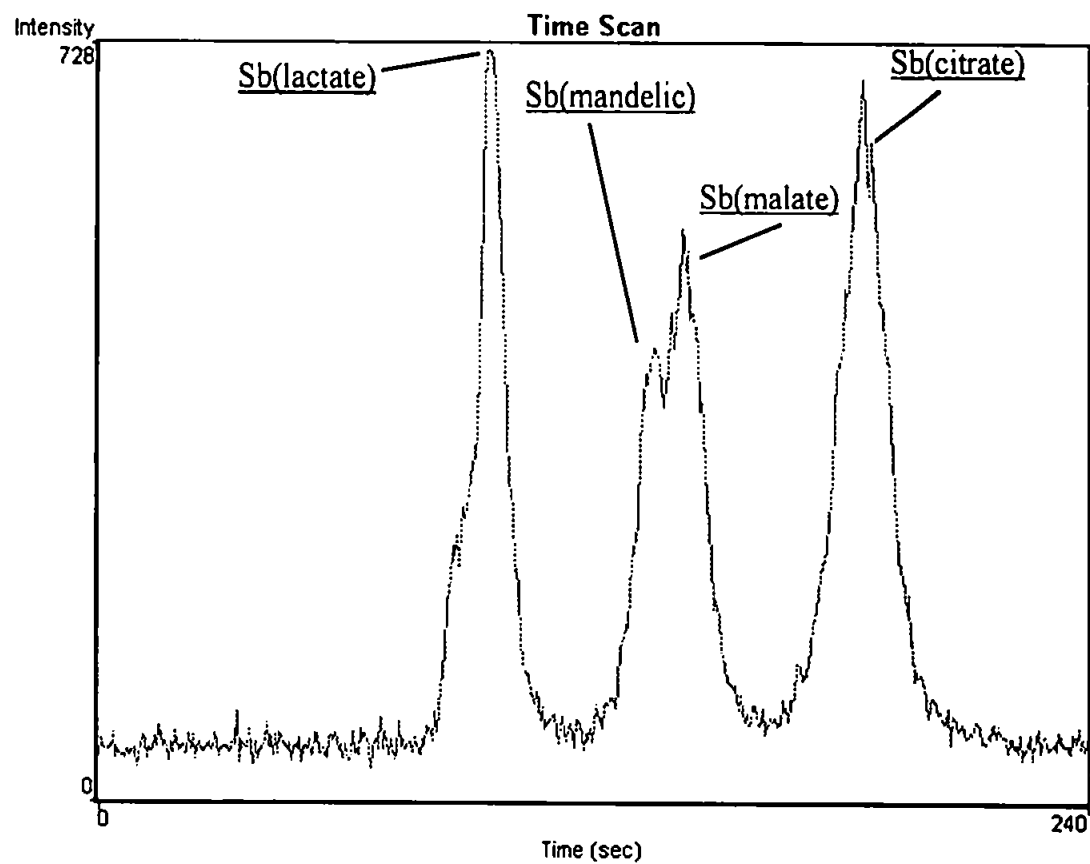


Figure 4.11 Separation of Sb(V): α -hydroxyacid complexes. 20 mM Cl^- mobile phase at 1.0 ml min^{-1} , pH 3. AS4A column

A preliminary investigation to test this arrangement was carried out. Figure 4.12 a) shows the wavelength scan for a 10 mg l^{-1} standard of SbCl_3 solution; Figure 4.12 b) shows the wavelength scan for a 0.5 mg l^{-1} sample of SbCl_3 after hydride generation; and Figure 4.12 c) shows the blank signal under HG operating conditions. The improvement in signal was estimated at 20 times, based upon signal-to-background ratio (SBR). Following a calibration run from $0\text{-}50 \text{ }\mu\text{g l}^{-1}$ the l.o.d. was calculated as $1.3 \text{ }\mu\text{g l}^{-1}$, based upon blank signal plus 3s of the blank. This was an improvement of just under 24 times better than the l.o.d. for continuously nebulised Sb.

A full study of the response from the three main Sb standards used in this study was undertaken. Two emission lines were used and compared for response, 217.581 and 206.583 nm. SbCl_3 and antimonyl tartrate needed no pre-reduction step as they are already in the preferred +III oxidation state. The calibration graphs for these compounds are given in Figure 4.13 a) and b) respectively. The emission line at 217.581 nm gave a better slope and lower background in both cases.

Figure 4.13 c) shows the calibration graph for KSb(OH)_6 without a pre-reductant. The response shows a limited formation of SbH_3 , and at $\leq 10 \text{ }\mu\text{g l}^{-1}$ the levels produced would not interfere with analysis of Sb(III). With a pre-reductant (upto 30% KI) there was a much improved response, Figure 4.13 d).

An analysis of several samples, i.e. spoil heap runoff and adit entrance water was carried out. Table 4.2 gives the results obtained using HG-ICP-AES and a comparison with the results of ICP-MS analysis.

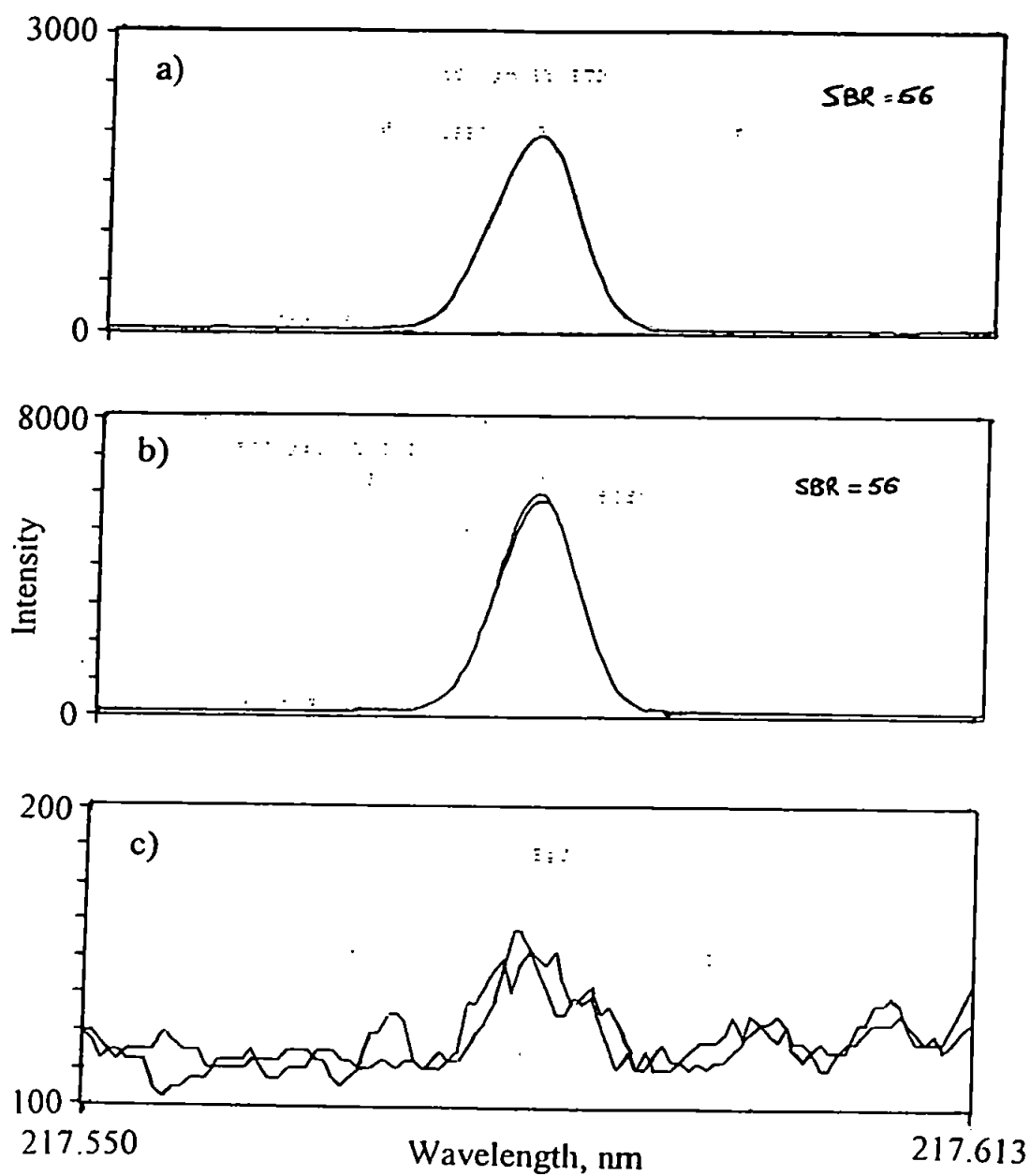


Figure 4.12 Wavelength scans for a) 10 mg l⁻¹ SbCl₃ solution; b) 0.5 mg l⁻¹ SbCl₃ with HG; and c) blank solution with HG.

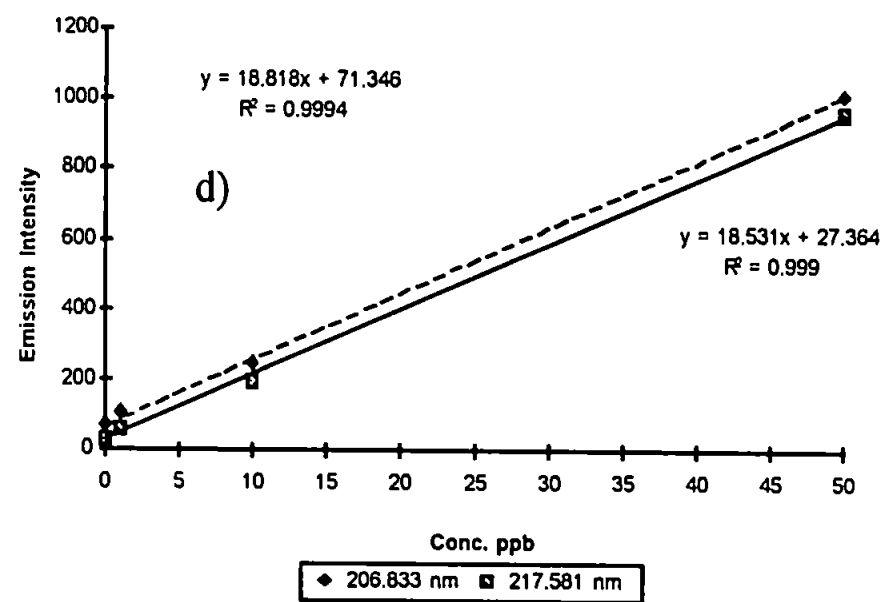
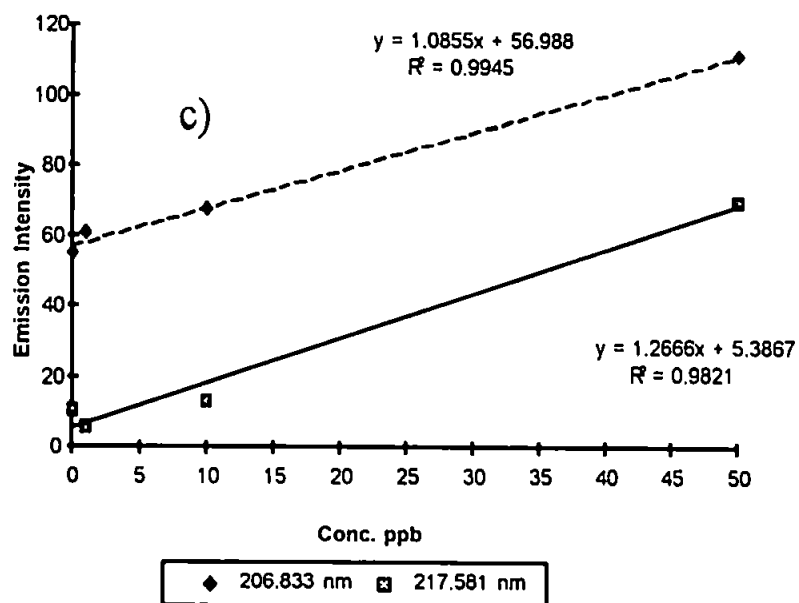
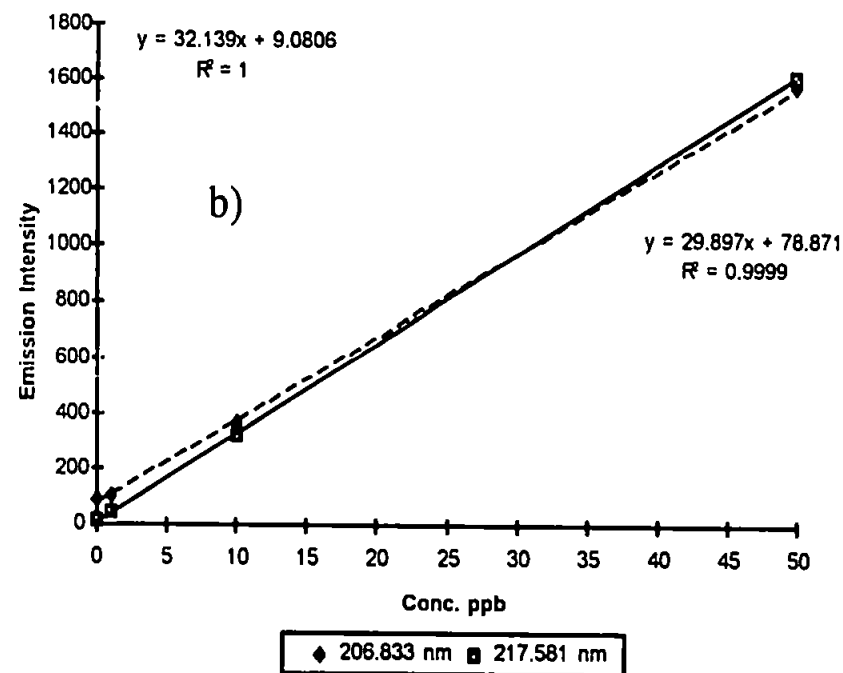
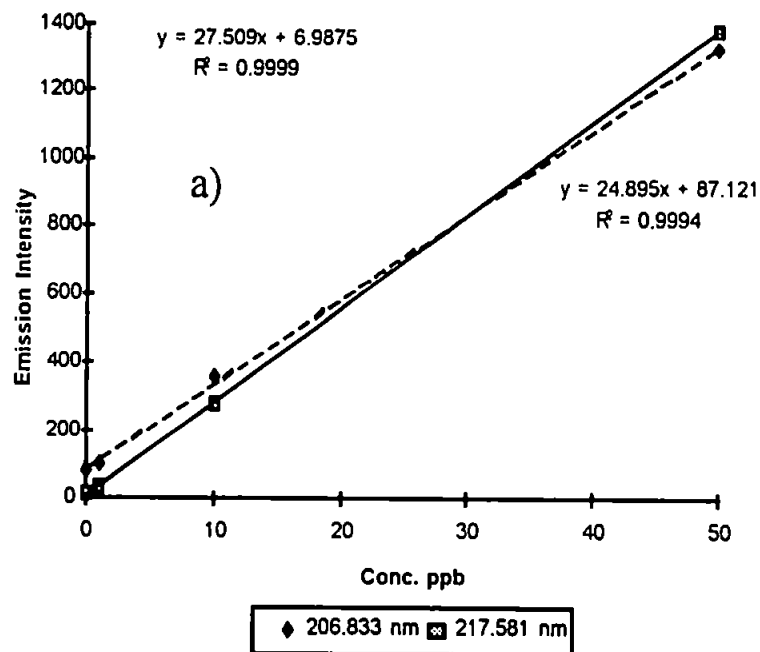


Figure 4.13 Calibration graphs for a) SbCl_3 ; b) antimonyl tartrate; c) KSb(OH)_6 without KI; & d) as c) with KI.

Table 4.2 Comparison of sample analyses by HG-ICP-AES with ICP-MS

Sample	Total Sb by HG-ICP-AES ($\mu\text{g l}^{-1}$)	Total Sb by ICP-MS ($\mu\text{g l}^{-1}$)
Spoil Heap	10.48 ± 0.48	13.34 ± 0.35
As above + $5 \mu\text{g l}^{-1}$	16.47 ± 0.41	
Spoil heap (undiluted)	11.66 ± 1.99	13.34 ± 0.35
Adit entrance	6.41 ± 0.54	6.79 ± 0.25

Figure 4.14 a) and b) give the calibration graphs for the determination of $(\text{CH}_3)_3\text{SbBr}_2$ (TMSbBr_2) by HG-ICP-AES with and without a pre-reductant. This demonstrates that not all Sb compounds will form the hydride using HG conditions reported for Sb^(106,115,116,117,143,148&157). A modification to this basic method was reported by Dodd *et al.*⁽⁷⁸⁾. These workers used an acetic acid carrier instead of HCl. Indeed, using this modification both TMSb and Sb(V) formed the hydride without pre-reduction. The addition of citric acid suppressed hydride formation for Sb(V), as described by Apte and Howard⁽¹⁴³⁾ and Mohammad *et al.*⁽¹⁴⁴⁾ but not for TMSb, Figure 4.15.

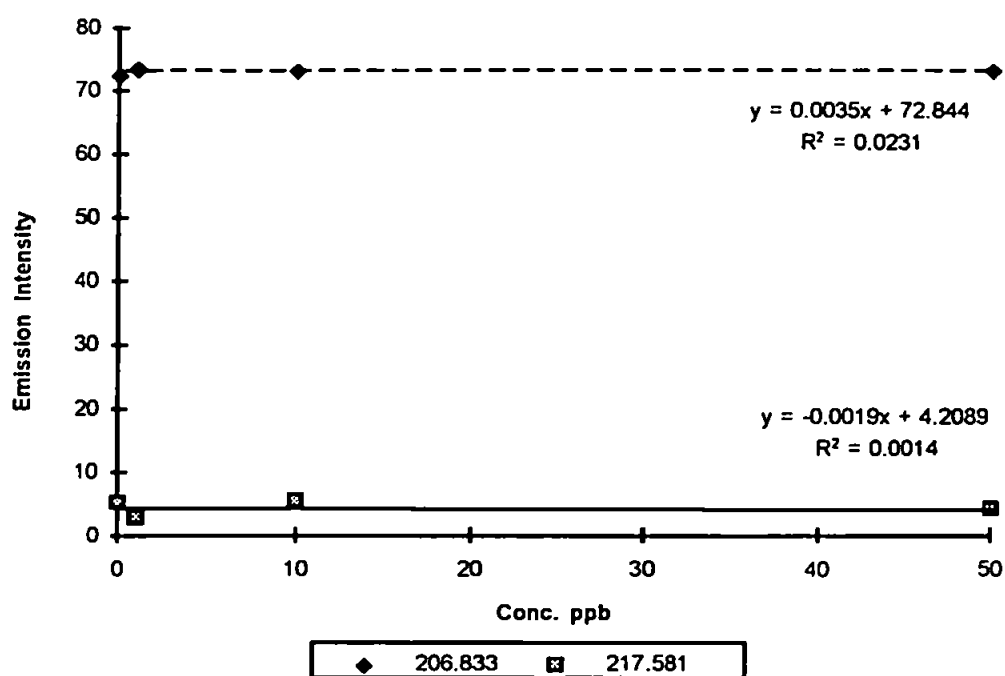
4.3.3 Determination of Antimony by ICP-MS and HPLC-ICP-MS

4.3.3.1 Continued method development using Ion-Exchange Chromatography

Although there was a period during the method development for the HPLC separation where both ICP-AES and ICP-MS were used as detectors, they have been separated for convenience of discussion.

It was while the eluents KNO_3 , NH_4NO_3 and NH_4Cl were being investigated using ICP-MS detection that the first significant result of instrumental sensitivity was observed.

a)



b)

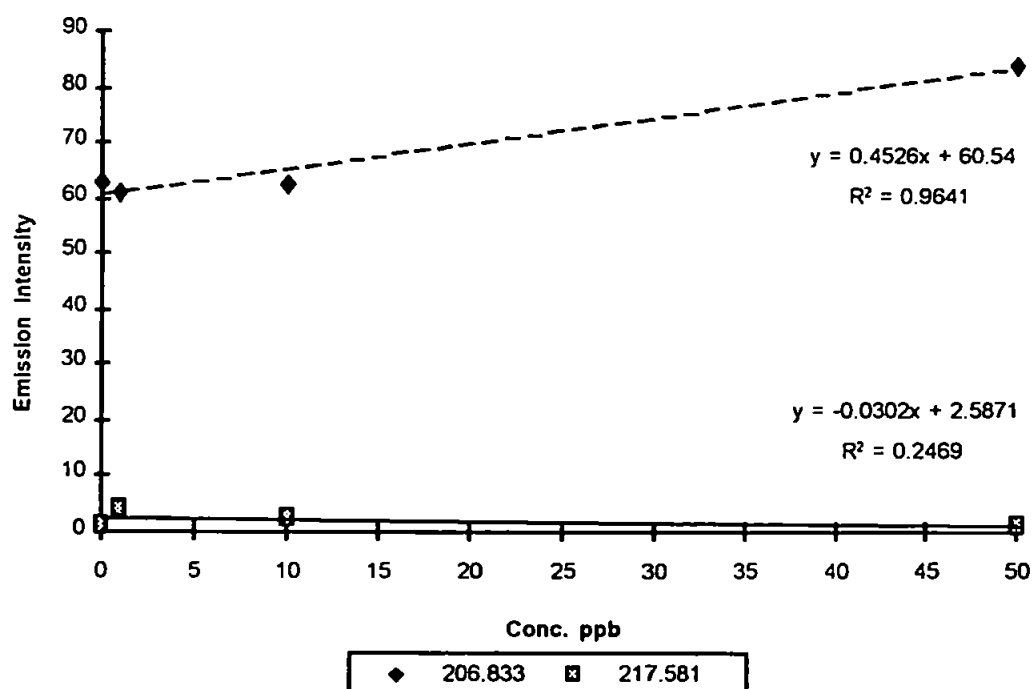


Figure 4.14 Calibration graphs for a) TMSbBr₂ without KI; and b) TMSbBr₂ with KI.

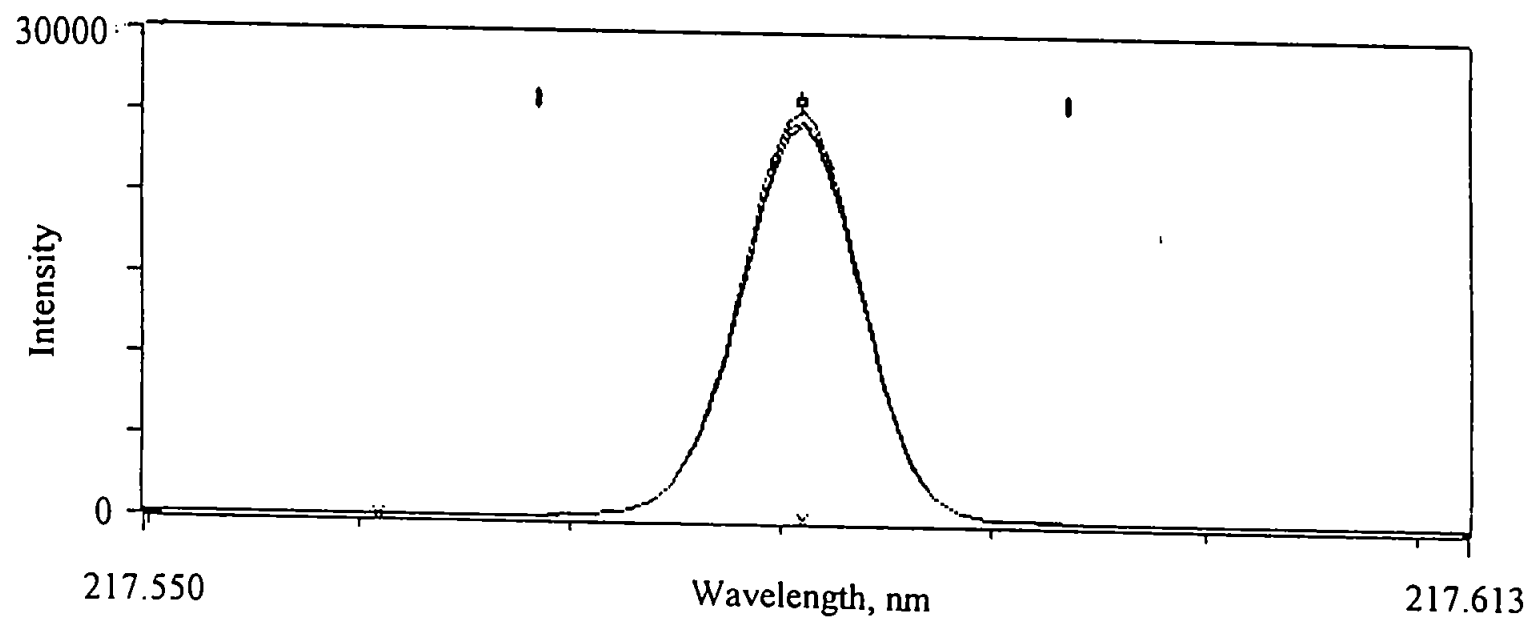
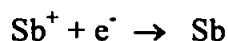


Figure 4.15 Wavelength scan for 1 mg l⁻¹ TMSb by HG in the presence of citric acid.

When investigating the two NO_3^- eluents for the separation of Sb(V) from Sb(V)citrate it became obvious that the choice of nitrate eluent was important. Figure 4.16 compares the separations achieved with 20 mM a) KNO_3 and b) NH_4NO_3 . It shows that with KNO_3 the intensity of the peaks were less than for the NH_4NO_3 eluent. This is believed to be due to the presence of K^+ in the mobile phase. K^+ is an easily ionizable element with the 1st ionisation energy at 419 kJ mol^{-1} (4.34 eV) compared with Sb at 834 kJ mol^{-1} (8.64 eV). In the example presented in Figure 4.16, the concentration of Sb in the discrete volume is approximately 1×10^{-5} that of K^+ in the mobile phase. When the potassium is ionised in the plasma the excess electrons produced could suppress the number of Sb ions reaching the mass analyser:



The use of ammonium nitrate did not produce significantly different retention times compared to that of KNO_3 , thus this compound was used as the source of NO_3^- in the mobile phase for future work.

Two visits were made to the mine site to collect water, sediment and plant samples. The first visit was in December 1997 and the second in May 1998. Total Sb analyses were made for the water samples, and water soluble extracts of sediment samples. A reference water was also analysed for Sb. Table 4.3 summarises these results.

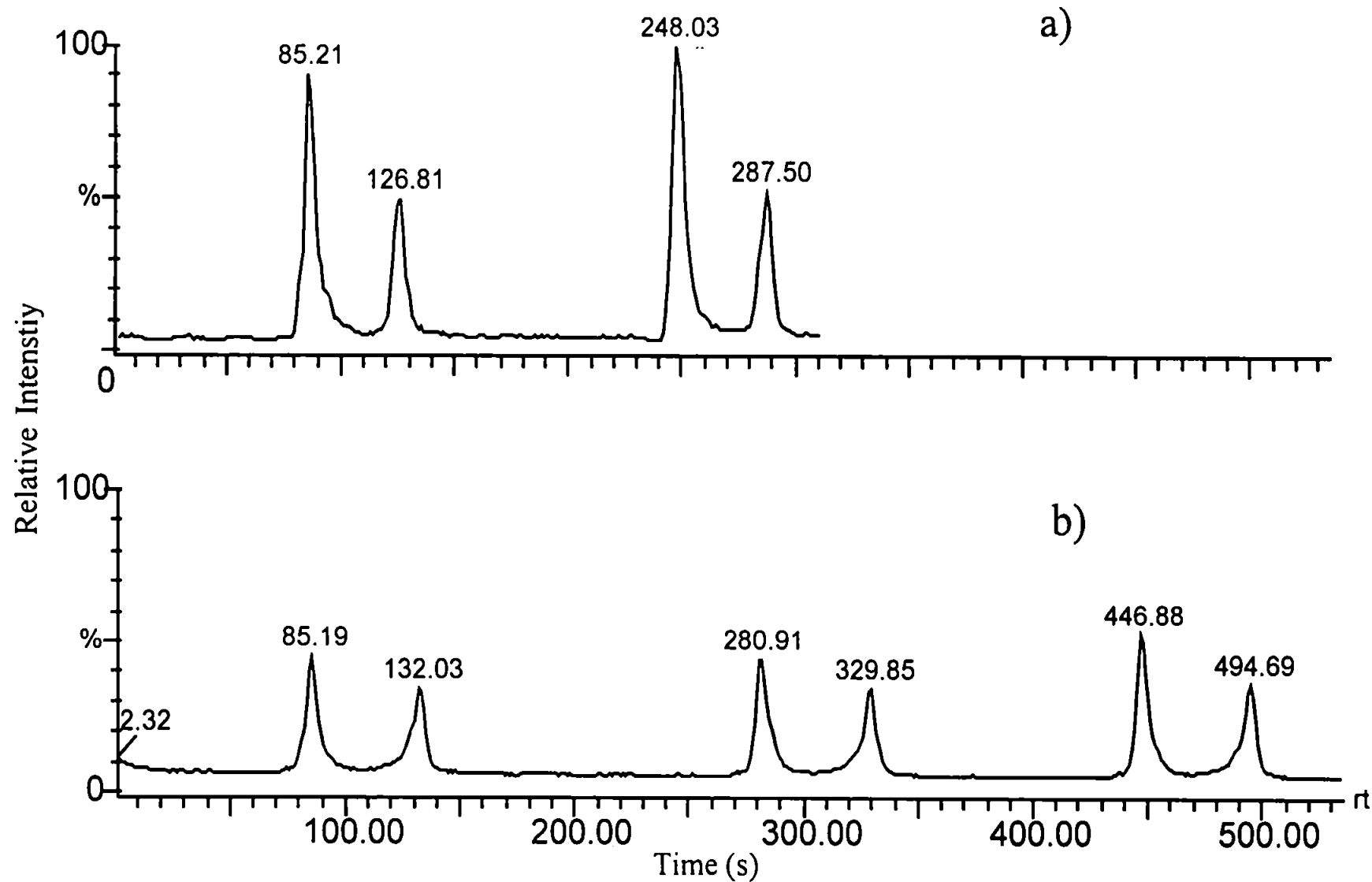


Figure 4.16 Chromatograms obtained for repeat injections of $20 \mu\text{g l}^{-1}$ Sb(V) and Sb(V)citrate mix with a) $20 \text{ mM NH}_4\text{NO}_3$ mobile phase; and b) 20 mM KNO_3 mobile phase at 1.0 ml min^{-1} , pH3, AS4A anion exchange column.

Table 4.3 **Summary of total Sb analyses of water samples and water soluble extracts of sediment samples**

Sample	Collection Date	Concentration ($\mu\text{g l}^{-1}$ unless stated otherwise)
Adit entrance	Dec. 1997	6.83 ± 0.21
Adit discharge	"	6.92 ± 0.20
Spoil heap runoff	"	$13.34 \pm .35$
Adit entrance + $2 \mu\text{g l}^{-1}$ Sb	"	8.95 ± 0.20 (101% recovery)
Spoil heap, UF	"	14.23 ± 0.40
Spoil heap, UF + $2 \mu\text{g l}^{-1}$ Sb	"	16.14 ± 0.25 (96% recovery)
Stream, below spoil heap	"	0.68 ± 0.02
Stream, above high tide mark	"	2.28 ± 0.12
Stream issue	"	0.04 ± 0.06
Deep adit pool, UF, H^+	"	1.27 ± 0.02
Deep adit pool, F, H^+	"	1.40 ± 0.03
Deep adit pool, UF	"	1.34 ± 0.04
Adit entrance	May 1998	6.89 ± 2.07
Spoil heap runoff	"	31.08
Spoil heap sediment, (H_2O)	"	$1.78 \pm 0.53 \text{ mg kg}^{-1}$
Adit trail sediment, (H_2O)	"	$1.087 \pm 0.38 \text{ mg kg}^{-1}$
Deep adit sediment, (H_2O)	"	$1.09 \pm 0.10 \text{ mg kg}^{-1}$
Adit mouth sediment, (H_2O)	"	$0.37 \pm 0.09 \text{ mg kg}^{-1}$
Stream sediment, (H_2O)	"	$0.13 \pm 0.04 \text{ mg kg}^{-1}$
*Deep adit pool sediment (H_2O)	December 1997	$0.07 \pm 0.01 \text{ mg kg}^{-1}$
SLRS-2		0.15 ± 0.03 (58 % recovery) [#]

* ^{115}In counts 50% that of average internal standard count.

UF, unfiltered

F, filtered

H^+ , acidified

H_2O , water soluble extract.

[#] Poor recovery could be due to age of ref. solution at approx. 4 years.

It was expected in this study that the major component in the water samples and the water soluble sediment extracts would be Sb(V) and not Sb(III). However, this could not be assumed to be true without further analysis by chromatographic means. HG analysis has been shown to demonstrate marked differences in response for each Sb species, hence the continued need for chromatography.

The analysis of these samples was therefore incorporated directly into the development of the chromatography. This was to ascertain how the Sb species in the matrix responded to the chromatographic protocol when compared with standard species. In addition, it was important to see how spiking the samples affected the analyses. The use of citric acid as a complexing agent pre-column was introduced to see if the Sb in the water samples would complex with it the same way as $[\text{Sb}(\text{OH})_6]^-$ in standard solutions. This experiment was carried out in order to investigate the form of Sb(V) in the samples. If the same complex is formed then the elution profile of the sample complex and the synthetic complex should match.

When the methods developed for the ICP-AES were transferred to the ICP-MS Sb(III) peaks were no longer observed. This is discussed in a later section. Different eluents were introduced to the study providing a broader range of varying strength ion exchange candidates with the order being $\text{SO}_4^{2-} > \text{phthalate (pH dependent)} > \text{NO}_3^- > \text{Cl}^- > \text{OH}^-$.

The SO_4^{2-} at 5 mM concentration did provide a separation, however, the Sb(III) and TMSb peaks co-eluted and the response for both of these compounds was very poor. Figure 4.17 shows an example of a typical chromatogram obtained for a standard mix of Sb(V) and (III). Such a protocol would be unsuitable for analytical purposes when looking at environmental samples and increasing the SO_4^{2-} concentration only led to problems of salt build-up in the torch which left unchecked eventually extinguished the plasma.

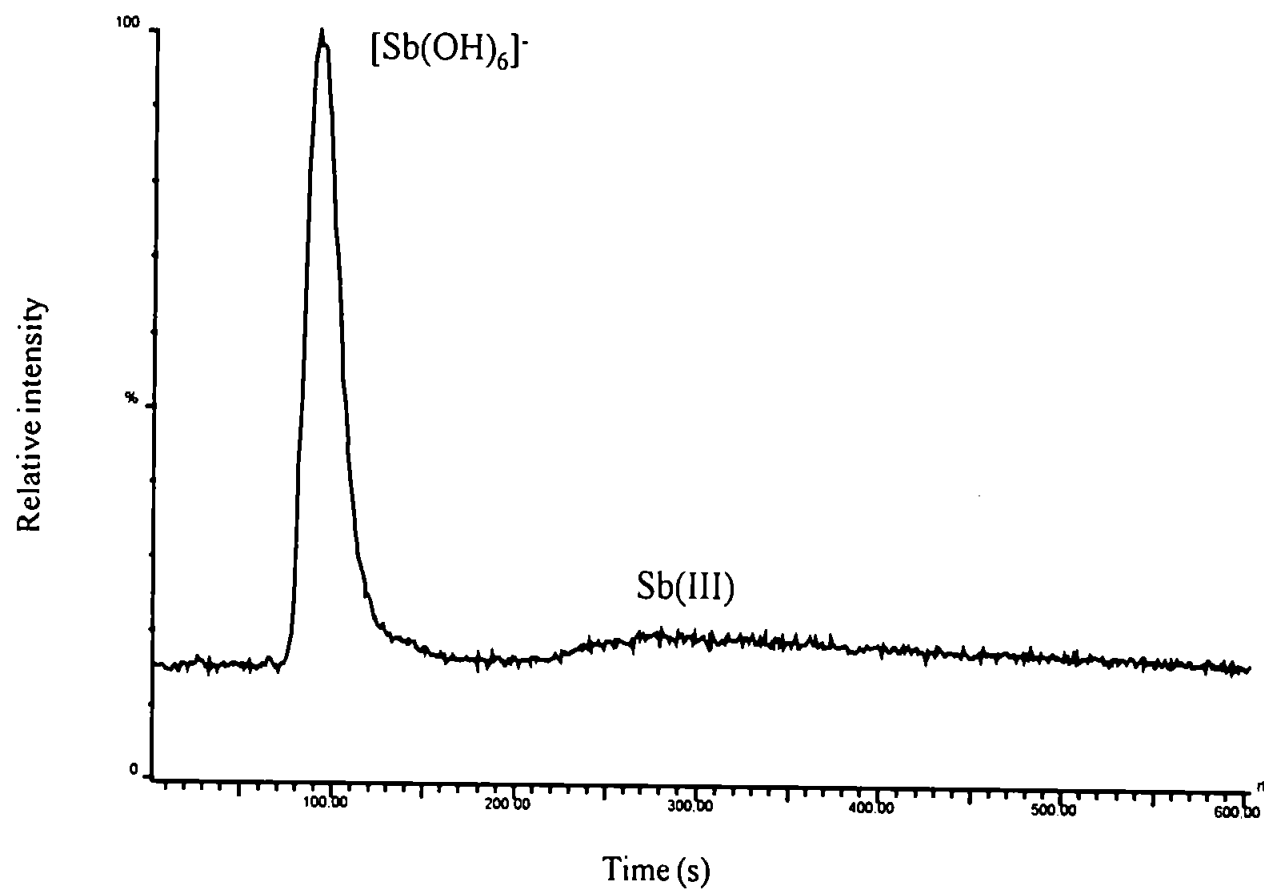


Figure 4.17 Chromatogram for $100 \mu\text{g l}^{-1}$ $[\text{Sb}(\text{OH})_6]^-$ and antimonyl(III) tartrate solution, 5 mM SO_4^{2-} mobile phase at 0.35 ml min^{-1} , AS11 anion exchange column.

The experiment to assess the effect of adding citric acid to the sample provided more useful results. Figure 4.18 shows a chromatogram for a) $20\ \mu\text{g l}^{-1}\ \text{Sb(V)}$; b) $10\ \mu\text{g l}^{-1}\ \text{Sb(V)}$ with citric acid; c) spoil heap runoff; and d) spoil heap runoff with citric acid. As can be seen from Figure 4.18 the elution profiles for both the standard and sample are identical as are the equivalent citric acid complexes. The amount of citric acid required to bring about complete complexation was estimated to be around 3000x molar excess of the amount of Sb in the sample. This was thought to be due to other metals in sample solution competing for citric acid. It could be assumed that the large excess of citric acid present in the matrix might provide sufficient citrate ions that could merely affect the elution profile by altering the ion-exchange characteristics of the Sb in the solution. Figure 4.19 shows the chromatograms obtained for the spoil heap runoff as the Sb present was gradually forming the complex. The two peaks present in the one chromatogram would discount the citrate ion-exchange theory. Chapter 3 covers this aspect of Sb interaction with citric acid more thoroughly.

However, all of the Sb present in the sample appeared to change to the citrate complex in solution, strongly supporting the presence of Sb in the form $[\text{Sb(OH)}_6]^-$. Changing the eluent to 5 mM NH_4NO_3 and NH_4Cl with small pH adjustments to facilitate elution of the citrate complex produced similar patterns of elution for standards and samples to those seen in the sulphate mobile phase.

A calibration was attempted for Sb(V) as $[\text{Sb(OH)}_6]^-$ followed by analysis of selected samples, with and without the addition of standards, by HPLC-ICP-MS.

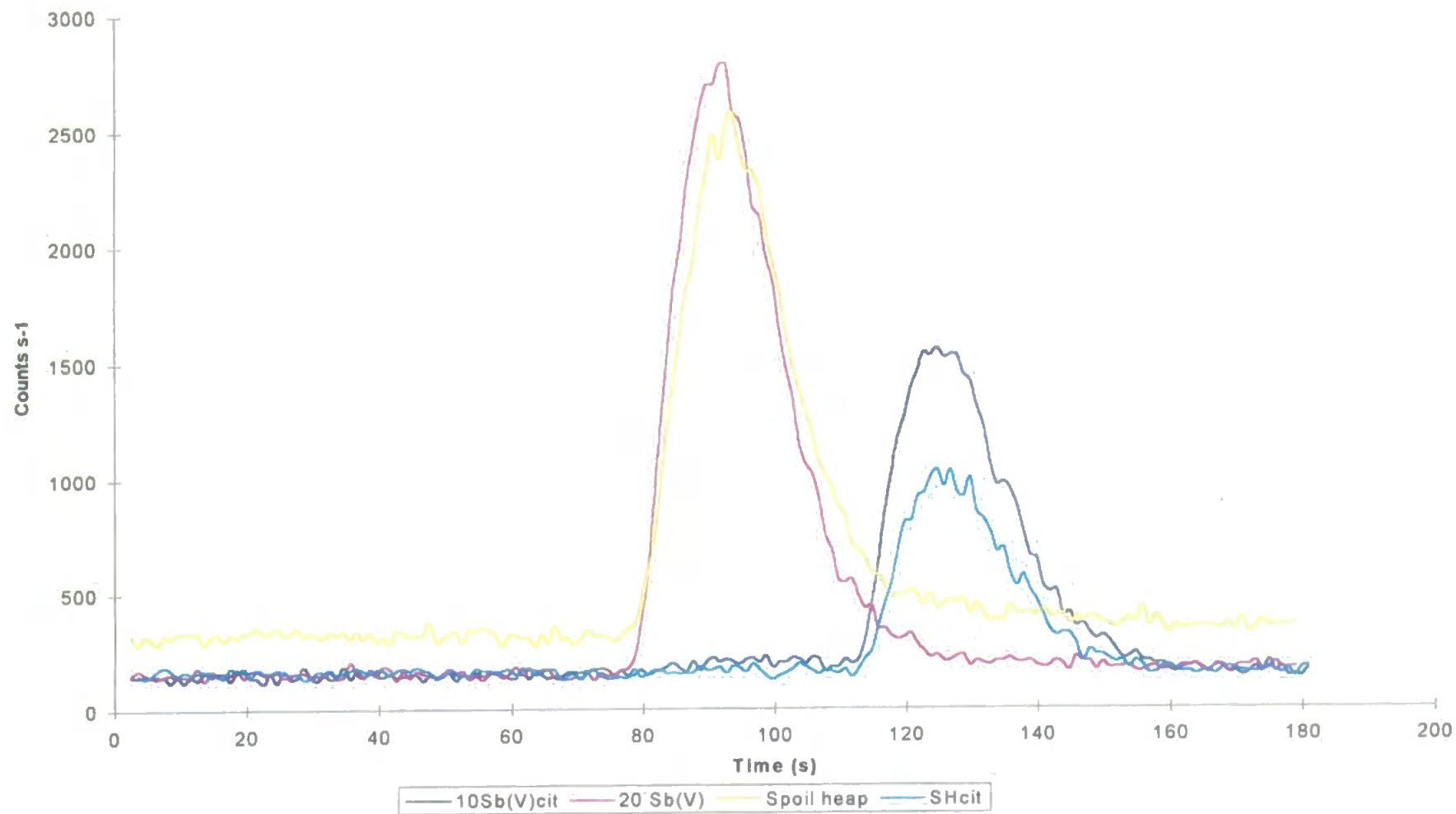


Figure 4.18 Chromatograms for injections of standards and samples with and without citric acid

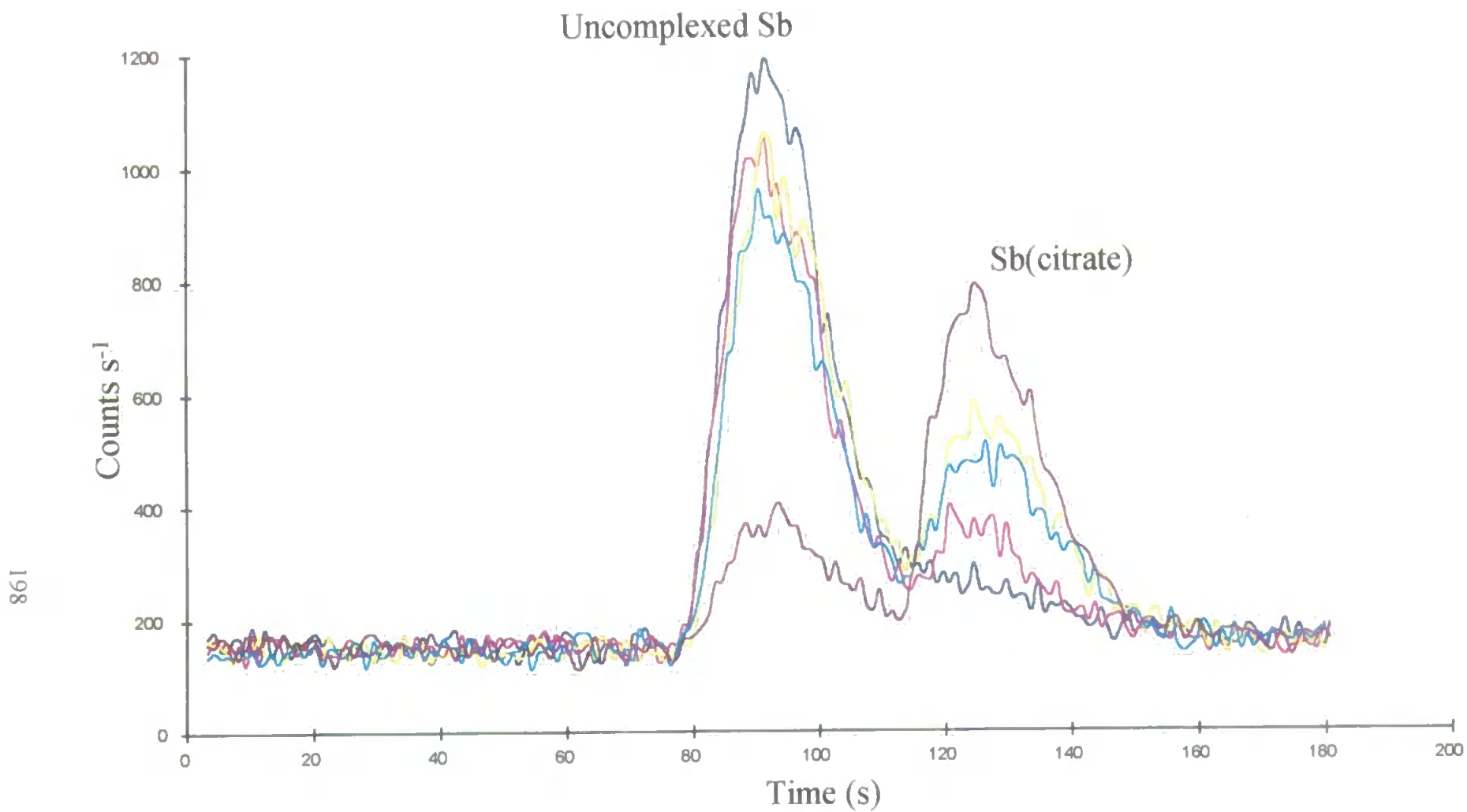


Figure 4.19 Chromatograms obtained from spoil heap runoff as the Sb formed the complex with the citric acid

Table 4.4 Summary of HPLC-ICP-MS results for Sb(V) using 5 mM Cl⁻ eluent at 0.35 ml min⁻¹, AS11 anion exchange column

Sample	Concentration (µg l ⁻¹)
Spoil heap runoff	15.52 ± 0.91
Spoil heap runoff + 4 µg l ⁻¹ Sb(V)	21.01 ± 2.01 (107%)
Adit entrance	8.38 ± 0.16
Adit entrance + 4 µg l ⁻¹ Sb(V)	13.60 ± 0.60 (110%)

Figure in parentheses are percentage recoveries.

The limit of detection for this method calculated as the blank signal plus 3s of the blank was 0.95 µg l⁻¹, or 19 pg on-column.

The use of the OH⁻ eluent with the AS11 column instantly demonstrated an ability to separate Sb(V) from TMSb with Sb(V) being the most retained species. At OH⁻ concentrations of 1 mM the separation was baseline resolved in less than two minutes from injection. This separation was optimised following an investigation of the nebuliser/spray chamber assembly and the minimisation of extra-column dispersion. Chapter 5 deals with this aspect of the study.

Figure 4.20 shows a calibration set of chromatograms for the separation of TMSb and [Sb(OH)₆]⁻. The limits of detection calculated for these species were 4.43 and 8.51 pg on-column for a 20 ml sample volume of TMSb and [Sb(OH)₆]⁻ respectively. Analysis of the water soluble extract of sediment from the base of the spoil heap showed no TMSb present and the peak area for the peak at the Sb(V) retention time indicated a concentration in solution of 8.8 µg l⁻¹. This result was considerably lower than that of the totals analysis at 111.09 µg l⁻¹. Therefore not all of the Sb present in the solution was being recovered from the column by this method.

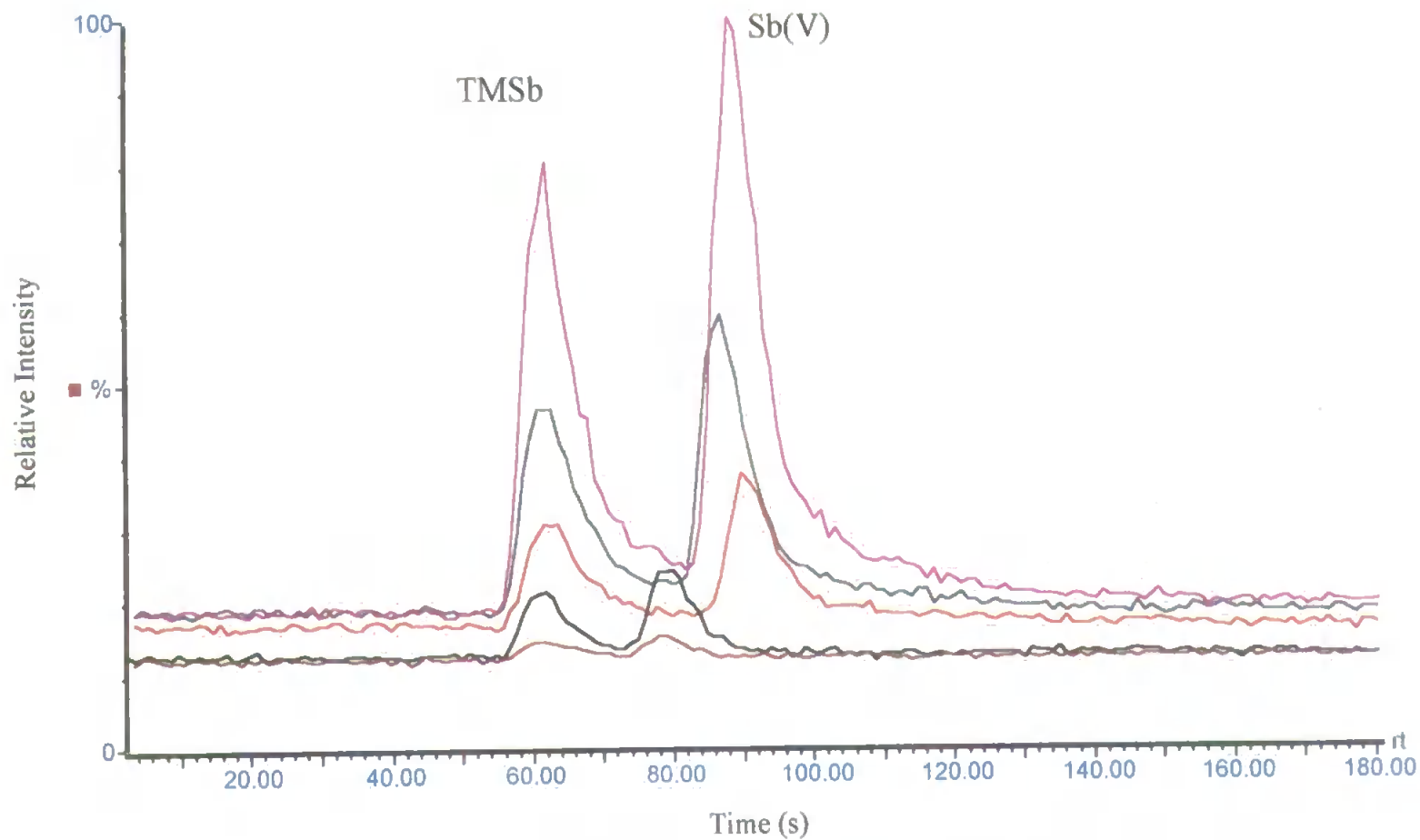


Figure 4.20 Calibration set for separation of TMSb and Sb(V). 1 mM OH⁻ mobile phase at 0.35 ml min⁻¹, AS11 column. Concentration set: 1, 5, 10, 20 and 40 µg l⁻¹.

Thus, after all the attempts to obtain a method utilising ion exchange another approach was deemed necessary to try and recover more of the Sb from the column. It has already been shown that Sb(V) in solution can react with compounds such as α -hydroxyacids. As such, if there is any chance that the water soluble extracts contained dissolved species that might complex with Sb then they might also share the pH dependence of Sb, α -hydroxyacids.

In Chapter 3 it was shown that the Sb, α -hydroxyacid complexes could be separated with an H₂SO₄ eluent. Such an elution protocol is normally applied to the elution of organic acids from a reversed-phase column such as an C₁₈ or C₈ packed column⁽²⁰⁸⁾. However, as described in Chapter 3, the AS11 column is highly cross-linked and demonstrated a capacity for mixed-mode separation mechanisms, possibly including ion-suppression characteristics. Hence the application of a H₂SO₄ mobile phase to the separation of Sb species offered another possibility for investigation.

4.3.3.2 Determination of antimony in H₂O and 0.2 M Acetic acid extracts of plant and sediment samples by HPLC-ICP-MS

In an attempt to extract more Sb from the sediment samples whilst maintaining the integrity of the Sb species, 0.2 M acetic acid was used as an extraction solvent. As with the water extracts 2.5 g of each sediment sample was weighed into a clean sample tube, to which was added 40 ml 0.2 M acetic acid. The tube was then sealed with a screw cap and then shaken for up to 8 hours. The solution was then allowed to settle, and the supernatant then filtered through a 0.45 μ m cellulose acetate filter.

Moss and liverwort samples (0.25 g) were homogenised with a few mls of 0.2 M acetic acid, then sonicated for 6 hours after being made up to final volume with 0.2 M acetic acid (15-16 ml). A reference material was used for the plant samples, BCR No.61, *Platihypnidium riparioides* (aquatic moss). Table 4.5 gives the pH values of the extracts.

Table 4.5 pH ranges of the 0.2 M acetic acid extracts

Sample	pH
Adit mouth moss	3.36
Liverwort	3.11-3.25
Spoil heap moss	3.67-3.82
Adit mouth sediment	3.30-3.32
Spoil heap sediment	4.5-4.52
BCR No. 61 (aquatic moss)	3.62-3.63

The water soluble extracts had a pH range from 6.84-7.6 and the water sample taken from the site were in the pH range 7.4-7.65.

Figure 4.21 shows the chromatograms obtained for the adit mouth moss sample in 0.2 M acetic acid extract and the variation in retention times with H₂SO₄ eluent concentration.

Table 4.6 summarises the results for other samples analysed.

Table 4.6 Summary of peak data for sample extracts, all 0.2 M acetic acid except where indicated.

Sample	No. of Peaks	Figure No.
Liverwort	4-5	4.22
Spoil heap moss	4	4.23
BCR No. 61	3	4.24
Spoil heap sediment	2	4.25
Adit mouth sediment	2	4.26
Adit trail sediment (H ₂ O)	3	4.27
Spoil heap sediment (H ₂ O)	2	4.28
Adit mouth moss	4	4.29

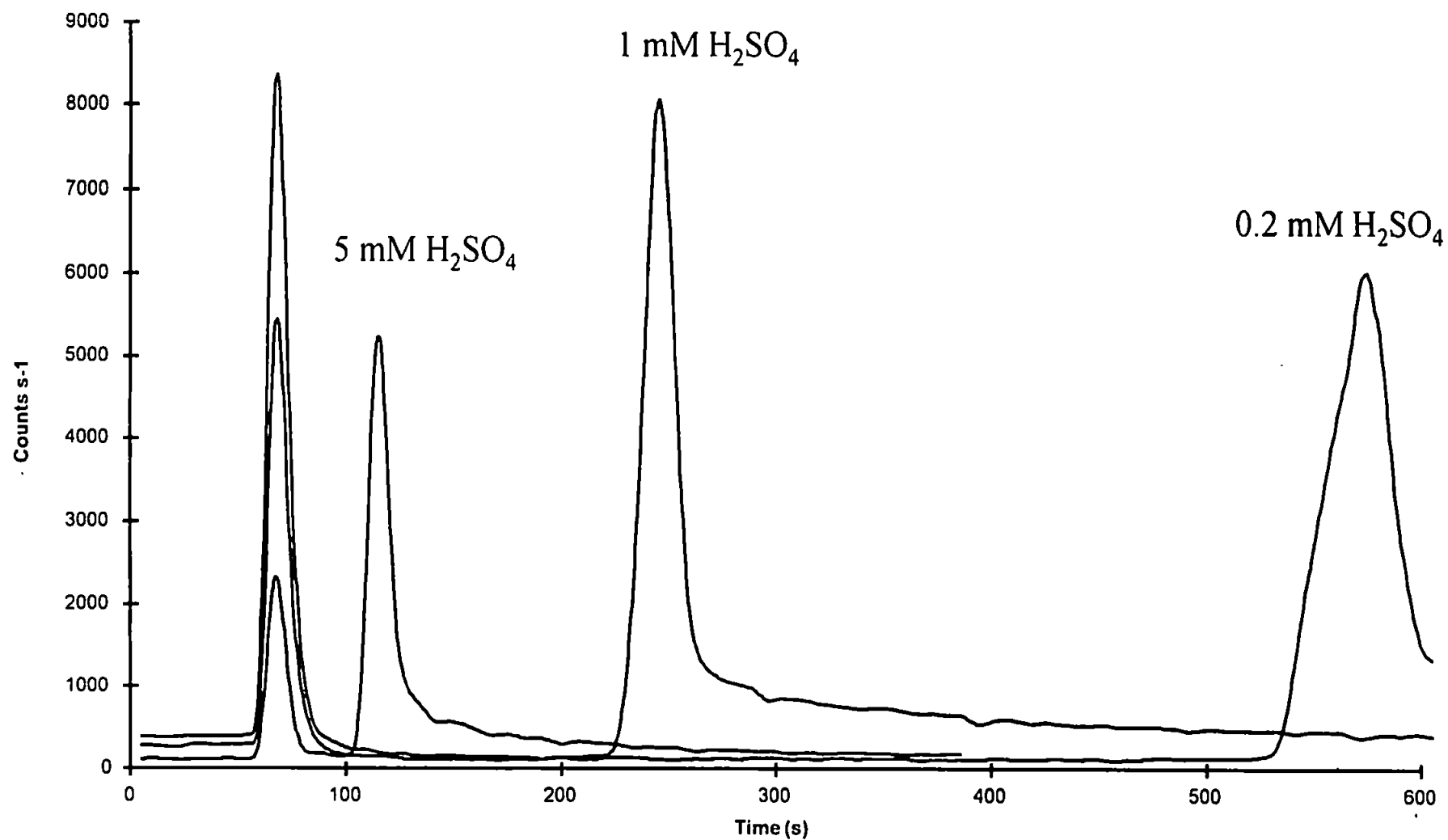


Figure 4.21 Chromatograms illustrating the effect of H_2SO_4 concentration on the elution profile of a 0.2 M acetic acid extract of a moss sample taken from the mine adit mouth. AS11 column. ICP-MS detection

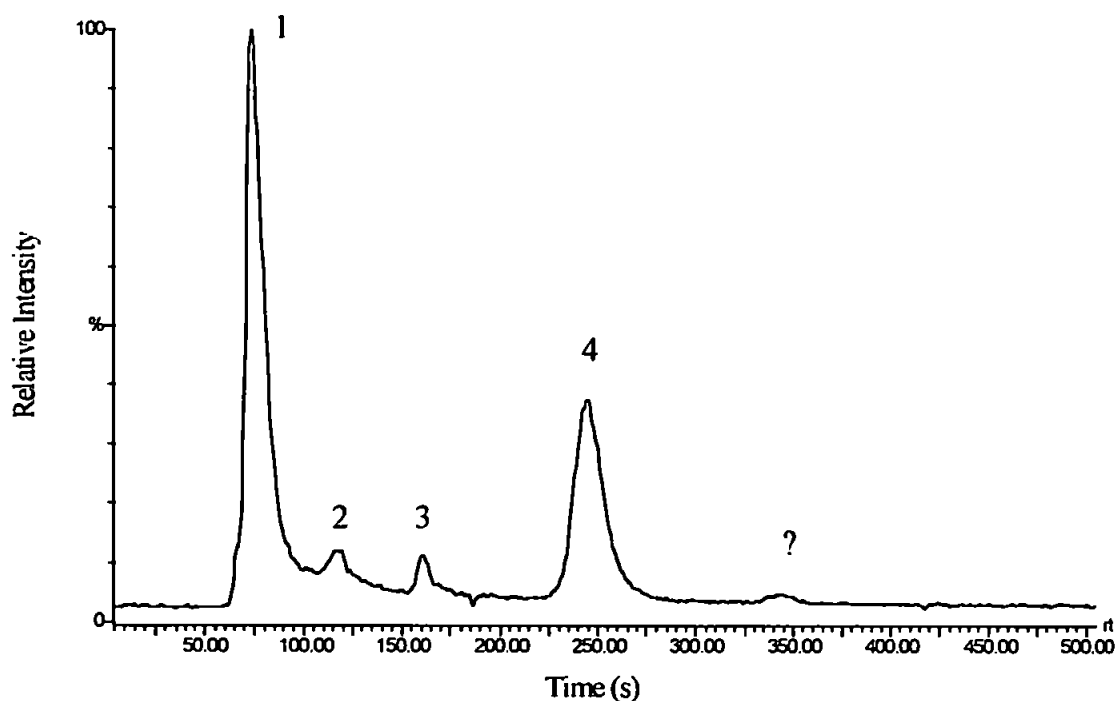


Figure 4.22 Chromatogram obtained from a sample of liverwort taken from the mine site. 0.5 mM H_2SO_4 mobile phase at 0.35 ml min^{-1} . AS11 column. ICP-MS detection

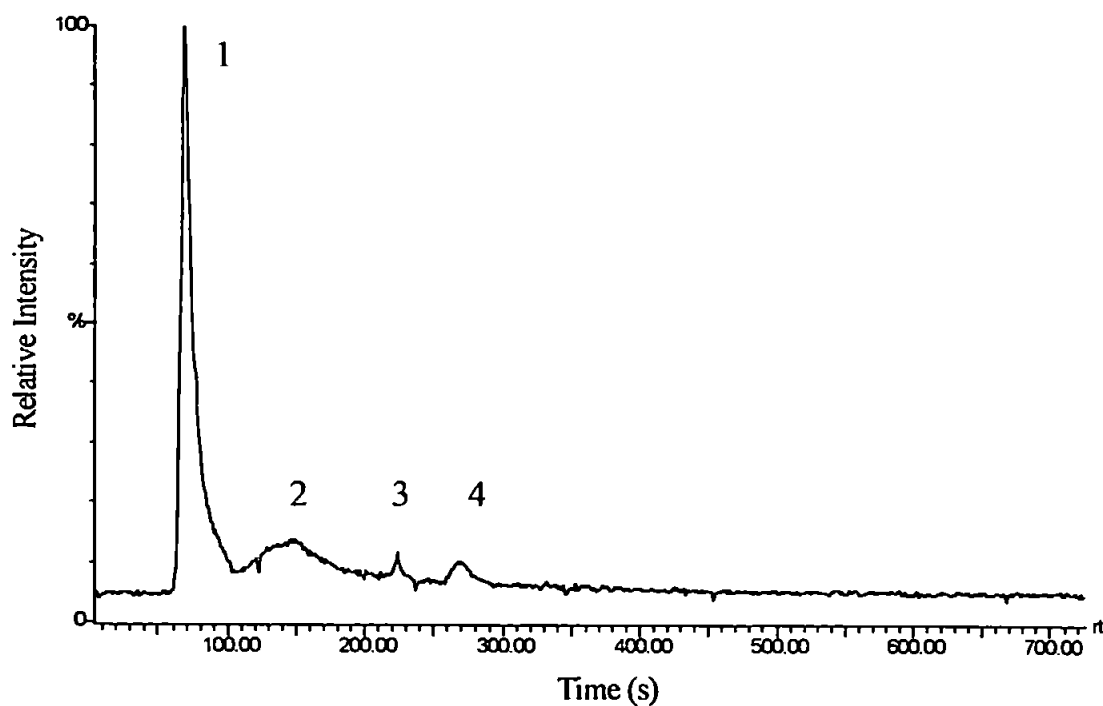


Figure 4.23 Chromatogram obtained from a sample of moss taken from the spoil heap. 0.5 mM H_2SO_4 mobile phase at 0.35 ml min^{-1} . AS11 column. ICP-MS detection

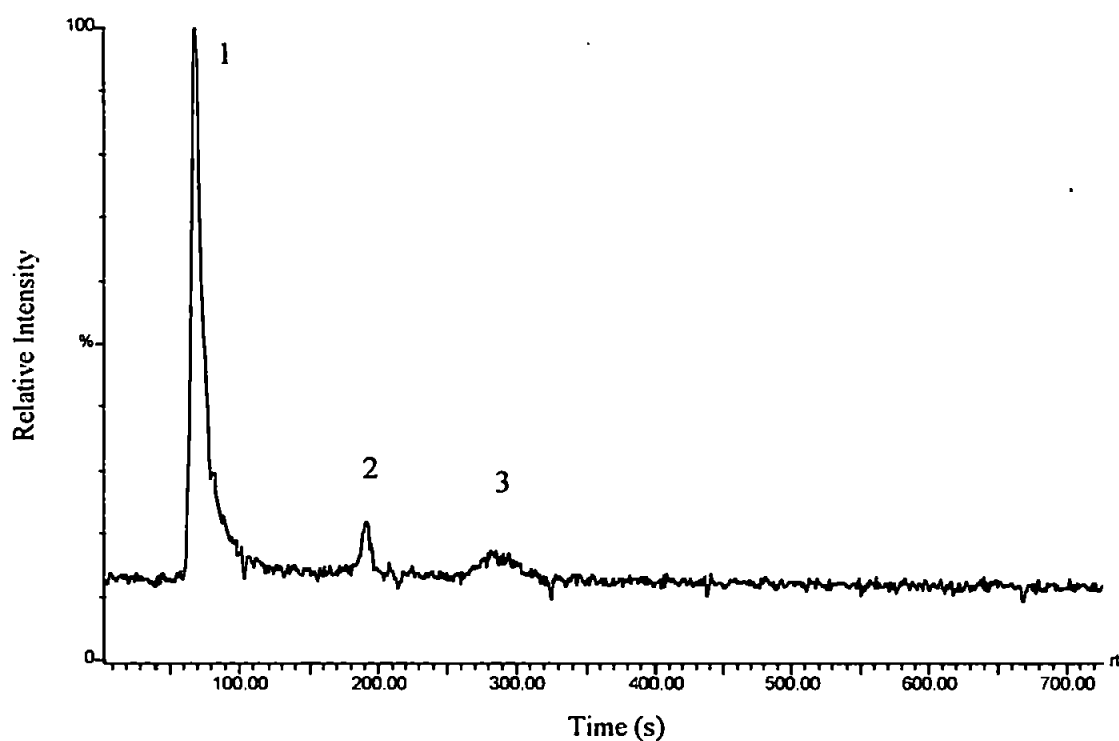


Figure 4.24 Chromatogram from the BCR reference material No.61. *Platyhypnidium riparoides* (aquatic moss) 0.5 mM H₂SO₄ mobile phase at 0.35 ml min⁻¹. AS11 column. ICP-MS detection

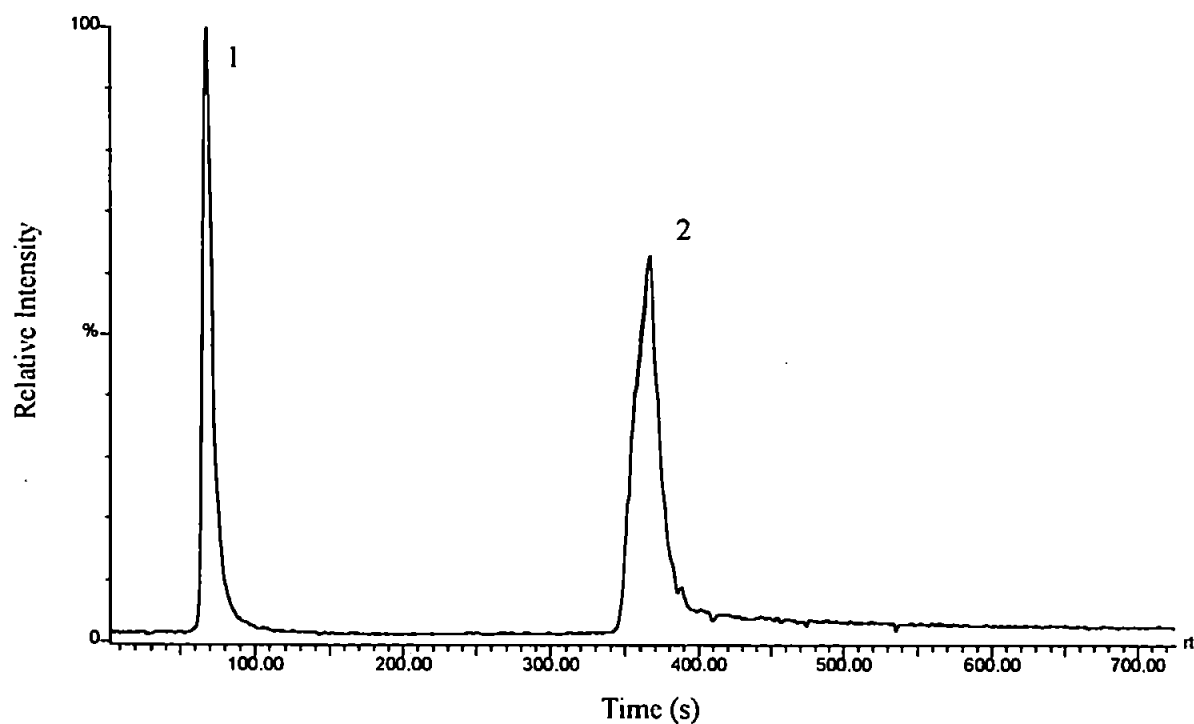


Figure 4.25 Chromatogram obtained from the spoil heap sediment. 0.5 mM H₂SO₄ mobile phase at 0.35 ml min⁻¹. AS11 column. ICP-MS detection

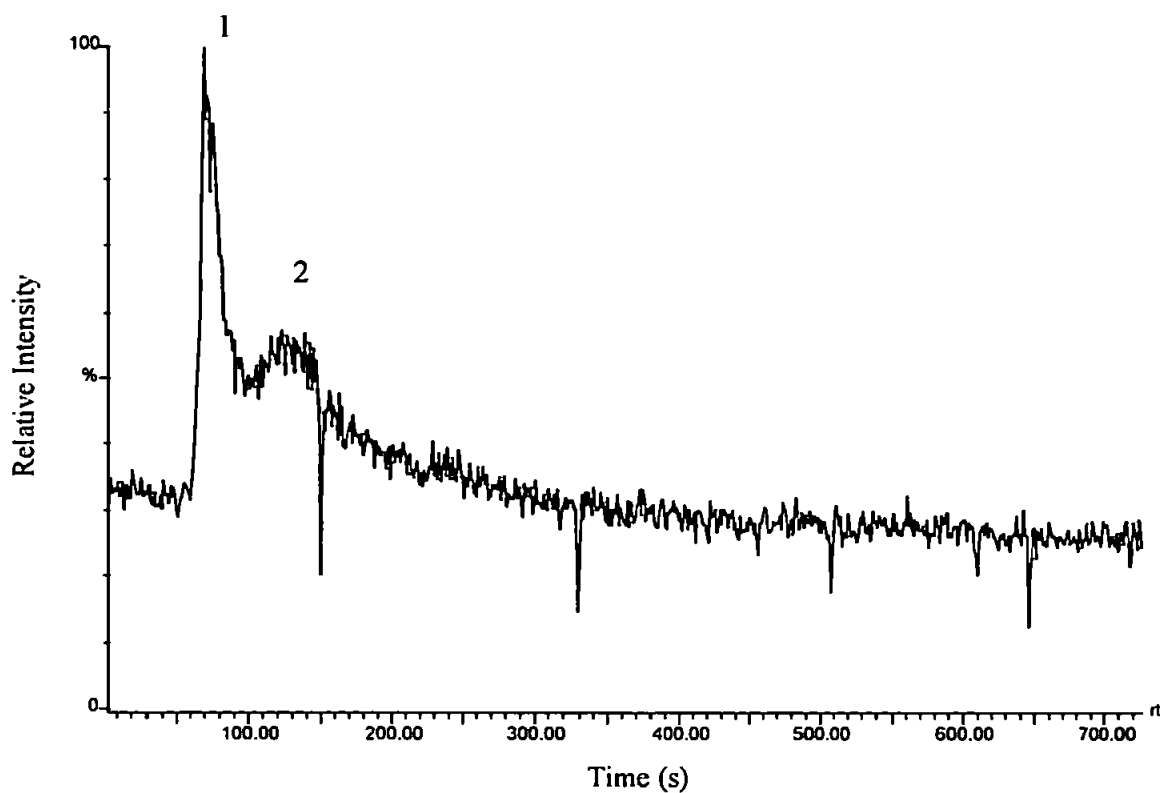


Figure 4.26 Chromatogram obtained from the adit mouth sediment. 0.5 mM H_2SO_4 mobile phase at 0.35 ml min^{-1} . AS11 column. ICP-MS detection

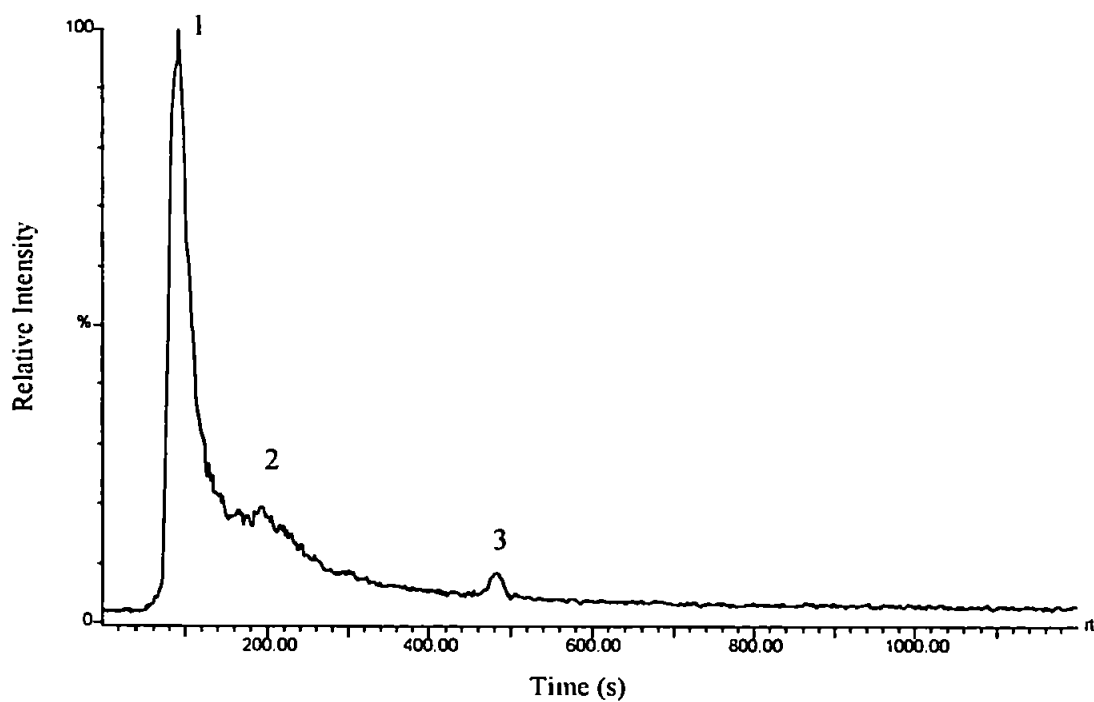


Figure 4.27 Chromatogram obtained from the adit trail sediment in H_2O . 0.4 mM H_2SO_4 mobile phase at 0.35 ml min^{-1} . AS11 column. ICP-MS detection

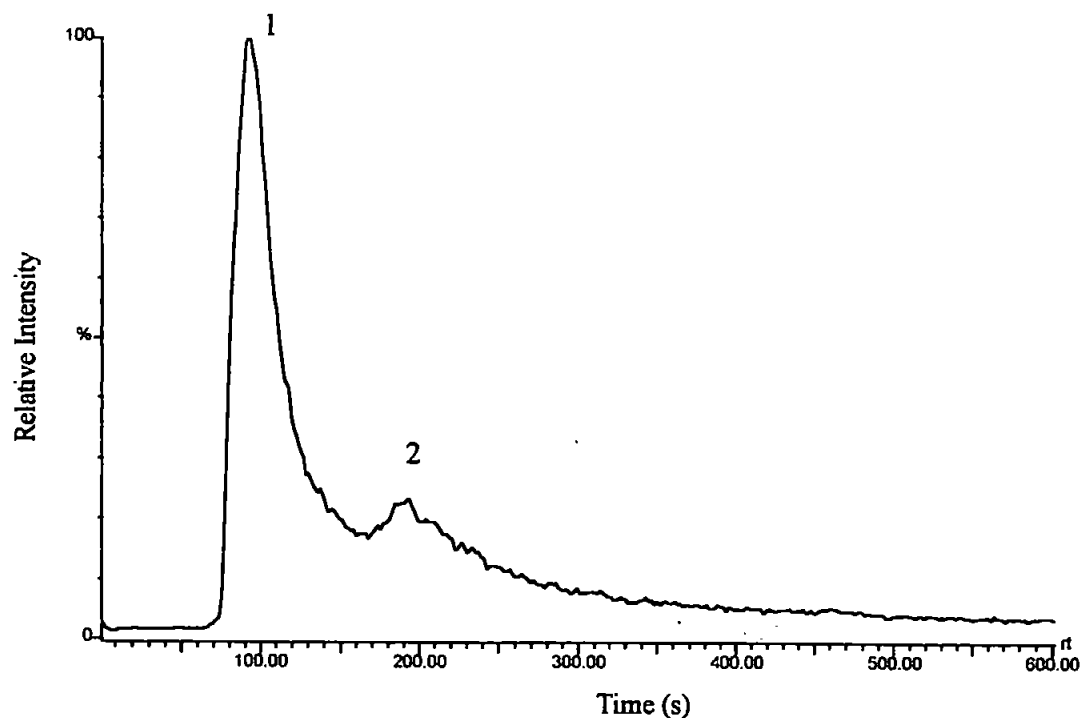


Figure 4.28 Chromatogram obtained from the spoil heap sediment in H_2O . $0.4 \text{ mM H}_2\text{SO}_4$ mobile phase at 0.35 ml min^{-1} . AS11 column. ICP-MS detection

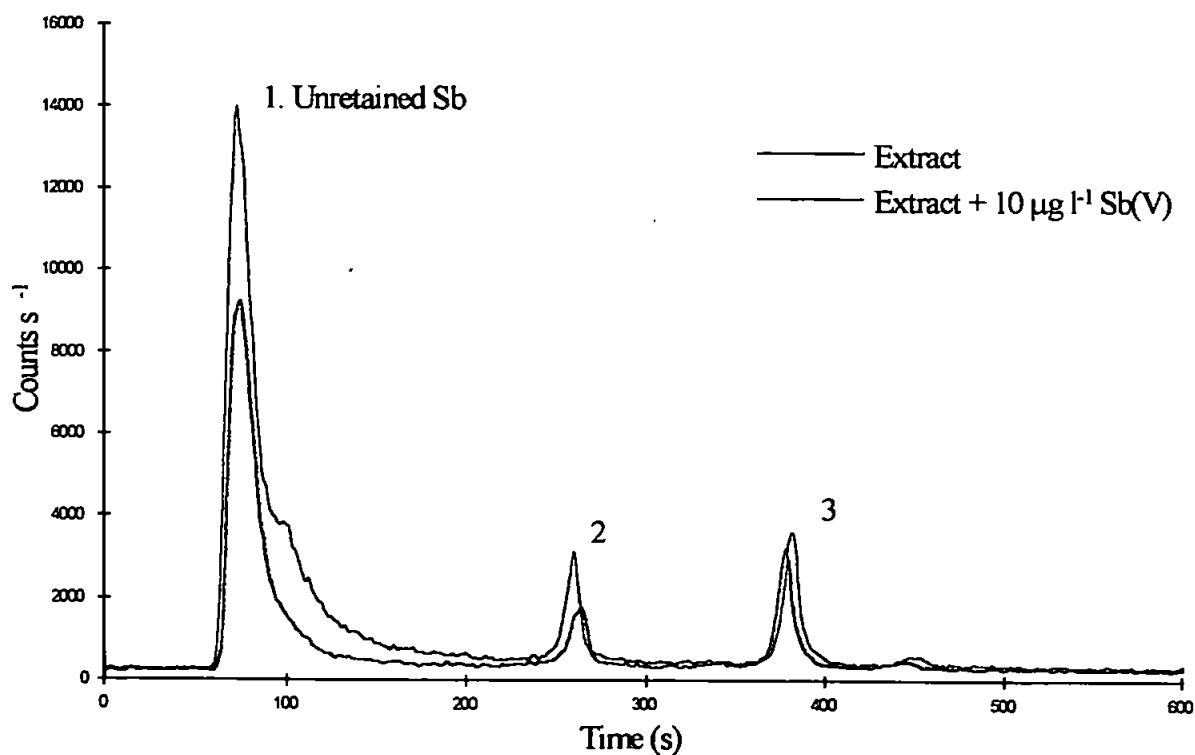


Figure 4.29 Chromatograms obtained from the adit mouth moss extracts with and without a Sb(V) spike. $0.4 \text{ mM H}_2\text{SO}_4$ mobile phase at 0.35 ml min^{-1} . AS11 column. ICP-MS detection

The next stage of the analysis was to investigate how the separation would be affected by spiking the samples with standards.

Figure 4.29 a) shows the chromatogram obtained from a moss sample from the adit mouth. There are three distinct peaks and one small hump at about 450 s. With the addition of a $10\ \mu\text{g l}^{-1}$ spike of Sb(V) all of the main peaks increase in intensity, Figure 4.29. Figure 4.30 shows the chromatogram obtained from a spoil heap moss extract. There are 5 clear peaks observed although not all are baseline resolved. When a $10\ \mu\text{g l}^{-1}$ spike of Sb(V) was added to this sample a pronounced increase occurs only in peak 2, Figure 4.30. For reference Figure 4.31 shows the chromatogram for $10\ \mu\text{g l}^{-1}$ Sb(V) in 0.2 M acetic acid.

These results suggest two things. There is a variation in Sb species between plants of the same type at different points of the site. None of the retention times cross-correlate between chromatograms. Secondly, the effect of spiking these extracts is significantly different, with the Sb species in the adit mouth moss sample being practically impossible to quantify with the standards available and without a much more detailed analysis of the biogeochemical pathways.

However, this whole section of the study utilising chromatography involving a significant amount of reversed-phase has shown the most promise for Sb speciation analysis.

4.3.3.3 Analysis of Mine Site samples by HPLC-HG-ICP-MS

The instrumentation utilised for this study was basically the same as that shown in Figure 4.2 except the sample line was swapped for the HPLC column outlet. The acid concentration was 3M HCl and the reductant was 0.5% NaBH₄. KI (30% w/v) was used as a pre-reductant. Figure 4.32 shows the chromatograms obtained from the spoil heap sediment extracts (0.2M acetic acid) using this method without and with the pre-reductant present in the acid carrier. The response for both peaks increased significantly using the pre-reductant. Figure 4.33 shows chromatograms obtained from the spoil heap

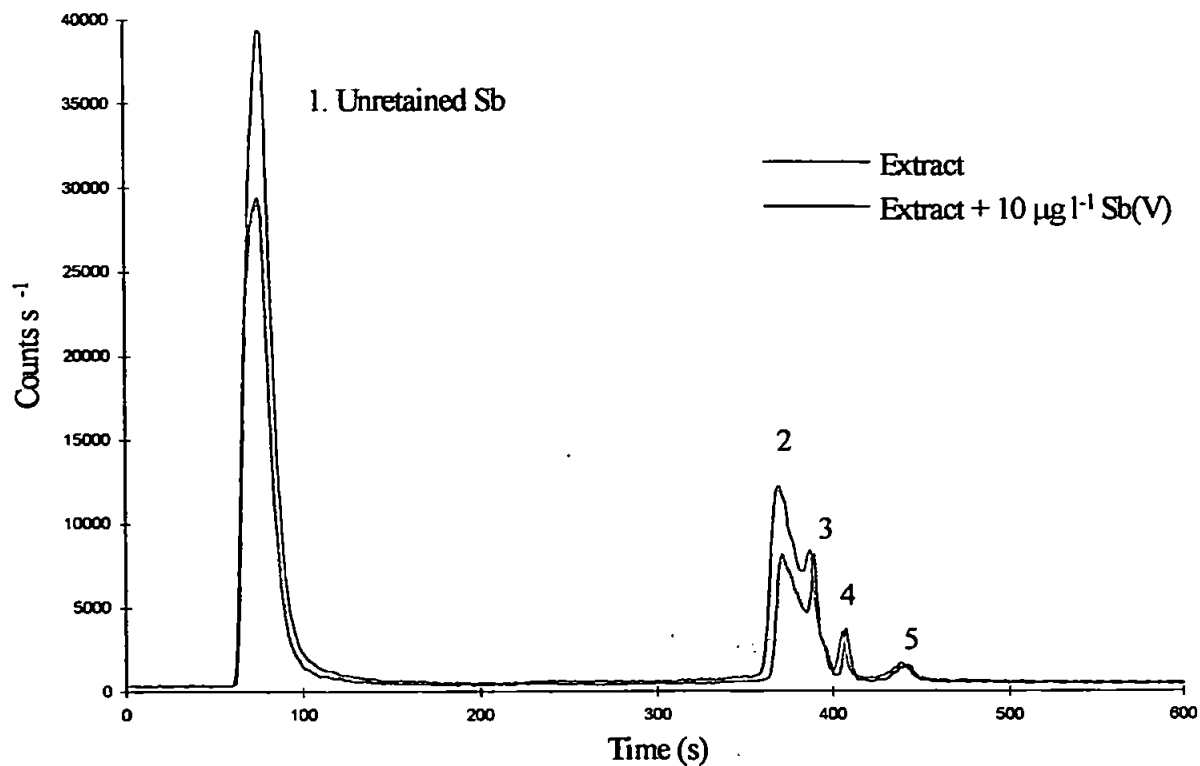


Figure 4.30 Chromatogram obtained from the spoil heap moss extracts with and without a Sb(V) spike. 0.4 mM H_2SO_4 mobile phase at 0.35 ml min⁻¹. AS11 column. ICP-MS detection

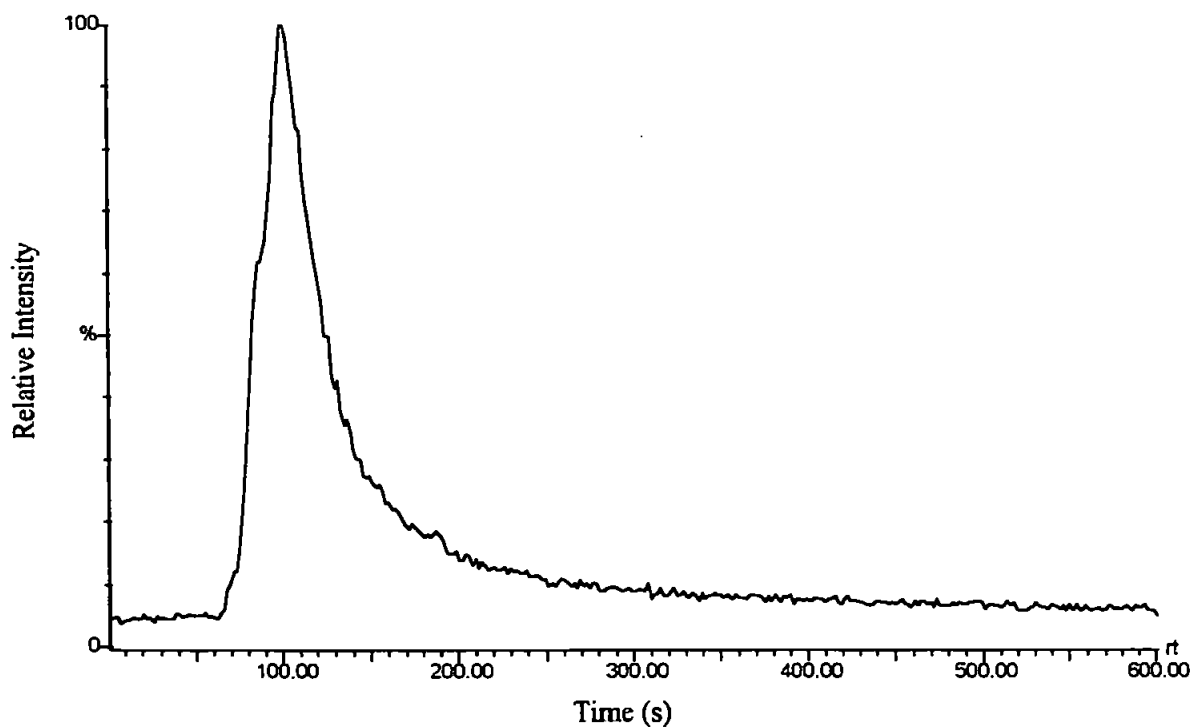


Figure 4.31 Chromatogram obtained for 10 µg l⁻¹ Sb(V) in 0.2 M acetic acid. 0.4 mM H_2SO_4 mobile phase at 0.35 ml min⁻¹. AS11 column. ICP-MS detection

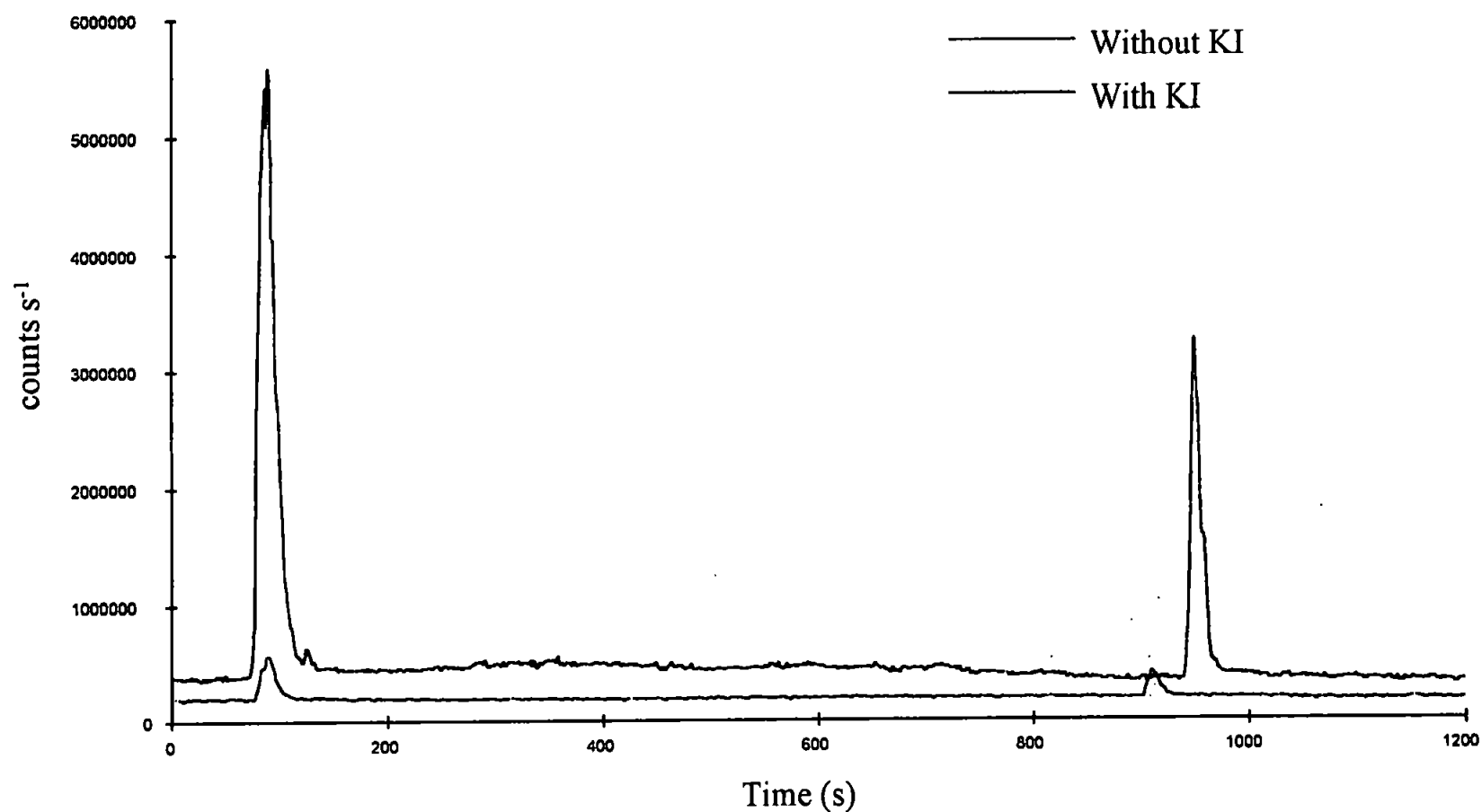


Figure 4.32 Chromatograms for spoil heap sediment in 0.2 M acetic acid by HPLC-HG-ICP-MS with and without a pre-reductant. 0.4 mM H₂SO₄ mobile phase at 0.35 ml min⁻¹. AS11 column. ICP-MS detection

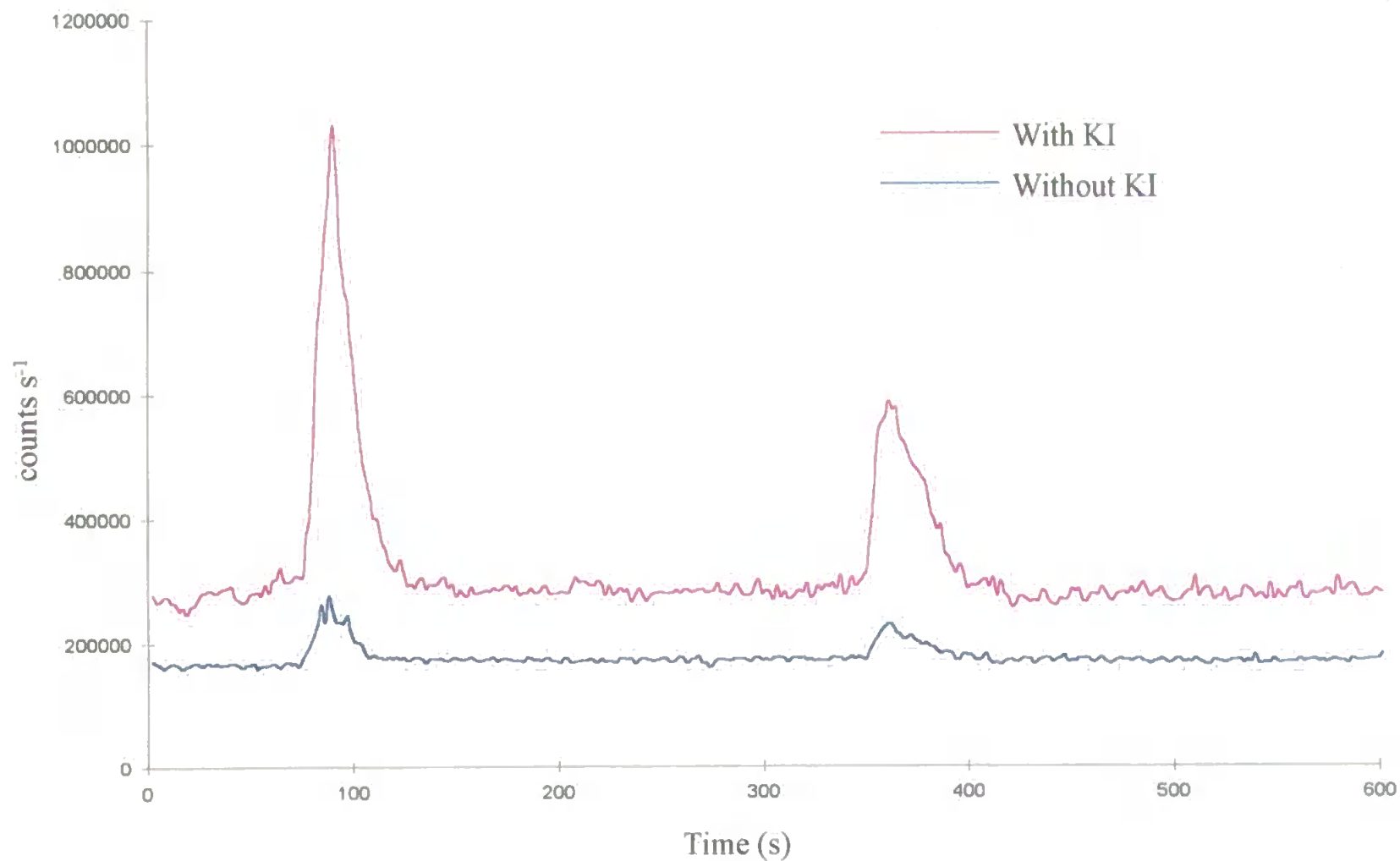


Figure 4.33 Chromatograms for spoil heap moss in 0.2 M acetic acid by HPLC-HG-ICP-MS with and without a pre-reductant. 0.4 mM H₂SO₄ mobile phase at 0.35 ml min⁻¹. AS11 column. ICP-MS detection

moss; a) without KI; and b) with KI. A comparison with the same sample using HPLC-ICP-MS with HG treatment shows that using HG three peaks are not observed. The liverwort sample showed a similar result with the loss of two peaks when using HG compared to analysis without HG.

Thus, even though HG in a continuous flow arrangement without prior species separation and careful choice of acid carrier cannot be used solely in speciation studies of Sb in the environment, it can be used to provide valuable information as to those species that do resist hydride formation. This is an important factor in the continuing development of methods for the elucidation of biogeochemical pathways for this metalloid.

4.4 Conclusions

This study set out to investigate the speciation of antimony in environmental samples from a disused mine site. The development of the methods utilising chromatography found much of the anion exchange methodology lacking for most purposes of environmental analysis except in limited applications such as the analysis of water samples. When simple water soluble extracts of sediments were analysed, the lack of Sb recovery from the column indicated that either the Sb present was in a strongly ionic, polycharged form, or that the Sb species were of a form that interacted with the backbone of the column itself rather than acting as a simple ion exchanger.

Although the sulphuric acid method is normally used for organic acids it proved a good starting point to start with considering the results from the chromatography with the Sb, α -hydroxyacids. This protocol provided many interesting results for both the water soluble extracts and acetic acid extracts.

The results obtained also showed how it may be possible that the same family of plants in different parts of the site may metabolise Sb in different ways. This may be due to the form in which the Sb is present in those parts of the sites. However, this cannot be confirmed without a great deal of investigation of the biogeochemistry of antimony. This in turn requires more organoantimony standards to be synthesised to aid identification and quantification of the Sb present in these samples.

In the absence of reference materials, sample spiking was attempted and this only served to reinforce the need for further biogeochemical analysis.

The chromatograms for the spiked samples of plant extracts also showed a very interesting result. In one sample the spike response was different to the other. The fact that in one case only one retained peak increased in intensity with a spike of Sb(V) suggests that that peak might be due to Sb(V) in the form in which it was spiked. However, the other sample

analysed after it was spiked had all of the retained peaks increase in intensity. These peaks cannot all be due to Sb(V) in the form in which it was introduced as a spike. Therefore, the results seem entirely analogous with those obtained for the Sb, α -hydroxyacid study, i.e. that Sb(V) is forming stable complexes in solution with dissolved chelates, most likely organic. These complexes can be determined in the presence of each other.

This result is important because as far as the author can discern this is the first time that such a chemical effect has been observed directly in environmental matrices during the analysis of antimony.

Although it has been suggested in this thesis that hydride generation is not the analytical method of choice for Sb speciation, mostly because it does not provide enough information, hydride generation does have a firm place in the analysis of unknown species when coupled with HPLC-ICP-MS as such a method can provide information on reducible species. This was shown in the ICP-MS studies when a number of species observed in the HPLC-ICP-MS analysis were clearly not observed in the HPLC-HG-ICP-MS analysis. This backs up the argument that it is possible to obtain Sb compounds that resist HG, most likely stable organoantimony compounds. This statement is supported by the results presented in this chapter on the unsuccessful attempt to produce a hydride from the TMSb species when using a mineral acid carrier. The use of hydride generation might allow for the pinpointing of these stable Sb compounds for further chemical analysis.

The methods developed and applied in this study are suitable for analysis of trace levels of antimony species and should be considered for further investigation as tools in the search for biogeochemical pathways of Sb in the environment.

Chapter 5

5.1 Nebuliser and Spray-Chamber effects on Post-Column Dispersion and Resolution in High Performance Liquid Chromatography-Inductively Coupled Plasma-Mass Spectrometry

5.1.1 Introduction

The coupling of high performance liquid chromatography (HPLC) with inductively coupled plasma-mass spectrometry (ICP-MS) is now widely used for speciation studies. Examples of metals and metalloids determined in this way include As, Se, Sn, Pb and Cr⁽²¹⁴⁻²¹⁸⁾. However, unlike gas chromatography (GC) where coupling interfaces have been specifically designed⁽²¹⁹⁻²²⁰⁾ HPLC couplings are often no more than a connecting tube between the end of the HPLC and the nebuliser.

Although GC couplings have specific problems associated with the interface, primarily involving the thermal equilibrium in the interface between the GC oven and the plasma torch, such arrangements avoid the need to use the nebuliser/spray-chamber and hence avoid the region where dispersion is most likely. HPLC systems however are usually connected via the nebuliser/spray-chamber in most interfaces, and although such arrangements do work, the results obtained often do not reflect either the separation achieved by the chromatography or the analyte sensitivity expected from the ICP-MS.

When commencing with any chromatographic optimisation procedure one of the key parameters to minimise is the effects of extra-column dispersion. Such effects can cause band-broadening with concomitant peak tailing and loss of efficiency. Such dispersion is usually caused by zones of dead volume either in the injection valve, the detector, or between the column outlet and the detector.

This study extends work previously carried out at Plymouth⁽¹⁷⁸⁾ to reduce the dispersion in the nebuliser/spray-chamber assembly. The nebulisation characteristics in terms of sample signal to background ratios were also studied. This was achieved by direct comparison of different nebuliser/spray-chamber combinations.

There have been a number of in-depth studies of aerosol-production and the relative performances of nebulisers for continuously nebulised samples in terms of noise characteristics⁽²²¹⁻²²²⁾, as well as the role of the spray-chamber^(176,177,179,180,182&223).

However, little attention has been paid to how these effect HPLC where the sample is introduced as a discrete volume in a continuous flow of mobile phase.

For this study the separation parameters (resolution etc.) were characterised by using two antimony species in an aqueous matrix.

5.1.2. HPLC-ICP-MS and Post-Column Dispersion.

Many conventional HPLC systems based on conductivity, UV/VIS absorption or refractive index detection are often designed in such a way as to minimise post-column dispersion by using narrow-bore tubing and zero dead-volume connectors. However, although ICP-MS has been long recognised as the detector of choice (when available), for speciation studies, the design of the nebuliser/spray-chamber assembly has not been subjected to a great deal of scrutiny with respect to the effects of dispersion on chromatographic separations.

Snyder, Glajch and Kirkland⁽¹⁶⁸⁾ state that retention and resolution variations in HPLC caused by extra-column effects are due to large tubing between column and detector and large volume fittings, amongst a range of other effects. They also state that these effects can combine to increase peak tailing. This type of tailing is most pronounced for early-eluting peaks (short retention times) since they have the smallest volume. The trend where early peaks tail most is a good indicator of extra-column effects in the apparatus.

Thus these effects should be eliminated or minimised before attempting to optimise a separation.

The authors⁽¹⁶⁸⁾ also suggested a number of ways to help eliminate these effects; i) inject small sample volumes, $< 25 \mu\text{l}$; ii) use minimal lengths of connecting tubing of small i.d. $< 20 \text{ cm}$ of $0.01''$ i.d.; iii) make sure that all tubing connections are made correctly from “matched” fittings; and iv) use a cleanly swept, low-volume detector cell ($< 10 \mu\text{l}$).

The dispersion of the analyte bands, band-broadening, is greatly influenced by the parabolic velocity profile of the mobile phase in a tube, Figure 5.1. Although this is sometimes considered secondary to the mixing effects that are caused by large dead volumes in HPLC couplings. The solute in the centre of the tubes moves more rapidly through the tube than solute situated initially at the wall of the tube⁽¹⁶⁹⁾.

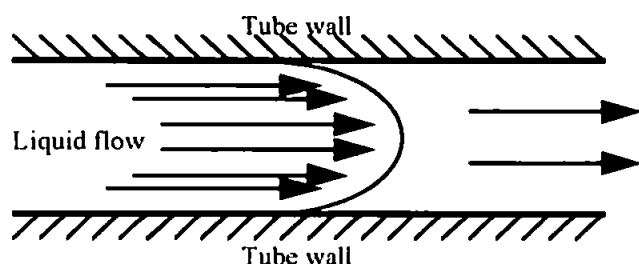


Figure 5.1 Parabolic flow of mobile phase through a tube

Thus the bands of solute become elongated and spread. Many HPLC separations are carried out on columns with 4.6 mm i.d. These columns have large enough peak volumes to make the extra-column volume band dispersion relatively unimportant. However, if the peak volume is reduced extra-column volume becomes very important. Peak volume is also reduced by a reduction in column i.d.

Snyder and Kirkland state that in columns $10\text{--}15 \text{ cm}$ long with narrow i.d., $< 4 \text{ mm}$, packed with $5 \mu\text{m}$ particles it is particularly important to eliminate tailing of early eluting bands⁽¹⁷⁰⁾. In this study the main column used was 25cm long with an i.d. of just 2 mm .

The column used in this study therefore conforms to the criteria where extra-column effects are more critical to eliminate or minimise.

5.1.2.1 The Nebuliser and Spray Chamber Assembly

The types of nebuliser and spray chambers commonly utilised in ICP spectroscopy are described in Chapter Two. In that chapter the inefficiency, in terms of sample transport, of the double-pass spray chamber is also described.

In chromatography discrete volumes of the analyte have to be detected in a bulk matrix (mobile phase) in the time in which they elute. This is as opposed to continuously nebulised analytes from which a total signal can be integrated over time. If the peak volume is minimised then the peak maxima should be greater in intensity and therefore easier to determine. If the spray-chamber is at best just 2% efficient in sample transport, the demand for a peak volume to be as narrow as possible is paramount. This concentrates the analyte into as narrow a time slot as can be achieved to ensure the best possible sensitivity. Thus, if a narrow-bore analytical column is used, and narrow-bore tubing is cut to a minimal length so that the column outlet is connected as close as possible to the nebuliser then the nebuliser/spray-chamber assembly is the only part of the system that can contribute significantly to post-column dispersion.

Figure 5.2 gives schematic representations of the nebulisers utilised in this study: a) the concentric glass; b) Burgener; c) de Galan; d) Ebdon-type V-groove; and e) a V-groove nebuliser modified with HPLC tubing.

The nebulisers a-d have varying dimensions for the sample introduction bores and as such can be used to compare the effect of varying post-column volumes on peak-tailing. Such a comparison must be made with the same spray chamber. Figure 5.2 e) shows the modified nebuliser. This modification meant that the eluent did not encounter any change in post-column volume until it was nebulised. Theoretically this should provide

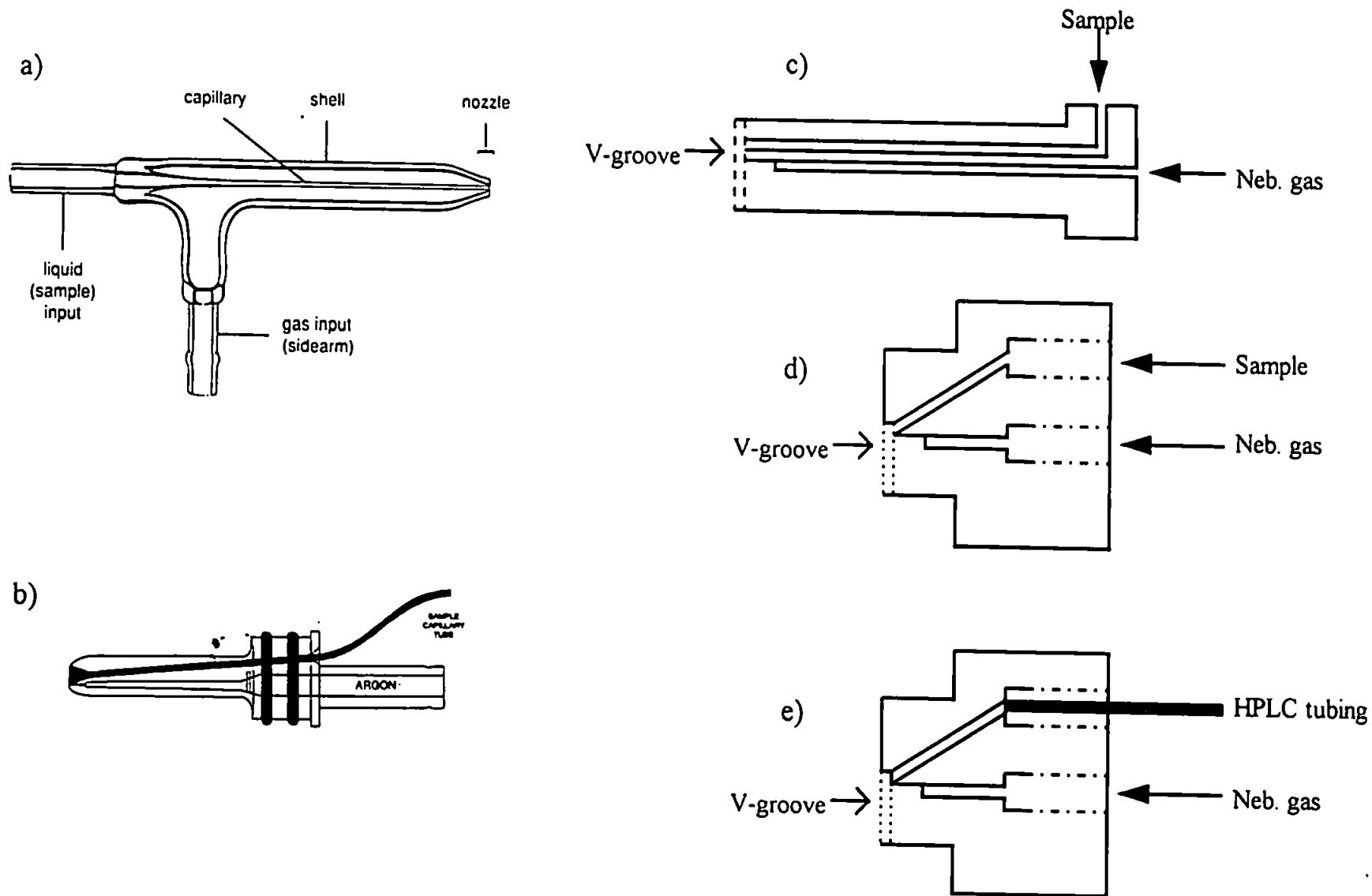


Figure 5.2 Schematic diagrams of nebulisers utilised in this study. a) concentric glass (MN); b) Burgener (BGN); c) de Galan; (DGN) d) Ebdon type V-groove (EUM); and e) modified V-groove (MOD)

the best separation characteristics when compared to the other nebulisers. This, however, is very dependent on the nebulisation characteristics and the spray-chamber.

The spray-chamber part of the sample introduction assembly is obviously a large volume fitting when compared with the rest of the sample introduction apparatus. However, transportation to the plasma is via the nebuliser gas flow at a flow rate typically of 0.8 - 1.0 l min⁻¹, and through spray-chambers of internal volume usually no greater than 0.1 l. Thus ignoring material that is incorporated from the walls of the spray-chamber, the residence time for most of the analyte in conventional spray-chambers is a few seconds. In LC systems peak widths are wider than for GC systems and as such elution times per peak, even with good separations, can be 30-60s. Therefore a 2-3 s residence time in a spray chamber should not significantly add to peak-tailing. It is the overall transport efficiency of the spray-chamber that will have the greatest impact upon the effectiveness of the interface, assuming the background signal can be minimised.

Thus, within the confines of this study the two most commonly used spray-chambers were investigated, the double-pass and the cyclonic spray chambers. Although Sharp^(181,182) has set out methods to measure the performance of nebulisers and spray-chambers Sharp's work is more concerned with continuously nebulised samples and he only made a limited reference to HPLC arrangements. Thus the special requirements of an HPLC-ICP-MS system has not undergone similar investigation. The gathering of empirical data in this part of the study provided a valuable insight into the importance of the interface design in HPLC-ICP-MS studies.

5.1.3 Instrumentation

The HPLC system employed for this study comprised an inert pump (Model 9010, Varian, Walnut Creek, Calif., USA) used at 0.350 or 1.0 ml min⁻¹. The chromatographic columns used were an IonPac AS11-SC (25cm x 2 mm i.d.) and an IonPac AS4A (25cm x 4 mm i.d.), both anion exchange columns (Dionex, Calif., USA). Sample introduction was via a six-port injection valve (Rheodyne type 7125) with a 20 µl stainless steel sample loop. The ICP-MS instrument was a Fisons PQ2+ (Fisons Instruments Elemental, Cheshire, U.K.), using typical operating conditions of 1340W forward power, 15.0 l min⁻¹ coolant gas flow rate, 1.0 l min⁻¹ auxiliary gas flow rate and a nebuliser gas flow rate of 0.868 l min⁻¹ for the double-pass spray-chamber and 0.800 l min⁻¹ with the cyclonic spray-chamber. The nebulisers investigated were: concentric glass (Meinhard type), Burgener (high solids), de Galan (high solids), V-groove (Ebdon type, high solids) and a V-groove modified with standard HPLC tubing (PEEK, i.d. 0.007"). Figures 5.3 shows schematic representations of the two spray-chambers investigated in this study.

5.1.4 Reagents

All reagents used were of analytical grade unless otherwise stated. Stock solutions of 1000 mg l⁻¹ K[Sb(OH)₆] and (CH₃)₃SbBr₂ were made by dissolving potassium hexahydroxyantimonate(V) (Aldrich, Kent, UK), and trimethyl antimonydibromide ((CH₃)₃SbBr₂, de Montfort University, Leicester, U.K.) in H₂O. Working solutions of these compounds were obtained by serial dilution of aliquots from the stock solutions. The required concentrations of KOH (Aldrich, Kent, UK) and CH₃COONH₄ (Aldrich, Kent, UK) for the mobile phases were obtained using the inert pump. MilliQ (Millipore, Mollsheim, France) water was used in all cases. The ¹¹⁵In standard used for tuning of the ICP-MS was obtained by dilution of a 10 mg l⁻¹ In solution in 2% HNO_{3(aq)}.

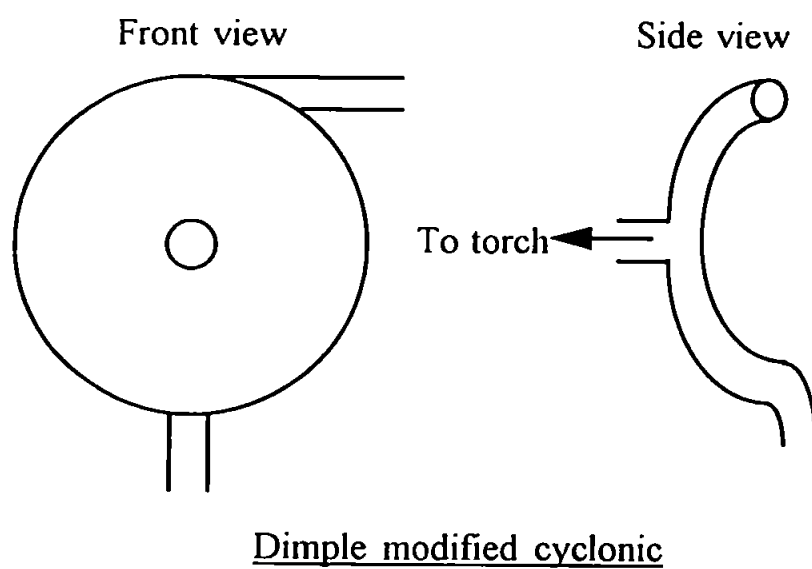
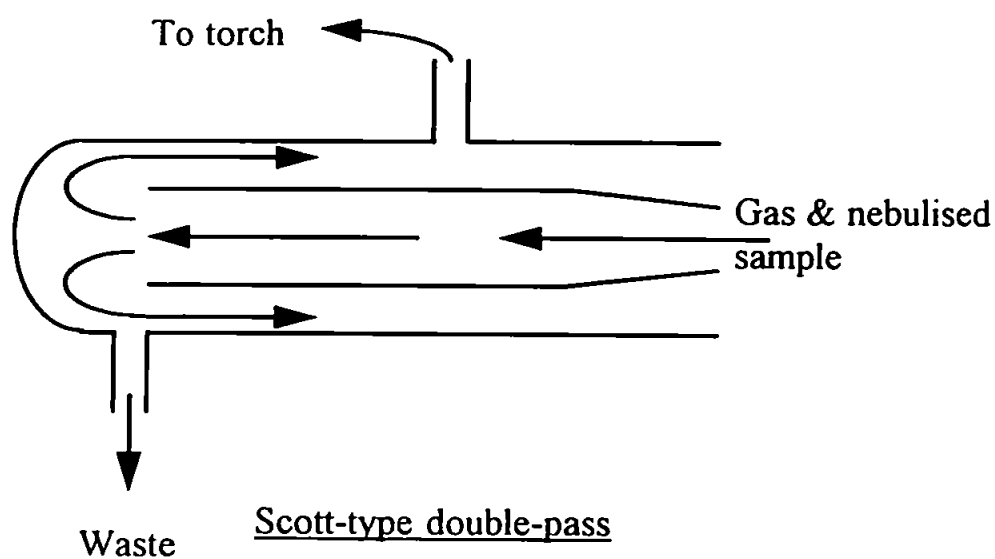


Figure 5.3 Schematic diagrams of spray-chambers used in this study

5.1.5 Experimental

5.1.5.1 Nebuliser Comparison with Double-Pass Spray-Chamber

Each nebuliser was first of all inserted into the double-pass spray-chamber and a $100 \mu\text{g l}^{-1}$ ^{115}In standard was continuously nebulised in order to tune the ICP-MS. This was carried out to assess how each nebuliser performed under the conditions set for analysis in terms of the maximum counts possible for In. Following tuning of the ion lenses, the HPLC system was set-up and the 'model' separation of the two Sb species was carried out in replicate ($n=3$). A chromatogram of the background response was also acquired.

Three HPLC parameters were assessed. The first of these was resolution (R_s), i.e. the extent of separation of the peaks, using the simple equation;

$$R_s = \frac{2(t_{RB} - t_{RA})}{(w_A + w_B)}$$

Figure 2.1 shows how these terms relate on the chromatogram. The second parameter was signal-to-background ratio, based upon peak height and area against average signal for acquired background. Finally the total elution time from peak front of t_1 to the end of peak t_2 was recorded.

The post-column dimensions, i.e. the dimensions (and volumes) of the nebuliser sample introduction bores that the mobile phase flows through between the column outlet and the point of nebulisation, were estimated as accurately as possible. These measurements were then related to the performance of the nebuliser and the efficiency of the separation. The flow/volume transitions were also noted, i.e. whether the mobile phase flowed through zones of different i.d. prior to nebulisation and after it had left the column.

5.1.5.2 Comparison of cyclonic and double-pass spray-chamber, and the concentric and

Burgener nebuliser with the cyclonic spray-chamber.

Using both the concentric glass and Burgener nebulisers, the performance of the cyclonic spray-chamber was compared to the double-pass spray-chamber when used with HPLC.

Primarily the performance was assessed in terms of SBR and peak width, to assess changes in residence time in the spray-chamber and if any affect can be observed.

When comparing the glass concentric and Burgener nebulisers with the cyclonic spray-chamber the parameters assessed were the same as those outlined in Section 5.1.5.1.

5.1.6 Results

5.1.6.1 Comparison of nebulisers when used with double-pass spray-chamber

The results of the instrument tuning process are summarised in Table 5.1

Table 5.1 Summary of tuning process for the nebulisers with a double-pass spray-chamber using a continuously nebulised solution of ^{115}In ($100\ \mu\text{g l}^{-1}$)

Nebuliser	^{115}In counts ppm^{-1}
de Galan	1.0×10^6
Burgener	1.0×10^6
Concentric glass	6.5×10^5
Unmodified V-groove	1.0×10^5
Modified V-groove	1.0×10^5

Although not reported in Table 5.1 some adjustment was required for the ion lens settings when changing the nebulisers to optimise the signal.

Figure 5.4 presents chromatograms for the separation of the two Sb species for each nebuliser. Table 5.2 and Table 5.3 summarise the chromatographic parameters; retention times, resolution, elution period; background stability; and calculated SBR's based on peak area and peak height for the separations with each nebuliser, respectively. Table 5.4 gives the estimated extra-column volumes associated with each nebuliser and the flow transitions between the column and point of nebulisation.

Table 5.2 Summary of chromatographic parameters for comparison of nebulisers with double-pass spray-chambers

Nebuliser	Retention times (s)		Background & stability (%rsd)	Rs	Elution Period (s)
	TMSb	[Sb(OH) ₆] ⁻			
Concentric	57.5	75.2	486.3(6.7)	0.97	49
Burgener	61.5	79.8	1128.7(3.9)	0.91	49
de Galan	64.5	90.0	691.1(5.6)	0.95	58
Unmod ^d V-groove	65.0	78.5	137.7(11.1)	0.54	58
Mod ^d V-groove	57.5	73.2	154.8(9.3)	0.80	49

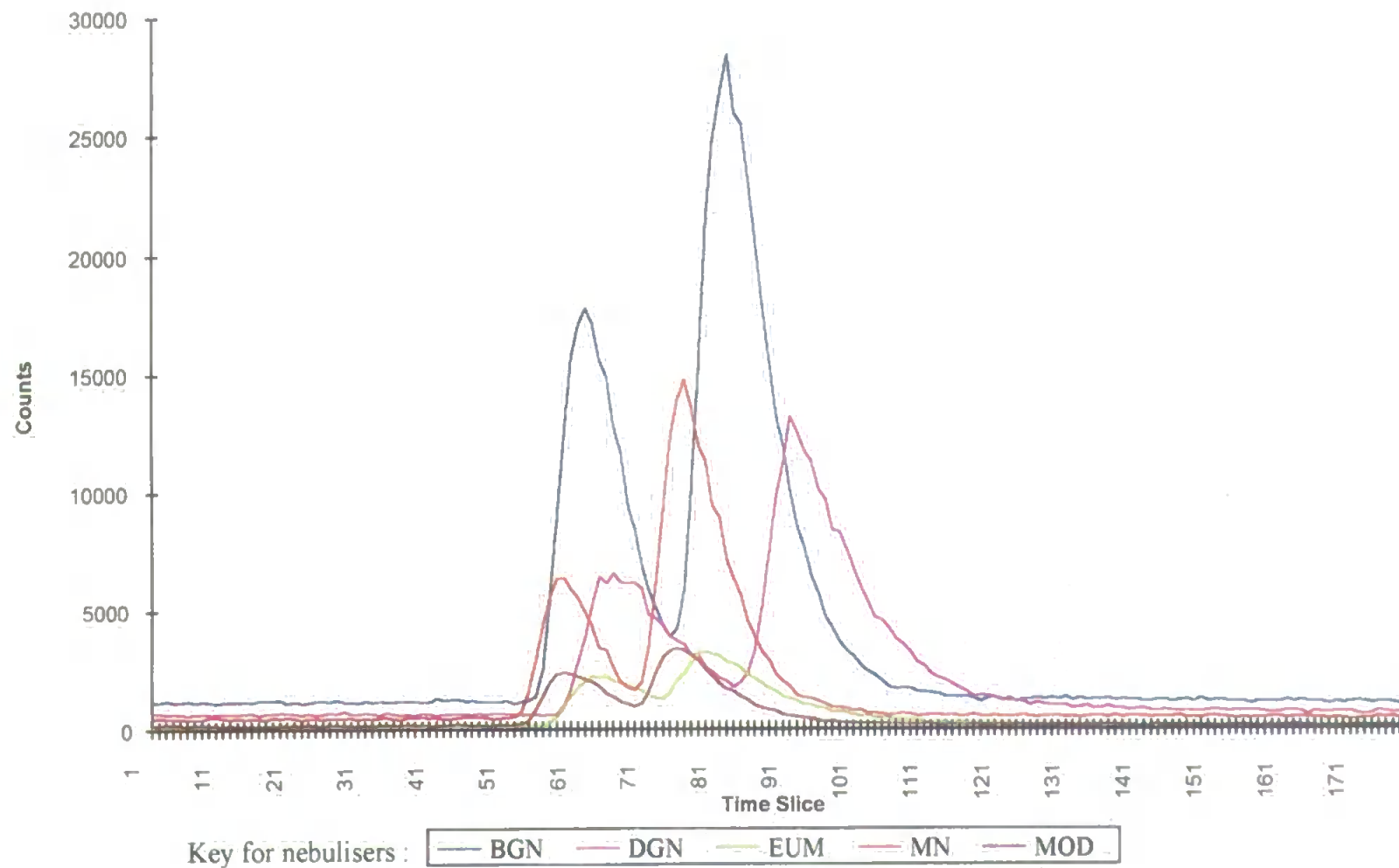


Figure 5.4 Chromatograms obtained for the separation of Sb species using the nebulisers shown in Figure 5.2

Table 5.3 Summary of signal-to-background ratios for the nebuliser study with a double-pass spray-chamber

Nebuliser	Peak height/bkg ratios		Peak area/bkg ratios	
	TMSb	[Sb(OH) ₆] ⁻	TMSb	[Sb(OH) ₆] ⁻
Modified V-groove	17.86	29.56	185.61	321.41
Concentric	14.14	29.42	90.51	311.23
Burgener	15.92	25.05	167.34	297.40
Unmodified V-groove	14.81	22.97	169.43	345.03
de Galan	9.30	17.03	122.26	249.76

Table 5.4 Extra-column volumes and changes in i.d. in the interface associated with each nebuliser

Nebuliser	Post-Column Volume (mm ³)	Post-Column Flow dimensions
Meinhard	85	0.18 mm to 2.5 mm(x15 mm) > ≈0.25 mm(40 mm)
Burgener	26	0.18 mm to 0.38 mm(x230 mm)
de Galan	38	0.18 mm(x85 mm) to 1 mm(x45 mm)
Unmodified V-Groove	78.55	0.18 mm to 1.59 mm(x25 mm)

The 0.18 mm tubing is the narrow-bore HPLC tubing connecting the column to each nebuliser. This was kept at a constant length for each nebuliser.

5.1.6.2 Comparison of spray-chambers

Figure 5.5 shows the chromatograms obtained when comparing the cyclonic with the double-pass spray-chamber, and Table 5.5 gives the key parameters for this comparison.

Table 5.5 Key results from the spray-chamber comparison using a Burgener nebuliser

Spray-chamber	SBR		Background & Stability (%rsd)	Rs	Elution Period (s)
	TMSb	[Sb(OH) ₆] ⁻			
Cyclonic	11.6	14.2	5317(4.2)	1.27	32.5
Double-pass	16.7	26.6	1121(3.6)	0.99	37.5

Under optimised conditions the cyclonic spray-chamber gave over 2×10^6 counts ppm⁻¹ ¹¹⁵In. This clearly indicates an improved transport of the analyte. The transport efficiency of both of these spray-chambers were reported as 8.0% and 2.5% for the cyclonic and double-pass respectively⁽¹⁷⁸⁾. Obviously, if the cyclonic spray chamber provides an improved sample transport then the increase in background is to be expected also. The overall signal-to-background ratios were worse for the cyclonic spray-chamber, however, the decreased residence time of the analytes in the spray-chamber compared to the double pass spray-chamber clearly played a significant role in the calculation of resolution.

5.1.6.3 Comparison of nebulisers with the cyclonic spray-chamber

Figure 5.6 demonstrates how the concentric and Burgener nebulisers compared with the cyclonic spray-chamber, using examples of the chromatograms acquired with each combination.

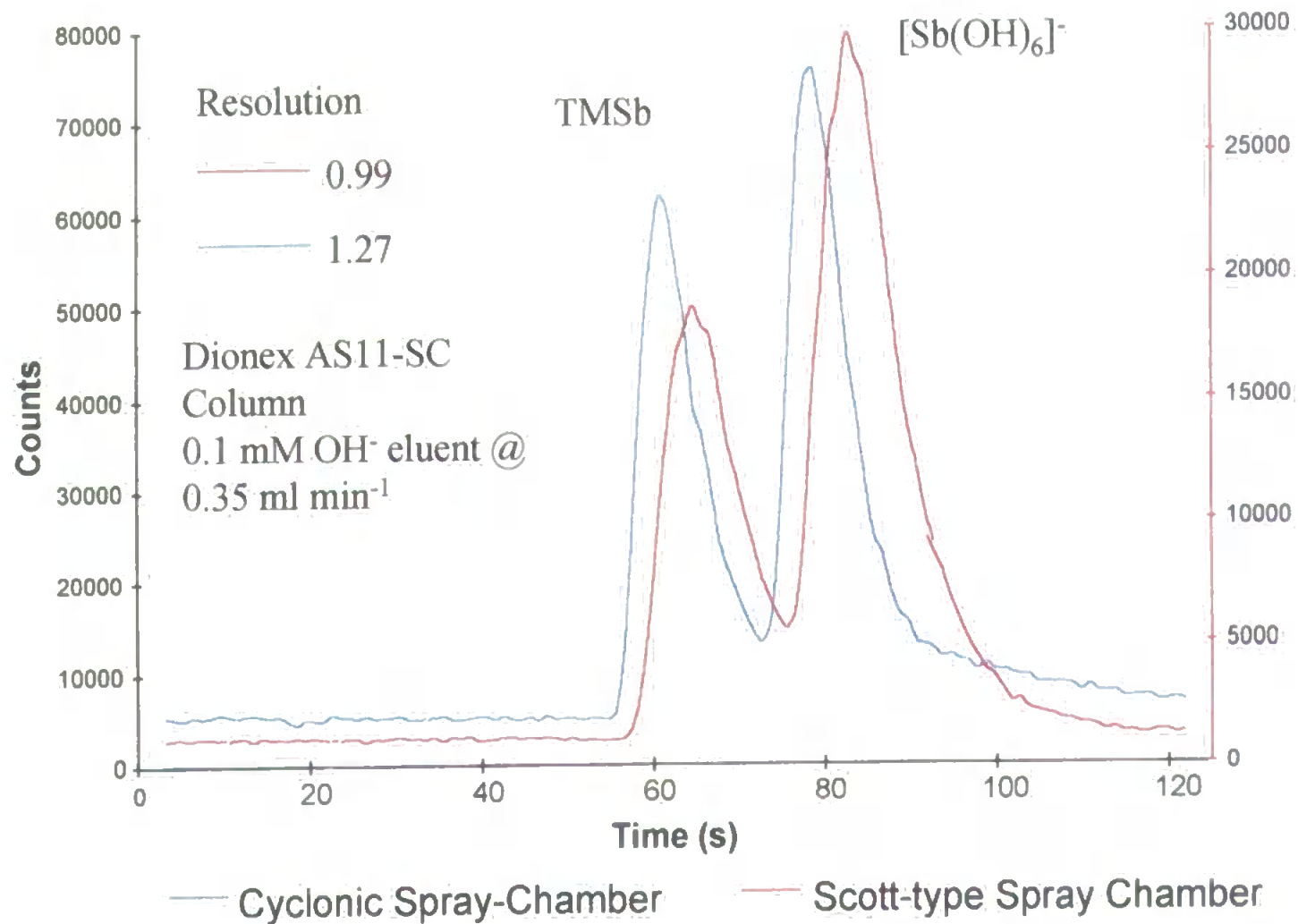


Figure 5.5 Chromatograms obtained for the separation of the Sb species using the cyclonic and double pass spray-chambers.

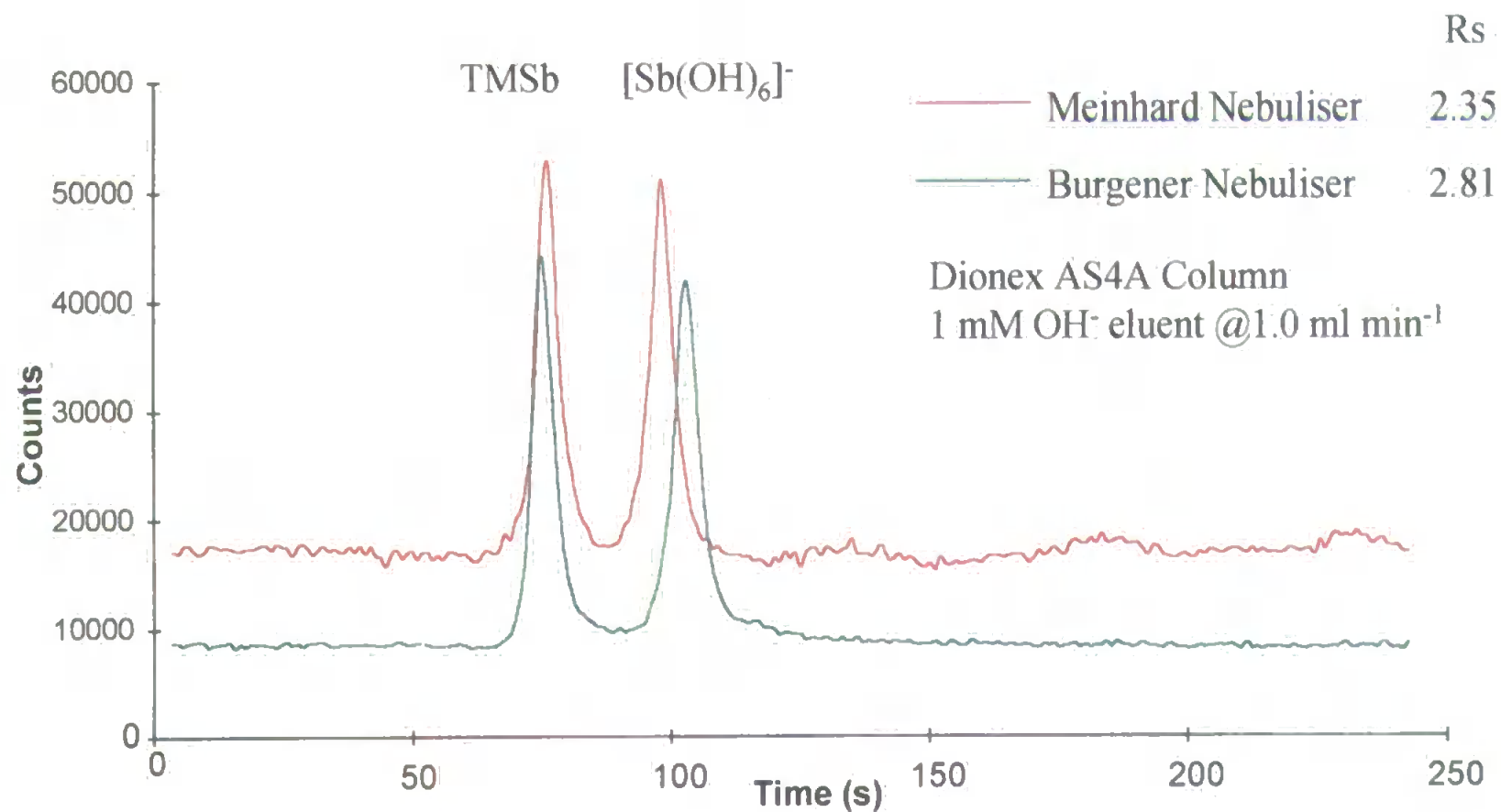


Figure 5.6 Chromatograms obtained for the separation of the Sb species using the cyclonic spray-chamber with the concentric glass and Burgener nebulisers.

5.1.7 Discussion

5.1.7.1 Nebuliser comparison with double-pass spray-chamber

The results from Table 5.1 indicate how much the difference in signal can vary between nebulisers run at the same nebuliser pressure. This is intuitive, however the difference between the 'best' and the 'worst' signals seem unlikely to be bridged by optimisation of the gas flow rates although this was not evaluated experimentally.

From the results in Tables 5.2 and 5.3, it can be seen that a combination of either the concentric nebuliser or the modified V-groove nebuliser with the double-pass spray-chamber offered the best options for HPLC coupling in terms of a compromise between resolution (R_s), SBR and ease of coupling. Even though the resolution was poorer for the modified nebuliser, the signal-to-background ratios for the modified nebuliser were much better than the other nebulisers overall, with no difference in the total elution time. The de Galan and the unmodified V-groove had the worst overall performance and longest elution periods. The retention times for the species when using the de Galan and the unmodified V-groove nebuliser were also considerably longer than the retention times when using the other nebulisers. If this data is used in conjunction with that of the post-column flow transitions from Table 5.4, it can be seen that the last section of pre-nebulisation flow in both of these nebulisers is in bores of i.d. much greater than for the other three nebulisers. This would seem to suggest that the V-groove poor R_s is due to this factor. The de Galan had a calculated R_s of 0.95 which was the second best of all of the nebulisers tested, but the SBR's were very poor. It is unclear why this should be so.

The use of a modified V-groove also has another advantage over the concentric nebuliser in that such a modification is a low cost option compared to purchasing a nebuliser specifically for HPLC use, i.e. one with a manufactured narrow-bore sample introduction geometry. Such nebulisers could also prove difficult to maintain if blocked through misuse. With a modified V-groove, if it blocks, the tube can be replaced easily. Also the concentric

glass nebuliser has a self-aspiration effect (venturi) which could slightly distort the characteristics of the separation, especially when using low-flow LC systems, i.e. where the volume pumped is less than the volume self-aspirated at a given nebuliser gas-flow.

5.1.7.2 Comparison of spray-chambers

Firstly, the results of the ^{115}In counts used to tune the ICP-MS is significant. The cyclonic spray-chamber used in this study demonstrated a 100% improvement in performance compared to that of the double-pass spray-chamber, although there was also an increased background level, (Table 5.5). The stability of the background signal was comparable to that of the double-pass spray-chamber and the resolution for the separation and the elution period were much improved when using the cyclonic spray-chamber. The internal volume of the cyclonic spray-chamber was much less than for the double-pass. This could explain the reduction in total elution time. However, the improvement in R_s might well be as a result of decreased residence-time (improved wash-out efficiency) of each peak volume in the chamber. This is more significant for the early eluting peak. The overall SBR's for the cyclonic spray-chamber were not as good as for the double-pass spray-chamber, although it may be further improved by optimisation of the nebuliser/aerosol production characteristics.

It is clear from these results that a greater proportion of the nebulised sample is reaching the plasma when using the cyclonic chamber.

5.1.7.3 Comparison of Burgener and concentric nebulisers with cyclonic spray-chamber

It was immediately obvious from these results that the background noise levels using the Burgener nebuliser were much lower than for the concentric nebuliser. This is completely opposite to that of the equivalent comparison for the two nebulisers with the double-pass spray-chamber. The SBR's for both Sb species are thus considerably better for the Burgener nebuliser compared to the concentric nebuliser.

When the Burgener nebuliser was used with a double-pass spray-chamber the overall SBR's were hampered by the background levels, but were not much inferior to those of the concentric nebuliser. Thus, the Burgener appears to be an excellent all round nebuliser for HPLC coupling.

There was also a noticeable improvement in Rs with the Burgener nebuliser. Although in the example shown in Section 5.1.6.3. Figure 5.6, resolution was not a problem this result was significant for the following reason.

If the optimum combination of nebuliser and spray-chamber are utilised with real samples, complex separations are more achievable and there is a reduced risk of 'losing' peaks through co-elution or poor resolution.

Indeed in the preceding Chapter the combination of Burgener nebuliser with the cyclonic spray-chamber was used for the plant and soil extract analysis by HPLC-ICP-MS. The plant extracts revealed a number of multiple peaks that may well have been unresolved if the assembly had not been optimised.

5.1.8 Conclusions

The effect of the nebuliser upon chromatographic resolution and signal-to-background ratios has been demonstrated. The de Galan and Ebdon type V-groove nebulisers have been shown to be the least suitable for HPLC coupling to ICP-MS in this study.

The concentric glass nebuliser (Meinhard type) has been shown to be an excellent nebuliser when used with the double-pass spray-chamber, offering good SBR's and resolution, but it suffers from high background levels when used with the cyclonic spray-chamber.

The modified V-groove nebuliser gave excellent SBR's when used with the double-pass spray-chamber, but poorer resolution than for both the concentric glass and Burgener nebulisers. However, this nebuliser was the one of choice when used with the double-pass spray-chamber as it was the most robust of all the nebulisers and the easiest to maintain.

The Burgener nebuliser was considered to be the best all round nebuliser within the confines of this study although an improvement to this design should be considered, see Future Work - Chapter 6.

The combination of the Burgener nebuliser with the cyclonic spray-chamber was seen as the optimum coupling for the purposes of HPLC-ICP-MS in this study of antimony species in environmental samples.

5.2 Investigation of Antimony in Organic Matrices

5.2.1 Introduction

In Chapter One a section is given over to discussion of the industrial applications of Sb as well as some of the methods utilised to analyse for Sb in a range of materials. However, two of the primary applications for Sb have been as flame retardents or as catalysts in polymer production.

It is as a flame retardent in mattress covers that Sb hit the headlines by being implicated as contributing to Sudden Infant Death Syndrome⁽⁷¹⁾. This was postulated as being due to microbial generation of the highly toxic gas stibine, SbH_3 . However, since this original paper in 1990 many studies have been carried out to simulate this fungal generation but none have been able to prove such a link between SIDS and Sb exists. It has however encouraged extensive interest in the element and particularly the biomethylation of Sb^(76,77,111). Khalturinskij and Tsirekidze⁽³⁶⁾ have reported that 'antimony trioxide (Sb_2O_3) is the most commonly used burning inhibitor' in polymeric materials, but it was in 1947 that Little⁽²²⁴⁾ proposed the inhibitory mechanism of polymer burning by Sb_2O_3 and halogen containing compounds. The authors of the former work also state that the experimental data available at that time did not allow final conclusions concerning the inhibition properties of antimony antipyrens. The only consistent feature is that the synergism between antimony and the halogen compounds in the polymer appears to be central to the inhibitory effects. However, Moy⁽³⁷⁾ confidently stated that the formation of SbCl_3 and oxychlorides render the combustible gases (evolved in degradation of the polymer) non-flammable.

As a catalyst in polymer production, Sb compounds have been used in the formation of lactic acid prepolymers⁽²²⁵⁾ and oxiranes^(35,226). But it is the use of Sb in the production of

polymers used in the food industry that has been of interest in this project. Antimony is, in some cases, used as a catalyst element in the production of polymers such as poly(ethylene terephthalate) or PET. The monomer has the formula $[-OCH_2CH_2OCO(p-C_6H_4)CO-]_n$. A polyester, PET is synthesised by polycondensation of ethylene glycol, $HOCH_2CH_2OH$, with either terephthalic acid, $HOOC(p-C_6H_4)COOH$ or dimethyl terephthalate, $CH_3OOC(p-C_6H_4)COOCH_3$. It was first discovered in 1941 and went into commercial production in 1953⁽²²⁷⁾. PET is an example of a melt-polymerised polyester. The following method was patented in 1946 and is an example of Sb_2O_3 catalysed polymerisation of PET^(34,228).

'In a polymer tube place 15.5 g (0.08M) dimethyl terephthalate, 11.8 g (0.19M) ethylene glycol, 0.025 g calcium acetate dihydrate and 0.006 g Sb_2O_3 . The mixture is melted at 197°C in a vapour bath and N_2 is introduced through the melt via a capillary. MeOH is distilled from the mixture over a 60 min period. The polymer tube is immersed as far as is practical in the vapour bath and left for a further 2 hours to remove the last traces of MeOH.

The tube is then heated for a further 20 minutes at 222°C (methyl salicylate) then transferred to another vapour bath at 283°C (dimethyl phthalate). After 10 mins the pressure is reduced to 0.3 mm or less over 15-20 mins.

Polymerisation is continued for 3 hours before the tube is allowed to cool under N_2 . Polymer yield is quantitative if no dimethyl terephthalate was distilled in the early stages'. (Method, Sorenson & Campbell⁽²²⁹⁾).

In this method the total PET could be 0.08 M or 15.360 g, added to which is 0.025 g calcium acetate dihydrate and 0.006 g Sb_2O_3 provided all the catalyst remnants are held in the polymer giving a total mass of 15.391 g. Of this total 0.005 g will be as Sb. This is the equivalent of 0.325 g kg^{-1} (325 ppm).

Two recent papers have also considered the possibility that during the polymerisation of PET the Sb(III) is reduced to elemental Sb^(164,230).

The applications of PET include fibres and thermoplastics for bottles. Because of this usage in drinks bottles the interest lies in whether Sb migrates from the polymer into

artificial food simulants such as water, 3% acetic acid and 15/95% ethanol. Any leachable, soluble Sb will enter the food chain.

This section presents results for samples of leachate solutions by the analytical methods developed and employed in this study. These samples were either provided by ICI or produced at the University of Plymouth.

5.2.2 Experimental

5.2.2.1 Instrumentation

The methodology applied to the analyses of these samples was the same as for the environmental samples referred to in Section 4.2.1. and 4.2.3.

5.2.2.2 Reagents

All reagents used were of analytical grade unless otherwise stated. For stock standard solutions refer to Section 4.2.2. 3% acetic acid was made up by diluting (with deionised H₂O) the appropriate volume of glacial acetic acid (BDH, Poole, Dorset, UK.).

5.2.2.3 Sample Preparation (University of Plymouth)

Approximately 2.5 g of PET (coke or sprite bottles) were weighed into round-bottom flasks, to which was added 40 mls of 3% acetic acid. The sample was then refluxed for 6 hrs. The solution was then decanted and allowed to cool. All other samples described in this Section were supplied by ICI Wilton.

5.2.3 Results

The development of the HPLC methodology using both a conductivity detector and ICP-AES was problematic because the sensitivity of these methods were not low enough to determine Sb in the samples provided (3 - 40 µg l⁻¹).

When the methodology was transferred to the ICP-MS, analysis of these samples was attempted.

Figure 5.7 a) shows the chromatogram obtained for the 15% ethanol blank sample provided by ICI. An OH^- mobile phase was used, i.e. the same mobile phase that separated the TMSb species from $[\text{Sb}(\text{OH})_6]^-$ in water samples. Figure 5.7 b) shows the chromatogram obtained for repeat injections of the 15% ethanol sample that contained approximately $20 \mu\text{g l}^{-1}$ Sb. The first injection was atypical but the second and third injections clearly indicate the presence of Sb. The retention time of this species suggested that it was in the form of Sb(V). The smaller peak in each case appears to be due to Sb carried in the solvent front.

Figure 5.8 a) and b) are chromatograms obtained from aliquots of 3% acetic acid blank and sample supplied by ICI. The sample was estimated to contain $40 \mu\text{g l}^{-1}$ Sb. With the exception of a very small peak on the solvent front there was no other observed peak. Elution conditions were as follows for both sample types : 0.1 mM OH^- eluent at 0.35 ml min^{-1} using an AS11 anion exchange column.

Figure 5.9 a) - d) give chromatograms for the same samples and blanks but using a 5 mM SO_4^{2-} mobile phase. The column used was again the AS11 and the mobile phase flow rate was 0.35 ml min^{-1} .

Figure 5.10 presents chromatograms for a) 3% acetic acid blank; b) 3% acetic acid sample ($40 \mu\text{g l}^{-1}$); and c) 3% acetic acid with $33 \mu\text{g l}^{-1}$ Sb(V). The double peak does not appear on the blank chromatogram, indicating a difference between the sample and the standard solutions, i.e. the possibility that there is more than one Sb species present in the 3% acetic acid ICI sample. This is, however, by no means certain.

In Figure 5.11 we can see the chromatogram for 95% ethanol blank provided by ICI. The signal may be due to a perturbation of the plasma or that the ethanol has mobilised some strongly retained Sb(III). The elution conditions used; $0.4 \text{ mM H}_2\text{SO}_4$ at 0.35 ml

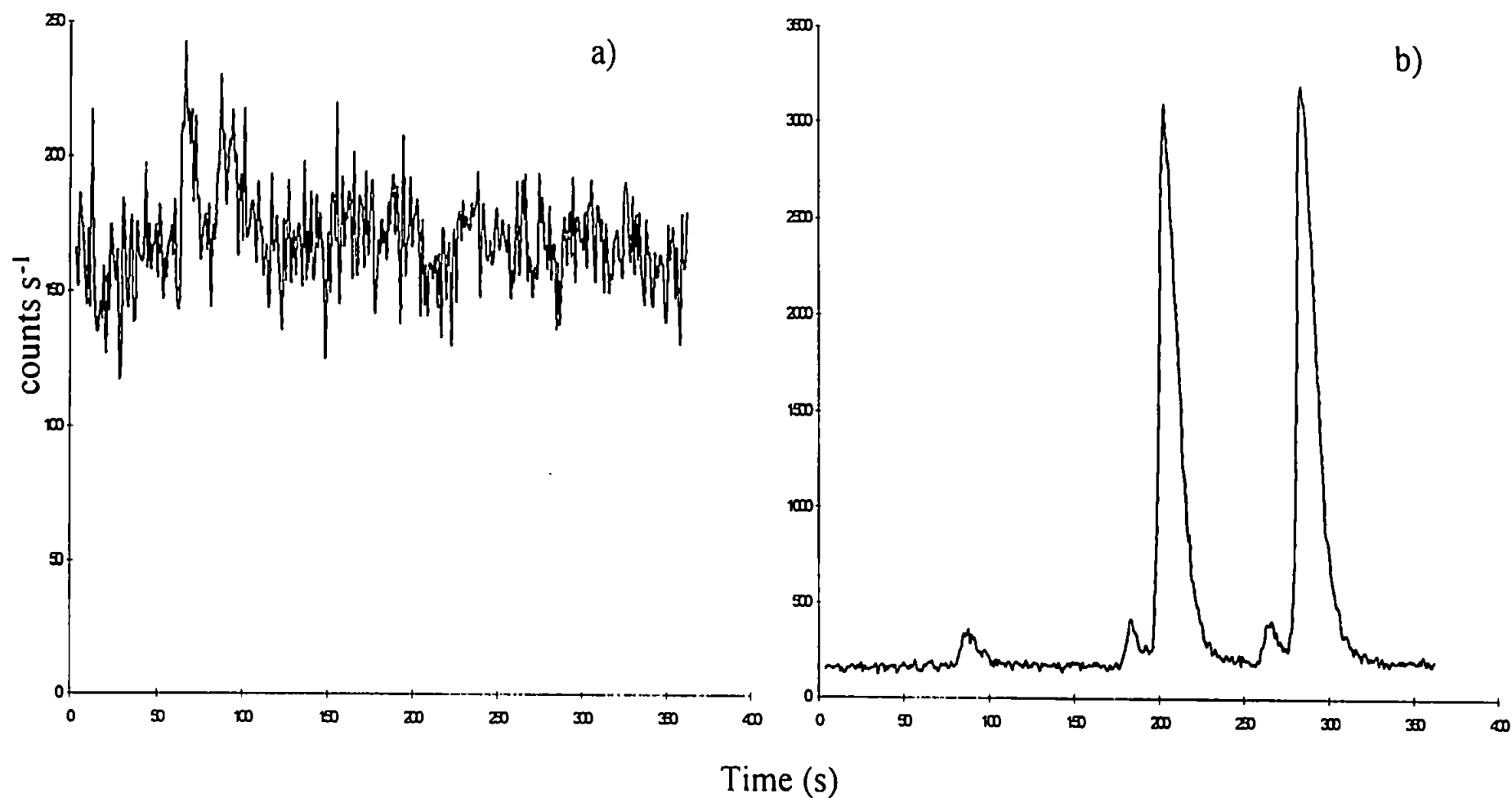


Figure 5.7 a) Chromatogram for 15% ethanol from ICI; and b) Chromatogram for repeat injections of 15% ethanol sample. 0.1 mM OH⁻ mobile phase at 0.35 ml min⁻¹. AS11 column. ICP-MS detection

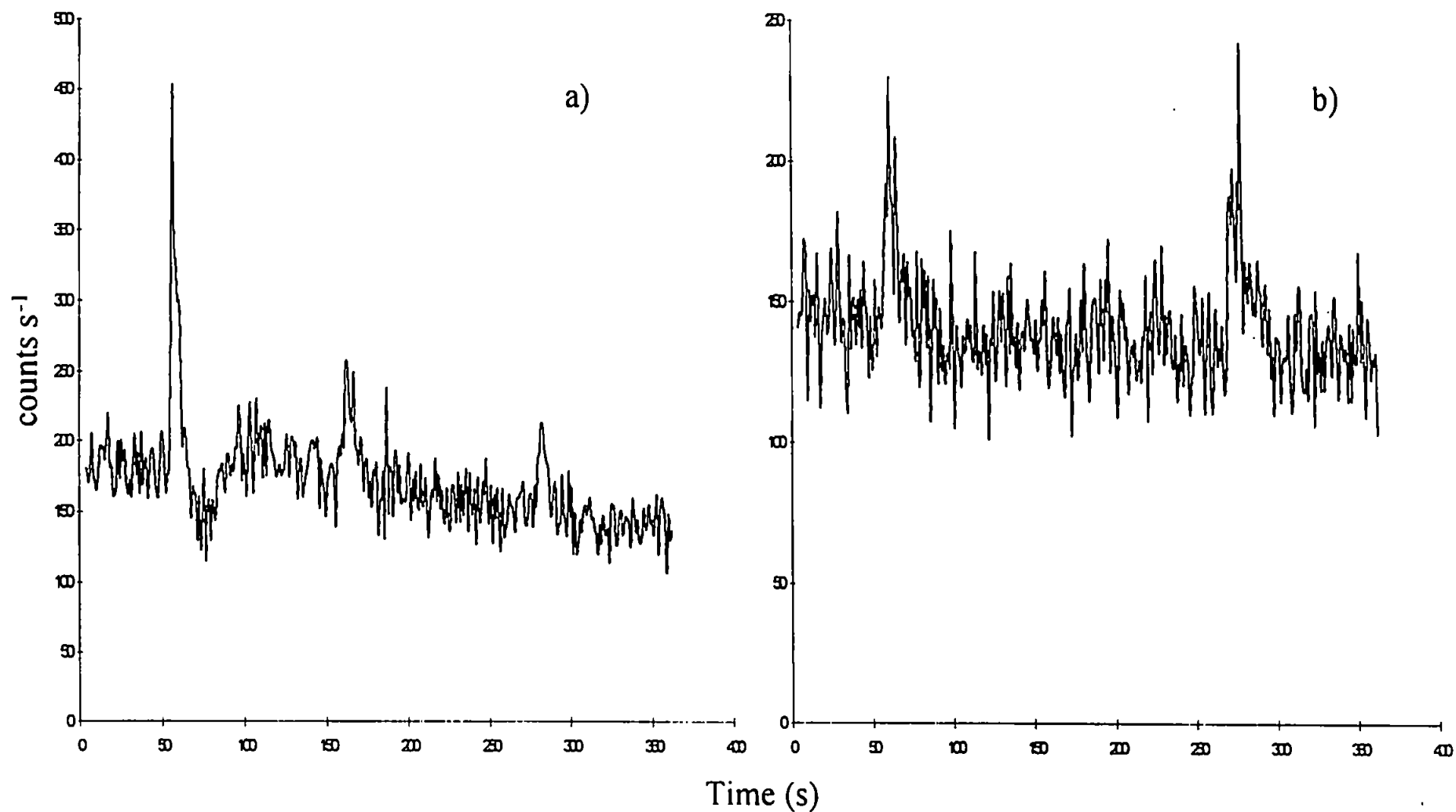


Figure 5.8 a) Chromatogram obtained for repeat injections of 3% acetic acid blank; and b) chromatogram for repeat injections of approx. $40 \mu\text{g l}^{-1}$ Sb in 3% acetic acid sample. (both samples obtained from ICI, Wilton)

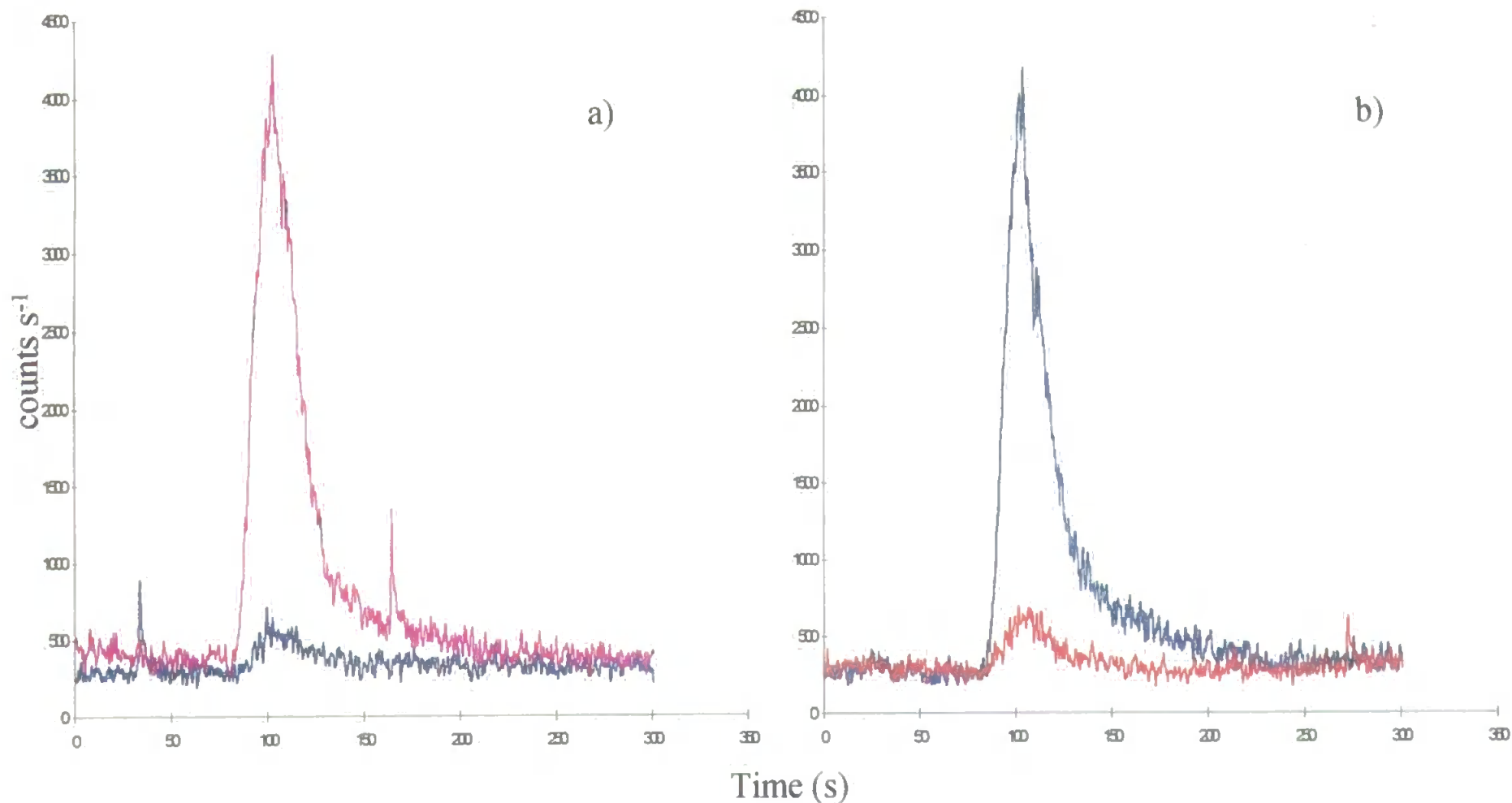


Figure 5.9 a) Chromatograms obtained from 3% acetic acid blank (blue line), and 3% acetic acid sample (purple line); and b) Chromatograms for 15% ethanol blank (red line), and 15% ethanol sample. 5 mM SO₄²⁻ mobile phase at 0.35 ml min⁻¹.

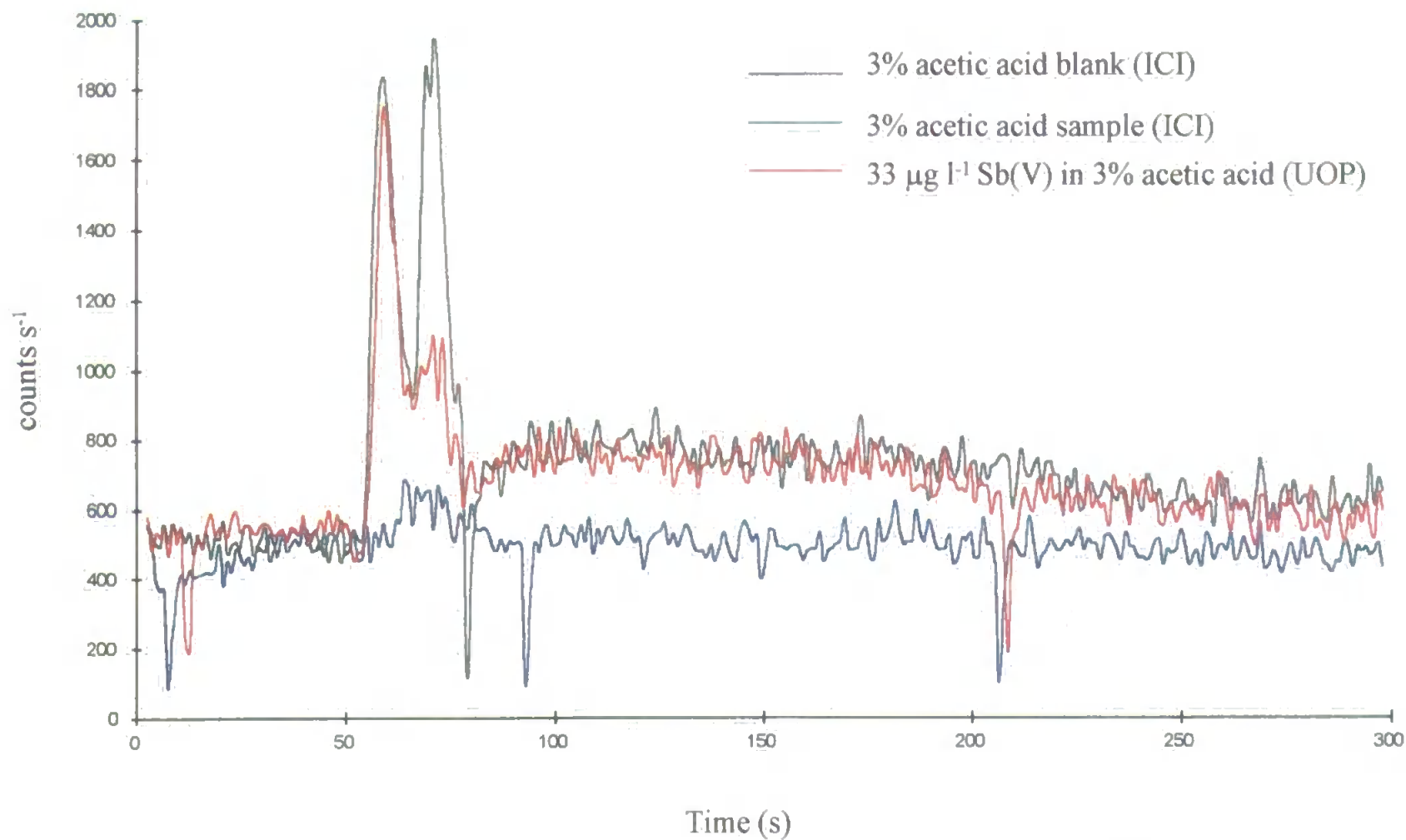


Figure 5.10 Chromatograms obtained for solutions of 3%acetic acid. 0.2 mM H_2SO_4 mobile phase at 0.35 ml min⁻¹.

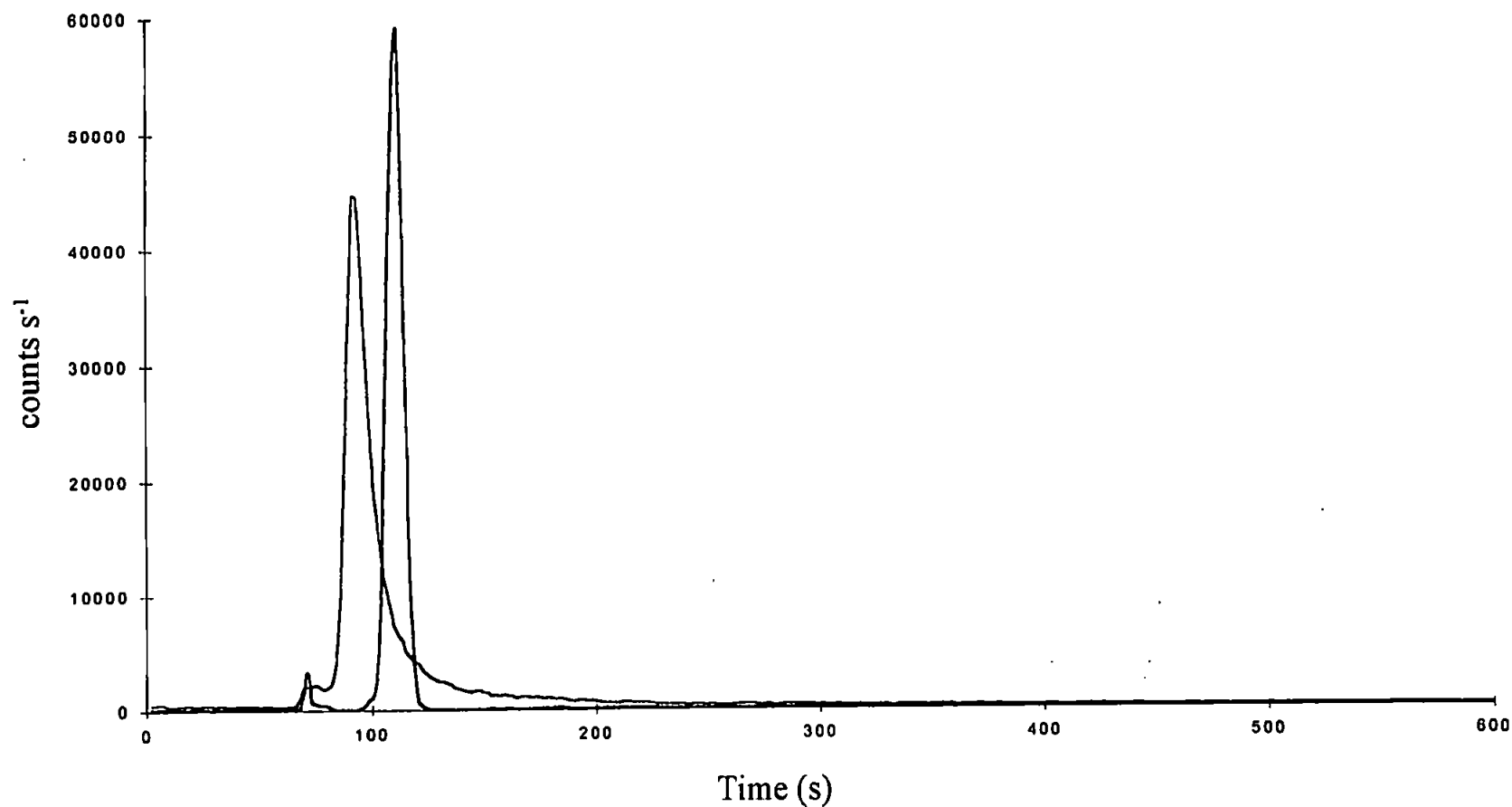


Figure 5.11. Chromatograms obtained for 15% ethanol and 95% ethanol samples from ICI. The 15% ethanol sample contains approximately $20 \mu\text{g l}^{-1}$ Sb. $0.4 \text{ mM H}_2\text{SO}_4$ mobile phase at 0.35 ml min^{-1} .

min⁻¹ using the AS11 column. Figure 5.12 presents chromatograms for the PET extracts (UOP) in 3% acetic acid using the same elution conditions as those in Figure 5.11. Figure 5.13 shows however that significant levels of Sb were in the extracts injected on column. This figure represents aliquots of 3% acetic acid, Sprite® PET extract and coke bottle PET extract continuously nebulised into the ICP-MS. This experiment suggests that over 10 µg l⁻¹ Sb were in the extracts, and the total Sb analysis by ICP-MS confirmed this. The coke bottle extract contained 16.40 ± 3.12 µg l⁻¹ and the Sprite® bottle extract contained 18.38 ± 3.49 µg l⁻¹ Sb. The ICI sample of 3% acetic acid estimated by ICI to contain approximately 2 µg l⁻¹ Sb was determined by this method to contain 2.04 ± 0.19 µg l⁻¹.

A subsequent analysis of the cola contained in a PET bottle and a cola can was carried out. The instrument calibration was established using aqueous standards of Sb. The liquid from each container was diluted by a factor of 2 with water and analysed. The analysis of spiked samples was also carried out. Table 5.6 summarises the results of this study.

Table 5.6 **Summary of analysis of cola samples from both a can and a PET bottle**

Sample	Concentration, µg l ⁻¹ .
Tin 1	3.51
Tin 2	1.31
Bottle 1	1.78
Bottle 2	0.90
Tin + 5 µg l ⁻¹ Sb	13.93

Following this analysis a standard addition method was carried out. This method showed that there was less than 1.5 µg l⁻¹ Sb in the coke sample allowing for the dilution factor.

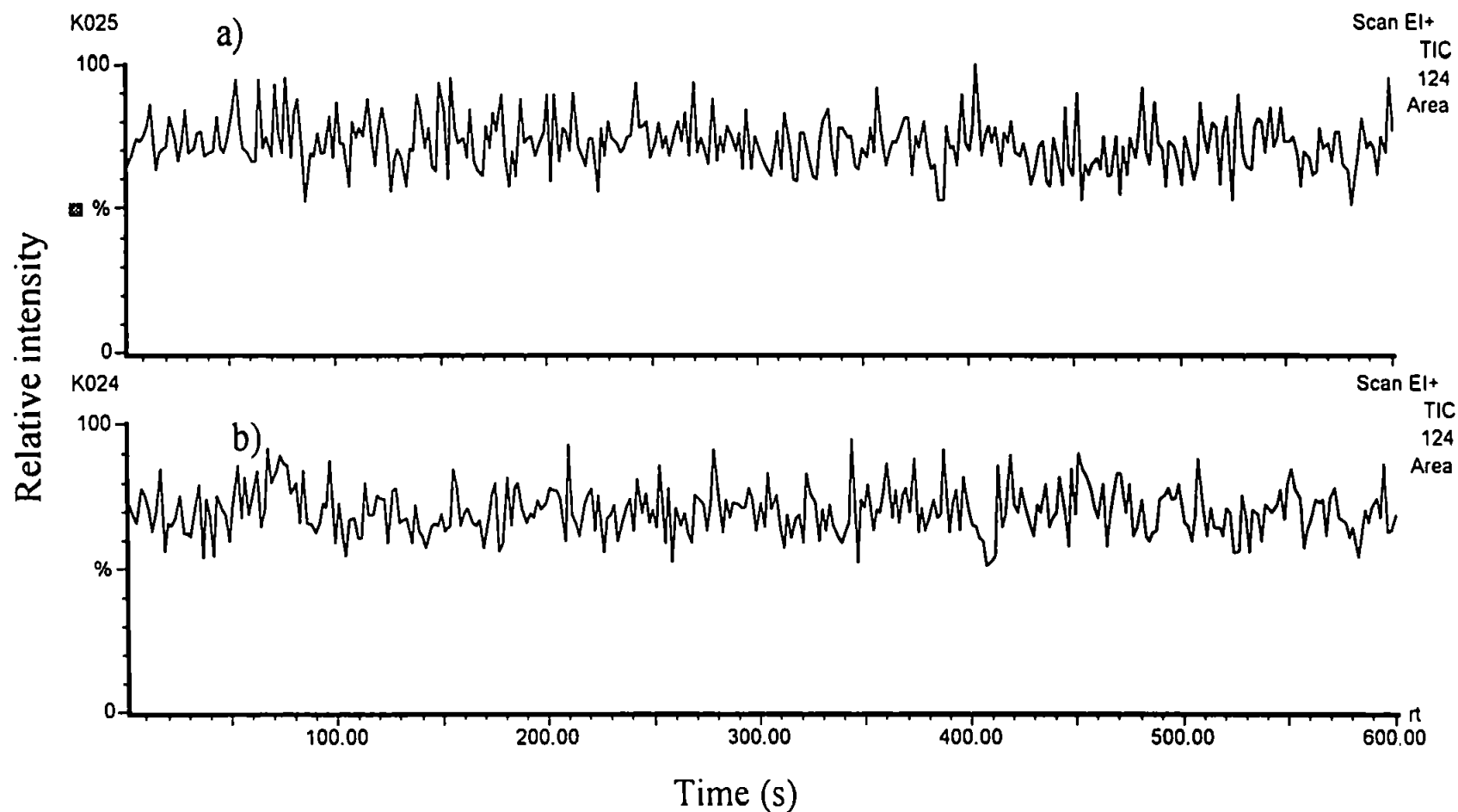


Figure 5.12. Chromatograms obtained for a) 3% acetic acid extract of poly(ethylene terephthalate), PET, from a coke bottle; and b) 3% acetic acid extract of PET from a sprite bottle. 0.4 mM H_2SO_4 mobile phase at 0.35 ml min^{-1} . AS11 column. ICP-MS detection.

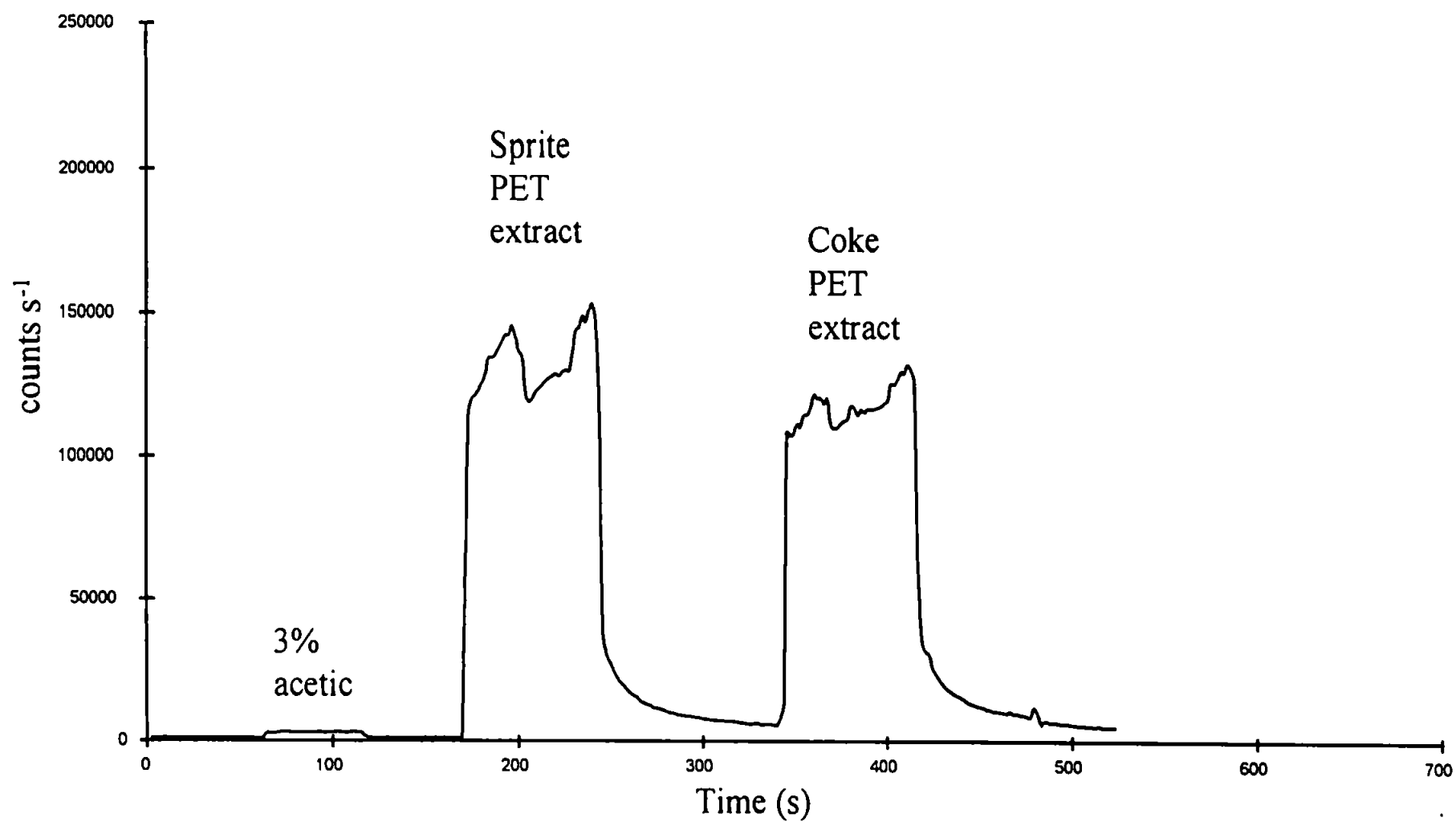


Figure 5.13. Aliquots of continuously nebulised solutions of 3% acetic acid, Sprite bottle and coke bottle extract. ICP-MS detection.

This was certainly considerably lower than the amount extracted by the 3% acetic acid reflux.

When the ICI samples were analysed by HG-ICP-AES under the acetic acid conditions described in Chapter 4, Section 4.3.2.2. the results showed that in all cases the citric acid addition had no effect upon the signal observed. Figure 5.14 a) - e) shows examples of this. This indicated that Sb was present in the sample but most likely not in an inorganic Sb(V) form.

5.2.4 Discussion

The results obtained from the ICI samples confirm the presence of Sb, but no separations were achieved except when the 3% acetic acid samples were analysed using the H_2SO_4 eluent. In this case a double peak was observed, when compared to an Sb(V) standard in 3% acetic acid there was an unidentified peak in the sample chromatogram.

However, when considering the details in the introduction regarding the use of Sb_2O_3 as the catalyst in the production of PET it seems likely that very little Sb would be seen by the HPLC methods used. The polymerisation process itself would not appear to provide conditions to produce Sb(V) species. In fact quite the contrary appears to be the case if the literature^(164,230) is to be believed. If the Sb(III) present is reduced to Sb^0 then this should be considered a greater cause for any concern as elemental Sb is considered more toxic than Sb(III).

As was observed in the HPLC results for Chapter 4, Sb(III) appears to be strongly retained on these columns. The discussion of this effect has been left until now to avoid repetition. In Chapter One a mention was made about Menshutkin Complexes. These complexes are formed between the lone pair on Sb(III) with the delocalised electrons on, for example, benzene rings. Although the following theory has yet to be tested, one very

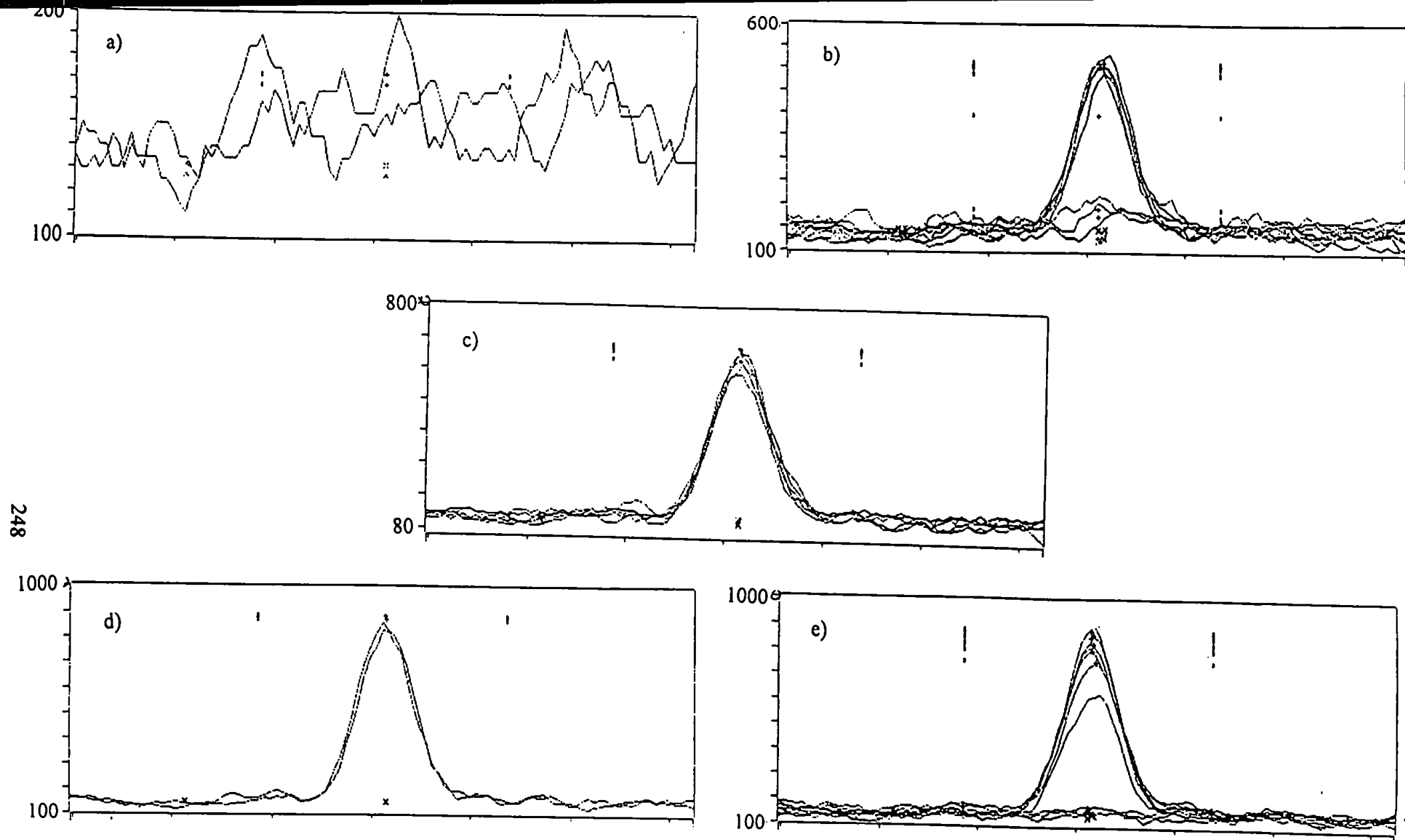


Figure 5.14. Wavelength scans 217.550 to 217.613 nm for a) 15% ethanol; b) approx. $20 \mu\text{g l}^{-1}$ Sb in 15% ethanol sample; c) as b) but with citric acid; d) approx. $40 \mu\text{g l}^{-1}$ Sb in 3% acetic acid sample; and e) as d) with citric acid. Analysis by HG-ICP-AES. 2 M acetic acid carrier, 1% NaBH_4 reductant.

possible reason for Sb(III) being strongly retained on the analytical column is by the interaction of the Sb(III) lone pairs with the divinylbenzene cross-linkage in the packing. The AS4A is only 4% cross-linked (although the backbone contains benzene rings) and Sb(V)/Sb(III) separations were possible. The AS11 column is 55% cross-linked. It is this cross-linkage difference that appears to provide the possible source of Menshutkin like interactions of Sb(III) with the column packing. One way to test this might be to remove the resin from the column and analyse it by x-ray microanalysis or electron microscope methods to see if the Sb present has been sorbed or formally bound to the resin surface. This would destroy the very expensive analytical column. Alternatively fresh packing material could be bought and a controlled experiment carried out with Sb(III) and Sb(V) to assess the uptake of each species and their removal by ion exchange mobile phases. The resin could be analysed again in similar ways as before to see if it really is forming a bond with the Sb(III). Alternative packing materials could be used and this type of column disregarded completely for future work in Sb analysis.

5.2.5 Conclusion

Antimony was observed in acetic acid and ethanol extracts of poly(ethylene terephthalate) by HPLC-ICP-MS, ICP-MS and HG-ICP-AES. Although not quantified, Sb(V) was believed to make up very little of the total Sb in acetic acid samples.

In the absence of a suitable HPLC method for the very low levels of Sb(III) likely to be seen in these samples, hydride generation is seen as the only analytical method that can currently be utilised for Sb speciation in these matrices. As with environmental samples HG results must always be considered against results of totals analysis by ICP-MS as there may be stable complexes of Sb formed that resist volatile hydride formation.

Chapter 6. Conclusions and Future Work

6.1 Conclusions

The literature review in Chapter One demonstrated that advances in the knowledge of antimony chemistry at trace levels were required to achieve improved chromatographic separations of antimony species. This improved knowledge and application to the speciation of Sb was demonstrated by the investigation of Sb, α -hydroxyacid complexes and their separation by ion exchange and reversed phase chromatography.

This particular study successfully utilised nuclear magnetic resonance (N.M.R.) to confirm the existence of a bond between the acids and Sb by analysing ^1H and ^{13}C spectra of the acid ligand in or not in the presence of antimony. The simultaneous determination of Sb and C by ICP-AES coupled to ion-exchange chromatography permitted the use of a 'mole ratio' method to calculate the stoichiometry of these complexes in terms of the metal:ligand (M:L) ratio. Electrospray ionisation mass spectrometry (ESI-MS) was used to try to determine these complexes. Major molecular ions that had been predicted by the mole-ratio method were determined by ESI-MS. The complexes were designated as:

- $\text{K}[\text{Sb}(\text{OH})_5(\text{citrate})]$;
- $\text{K}[\text{Sb}(\text{OH})_5(\text{OOCCH}_2\text{CH}(\text{OH})\text{COOH})]$, $\text{K}[\text{Sb}(\text{OH})_5(\text{OOCCH}(\text{OH})\text{CH}_2\text{COOH})]$;
- $\text{K}[\text{Sb}(\text{OH})_5(\text{mandelate})]$; and
- $\text{K}[\text{Sb}(\text{OH})_4(\text{mandelate})_2]$.

The HPLC methodology applied to the separation of these complexes was also applied to the determination of Sb in environmental samples (minewaters). The only determined

species was Sb(V) in the form $[\text{Sb}(\text{OH})_6]^-$. This was tested by reaction with citric acid and analysis by HPLC. The sample Sb was found to elute identically to that of the synthetic Sb(V) standard. This indicated the reaction should be identical. The investigation of the Sb, α -hydroxyacid complexes also led to development of a mixed-mode chromatographic method of separation of these compounds utilising a weak sulphuric acid eluent.

Aqueous separations of Sb(V) and Sb(III) were achieved with a range of ion-exchange elution protocols. The separation of $[\text{Sb}(\text{OH})_6]^-$ from antimony trihalides and antimonyl(III) tartrate was achieved using a phthalic acid eluent. Separations of $[\text{Sb}(\text{OH})_6]^-$ and trimethyl antimony were carried out utilising Cl^- , NO_3^- , SO_4^{2-} and OH^- mobile phases. The separation with the hydroxide mobile phase provided the most sensitive determination of both of these species at 8.51 and 4.43 pg on column for $[\text{Sb}(\text{OH})_6]^-$ and TMSb respectively. Application of this method to environmental analysis showed only $[\text{Sb}(\text{OH})_6]^-$ to be present in the samples.

Hydride generation ICP-AES determination of Sb(V) and Sb(III) confirmed this finding for the water samples. The use of hydride generation in ICP-AES determinations of Sb improved the detection limits for this instrument by a factor of 24. The findings of Apte and Howard⁽¹⁴³⁾ and Mohammad *et al.*⁽¹⁴⁴⁾ were confirmed in as much that citric acid addition to Sb(V) would suppress hydride generation of this species. The TMSb species would not form a hydride under mineral acid (3M HCl) carrier conditions but would when acetic acid (0.2 M) was used as the sample carrier.

The determinations by HPLC-ICP-MS and HG-ICP-AES showed acceptable recoveries compared with total Sb determinations by ICP-MS.

Mixed-mode (ion-suppression & ion exchange) chromatography was successfully applied to the separation of the Sb, α -hydroxyacids to assess whether the organic functionality of the complexes could be used to affect the separation. The methodology was then applied to water soluble sediment extracts and acetic acid (0.2 M) extracts of sediments and plant homogenates.

These samples showed that there were several peaks that demonstrated multiple antimony species, although none corresponded to standard peaks. Closer analysis of moss homogenates by spiking of samples with Sb(V) showed that in one sample only one of the retained peaks responded to spiking, whereas in the other moss sample from a different sampling site would show increases in all peaks. This result suggested that in all likelihood the Sb(V) was being taken up by dissolved agents that complexed with the Sb(V). In the sediment samples, the most likely candidate for complexing would be humic acid. In the plants it is very unclear as to what could be present in one plant of the same species but not the other. However, the input of Sb into the system for metabolism by the plants must be different to provide such striking differences in the chromatograms. What has been observed, however, appears to be as a result of Sb chemistry not yet seen in analysis of environmental Sb. The analysis of these samples by HPLC-HG-ICP-MS showed that not all of the peaks observed by HPLC-ICP-MS were due to Sb in a reducible form. This result suggests that these non-reducible species may well exist as stable organoantimony species analogous to the Sb, α -hydroxyacid complexes. Therefore, analysis of environmental samples for the determination of Sb can be facilitated by mixed-mode HPLC coupled to ICP-MS. However, the requirement for a more detailed investigation of the matrices and potential chelating species is obvious for quantification of Sb in addition to total determinations.

The investigation of the nebuliser/spray-chamber assembly has shown that both of these parts of the sample introduction system contributed to post-column dispersion. These contributions affected adversely the resolution of the model separation used to investigate and optimise the instrumental arrangement. When using a double-pass spray-chamber the nebulisers of choice were the concentric glass or the Ebdon-type V-groove modified with HPLC tubing connected directly to the HPLC column outlet. For the dimple modified cyclonic spray-chamber the Burgener nebuliser was deemed to be the best of those tested.

The significance of this optimisation was most obviously demonstrated by the analysis of the moss homogenate extract from the spoil heap where it is thought that at least one of the peaks would have been lost through co-elution.

Antimony was observed in acetic acid and ethanol extracts of poly(ethylene terephthalate) by HPLC-ICP-MS, ICP-MS and HG-ICP-AES.

However, hydride generation is seen as the only analytical method that can currently be utilised for Sb speciation in these matrices. As with environmental samples HG results must always be considered against results of totals analysis by ICP-MS as there may be stable complexes of Sb formed that resist volatile hydride formation.

The reason that HG was seen as the only analytical method for these types of samples lies with the observations relating to Sb(III) determinations by HPLC. These observations have been discussed in greater detail in Chapter 5 but the concluding remarks on this subject are that in the opinion of the author Sb(III) compounds have a large potential for more complex interactions with the organic backbone of the column packing via the stereochemically active lone pair of Sb(III). The scope for the interaction of the lone pair with aromatic rings is also demonstrated in the literature review, Chapter 1.

The primary aim of this study was to investigate chromatographic methods of antimony speciation with plasma spectroscopic detection. It is felt that this has been achieved in great measure. The study has been carried out without bias from previous studies on Sb and As speciation other than to critically assess previous methods prior to development of new methodology.

Therefore the aims and objectives as laid out in Chapter 1 have been achieved and have been added to by the analysis of plant extracts and the apparent discovery of chemical complexing of Sb analogous to that of the Sb, α -hydroxyacid complexes.

6.2 Future Work

6.2.1 HPLC Separations of Antimony Species

Although the use of a sulphuric acid eluent with the AS11 column facilitated the most interesting separation of Sb species in the environmental samples a great deal of work is required in this area.

1. The significant levels of unretained Sb in the peak fronts of many of the chromatograms indicate the requirement for more specialised columns designed for reversed-phase chromatography.
2. The use of more specialised columns will have to be coupled with continued modification of mobile phases. The sulphuric acid mobile phase has most application in the separation of organic acids, therefore the requirement for more suitable mobile phases for other organic functionalities not affected by this mobile phase is obvious.
3. This development for environmental and industrial analysis has to be coupled with increased experimentation in trace Sb chemistry. Therefore future work has to include complex determinations and studies as to what will complex with Sb in the matrices of interest. This means that investigations such as the study of the interaction of Sb with

humic and fulvic materials should commence. Another consideration might be the use of citric or tartaric acid as extractants for the polymer samples.

4. The need for a programme concentrating upon the development of suitable reference materials is the last and one of the most important aspects in the future work of Sb speciation by HPLC methodology

6.2.2 HPLC coupled to ICP-MS

The evidence presented in this study relating to the effects of the nebuliser/spray-chamber upon chromatographic performance shows that the need for an integrated study of the performance of the sample introduction system in low-flow systems, such as those of HPLC, is clear.

1. The design of the spray-chamber could be investigated such as the most efficient design for sample transport without the concomitant increases in noise characteristics.
2. Nebuliser design appears to be the most critical feature of the assembly in terms of the post-column dispersion effects. Therefore, a more detailed characterisation of nebuliser performance is required with respect to use with HPLC, namely an expansion of this study by investigating more nebulisers with the cyclonic spray-chamber. This might be further expanded to even include the investigation of nebulisers that completely by-pass the requirement for spray-chambers, i.e. direct injection nebulisers.

6.2.3 Sb, α -hydroxyacid Complexes

These complexes and analogous organic ligand groups need further investigation relating to the structure of these complexes.

1. There is a requirement to obtain a solid or a technique that facilitates definitive structure derivation for the Sb, α -hydroxyacid complexes.
2. Chemical parameters need to be established such as stability constants and ionic character. This type of information will benefit work relating to formation of Sb complexes with organic acids in the natural environment and what is thermodynamically preferred.

It is believed that this work opened the way to improving the chromatographic development for environmental analysis and demonstrated that new chemistries for Sb in the environment could be observed.

Therefore the future work must include a concerted effort in Sb co-ordination chemistry for Sb(V) and Sb(III) species in order to determine the biogeochemical pathways for Sb in soils and plants which is the ultimate test for workers in the study of Sb speciation.

References

1. Greenwood, N.N., and Earnshaw, A., from 'Chemistry of the Elements', 1984, Pergamon, Oxford
2. Cotton, F.A., and Wilkinson, G., from 'Advanced Inorganic Chemistry', 1988, 5th Ed., Wiley, New York
3. From 'Inorganic Chemistry: Series Two', Vol. Two, 1975, H.J. Emelius Consultant Editor, D.B. Sowerby Volume Editor, Butterworths, London. pp. 221-267
4. From 'Inorganic Chemistry: Series Two', Vol. Four, 1972, H.J. Emelius Consultant Editor, B.J. Aylett Volume Editor, Butterworths, London. pp.355-412
5. Lee, J.D., from 'Concise Inorganic Chemistry', 1991, 4th Ed., Chapman & Hall, London
6. Claire, P.P.K., Willey, G.R., Drew, M.G.B., *J. Chem. Soc. Dalton Trans.*, 1987, 263-265
7. Willey, G.R., Asab, A., Lakin, M.T., Alcock, N.W., *J. Chem. Soc. Dalton Trans.*, 1993, 365-370
8. Bricklebank, N., Godfrey, S.M., Lane, H.P., McAuliffe, C.A., Pritchard, R.G., *J. Chem. Soc. Dalton Trans.*, 1994, 1759-1763
9. Millington, P.L., Sowerby, D.B., *J. Organometallic Chemistry*, 1994, **480**, 227-234
10. Legoupy, S., Lassalle, L., Guillemin, J-C., Métail, V., Senio, A., Pfister-Guillouzo, G., *Inorg. Chem.*, 1995, **34**, 1466-1471
11. Knör, G., *Inorg. Chem.*, 1996, **35**, 7916-7918
12. Singh, R.P., Pandey, A.K., *Synth. React. Inorg. Met-Org. Chem.*, 1992, **22**, 1031-1039
13. Jagannath Rao, R., Prasad Rao, K., Singh, M.S., *Nat. Acad. Sci. Letters*, 1996, **19**, 193-196
14. Rastogi, M.K., *Asian J. of Chemistry*, 1997, **9**, 5-9
15. Gibbons, M.N., Sowerby, D.B., Silvestru, C., Haiduc, I., *Polyhedron*, 1996, **15**, 4573-4578
16. Wegener, J., Kirschbaum, K., Giolando, D.M., *J. Chem. Soc. Dalton Trans.*, 1994, 1213-1218

17. Said, M.A., Kumara-Swamy, K.C., Babu, K., Aparna, K., Nathaji, M., *J. Chem. Soc. Dalton Trans.*, 1995, 2151-2157
18. Clegg, W., Elsegood, M.R.J., Farrugia, L.J., Lawlor, F.J., Norman, N.C., Scott, A.J., *J. Chem. Soc. Dalton Trans.*, 1995, 2129-2135
19. Silvestru, C., Silvestru, A., Haiduc, I., Sowerby, D.B., Ebert, K.H., Brenning, H.J., *Polyhedron*, 1997, **16**, 2643-2649
20. Silvestru, C., Socaciu, C., Bara, A., Haiduc, I., *Anticancer Research*, 1990, **10**, 803-804
21. Kondyurin, A., *J. Phys. Chem.*, 1992, **96**, 11038-11042
22. Kondyurin, A., Mikov, S.N., Kozulin, A.T., *J. Raman Spectroscopy*, 1991, **22**, 249-252
23. Sharutin, V.V., Sharutina, O.K., Pakusina, A.P., Belsky, V.K., *J. Organometallic Chem.*, 1997, **536-537**, 87-92
24. Hartley, D.W., Smith, G., Sagatys, D.S., Kennard, C.H.L., *J. Chem. Soc. Dalton Trans.*, 1991, 2735-2739
25. Smith, G., Sagatys, D.S., Bott, R.C., Lynch, D.E., Kennard, C.H.L., *Polyhedron*, 1992, **11**, 631-634
26. Smith, G., Sagatys, D.S., Bott, R.C., Lynch, D.E., Kennard, C.H.L., *Polyhedron*, 1993, **12**, 1491-1497
27. Smith, G., Kennard, C.H.L., *Main Group Chemistry*, 1996, **1**, 175-177
28. Bencze, H., from 'Handbook on Metal in Clinical and Analytical Chemistry', 1994, Eds. Seiler, H.G., Sigel, A., & Sigel, H., Marcel Dekker, New York, pp 227-236
29. Al-Kaff, A., Al-Rajhi, A., Tabbara, K., El-Yazigi, A., *Annals of Saudi Medicine*, 1993, **13**, 1, 26-30
30. Al-Hazzaa, S.A.F. Krahn, P.M., *International Ophthalmology*, 1995, **19**, 83-88
31. Maeda, S., from 'The Chemistry of Organic Arsenic, Antimony and Bismuth Compounds', 1994, Ed. Patai, S., John Wiley, pp 725-755
32. Berman, E., from 'Toxic Elements and their Analysis', 1980, Heyden International Topics in Science, Heyden, London, pp 19-24
33. Brazeau, J., Wong, R.K., *J. Forensic Sciences*, 1997, **42**, 3, 424-428
34. Whinfield, J.R., Dickson, J.T., British Patent, 578079, June 1946
35. Nomura, R., Wada, Y., Matsuda, H., *J. Polymer Science: Part A, Polymer Chemistry*, 1988, **26**, 627-636

36. Khalturinskij, N.A., Tsirekidze, O.N., *Intern. J. Polymeric Mater.*, 1993, **20**, 75-90
37. Moy, P.Y., *Plastics Engineering*, 1997, **53**, 61-63
38. Jha, N.K., Misra, A.C., Bajaj, P., *Polymer Engineering and Science*, 1986, **26**, 332-336
39. Jha, N.K., Bajaj, P., Misra, A.C., Maurya, P.L., *J. Applied Polymer Science*, 1986, **32**, 4393-4403
40. Bajaj, P., Jha, N.K., Maurya, P.L., Misra, A.C., *J. Applied Polymer Science*, 1987, **344**, 1785-1801
41. Mark, H.F., Bibales, N., Overberger, G.C., and Menges, G., (Eds.), *Encyclopedia of Polymer Sci. and Eng.*, 1987, 2nd Ed., Vol. 10, Interscience, p 541.
42. Carraher Jr., C.E., Blaxall, H.S., *Angew. Makromol. Chem.*, 1979, **83**, 37
43. Cámara, C., de la Calle-Gutiñas, M.B., from 'Encyclopedia of Analytical Science', 1995, Academic Press Ltd., London, pp. 136-144
44. Elridy, M., Akbarieh, M., Kassem, M., Sharkawi, M., Tawashi, R., *International J. of Pharmaceutics*, 1989, **56**, 23-27
45. Elnahas, S., Temtamy, S.A., Dehondt, H.A., *Environmental Mutagenesis*, 1982, **4**, 83-91
46. Berger, B.J., Fairlamb, A.H., *Parasitology*, 1992, **105**, S71-S78
47. Jennings, F.W., *Tropical Medicine & Parasitology*, 1991, **42**, 135-138
48. Karak, N., Maiti, S., *J. Polymer Materials*, 1996, **13**, 179-190
49. Rosenbaum, W., Dormont, D., Spire, B., Vilmer, E., Gentilini, M., Griscelli, C., Montagnier, L., Barre-Sinoussi, F., Chermann, J., *Lancet*, 1985, **i**, 450
50. Paltrick, R.A.D., and Polya, D.A., (Eds.), from 'Mineralization in the British Isles', 1993, Chapman & Hall, London
51. Collins, J.H., from 'Observations on the West of England Mining Region', 1912, W. Brendon & Son Ltd., Plymouth, England
52. Dines, H.G., from 'The Metalliferous Mining Region of South West England', 1956, Vol. II, HMSO, England
53. Toll, R.W., and Barclay, C.F., 'A Report on Wheal Emily Antimony Mine, Knighton', 1922, Unknown Source
54. Leake, R.C., Brown, M.J., Smith, K., Rollin, K.E., Kimbell, G.S., Cameron, D.G., Roberts, P.O., Beddoe-Stephens, B.W., Mineral Reconnaissance Programme Report No. 79, British Geological Survey, NERC, 1985, Keyworth, Nottingham.

55. Elinder, C.G., and Friberg, L., from 'Handbook on the Toxicology of Metals', Friberg, L., Nordberg, G.F. & Vouk, V.B., eds., Elsevier, Amsterdam, 1979, 283-292
56. Gebel, T., *Chemico-Biological Interactions*, 1997, **107**, 131-144
57. Gerhardson, L., Brune, D., Nordberg, G.F., Wester, P.O., *J. Work Environ. Health*, 1982, **8**, 201-208
58. Groth, D.H., Stettler, L.E., Burg, J.R., Busey, W.M., Grant, G.C., Wong, L., *J. Toxicol. Environ. Health*, 1986, **18**, 607-626
59. Léonard, A., Gerber, G.B., *Mutation Research*, 1996, **366**, 1-8
60. Hayes, R.B., *Cancer Causes & Control*, 1997, **8**, 371-385
61. Brookins, D.G., Eh-pH Diagrams for Geochemistry, 1988, Springer, Berlin
62. Gregus, Z., Gyurasics, A., Koszorus, L., *Environmental Toxicology & Pharmacology*, 1998, **5**, 89-99
63. Kentner, M., Leinemann, M., Schaller, K-H., Weltle, D., Lehnert, G., *Int. Arch. Occup. Environ. Health*, 1995, **67**, 119-123
64. 'Antimony and its compounds: Health Hazards & Precautionary Measures', EH19 (Revised), 1996, HSE Books, Sudbury, U.K.
65. Breiger, H., Semisch, C.W., Stasney, J., Piatek, D.A., *Ind. Med. Surg.*, 1954, **23**, 521-523
66. Sundar, S., Sinha, P.R., Agrawal, N.K., Srivastava, R., Rainey, P.M., Berman, J.D., Murray, H.W., Singh, V.P., *American Journal of Tropical Medicine & Hygiene*, 1998, **59**, 139-143
67. Herwaldt, B.L., Kaye, E.T., Lepore, T.J., Berman, J.D., Baden, H.P., *J. of Infectious Diseases*, 1992, **165**, 968-971
68. Winship, K.A., *Adverse Drug Reactions & Toxicological Reviews*, 1987, **6**, 67-90
69. Council of European Communities, (1980), Council Directive Relating to the Quality of Water Intended for Human Consumption (80/778/EEC)
70. Threshold Limit Values & Biological Exposure Indices for 1989-1990, American Conference of Governmental Industrial Hygienists, Cincinnati, Ohio.
71. Richardson, B.A., *Lancet*, 1990,
72. Parris, G.E., Brinckman, F.E., *Environ. Sci. Technol.*, 1976, **10**, 1128-1134
73. Osaka, M., Machida, N., Tanaka, M., *Waste Management*, 1996, **16**, 519-526
74. Van der Hoek, E.F., van Elteren, J.T., Comans, R.N.J., *Intern. J. Environ. Anal. Chem.*, 1996, **63**, 67-79

75. Maeda, S., Fukuyama, H., Yokoyama, E., Kuroiwa, T., Ohki, A., Naka, K., *Applied Organometallic Chemistry*, 1997, **11**, 393-396
76. Gürleyük, H., van Fleet-Stalder, V., Chasteen, T.G., *Appl. Organometallic Chemistry*, 1997, **11**, 471-483
77. Jenkins, R.O., Craig, P.J., Goessler, W., Miller, D., Ostah, N., Irgolic, K.J., *Environ. Sci. Technol.*, 1998, **32**, 882-885
78. Dodd, M., Pergantis, S.A., Cullen, W.R., Li, H., Eigendorf, G.K., Reimer, K.J., *Analyst*, 1996, **121**, 223-228
79. Singh, I., Saini, R.K., *Indian J. of Chemistry*, 1995, **34A**, 666-667
80. Lacy, N., Christian, G.D., Ruzicka, J., *Anal. Chim. Acta*, 1989, **224**, 373-381
81. Raychaudhuri, A., Roy, S.K., *Talanta*, 1994, **41**, 171-178
82. Vartak, S.V., Gaudh, J.S., Shinde, V.M., *Mikrochimica Acta*, 1997, **127**, 41-44
83. Gao, H-W., Zhang, P-F., *Analyst*, 1994, **119**, 2109-2111
84. Irth, H., Brouwer, E., de Jong, G.J., Th. Brinckman, U.A., Frei, R.W., *J. Chromatography*, 1988, **439**, 63-70
85. Vin, Y.Y., Khopkar, S.M., *Mikrochimica Acta*, 1992, **107**, 49-54
86. Tripathi, A.N., Patel, K.S., *Fres. J. Anal. Chem.*, 1998, **360**, 270-272
87. Nalini, S., Balasubramanian, N., Ramakrishna, T.V., *Fres. J. Anal. Chem.*, 1994, **348**, 769-770
88. Jianhua, W., Ronghuan, H., *Toxicological & Environmental Chemistry*, 1993, **39**, 161-167
89. Enger, J., Marankov, A., Chekalin, N., Axner, O., *J. Anal. At. Spectrom.*, 1995, **10**, 539-549
90. Subramanian, K.S., Poon, R., Chu, I., Connor, J.W., *Archives of Environmental Contamination & Toxicology*, 1997, **32**, 431-435
91. Ward, R.J., Black, C.D.V., Watson, G.J., *Clin. Chim. Acta*, 1979, **99**, 143-152
92. Koch, I., Harrington, C.F., Reimer, K.J., Cullen, W.R., *Talanta*, 1997, **44**, 1241-1251
93. López-García, I., Sánchez-Merlos, M., Hernández-Córdoba, M., *Spectrochim. Acta B*, 1997, **52**, 437-443
94. Torgov, V.G., Vall, G.A., Demidova, M.G., Yatsenko, V.T., *Chemical Geology*, 1995, **124**, 101-107
95. Venkaji, K., Naidu, P.P., Rao, T.J.P., *Talanta*, 1994, **41**, 1281-1290

96. Marr, I.L., Anwar, J., Sithole, B.B., *Analyst*, 1982, **107**, 1212-1217
97. Kobayashi, R., Imaizumi, K., *Analytical Sciences*, 1989, **5**, 61-64
98. Dahl, K., Thomassen, Y., Martinsen, I., Radzink, Salba, B., *J. Anal. At. Spectrom.*, 1994, **9**, 1-5
99. Belarra, M.A., Belategui, I., Lavilla, I., Anzano, J.M., Castillo, J.R., *Talanta*, 1998, **46**, 1265-1272
100. Ainsworth, N., Cooke, J.A., Johnson, M.S., *Environmental Pollution*, 1990, **65**, 65-77
101. Brannon, J.M., Patrick Jr., W.H., *Environmental Pollution (Series B)*, 1985, **9**, 107-126
102. Ravichandra Babu, R., Rajan, S.C.S., Dikshitulu, L.S.A., *Talanta*, 1995, **42**, 2017-2020
103. Costantini, S., Giordano, R., Rizzica, M., Benedetti, F., *Analyst*, 1985, **110**, 1355-1359
104. Thompson, M., Thornton, I., *Environmental Toxicology*, 1997, **18**, 117-119
105. Raven, K.P., Reynolds, J.W., Loeppert, R.H., *Commun. Soil Sci. Plant Anal.*, 1997, **28**, 237-257
106. Anderson, K.A., Isaacs, B., *J. AOAC International*, 1994, **77**, 1562-1568
107. Morrow, A., Wiltshire, G., Hursthouse, A., *Atomic Spectroscopy*, 1997, **18**, 23-28
108. Bradford, G.R., Bakhtar, D., *Environ. Sci. Technol.*, 1991, **25**, 1704-1706
109. Lunzer, F., Pereiro-Garcia, R., Bordel-Garcia, N., Sanz-Medel, A., *J. Anal. At. Spectrom.*, 1995, **10**, 311-315
110. Arpadjian, S., Vuchkova, L., Kostadinova, E., *Analyst*, 1997, **122**, 243-246
111. Warnock, D.W., Delves, H.T., Campbell, C.K., Croudace, I.W., Davey, K.G., Johnson, E.M., Sieniawska, C., *Lancet*, 1995, **346**, 1516-1520
112. Kumamaru, T., Yamamoto, M., Nakata, F., Tsubota, H., Nishikida, K-I., *Analytical Sciences*, 1994, **10**, 651-653
113. Fairman, B., Catterick, T., *J. Anal. At. Spectrom.*, 1997, **12**, 863-866
114. Bowman, J., Fairman, B., Catterick, T., *J. Anal. At. Spectrom.*, 1997, **12**, 313-316
115. Chen, C-S., Jiang, S-J., *Spectrochimica Acta Part B*, 1996, **51**, 1813-1821
116. Santosa, S.J., Mokudai, H., Tanaka, S., *J. Anal. At. Spectrom.*, 1997, **12**, 409-415

117. Hall, G.E.M., Pelchat, J-C., *J. Anal. At. Spectrom.*, 1997, **12**, 103-106
118. Dietl, C., Reifenhauer, W., Peichl, L., *Sci. Total Environment*, 1997, **205**, 235-244
119. Delves, H.T., Sieniawska, C.E., Fell, G.S., Lyon, T.D.B., Dezateux, C., Cullen, A., Variend, J., Bonham, J.R., Chantler, S.M., *Analyst*, 1997, **122**, 1323-1329
120. Clemente, G.F., Ingrao, G., Santaroni, G.P., *Sci. of Total Environment*, 1982, **24**, 255-265
121. Zmijewska, W., *Biological Trace Element Research*, 1994, **43-45**, 251-257
122. Polasek, M., Jervis, R.E., *J. Radioanal. & Nuc. Chem.*, 1994, **179**, 205-209
123. Laporta-Ferreira, I.L., Santos, S.M.A., Santoro, M.L., Saiki, M., Vasconcelos, M.B.A., *J. Natural Toxins*, 1997, **6**, 103-110
124. Gentzis, T., Goodarzi, F., *Energy Sources*, 1997, **19**, 493-505
125. Fergusson, J.E., Forbes, E.A., Schroeder, R.J., Ryan, D.E., *Sci. of Total Env.*, 1986, **50**, 217-221
126. Haffer, E., Schmidt, D., Freimann, P., Gerwinski, W., *Spectrochim. Acta B*, 1997, **52**, 935-944
127. Pilarski, J., Waller, P., Pickering, W., *Water, Air & Soil Pollution*, 1995, **84**, 51-59
128. Sharma, P., Vyas, S., Sanganeria, S., *Bulletin of Electrochemistry*, 1997, **13**, 136-138
129. Khoo, S.B., Zhu, J., *Analyst*, 1996, **121**, 1983-1988
130. Van den Berg, C.M.G., *Estuaries*, 1993, **16**, 512-520
131. Zhou, C-L., Lu, Y., Li, X-L Luo, C-N, Zhang, Z-W., You, J-M., *Talanta*, 1998, **46**, 1531-1536
132. Kopanskaya, L.S., Vataman, I.I., *J. Anal. Chem. of the USSR*, 1986, **41**, 352-356
133. Guiyu, Y., Dibrov, I.A., *Russian J. Applied Chemistry*, 1996, **69**, 1126-1128
134. Bond, A.M., Kratsis, S., Newman, O.M.G., Pfund, B.V., *Electroanalysis*, 1997, **9**, 13-18
135. Rurikova, D., Pocuchova, M., *Chem. Papers*, 1997, **51**, 15-21
136. Mok, W-M., Wai, C-M., *Environ. Sci. Technol.*, 1990, **24**, 102-108
137. Chwastowska, J., Zmijewska, W., Sterlinska, E., *J. Radioanal. Nuclear Chem., Articles*, 1995, **196**, 3-9
138. Sato, S., *Talanta*, 1985, **32**, 341-344
139. Sharma, M., Patel, K.S., *Intern. J. Anal. Chem.*, 1993, **50**, 63-71

140. Rath, S., Jardim, W.F., Dórea, J.G., *Fres. J. Anal. Chem.*, 1997, **358**, 548-550
141. Huang, X., Zhang, W., Han, S., Yin, Y., Xu, G., Wang, X., *Talanta*, 1997, **45**, 127-135
142. Holak, W., *Anal. Chem.*, 1969, **41**, 1712
143. Apte, S.C., Howard, A.G., *J. Anal. At. Spectrom.*, 1986, **1**, 221-225
144. Mohammad, B., Ure, A.M., Reglinski, J., Littlejohn, D., *Chemical Speciation & Bioavailability*, 1990, **3**, 117-122
145. de la Calle-Guntiñas, M.B., Madrid, Y., Cámara, C., *Fres. J. Anal. Chem.*, 1992, **343**, 597-599
146. de la Calle-Guntiñas, M.B., Madrid, Y., Cámara, C., *Fres. J. Anal. Chem.*, 1992, **344**, 27-29
147. de la Calle-Guntiñas, M.B., Torralba, R., Madrid, Y., Palacios, M.A., Bonilla, M., Cámara, C., *Spectrochimica Acta*, 1992, **47B**, 1165-1172
148. D'Ulivo, A., Lampugnani, L., Pellegrini, G., Zamboni, R., *J. Anal. At. Spectrom.*, 1995, **10**, 969-974
149. Keenan, F., Cooke, C., Cooke, M., Pennock, C., ALSPAC Team, *Anal. Chim. Acta*, 1997, **354**, 1-6
150. de la Calle-Guntiñas, M.B., Madrid, Y., Cámara, C., *Anal. Chim. Acta*, 1991, **247**, 7-11
151. de la Calle-Guntiñas, M.B., Madrid, Y., Cámara, C., *J. Anal. At. Spectrom.*, 1993, **8**, 745-748
152. Smichowski, P., de la Calle-Guntiñas, M.B., Madrid, Y., Cobo, M.G., Cámara, C., *Spectrochimica Acta*, 1994, **49B**, 1049-1055
153. Smith, M.M., White, M.A., Wilson, H.K., *J. Anal. At. Spectrom.*, 1995, **10**, 349-352
154. Yan, X-P., van Mol, W., Adams, F., *Analyst*, 1996, **121**, 1061-1067
155. Garbos, S., Bulska, E., Hulanicki, A., Shcherbinina, N.I., Sedykh, E.M., *Anal. Chim. Acta*, 1997, **342**, 167-174
156. Dodd, M., Grundy, S.L., Reimer, K.J., Cullen, W.R., *Applied Organometallic Chemistry*, 1992, **6**, 207-211
157. Yamamoto, Tanaka, S., Hashimoto, Y., *Applied Organometallic Chemistry*, 1992, **6**, 351-356
158. de la Calle-Guntiñas, M.B., Adams, F.C., *J. of Chromatography A*, 1997, **764**, 169-175

159. Smichowski, P., Madrid, Y., de la Calle-Gutiñas, M.B., Cámara, C., *J. Anal. At. Spectrom.*, 1995, **10**, 815-821
160. Lintschinger, J., Koch, I., Serves, S., Feldmann, J., Cullen, W.R., *Fres. J. Anal. Chem.*, 1997, **359**, 484-491
161. Ulrich, N., *Fres. J. Anal. Chem.*, 1998, **360**, 797-800
162. Ulrich, N., *Anal. Chim. Acta*, 1998, **359**, 245-253
163. Skoog, D.A., Leary, J., from 'Principles of Instrumental Analysis', 1992, 4th Ed., Saunders College Publishing, Orlando
164. Aharoni, S.M, *Polymer Engineering & Science*, 1998, **38**, 1039-1047.
165. From 'High-Performance Liquid Chromatography:Advances and Perspectives', 1980, Ed. Csaba Horvath, Academic Press Inc., London
166. IUPAC Analytical Chemistry Division, Commission on Analytical Nomenclature "Recommendations on Nomenclature for Chromatography", *Pure Appl. Chem.*, 1974, **37**, 447-462
167. Weiss, J., 'Ion Chromatography', 1995, VCH, Weinheim
168. Snyder, L.R., Glajch, J.L., Kirkland, J.J., from 'Practical HPLC Method Development', 1988, John Wiley, Chichester
169. Heftmann, E. (Ed.), 'Chromatography:Fundamentals and Applications of Chromatographic and Electrophoretic Methods. Part A: Fundamentals and Techniques', Journal of Chromatography Library - Volume 22A, 1983, Elsevier, Oxford
170. Snyder, L.R., Kirkland, J.J., from 'Introduction to Modern Liquid Chromatography', 1979, John Wiley, Chichester
171. Lindsay, S., from 'High Performance Liquid Chromatography', Analytical Chemistry by Open Learning, Barnes, J. (Ed.), 1992, John Wiley, Chichester
172. Skoog, D.A., West, D.M., from 'Fundamentals of Analytical Chemistry', 1982, 4th Ed., Saunders College Publishing, Orlando
173. Ebdon, L., Evans, E.H. (Ed.), Fisher, A., Hill, S.J., from 'An Introduction to Analytical Atomic Spectrometry', 1998, John Wiley, Chichester
174. Hecht, E., from 'Physics in Perspective', 1980, Addison-Wesley, Mass.
175. From 'Inductively Coupled Plasma Spectrometry 1996; Methods for the Examination of Waters & Associated Materials', 1996, HMSO Books, London
176. Beres, S.A., Bruckner, P.H., Denoyer, E.R., *Atomic Spectroscopy*, 1994, March/April, 96-99
177. Wu, M., Hieftje, G., *Appl. Spectrosc.*, 1992, **46**, 1912-1918

178. Rivas, C., Ebdon, L., Hill, S.J., *J. Anal. At. Spectrom.*, 1996, **11**, 1147-1150
179. Wu, M., Madrid, Y., Auxier, J.A., Heftje, G., *Anal. Chim. Acta*, 1994, **286**, 155-167
180. Hettipathirana, T., Davey, D.E., *Appl. Spectrosc.*, 1996, **50**, 1015-1022
181. Sharp, B.L., *J. Anal. At. Spectrom.*, 1988, **3**, 613-652
182. Sharp, B.L., *J. Anal. At. Spectrom.*, 1988, **3**, 939-963
183. Houk, R.S., Fassel, V.A., Flesch, G.D., Svec, H.J., Gray, A.L., Taylor, C.E., *Anal. Chem.*, 1980, **52**, 2283-2289
184. Lambie, K., Hill, S.J., *Analyst*, 1995, **120**, 413-417
185. Marcos, A., Fisher, A., Rea, G., Hill, S.J., *J. Anal. At. Spectrom.*, 1998, **13**, 6, 521-525
186. Nickson, R.A., Hill, S.J., Worsfold, P.J., *Anal. Proc.*, 1995, **32**, 9, 387-395
187. Guy, A.B., Jones, P., Hill, S.J., *Analyst*, 1998, **123**, 1513-1518
188. Cairns, W.R.L., Hill, S.J., Ebdon, L., *Microchemical Journal*, 1996, **54**, 88-110
189. Cairns, W.R.L., Ebdon, L., Hill, S.J., *Fres. J. Anal. Chem.*, 1996, **355**, 202-208
190. Bloxham, M.J., Gachanja, A., Hill, S.J., Worsfold, P.J., *J. Anal. At. Spectrom.*, 1996, **11**, 145-148
191. Jackson, B.P., Miller, W.P., *J. Anal. At. Spectrom.*, 1998, **13**, 1107-1112
192. Rawcliffe, C.T., Dawson, D.H., from 'Principles of Inorganic and Theoretical Chemistry', 1974, 2nd Ed., Heinemann, London
193. Thompson, M., Pahlavanpour, B., Walton, S.J., Kirkbright, G.F., *Analyst*, 1978, **103**, 568
194. Agterdenbos, N. & J., Santosa, S.J., *Anal. Chim. Acta*, 1990, **237**, 189-199
195. Kemp, W., from 'Organic Spectroscopy', 1975, MacMillan Press, London
196. Sanders, J.K.M., Hunter, B.K., Modern NMR Spectroscopy. A Guide for Chemists, 1990, Oxford University Press, Oxford.
197. Duckworth, H.E., Barber, R.C., Venkatasubramanian, V.S., Mass Spectroscopy, 1986, 2nd Ed., Cambridge University Press, Cambridge
198. Ashcroft, A.E., 'Ionisation Methods in Organic Mass Spectrometry', Barnett, N.W. (Series ed.), RSC Analytical Spectroscopy Monographs, 1997, RSC, Cambridge

199. Holland, G., & Tanner, S.D. (Eds.), 'Plasma Source Mass Spectrometry. Developments and Applications', 1997, RSC, Cambridge
200. Wu, C., Siems, W.F., Reid Asbury, G., Hill Jr., H.H., *Anal. Chem.*, 1998, **70**, 23, 4929-4938
201. Casado, A.G., Hernandez, E.J.A., Espinoza, P., Vilchez, J.L., *J. of Chromatography A*, 1998, **826**, 49-56
202. Holmes, J.C., Morrell, *Appl. Spectrosc.*, 1957, **11**, 86
203. Dolnik, V., Dolnikova, J., *J. of Chromatography A*, 1995, **716**, 269-277
204. Barden, T.J., Croft, M.Y., Murby, E.J., Wells, R.J., *J. of Chromatography A*, 1997, **785**, 251-261
205. Prodromidis, M.I., Tzouwarakarayanni, S.M., Karayannis, M.I., Vadgama, P., Maines, A., *Analyst*, 1996, **121**, 435-439
206. Yoe, J.H., Jones, A.L., *Ind. Eng. Chem., Anal. Edition*, 1944, **16**, 111
207. Vosburgh, W.C., Cooper, G.R., *J. Am. Chem. Soc.*, 1941, **63**, 437
208. Jayaprakasha, G.K., Sakariah, K.K., *J. of Chromatography A*, 1998, **806**, 337-339
209. March, J., from 'Advanced Organic Chemistry', 1985, 3rd Ed., Wiley, New York, p. 117
210. Wifladt, A-M., Wibetoe, G., Lund, W., *Fres. J. Anal. Chem.*, 1997, **357**, 92-96
211. Smith, B.M., Griffiths, M.B., *Analyst*, 1982, **107**, 253-259
212. Ward, R.J., Black, C.D.V., Watson, G.J., *Clin. Chim. Acta*, 1979, **99**, 143-152
213. Andreae, M.O., Asmode, J.F., Foster, P., Van't Dack, L., *Anal. Chem.*, 1981, **53**, 1766-1771
214. Feldmann, J., *Anal. Comm.*, 1996, **33**, 11-13
215. Crews, H.M., Clarke, P.A., Lewis, J., Owen, L.M., Struut, P.R., Izquierdo, A., *J. Anal. At. Spectrom.*, 1996, **11**, 1177-1182
216. Wang, L., May, S.W., Browner, R.F., Pollock, S.H., *J. Anal. At. Spectrom.*, 1996, **11**, 1137-1146
217. Bergdahl, I.A., Schutz, A., Grubb, A., *J. Anal. At. Spectrom.*, 1996, **11**, 730-...
218. Tomlinson, M.J., Wang, J., Caruso, J.A., *J. Anal. At. Spectrom.*, 1994, **9**, 957-964
219. O'Connor, G., Ebdon, L., Evans, E.H., *J. Anal. At. Spectrom.*, 1997, **12**, 1263-1269

220. Kim, A.W., Foulkes, M.E., Ebdon, L., Hill, S.J., Patience, R.L., Barwise, A.G., Rowland, S.J., *J. Anal. At. Spectrom.*, 1992, 7, 1147-1149
221. Koropchak, J.A., Aryamanya-Mugisha, H., *J. Anal. At. Spectrom.*, 1994, 4, 291-294
222. Luan, S., Pang, H.M., Shum, S.C.K., Houk, R.S., *J. Anal. At. Spectrom.*, 1992, 7, 799-805
223. Koropchak, J.A., Sadain, S., Szostek, B., *Spectrochim. Acta, Part B*, 1996, 51, 1733-1745
224. Little, R.W., American Chemical Society Monograph No. 104, New York, 1947
225. Hittunen, K., Seppala, J.V., *J. Appl. Polymer Science*, 1998, 67, 1011-1016
226. Matsuda, H., Urabe, A., Nomura, R., *Ind. Eng. Chem. Prod. Res. Dev.*, 1984, 23, 422-425
227. Elias, H-G., from 'An Introduction to Polymer Science', 1997, VCH, Weinheim
228. Whinfield, J.R., *Nature*, 1946, 158, 930
229. Sorenson, W.R., Campbell, T.W., from 'Preparative Methods of Polymer Chemistry', 1968, 2nd Ed., John Wiley, London
230. James, D.E., Packer, L.G., *Ind. & Eng. Chem. Research*, 1995, 34, 4049-4057

Published work :

1. **'Identification and Chromatographic Separation of Antimony Species with α -hydroxyacids.'** Guy, A.B., Jones, P., and Hill, S.J., *Analyst*, **123**, No.7, 1513-1518, 1998.

Conference Presentations :

'The Development Of A High Performance Liquid Chromatography-Plasma Spectroscopy Technique For The Speciation Of Antimony (III) And (V).'

Alen Guy, Phil Jones & Steve J. Hill, at 8th Biennial National Atomic Spectroscopy Symposium, University of East Anglia, Norwich, U.K., 17-19 July 1996.

'Antimony Speciation : The Determination of Sb(V) and Sb(III) by Ion Chromatography - Inductively Coupled Plasma Optical Emission and Mass Spectroscopy.'

Alen Guy, Phil Jones & Steve J. Hill., at 1997 European Winter Conference on Plasma Spectrochemistry, University of Gent, Belgium, 12-17 January 1997.

'An Investigation of the Structure of Antimony Complexes.'

Alen Guy, Phil Jones, John Marshall & Steve J. Hill., at Research & Development Topics in Analytical Chemistry, University of Northumbria, 2-3 July 1997.

'HPLC-ICP-AES Determination of Sb Complexes in Solution: Application to Speciation of Sb(III) and (V).'

Alen Guy, Phil Jones & Steve J. Hill, at 1998 Winter Conference on Plasma Spectrochemistry, Scottsdale, Arizona, 5-10 January 1998.

'Speciation of Antimony(III) & (V) by Ion Chromatography with ICP-OES and ICP-MS.' Oral Presentation

Alen Guy, Phil Jones & Steve J. Hill. John Marshall, at Atomic Spectroscopy Group Meeting entitled 'Interesting Applications of Elemental Analysis', Sheffield Hallam University, 21st May 1997.

'HPLC-Plasma Spectroscopic Determination and Speciation of Antimony in Environmental Samples', Oral Presentation

Alen Guy, Phil Jones & Steve J. Hill, at 9th Biennial National Atomic Spectroscopy Symposium, University of Bath, U.K., 8-10 July 1998.

'Speciation Studies of Antimony from a disused mine Site by HPLC-ICP-MS and HPLC-HG-ICP-MS',

Alen Guy, Phil Jones and Steve J. Hill, 1999 European Winter Conference on Plasma Spectrochemistry, Pau, France, 10-15 January 1999.